Acta Universitatis Agriculturae Sueciae

Doctoral Thesis No. 2023:53
Faculty of Natural Resources and Agricultural Sciences

Innovative treatment technologies for PFAS-contaminated water

Utilizing foam partitioning and exploring electrochemical oxidation

Sanne J. Smith

Innovative treatment technologies for PFAS-contaminated water

Utilizing foam partitioning and exploring electrochemical oxidation

Sanne J. Smith
Faculty of Natural Resources and Agricultural Sciences
Department of Aquatic Sciences and Assessment
Uppsala

SLU
SWEDISH UNIVERSITY OF AGRICULTURAL SCIENCES

DOCTORAL THESIS
Uppsala 2023

Acta Universitatis Agriculturae Sueciae
2023:53

Cover: PFAS in foam
(picture created with Adobe Firefly and Adobe Photoshop by S.J. Smith)

ISSN 1652-6880
ISBN (print version) 978-91-8046-158-0
ISBN (electronic version) 978-91-8046-159-7
https://doi.org/10.54612/a.6p8i5lbs8l

Swedish University of Agricultural Sciences, Department of Aquatic Sciences & Assessment, Uppsala, Sweden
Print: SLU Grafisk Service, Uppsala 2023

Innovative treatment technologies for PFAS-contaminated water

Utilizing foam partitioning and exploring electrochemical oxidation

Abstract

The presence of per- and polyfluoroalkyl substances (PFAS) in the aquatic environment has become a global cause for concern. PFAS are persistent anthropogenic chemicals, and certain PFAS are known to be mobile, bioaccumulative and toxic. PFAS are often found in landfill leachate, effluents from industrial and municipal wastewater treatment plants, and groundwater contaminated with aqueous film-forming foam (AFFF). Conventional wastewater treatment technologies are typically inefficient towards the removal of PFAS. Therefore, this thesis aimed to explore the effectiveness of foam fractionation (FF) and electrochemical oxidation (EO) for PFAS removal and degradation.

In FF, PFAS adsorb to rising air bubbles and are separated from the water as a concentrated foam. In this thesis, a continuous pilot-scale FF reactor was optimized for PFAS removal from landfill leachate, reaching ΣPFAS removal efficiencies of 60%. Gaps in the mass balance were identified, so a follow-up study assessed if emissions to air could explain this loss of PFAS. Here, FF could remove up to 84% of ΣPFAS from AFFF-contaminated industrial water. While the measured PFAS emissions to air were high, they did not contribute significantly to the mass balance.

EO was tested as a destructive technology for the treatment of fractionated foam produced from groundwater and landfill leachate. Treatment effectiveness was assessed with thorough analysis strategies, including target analysis, PFAS sum parameters and effect-based methods, and a coupled numerical model was developed to describe the PFAS degradation kinetics. While the total degradation was higher with EO only, the energy efficiency of the FF+EO system was higher.

Finally, the potential of integrating foam fractionation with existing treatment processes was investigated. Foam was sampled from ten different full-scale water treatment plants, and it was found that the ΣPFAS enrichment relative to the influent reached up to a factor of 10^5. However, no PFAS removal from influent to effluent was found, possibly because the foam was not actually removed in any of the processes. Altogether, this thesis contributes to an increased understanding of treatment options for PFAS-contaminated water, with a particular focus on FF and EO.

Keywords: PFAS, wastewater treatment, foam fractionation, electrochemical oxidation

Innovativa behandlingsmetoder för PFAS-förorenat vatten – Utnyttjning av partitionering till skum och utforskning av elektrokemisk oxidation

Sammanfattning

Förekomsten av per- och polyfluoralkylämnen (PFAS) i vattenmiljön har blivit en orsak till oro världen över. PFAS är persistenta, antropogena kemikalier och vissa PFAS är mobila, bioackumulerande och toxiska. PFAS detekteras ofta i lakvatten från avfallsdeponier, avlopp från industriella och kommunala vattenreningsverk och grundvatten förorenat med brandsläckningsskum (AFFF). Konventionella vattenbehandlingstekniker är vanligtvis ineffektiva för PFAS. Syftet med denna avhandling var därför att utforska effektiviteten av skumfraktionering (FF) och elektrokemisk oxidation (EO) för avlägsnande och nedbrytning av PFAS.

I FF adsorberas PFAS till stigande luftbubblor och separeras från vattnet som ett koncentrerat skum. I denna avhandling optimerades en kontinuerlig FF-reaktor för avlägsnande av PFAS från lakvatten från en avfallsdeponi, och en ΣPFAS-avskiljningseffektivitet på 60 % uppnåddes. Massbalansen var inte 100 %, så en uppföljande studie bedömde om utsläpp till luft kunde förklara denna förlust av PFAS. FF kunde i den studien ta bort upp till 84 % av ΣPFAS från AFFF-förorenat industrivatten. Även om de upptäckta PFAS-utsläppen till luft var höga, bidrog de inte nämnvärt till massbalansen.

EO testades som en destruktiv teknologi för behandling av fraktionerat skum från grundvatten och lakvatten från en deponi. Behandlingseffektiviteten utvärderades med omfattande analysstrategier, inklusive kvantitativ masspektrometrisk analys, bred karakterisering av fluorerade organiska ämnen och effektbaserade metoder. Därutöver utvecklades en kopplad numerisk modell för att beskriva kinetiken för nedbrytningen av PFAS. Den totala nedbrytningen visade sig vara högre med endast EO, medan energieffektiviteten var högre för FF+EO-systemet.

Slutligen undersöktes potentialen för att integrera skumfraktionering med befintliga behandlingsprocesser. Skum provtogs från tio olika fullskaliga reningsanläggningar, och det visade sig att ΣPFAS-koncentrationen i skummet var upp till en faktor 10^5 högre än i inflödet. PFAS-halterna reducerades dock inte under processen (från inflöde till utflöde), möjligen för att skummet inte togs bort i någon av processerna. Sammantaget bidrar denna avhandling till en ökad förståelse för behandlingsalternativ för PFAS-förorenat vatten, med särskilt fokus på FF och EO.

Nyckelord: PFAS, vattenreningsverk, skumfraktionering, elektrokemisk oxidation

Innovatieve waterzuiveringsmethoden voor PFAS – benutten van verrijking in schuim en verkennen van elektrochemische oxidatie

Samenvatting

De wijdverspreide aanwezigheid van per- en polyfluoroalkylstoffen (PFAS) in het aquatische milieu is reden tot zorg. PFAS zijn persistente antropogene chemicaliën, en bepaalde PFAS zijn mobiel, bioaccumulerend en giftig. PFAS worden vaak aangetroffen in percolaat van stortplaatsen, stedelijk en industrieel afvalwater en water verontreinigd met brandblusschuim (AFFF). Conventionele waterbehandelingstechnologieën zijn doorgaans niet effectief voor deze stoffen. In dit proefschrift is de effectiviteit van schuimfractionering (FF) en elektrochemische oxidatie (EO) voor de verwijdering en afbraak van PFAS onderzocht.

In FF adsorberen PFAS aan stijgende luchtbellen en worden ze als geconcentreerd schuim van het water gescheiden. In deze scriptie is een continue FF reactor geoptimaliseerd voor de verwijdering van PFAS uit percolaat, met een uiteindelijke ΣPFAS verwijderingsefficiëntie van 60%. De massabalans sloot niet volledig, dus in een vervolgstudie werd beoordeeld of emissies naar de lucht dit verlies van PFAS konden verklaren. Hier kon FF tot 84 % van ΣPFAS verwijderen uit AFFF-verontreinigd industrieel water. Hoewel er hoge PFAS emissies naar lucht gemeten werden, droegen deze niet significant bij aan de massabalans over de FF.

EO is getest als destructieve technologie voor gefractioneerd schuim van percolaat en grondwater van een stortplaats. De effectiviteit van deze behandeling werd grondig geanalyseerd, met PFAS doel-analyses, ‘totaal PFAS’ parameters en effectgerichte analyses. Daarnaast is ook een gekoppeld numeriek model ontwikkeld, om de kinetiek van de PFAS degradatie te beschrijven. Hoewel de totale degradatie hoger was met alleen EO, was de energie-efficiëntie hoger bij gebruik van het FF+EO systeem.

Tenslotte is het potentieel van geïntegreerde schuimfractionering binnen bestaande waterzuiveringsinstallaties onderzocht. Schuim afkomstig van tien bestaande waterzuiveringsinstallaties is bemonsterd, en de ΣPFAS concentraties in het schuim waren tot 10^5 maal hoger dan in de influent. Er werd echter geen ΣPFAS verwijdering van influent naar effluent gevonden, mogelijk omdat het schuim niet daadwerkelijk verwijderd werd in de processen. Al met al draagt dit proefschrift bij aan een verbeterd begrip van behandelingsopties voor PFAS-vervuild water, met een focus op FF en EO.

Trefwoorden: PFAS, waterzuivering, schuimfractionering, electrochemische oxidatie

Dedication

To Hans. Thanks for the company!

Contents

List of publications

This thesis is based on the work contained in the following papers, referred to by Roman numerals in the text:

I. **Smith, S. J**.; Wiberg, K.; McCleaf, P.; Ahrens, L. (2022) Pilot-Scale Continuous Foam Fractionation for the Removal of Per- and Polyfluoroalkyl Substances (PFAS) from Landfill Leachate. ACS ES&T Water, 2 (5), 841–851.

II. **Smith, S. J**.; Lewis, J.; Wiberg, K.; Wall, E.; Ahrens, L. (2023) Foam Fractionation for Removal of Per- and Polyfluoroalkyl Substances: Towards Closing the Mass Balance. Sci. Total Environ., 871, 162050.

III. **Smith, S. J**.; Lauria, M.; Ahrens, L.; McCleaf, P.; Hollman, P.; Bjälkefur Seroka, S.; Hamers, T.; Arp, H. H. P.; Wiberg, K. (2023) Electrochemical Oxidation for Treatment of PFAS in Contaminated Water and Fractionated Foam - A Pilot-Scale Study. ACS ES&T Water, 3 (4), 1201-1211.

IV. **Smith, S. J**.; Keane, C.; Ahrens, L.; Wiberg, K. (2023) Integrated Treatment of Per- and Polyfluoroalkyl Substances in Existing Water Treatment Plants – Scoping the Potential of Foam Partitioning. ACS ES&T Engineering, accepted.

The contribution of Sanne J. Smith to the papers included in this thesis was as follows:

I. Planned the study together with the co-authors. Had main responsibility for the on-site pilot-scale experiments, laboratory analyses, data handling, data analysis, interpretations, writing and submitting.

II. Planned the study together with the co-authors. Had main responsibility for the on-site pilot-scale experiments, laboratory analyses, data handling, data analysis, interpretations, writing and submitting.

III. Planned the study together with the co-authors. Had main responsibility for the on-site pilot-scale experiments, all laboratory analyses except the extractable organofluorine measurements (which were done by M. Lauria), data handling, data analysis, numerical modelling, interpretations, writing and submitting.

IV. Planned the study together with the co-authors. Had main responsibility for the sample collection, laboratory analyses, data handling, data analysis, interpretations, writing and submitting.

Abbreviations

AFFF	Aqueous film-forming foams
AIX	Anion exchange
BDD	Boron-doped diamond
COD	Chemical oxygen demand
DOC	Dissolved organic carbon
DOM	Dissolved organic matter
ECHA	European chemicals agency
EE/O	Electrical energy per order of magnitude degradation
EF	Enrichment factor
EFSA	European food safety authority
EO	Electrochemical oxidation
EOF	Extractable organofluorine
FASA	Perfluoroalkyl sulfonamides
FF	Foam fractionation
FTSA	Fluorotelomer sulfonic acids
GAC	Granular activated carbon
MB	Mass balance
MBBR	Moving bed biofilm reactor
MCL	Maximum contaminant level

MOA	Mode of action
NF	Nanofiltration
PEQ	PFOA equivalents
PFAA	Perfluoroalkyl acids
PFAS	Per- and polyfluoroalkyl substances
PFCA	Perfluoroalkyl carboxylic acids
PFSA	Perfluoroalkyl sulfonic acids
PP	Polypropylene
RO	Reverse osmosis
SIPs	Sorbent-impregnated polyurethane foam discs
T_4	Thyroxine
TOC	Total organic carbon
TOP	Total oxidizable precursors
TTR	Transthyretin
TWI	Tolerable weekly intake
VOC	Volatile organic carbon

For full names of individual PFAS, see papers **I-IV**.

1. Introduction

Throughout history, science and innovation have made people's lives more comfortable. From using flints to create fire to the discovery of penicillin, inventors have successfully increased the quality of human life. However, sometimes innovations come with unintended consequences that can be detrimental, which happens particularly often within the chemical industry. Perhaps the most famous example hereof is DDT, or dichlorodiphenyltrichloroethane, an insecticide that became infamous for its environmental impacts (Carson, 1962), but the ozone-depleting capacity of Freon (Wofsy et al., 1975) and the addition of toxic tetraethyl lead to gasoline (Nriagu, 1990) are notable as well. In recent years, per- and polyfluoroalkyl substances (PFAS) have become the newest addition to this list of regrettable chemical inventions (Arp et al., 2023).

1.1 Per- and polyfluoroalkyl substances (PFAS)

PFAS are a class of chemical compounds characterized by the presence of at least one perfluoroalkyl moiety (R-CF_2-R'; R, R' ≠ H/Cl/Br/I) in their chemical structure (Z. Wang et al., 2021). Almost all PFAS are anthropogenic and they are widely used in consumer products, mostly for their repellent properties (Sunderland et al., 2019). The high stability, hydrophobicity and oleophobicity of PFAS are exploited in coating applications for clothing, furniture, paper, carpet and cookware. Another widespread use of PFAS is in aqueous film-forming foams (AFFFs). Finally, PFAS are used industrially, e.g. for semiconductor production, in laboratory equipment and in medical implants (Lemal, 2004; Sunderland et al., 2019; Z. Wang et al., 2017).

The extensive usage and high persistency of PFAS caused them to become widespread in the environment. PFAS have been detected worldwide in surface water, rainwater, groundwater, air, soil and ice caps (Cousins et al., 2022; Lau et al., 2007). Moreover, PFAS were detected in the blood of wildlife. The highest concentrations were found in samples originating from fish or fish-eating animals (Lau et al., 2007). PFAS have even been detected in human blood, breastmilk and liver tissue (Göckener et al., 2020; Lau et al., 2007).

1.1.1 PFAS classification

The reported PFAS concentrations in the environment, wildlife and human samples vary extremely per type of PFAS. Historically, perfluorooctanoic acid (PFOA) and perfluorooctane sulfonic acid (PFOS) were the most prevalent PFAS, both in terms of industrial production and as subject for academic research (Paul et al., 2009; Prevedouros et al., 2006). These two compounds are still amongst the most frequently detected. However, many more PFAS exist, and Buck et al. (2011) have classified the broad family of PFAS into different subclasses. The first distinction is between fluorinated polymers, such as polytetrafluoroethylene (PTFE or Teflon), and nonpolymeric PFAS. Of these, nonpolymeric PFAS are most relevant with regards to environmental contamination and water treatment.

Nonpolymeric PFAS are further divided into polyfluoroalkyl and perfluoroalkyl substances, see also Table 1. In *per*fluoroalkyl substances, all hydrogens on *all* alkyl carbon atoms have been replaced by fluorines. The most well-known class of perfluorinated compounds are the perfluoroalkyl acids (PFAA), which encompasses the perfluoroalkyl carboxylic acids (PFCA) and perfluoroalkane sulfonic acids (PFSA). PFOA and PFOS are examples of these respective classes. Conversely, in *poly*fluoroalkyl substances, such as the fluorotelomer sulfonic acids (FTSA), all hydrogens on *at least one,* but not all, carbon atoms have been replaced by fluorine. Many nonpolymeric PFAS are used as surfactants and thus consist of a polar hydrophilic head group and an apolar hydrophobic perfluoroalkyl tail (Buck et al., 2011).

Table 1: Overview of common non-polymeric PFAS classes, with examples of compounds. Adapted from (Ahrens & Bundschuh, 2014).

Name	Acronym	Structure	Example
Perfluorinated			
Perfluoroalkyl sulfonates	PFSA	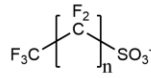	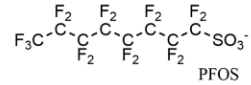 PFOS
Perfluoroalkyl carboxylates	PFCA	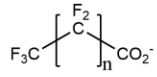	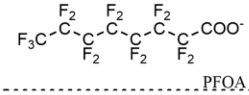 PFOA
Perfluoroalkyl phosphonates	PFPA	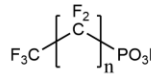	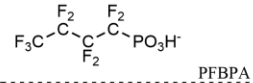 PFBPA
Perfluoroalkyl sulfonamides	FASA	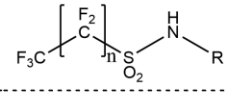	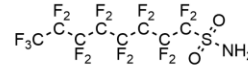 FOSA
Perfluoroalkyl sulfonamido-ethanols	FASE	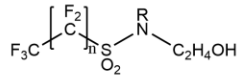	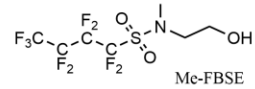 Me-FBSE
Perfluoroalkyl sulfonamido-acetic acids	FASAA	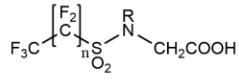	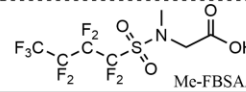 Me-FBSAA
Polyfluorinated			
Polyfluoroalkyl phosphoric acid esters	PAP	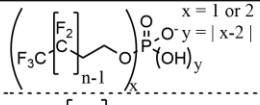	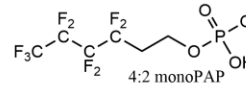 4:2 monoPAP
n:2 Fluorotelomer alcohols	n:2 FTOH	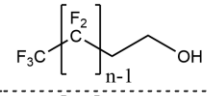	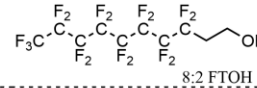 8:2 FTOH
n:2 Fluorotelomer sulfonates	n:2 FTSA	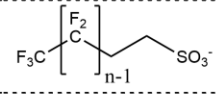	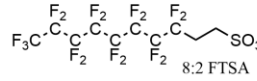 8:2 FTSA
n:2 Fluorotelomer carboxylates	n:2 FTCA	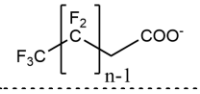	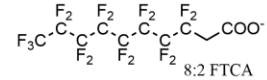 8:2 FTCA
n:2 Fluorotelomer unsaturated carboxylates	n:2 FTUCA	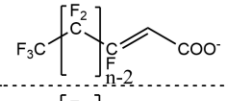	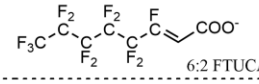 6:2 FTUCA
n:2 Fluorotelomer saturated aldehydes	n:2 FTAL	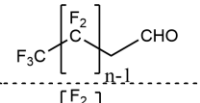	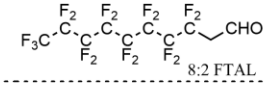 8:2 FTAL
n:2 Fluorotelomer unsaturated aldehydes	n:2 FTUAL	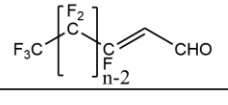	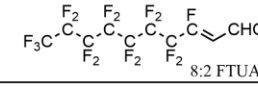 8:2 FTUAL

Classification of nonpolymeric PFAS based on their perfluorinated chain length is also common. Many PFAS have the general formula $C_nF_{2n+1}R$, where R can be a carboxylic acid, sulfonic acid, ether or phosphoric acid group. However, less well-known terminal groups also occur (Buck et al., 2011; Rayne et al., 2008). PFSA are commonly considered to be short-chain for a chain length below or equal to five ($C_nF_{2n+1}SO_3H$, $n \leq 5$) and PFCA for a chain length below or equal to six ($C_nF_{2n+1}COOH$, $n \leq 6$) (Buck et al., 2011).

In addition to specific PFAS compounds, precursor compounds also contribute to PFAS contamination. Precursors are polyfluorinated compounds that can degrade to perfluorinated PFAS, but are usually not measured during standard analysis. Their presence thus leads to an underestimation of the eventual actual exposure to PFAS (Buck et al., 2011; Sunderland et al., 2019). Examples of such precursors include fluorotelomer compounds, perfluoroalkyl sulfonamides and polyfluoroalkyl phosphates (Buck et al., 2011). Certain fluoropolymers may also be considered PFAS precursors.

1.1.2 (Eco)toxicity of PFAS

PFAS have been associated with a wide range of health effects in animals as well as humans. Controlled lab-animal studies are abundant and lethal concentrations (LC_{50}) have been determined for comparatively many PFAS and animal species (Ankley et al., 2021). Generally, these concentrations exceed concentrations relevant for human exposure by multiple orders of magnitude (Fenton et al., 2021). Studies into the effects of PFAS on wildlife exist as well, but are difficult to interpret (Ankley et al., 2021). Confounding factors can often not be excluded, and there is an extreme variability in the organisms and toxic endpoints studied, which may lead to contradictory results. Nonetheless, effects have been observed in some studies, for example a decrease in reproductive success of certain bird species at high PFOS exposures.

Bioaccumulation plays a role in certain chronic effects of PFAS, since it leads to increasing PFAS concentrations in organisms over time (De Silva et al., 2021). Particularly long-chain PFAA have a high bioaccumulation potential. Trophic magnification, meaning increased PFAS concentrations in top-predatory animals due to dietary exposure, is most important in avian and marine mammalian food webs. Accordingly, also in humans, eating fish

from PFAS-contaminated waterbodies may result in a significant increase of PFAS levels in blood serum (Barbo et al., 2023).

Definitive evidence of toxic effects in humans only exists for very few substances. A systematic literature review into human health effects of PFAS, commissioned by the Australian Government Department of Health, found sufficient evidence of associations between PFOS and PFOA exposure and elevated blood cholesterol, and limited evidence of associations with high blood uric acid concentration, impaired glomerular filtration rate, chronic kidney disease, kidney cancer, testicular cancer and impacts on vaccine-derived immunity (Kirk et al., 2018). Additionally, PFAS have often been associated with liver disease, altered thyroid function and adverse reproductive outcomes (Fenton et al., 2021; Rickard et al., 2022). For most of these effects, modes of action (MOA) have not been reliably determined (Fenton et al., 2021).

The wide variety of PFAS to which humans are exposed makes it challenging to assess human health effects. Most experts agree that grouping 'all PFAS' together for the purpose of assessing human health risk is illogical (Anderson et al., 2022). PFAS vary substantially in their physicochemical properties, and toxicological effects attributed to e.g. a long-chain PFCA may not be relevant to a short-chain PFSA or vice versa. Because PFAS typically occur as mixtures, this makes it difficult to assess human health risks accurately. Grouping PFAS based on toxic MOAs or target organs and evaluating mixture toxicities accordingly would be most reliable, but this information is scarce for most PFAS.

1.1.3 Persistency of PFAS

While toxicity and bioaccumulation potential are vastly different between the different types of PFAS, almost all PFAS are either non-degradable or form stable degradation products that are still PFAS (Cousins et al., 2020). This extreme resistance to degradation originates from the perfluoroalkyl moiety that is present in all PFAS. Perfluoroalkyl moieties contain multiple C-F bonds to the same carbon, which shortens and thereby strengthens these already exceptionally strong bonds. The presence of multiple perfluorinated carbon atoms further stabilizes the molecule by preventing nucleophilic attack and strengthening the C-C bonds in the carbon chain, due to the high electronegativity of fluorine.

The high persistency of the entire class has been argued to warrant phase-out of all "non-essential" uses of PFAS. Because of the persistency of PFAS, continuous emissions will lead to continuously increasing concentrations in the environment (Cousins et al., 2019). Experimentally determining dose-response curves for all PFAS and all toxicological endpoints is an infeasible task, but these increasing concentrations will most probably lead to an eventual harmful effect. Accordingly, to prevent costly and challenging remediation efforts, regulation of these chemicals that prevents their emission is crucial (Cousins et al., 2020).

This reasoning forms the basis of a recent EU proposal that aims to ban the production and use of around 10,000 PFAS, with exceptions for essential uses, because of their high persistency and mobility (European Chemicals Agency, 2023b). The detailed proposal is open for public consultation until the 25th of September 2023, after which the European Chemicals Agency (ECHA) will send their opinion to the European Commission, who will decide on the implementation of the ban. If the proposal is implemented, industries will be given a transition period of between 1.5 and 13.5 years to find replacements for all non-essential uses of PFAS as defined in the restriction (European Chemicals Agency, 2023a).

1.1.4 Human exposure to PFAS

Exposure routes for PFAS include ingestion of food and water, inhalation of air and dust and dermal absorption (De Silva et al., 2021). For the general population, dietary exposure is probably the most important contributor to PFOS and PFOA exposure, with animal-based products as the main source. Conversely, drinking water is often the main PFAS exposure pathway for people living near contaminated sites. The relative contributions of air inhalation and dermal exposure from dust and personal care products are uncertain, but particularly PFAS-contaminated house dust may contribute significantly to the total PFAS exposure (De Silva et al., 2021; DeLuca et al., 2022).

1.1.5 Current regulation of PFAS

After voluntary phase-out by production companies and the introduction of legal restrictions, the production and use of PFOS and PFOA have been largely eliminated in the US and Europe (Ahrens & Bundschuh, 2014; Paul et al., 2009; Prevedouros et al., 2006). PFOS, PFOA and perfluorohexane

sulfonic acid (PFHxS) have also been listed as persistent organic pollutants under the Stockholm convention (Secretariat of the Stockholm Convention, 2022), restricting their production and use. While worldwide, these 'legacy PFAS' may still be manufactured, PFAS production has mostly shifted to short-chain and precursor compounds, which are now becoming increasingly prevalent in the environment (S. Liu et al., 2022).

Guidelines for tolerable PFAS concentrations in environmental waters typically exist only for PFOS and PFOA and vary widely per country. For example, in Sweden, the advised maximum yearly-averaged concentration of PFOS in inland surface water is 0.65 ng L^{-1} (Swedish Agency for Marine and Water Management, 2019). In the Netherlands, advisory risk limits for PFOA and PFOS in surface water are 0.3 ng L^{-1} and 0.007 ng L^{-1}, respectively (National Institute for Public Health and the Environment (RIVM), 2022). In a draft recommendation, the US EPA set quality criteria for PFOA and PFOS concentrations (four-day average) in freshwater at 94 µg L^{-1} and 8.4 µg L^{-1}, respectively (US EPA, 2022a, 2022b).

Ultimately, surface water quality is not only protected for the sake of aquatic life, but also to protect drinking water sources. The US EPA recently proposed maximum contaminant levels (MCLs) for PFOA, PFOS, PFHxS, perfluorononanoic acid (PFNA), hexafluoroproylene oxide dimer acid (HFPO-DA, GenX) and perfluorobutane sulfonic acid (PFBS) in drinking water (US EPA, 2023). The proposed MCLs of PFOS and PFOA are both 4 ng L^{-1}. PFNA, PFHxS, PFBS and GenX would be regulated as a hazard index, based on health-based concentrations of 10, 9, 2000 and 10 ng L^{-1}, respectively. The European drinking water directive currently defines a limit value for the sum of 20 PFAS at 100 ng L^{-1} and a 'PFAS total' limit of 500 ng L^{-1}, but technical guidelines for measuring 'PFAS total' remain to be determined (The European Parliament and the Council of the European Union, 2020). In Australia, guideline concentrations are 70 ng L^{-1} for the sum of PFOS and PFHxS, and 560 ng L^{-1} for PFOA (Australian Government - NHMRC; NRMMC, 2018).

Guideline concentrations for PFAS in drinking water are becoming lower over time, particularly in the USA (Post, 2021). The European Food Safety Authority (EFSA) defined a tolerable weekly intake (TWI) of 4.4 ng per kg bodyweight per week for the sum of PFOA, PFOS, PFNA and PFHxS (EFSA, 2020). Translating this TWI to drinking water guidelines would result in a maximum concentration of 4.4 ng PFOA-equivalents (PEQs) L^{-1},

with PFOS, PFNA and PFHxS concentrations being expressed as PEQs using their relative potency factors (RIVM, 2021). This value of 4.4 ng PEQs L^{-1} is lower than the current EU drinking water directive limit of 100 ng L^{-1} for the sum of 20 PFAS, and some European countries are thus already preparing their drinking water infrastructure for more stringent guidelines (Danish EPA, 2021; RIVM, 2021; Swedish Food Agency, 2022).

1.2 Water treatment technologies for PFAS

Effluent streams from municipal and industrial wastewater treatment plants and the disposal of landfill leachate are major discharge routes of PFAS into the aquatic environment (Ahrens & Bundschuh, 2014). Additionally, AFFF application can contaminate soils and groundwater with PFAS, which may eventually spread to nearby water bodies. Remediation of such contaminated waters is a crucial way of protecting drinking water sources, and thereby preventing human exposure to PFAS.

Unfortunately, most conventional wastewater treatment technologies are ineffective towards the removal of PFAS. While biological treatment may result in some PFAS removal due to adsorption to sludge, the degradation of PFAA precursors may also lead to an increase of measurable PFAS concentrations in the effluent (Lenka et al., 2021). Accordingly, for reliable removal of PFAS from contaminated water, more advanced technologies are necessary.

1.2.1 Removal technologies

Removal technologies for PFAS-contaminated water aim to relocate the PFAS from the water, rather than destroy them. Removal technologies include sorption technologies and concentration technologies. Sorption technologies transfer PFAS from the aqueous phase to a solid phase, whereas concentration technologies generate a PFAS-enriched aqueous waste stream. Examples of sorption technologies are treatment with activated carbon and ion exchange, and examples of concentration technologies are membrane filtration and foam fractionation. Additionally, less well-known removal technologies include phytoremediation and electrocoagulation, but these are not commonly used yet on full-scale.

Activated carbon

Historically, adsorption to granular activated carbon (GAC) has been the most-used treatment technology for PFAS-contaminated water (Zhi & Liu, 2015). GAC is activated carbon with a particle size of ≥ 0.2 mm, and is particularly effective for the removal of long-chain PFAA from low-strength waters (P. Li et al., 2019; Wei et al., 2019). The presence of dissolved organic carbon (DOC) or other co-contaminants can reduce the PFAS removal by GAC, and once the GAC is saturated, breakthrough of PFAS will occur (Tröger et al., 2020; Ullberg et al., 2021).

Long-chain PFAS are usually removed better than short-chain PFAS. Over time, concentrations of short-chain PFAS in the effluent may become even higher than their influent concentrations, due to desorption and displacement by other chemicals (Belkouteb et al., 2020; C. J. Liu et al., 2019). For the same perfluoroalkyl chain length, breakthrough for different head-groups typically occurs in the order: ~COO^- < ~SO_3^- < ~$CH_2CH_2SO_3^-$ (FTSA) < ~SO_2NH^- (perfluoroalkyl sulfonamides; FASA) (McCleaf et al., 2017; Rodowa et al., 2020; X. Xiao et al., 2017).

GAC needs to be regenerated or replaced once a certain level of breakthrough occurs that depends on the treatment goals (Belkouteb et al., 2020). The costs of regeneration or replacement tend to dominate the total treatment costs, and regeneration uses high amounts of solvents or energy (McNamara et al., 2017; Siriwardena et al., 2021). When GAC is not regenerated, the disposal of the PFAS-laden GAC poses an issue. Moreover, while virgin GAC can be produced from renewable materials, such as coconut shells, it is also often produced from coal.

Ion exchange

PFAS removal by anion exchange (AIX) works by reversibly exchanging ionic PFAS with negatively charged counter ions from the surface of a resin (Dixit et al., 2021). AIX resins specifically designed for the removal of PFAS have become popular in recent years. Typically, PFSA are removed better than PFCA, and long-chain PFAS better than short-chain PFAS. PFAS removal with AIX is generally higher than with GAC, particularly for short-chain compounds (Dixit et al., 2021; McCleaf et al., 2017; Woodard et al., 2017). While the media cost is higher for AIX resins than for GAC, the overall treatment costs can be lower for AIX, because of its higher PFAS adsorption capacity (Murray et al., 2021).

Similar to GAC, AIX resins need to be regenerated or replaced when treatment goals are no longer met. Matrix compounds such as sulfates, phosphates, nitrates and organic compounds may compete with PFAS for exchange sites, and thus cause higher resin change-out frequencies (Dixit et al., 2021). PFAS-loaded AIX resins can be regenerated with organic solvents, inorganic salt solutions, or combinations of these two, creating a PFAS-laden brine that requires destructive treatment. The organic solvent is sometimes recovered from the regenerant solution by distillation, resulting in an even more concentrated still-bottom. Conversely, non-regenerable resins are disposed of by incineration or landfilling and then replaced with virgin resins.

Membrane filtration

High pressure membrane processes such as nanofiltration (NF) and reverse osmosis (RO) can effectively remove both short- and long-chain PFAS from water (Lee et al., 2022). In NF and RO, part of the feed stream passes through the membrane pores, becoming a PFAS-depleted permeate. The remaining water contains all solutes that were rejected by the membrane, and is referred to as the retentate or concentrate. Membrane systems aim to maximize the permeate productivity as well as the recovery, i.e. the fraction of permeate produced from the feed water. Recoveries are typically limited to at most 90% (Tow et al., 2021).

The predominant mechanism of PFAS separation in membrane processes is size-exclusion. Removal of short-chain PFAS can exceed 90% (Appleman et al., 2013), but is still generally slightly lower than that of long-chain PFAS due to their smaller size. RO membranes have smaller pore sizes (< 1 nm) than NF membranes (1-10 nm), resulting in a higher PFAS rejection. Locally increased PFAS concentrations at the membrane surface can cause a high concentration gradient over the membrane, leading to diffusive PFAS transport through the membrane. This phenomenon is known as concentration polarization. Concentration polarization is often more severe for NF membranes, due to their higher permeate flux, and thus contributes to the lower PFAS rejection of NF membranes (Lee et al., 2022; Soriano et al., 2017).

Effects of the water matrix on the efficiency of membrane filtration are three-fold (Lee et al., 2022). Firstly, the presence of cations may neutralize PFAS' negative charge, leading to lower electrostatic repulsion by negatively charged membrane surfaces and thus lower rejection. Conversely,

cations may also increase the rejection by size exclusion when they form large complexes with PFAS. Finally, the formation of complexes or the presence of co-solutes may lead to pore blocking and membrane fouling, which can reduce the membranes' life span and increase the energy demand. Typically, extensive pre-treatment of heavy matrix waters is required to prevent excessive levels of membrane fouling (Baudequin et al., 2011; X. Liu et al., 2023).

Foam fractionation

Foam fractionation exploits the surface-active properties of many non-polymeric PFAS by adsorbing them on rising air bubbles (Buckley et al., 2021). If the surface tension is reduced sufficiently, which sometimes requires dosing of additional surfactants, these bubbles will form a PFAS-enriched foam at the air/water interface. Collecting and collapsing this foam generates a PFAS-rich foamate and a PFAS-depleted liquid pool or effluent. Compared to the other PFAS removal technologies, foam fractionation has a low use of consumables and is relatively unaffected by heavy matrices, so it can be applied without extensive pre-treatment (Burns et al., 2021; McCleaf et al., 2021). However, foam fractionation is only capable of removing surface-active compounds, so it is less effective for the separation of short-chain or non-amphiphilic PFAS, and the effluent PFAS concentrations are not as low as after membrane treatment.

Foam fractionation can achieve higher water recoveries than membrane filtration, i.e. foamate volumes are typically lower than membrane concentrate volumes. These high recoveries can be reached by adopting multi-stage foam fractionation, in which the foam from the first stage is subjected to foam fractionation again to reduce its volume (Burns et al., 2021; Y. Wang et al., 2023). The foam fraction is the percentage of influent volume recovered as foam. Most often, up to three stages are included to reduce the foam fractions sufficiently. However, low ($\leq$ 2%) foam fractions have been achieved already in the first stage as well (McCleaf et al., 2023; Meng et al., 2018; Vo et al., 2023).

An advantage of foam fractionation is its suitability for treating water matrices with high levels of co-contaminants. In fact, PFAS removal with foam fractionation is generally higher in the presence of cations and at higher ionic strength (Buckley et al., 2022; Y. Wang et al., 2023), because the PFAS adsorption constants to the air/water interface increase in the presence of electrolytes (Brusseau & Van Glubt, 2019). However, high concentrations of

Na, K, Mg or Ca ions may also suppress foam formation, and thereby prevent effective PFAS removal (Buckley et al., 2022).

While foam fractionation is not suitable for the removal of short-chain PFAS, recent papers show promising results when cationic surfactants are used as additives (Buckley et al., 2023; McCleaf et al., 2023; Vo et al., 2023). The addition of a cationic surfactant facilitated almost complete removal of the short-chain perfluorobutanoic acid (PFBA) from artificial PFAS solutions with low background salt concentrations (Buckley et al., 2023). However, cationic surfactant addition could not facilitate PFBA removal from saline landfill leachate or NF concentrate, although it did increase the removal efficiencies for other short-chain PFAS (McCleaf et al., 2023; Vo et al., 2023).

Phytoremediation

In phytoremediation, plants are used to remove PFAS from contaminated soil or water (Mayakaduwage et al., 2022). These plants must then be harvested and incinerated at sufficiently high temperatures to destroy the PFAS. For water treatment, constructed wetlands are the most common implementations of phytoremediation, which remove PFAS by plant uptake and adsorption to soil. Riparian plants with fibrous rooting systems can accumulate PFOA from water (Mudumbi et al., 2014) and up to 82% PFOA and 95% PFOS removal from water was achieved in a pilot-scale constructed wetland (Chen et al., 2012). Full-scale constructed wetlands have been used successfully to remove PFAS from landfill leachate (Yin et al., 2017).

Unlike the other removal technologies, phytoremediation works better for short-chain than long-chain PFAS (Mayakaduwage et al., 2022; Mei et al., 2021). Short-chain PFAS are more polar and mobile, and thus translocate through the plant body more easily, leading to higher removal efficiencies. Accordingly, combining phytoremediation with another removal technology in a treatment train may result in comprehensive removal of both long- and short-chain PFAS.

Electrocoagulation

In electrocoagulation, adsorbents are generated *in-situ* by the dissolution of a sacrificial anode in an electrochemical system (Moussa et al., 2017). Common anode materials include zinc, iron and aluminium, and their dissolution results in the formation of metal cations and metal hydroxides. The metal cations can act as coagulants, i.e. they decrease the zeta potential

of suspended particles, leading to their flocculation and precipitation. Metal hydroxides are poorly soluble and thus precipitate readily by themselves. Pollutants such as PFAS adsorb to the precipitates, and the resulting flocs are subsequently removed by filtration, sedimentation or flotation (Lin et al., 2015).

The removal of PFAS has been tested on laboratory scale, mostly using artificial PFAS solutions (Bao et al., 2020; Lin et al., 2015; Y. Liu et al., 2018; Yang et al., 2016). Electrocoagulation could also remove PFAS from landfill leachate (C. Zhang et al., 2014) and groundwater (Bao et al., 2020; Y. Liu et al., 2018), but typically with lower efficiencies, due to the presence of co-contaminants. A side-reaction in electrocoagulation is the evolution of hydrogen gas on the cathode, which leads to the formation of bubbles. Therefore, part of the observed PFAS removal in electrocoagulation may be due to PFAS adsorption to bubbles rather than metal flocs. Shi et al. confirmed that PFAS distribution into foam can play a role in the removal mechanism with electrocoagulation (Shi et al., 2021).

Comparison of removal technologies

Which removal technology is the best choice for a specific scenario depends on the treatment requirements, the water matrix and the energy costs. Figure 1 summarizes the four most mature removal technologies in terms of their capability of removing short-chain PFAS, their energy use, their sensitivity to matrix compounds (i.e. the extent of pretreatment that is required) and their ability to remove other contaminants (e.g. DOC, salts or other micropollutants) together with PFAS. For each parameter, the treatments were ranked from ‘worst’ to ‘best’ from a practical viewpoint, based on the information as summarized earlier in this section.

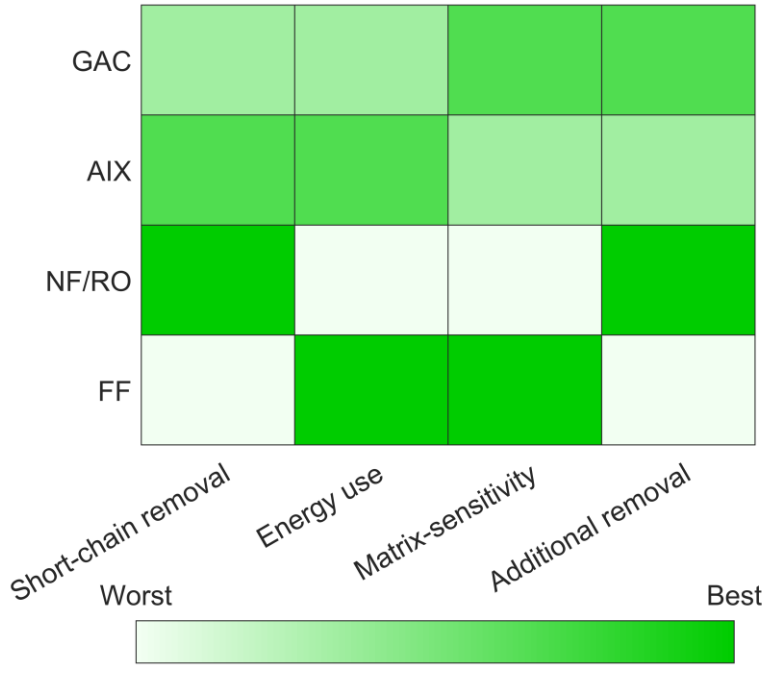

Figure 1: Qualitative comparison of different removal technologies for PFAS in terms of short-chain removal capacity, energy use (Boyer et al., 2021; Burns et al., 2022; Emery et al., 2019; G. Li et al., 2022; C. J. Liu et al., 2021), matrix sensitivity and removal of additional contaminants. GAC = granular activated carbon, AIX = anion exchange, NF/RO = nanofiltration/reverse osmosis, FF = foam fractionation. Energy use for GAC and AIX included the production and transport of sorbent. If only the electrical energy used on site is considered, the energy use of FF is higher than that of GAC and AIX.

Obviously, some of these parameters are interconnected and the exact ranking may be case-dependent. Nonetheless, the overview in Figure 1 may be helpful when determining which removal technology is most appropriate. For example, heavy-matrix water that is only contaminated with long-chain PFAS is probably best treated with foam fractionation, whereas a membrane process is most suitable when low short-chain PFAS concentrations in the effluent are required.

1.2.2 Degradation technologies

Degradation technologies aim to destroy PFAS, rather than merely remove them. A plethora of degradation technologies for PFAS in water exists, but many have only been tested on laboratory scale with artificial PFAS solutions in clean water. Here, only physicochemical degradation

technologies that have been tested with real water matrices at pilot or full scale will be discussed, and examples of up-scaled case studies are given. For completeness, a brief discussion of biological treatment is included as well, even though biological PFAS degradation in real water matrices has not yet been achieved successfully.

For degradation technologies, the terminology of 'mineralization', 'defluorination' and 'degradation' is important. Generally, mineralization of a PFAS is taken to mean complete defluorination, regardless of whether the carbon is fully oxidized to CO_2 (Horst et al., 2020). Defluorination of a PFAS can also be incomplete, in which case the product molecules are often still PFAS. Degradation is the transformation of a PFAS into another molecule, but does not have to include defluorination. For example, the degradation of precursors into PFAA does not necessarily involve defluorination.

Thermal degradation

The state-of-the art method for GAC regeneration is heating to high temperatures (typically 650-850 °C) in the presence of inert gases or steam (F. Xiao et al., 2020). Combustion of GAC or AIX resins is a common method for disposal of non-reusable PFAS-laden sorbents. Although these methods are widely used, the fate of PFAS in pyrolysis, combustion or thermal reactivation processes is often unknown (J. Wang et al., 2022). Long-chain PFAS are degraded and defluorinated less efficiently at the same temperatures than short-chain PFAS, with mineralization of PFOS and PFOA being found to occur at temperatures of ≥ 700-800 °C (Sonmez Baghirzade et al., 2021; F. Xiao et al., 2020).

The regeneration yield, i.e. the ratio of adsorption capacity of regenerated GAC versus virgin GAC, is often below 100% (Sonmez Baghirzade et al., 2021). Incomplete thermal mineralization may contribute to a lower regeneration yield, since it can cause blocked pores or adsorption sites to remain inaccessible. Regeneration yields in terms of GAC mass or surface area, rather than adsorption capacity, are often also below 100%, but the use of reactivation agents such as air or CO_2 can increase the regenerated surface area. Practically, regenerated GAC always needs to be supplemented with a portion of virgin GAC, to make up for the loss of yield.

Plasma treatment

Plasma treatment uses electrical discharge to ionize a gas, leading to the formation of reactive species such as free electrons, free radicals, ions and

photons (Barjasteh et al., 2021; Palma et al., 2022). Broadly, a distinction can be made between thermal plasma and non-thermal plasma. Thermal plasma forms when high amounts of energy are dissipated, such that the electrons and gas molecules reach thermal equilibrium, i.e. they have the same temperature. In non-thermal plasma, a lower pressure prevents the formation of thermal equilibrium, and the temperature of the electrons is higher than that of the bulk gas molecules. In water treatment applications, non-thermal plasma is mostly used, and different geometries for contacting the plasma with water exist. Since many PFAS accumulate at gas/liquid interfaces, the high reactivity of plasma can be exploited very efficiently for the degradation of PFAS in water (Palma et al., 2022).

During plasma treatment, the treated water acidifies, and PFAS degradation is inhibited when the pH gets too low. Similarly, high water conductivity and high nitrate or DOC concentrations can prevent effective treatment. Nevertheless, plasma treatment has been used successfully for defluorination of PFAS in landfill leachate with high concentrations of co-contaminants (Singh et al., 2021). In this study, a layer of foam formed on the water surface, where plasma was generated to degrade the accumulated PFAS. Many studies observe the formation of short-chain PFAS as byproducts of long-chain degradation, so complete PFAS mineralization is not always achieved (Palma et al., 2022).

Plasma treatment has been applied successfully on pilot-scale for the treatment of PFAS in investigation-derived wastewater from an AFFF-impacted site (Singh et al., 2019). Another pilot-scale study used plasma treatment for PFAS degradation in AFFF-contaminated groundwater (Nau-Hix et al., 2021). In both studies, removal efficiencies were highest (up to 100%) for long-chain PFAA, but PFBA was formed rather than degraded (Nau-Hix et al., 2021; Singh et al., 2019). PFBA is a degradation product of long-chain PFAA and precursors, and has a lower tendency to accumulate at bubble-liquid interfaces, so it is not degraded as efficiently as long-chain PFAA. The addition of a cationic surfactant significantly improved the degradation of short-chain PFAA, including PFBA (Nau-Hix et al., 2021).

Supercritical water oxidation

Supercritical water is water at temperatures and pressures above the critical point of 374 °C and 22.1 MPa (Savage, 1999). Supercritical water has a lower viscosity, lower dielectric constant and lower dissociation constant than ambient liquid water, and these properties can be tuned as preferred by

varying the pressure and temperature. Gases and organic compounds are much more soluble in supercritical water, and it contains high numbers of free radicals, making it a very suitable medium for oxidation reactions (J. Li et al., 2022). Salts, on the other hand, are less soluble and precipitate out, which can cause reactor plugging or corrosion.

PFAS degradation with supercritical water oxidation can reach up to 100%, particularly when additives such as air or iron are used (J. Li et al., 2022). While the degradation of long-chain PFAS may lead to the formation of short-chain PFAA, the recovery of fluoride is typically high, which indicates full mineralization. It should be noted that while supercritical water oxidation has been tested with AFFF dilutions, no studies on the treatment of real water matrices were found in the open literature, and the PFAS concentrations used in most existing studies were very high (µM range).

A pilot-scale study treating diluted AFFF found a total PFAS degradation of ≥ 99.999%, with a fluoride recovery of 63% (McDonough et al., 2022). Short-chain PFAA were degraded less efficiently than long-chain PFAA, but still with efficiencies exceeding 90%. A comparison between three commercially available continuous SCWO systems treating diluted AFFF found > 99% ΣPFAS degradation for each system (Krause et al., 2022). Fluoride in the effluent was only analysed for one system, which showed a fluoride recovery of > 300%, indicating the presence of unidentified PFAS in the influent.

Sonochemical degradation

Sonochemical treatment degrades PFAS molecules by applying ultrasonic waves to water, leading to the formation of cavitation bubbles (Cao et al., 2020). The collapse of these bubbles generates high local temperatures and pressures, leading to the degradation of PFAS molecules that accumulated at the bubble interface. Sonolysis of PFAS is hypothesized to occur by a combination of pyrolysis and radical oxidation (Sidnell et al., 2022). For most PFAS, degradation rates increase for higher power densities (W per volume) and are optimal at ultrasonic frequencies of 300-1000 kHz. Short-chain PFAA degrade fastest at higher frequencies than long-chain PFAA. Formation of short-chain PFAA is sometimes observed initially, but these degrade after continued treatment.

PFAS sonolysis is faster at higher concentrations and typically follows first-order kinetics (Cao et al., 2020; Sidnell et al., 2022). PFCA degrade faster than PFSA, and long-chain compounds faster than short-chain due to

the latter's lower affinity for bubble surfaces. Degradation efficiencies can be improved by using argon as dissolved gas instead of air, and by keeping the temperatures low. Additionally, additives such as sulfate, periodate, permanganate, bromide, perchlorate, nitrate and cationic surfactants can speed up the PFAS degradation and stimulate the oxidative degradation mechanism.

Sonochemical treatment has been shown to successfully degrade PFOS and PFOA in groundwater (Cheng et al., 2008, 2010). However, compared to MilliQ water, the high volatile organic carbon (VOC) content of groundwater from beneath a landfill decreased the sonolysis rate by up to 61% (Cheng et al., 2008). In groundwater with lower VOC concentrations, the presence of inorganic salts still decreased the degradation rate by up to 30% (Cheng et al., 2010). Pilot-scale sonochemical treatment of AFFF-impacted groundwater resulted in 93 – 100% ΣPFAS removal (Kulkarni et al., 2022). In another study, two types of diluted AFFF were treated for 13 h in a large-scale (91 L) sonochemical reactor, obtaining approximately 50% total defluorination for both AFFF formulations (Gole et al., 2018).

Photodegradation

Photodegradation encompasses different treatment processes that all use UV irradiation to facilitate PFAS degradation (Banayan Esfahani et al., 2022). Direct photolysis cannot effectively degrade PFAA, so photodegradation uses chemical mediators or catalysts to stimulate the PFAS degradation. Broadly speaking, photodegradation can be divided into photo-oxidation and photo-reduction, which are carried out by oxidising agents, such as $SO_4^{\cdot-}$, and by hydrated electrons, respectively.

Photo-oxidation uses oxidants, such as persulfate, ferric iron, carbonate and periodate (Banayan Esfahani et al., 2022). Alternatively, a photocatalyst may be used to promote the oxidative decomposition of PFAS. Heterogeneous catalysts include semiconductors, such as TiO_2, In_2O_3 and Ga_2O_3, but there is also a rapid development of novel engineered nanomaterials. Photoreduction uses a heterogeneous catalyst or additives such as sulfite, iodide, or ferrocyanide to generate hydrated electrons. Of all these, the UV/sulfite process is most promising for the mineralization of a wide range of PFAS.

Photo-oxidation is more effective at low pH and high dissolved oxygen, which is the opposite for photoreduction (Banayan Esfahani et al., 2022). Both processes may generate short-chain PFAA as byproducts of long-chain

PFAS degradation. Some studies report more efficient degradation of long-chain than short-chain PFAS, but this effect is not always found. VOC, dissolved organic matter (DOM), chloride, bicarbonate, sulfate, nitrate and ionic strength can prohibit effective photodegradation, by scavenging radicals, reducing light penetration and hindering the complexation between PFAS and mediators. Conversely, DOM, bicarbonate and ionic strength may also promote photodegradation, by acting as photosensitizer and generating reactive photo-induced species.

Photo-oxidation of various PFCA in spiked tap-water (C_0 > µg L^{-1}) was tested with a commercially available pilot-scale (16 L) photocatalytic reactor (Qanbarzadeh et al., 2021). Almost complete degradation of all PFCA was obtained after 20 min irradiation time, but fluoride recoveries ranged between 23 and 36%. Moreover, the addition of Cl^- and SO_4^{2-} at environmentally relevant concentrations diminished the degradation efficiency significantly. Another pilot-scale study reported > 90% ΣPFAS degradation in NF concentrate from AFFF-impacted groundwater after 8 h of treatment, using a UV/sulfite photoreduction process (C. J. Liu et al., 2021).

Electrochemical oxidation

In electrochemical oxidation (EO), PFAS are oxidized at the anode of an electrochemical cell. Boron-doped diamond (BDD) is often the anode material of choice, because of its high overpotential for the oxygen-evolution reaction, high stability and long service life (Radjenovic et al., 2020). However, BDD is expensive and the mining of Nb, a popular substrate for the diamond coating, comes with ethical concerns. For these reasons, alternatives, such as mixed metal oxide and ceramic Magnéli phase Ti_4O_7 anodes, have also been evaluated extensively for their PFAS degradation potential.

The initial direct electron transfer from PFAS to anode is generally accepted to be the rate-limiting step in EO. Therefore, promoting the mass transfer of PFAS to the electrode surface is crucial to increase reaction rates. Promising results have been obtained with porous flow-through electrode materials (Duinslaeger & Radjenovic, 2022; Sharma et al., 2022; Shi et al., 2019), so these anodes should be tested further with real matrices. Most research with real matrices until now has been done in parallel-plate or perforated electrode flow-through cells.

The presence of DOC, radical scavengers and other matrix compounds at high concentrations decreases PFAS oxidation rates (Barisci & Suri, 2020; Pierpaoli et al., 2021). Short-chain PFAA degrade more slowly than long-chain PFAS, and can form as degradation products of long-chain PFAS. Additionally, the formation of toxic oxyhalide anions or halogenated organic byproducts is a serious concern in EO (Radjenovic & Sedlak, 2015). Nevertheless, EO has significant advantages in terms of scalability, process safety, ease of automation, requirement of chemicals, compactness and flexibility, so it is one of the most extensively researched destructive technologies for PFAS.

EO has been used successfully for PFAS degradation in groundwater (Schaefer et al., 2018, 2019; Trautmann et al., 2015), landfill leachate (Maldonado et al., 2021; Pierpaoli et al., 2021; Urtiaga et al., 2022), industrial water (Nienhauser et al., 2022; Uwayezu et al., 2021), NF concentrate (Soriano et al., 2017) and AIX still-bottoms (Liang et al., 2018, 2022). Scale-up of EO is hampered by mass transfer limitations and the high cost of electrodes (Sharma et al., 2022), but the suitability of EO for treating concentrated waste streams has been demonstrated on pilot-scale.

Liang et al. used an on-site EO system with Ti_4O_7 anodes to treat still-bottom from AIX treatment of a contaminated groundwater (Liang et al., 2022). Treatment of 19 L still-bottom for ~80 hours resulted in long-chain PFAA degradation of 59-94% and short-chain PFAA degradation of 2.5-20%. Soriano et al. treated NF concentrate from industrial water with high levels of perfluorohexanoic acid (PFHxA) in 1 L batch EO experiments with BDD electrodes (Soriano et al., 2017). After 90 min, they obtained 91-98% PFHxA degradation. For both studies, the initial PFAS concentrations in the concentrated waste were extremely high, i.e. up to 10 - 1000 mg L^{-1}.

Biological degradation

In biological degradation, the metabolism of microorganisms is exploited for the degradation of PFAS. Generally, financial and energy costs are lower for biological treatment than for physicochemical degradation processes (Ji et al., 2020). Additionally, the formation of harmful byproducts is less of a concern than in energy-intensive degradation methods. Because of the presence of incompletely fluorinated carbon atoms in polyfluorinated substances, they are easier to degrade than perfluorinated substances. (Z. Zhang et al., 2022). Biological degradation of PFAA is particularly

challenging, because the high number of strong carbon-fluorine bonds shields the perfluorocarbon tail from degradation (Shahsavari et al., 2021).

To date, only very few bacterial strains capable of mineralizing PFAA have been found. Aerobic biodegradation of saturated PFAA has been reported, but either without investigating degradation products, or with a PFCA as terminal degradation product (Chetverikov et al., 2017; Kwon et al., 2014; Yi et al., 2016). A comment on the publication by Kwon et al. identified these issues and questioned the conclusion that PFOS was biodegraded (Mejia Avendaño et al., 2015).

Huang and coworkers have reported the most promising results on biodegradation of PFAA (Huang et al., 2022; Huang & Jaffé, 2019; Ruiz-Urigüen et al., 2022). In 2019, an enrichment culture of *Acidimicrobium sp*. strain A6 (A6) was found capable of anaerobically defluorinating PFOA and PFOS while reducing ferric iron and oxidizing ammonia or hydrogen (Huang & Jaffé, 2019). They achieved up to 60% removal of PFOS and PFOA within 100 days, and observed formation of fluoride, acetate and shorter-chain perfluorinated acids. Autoclaved replicates did not show PFAA degradation or fluoride formation, confirming the biological origin of the degradation. The recovery of fluoride indicated 37% mineralization of PFOA after 100 days, while the remaining fluorine was still contained in shorter chain PFAA.

More recently, it was demonstrated that A6 could also degrade PFOA in contaminated biosolids from an industrial wastewater treatment plant, still using ferric iron as electron acceptor (Huang et al., 2022). A6 could also defluorinate PFAS in a microbial electrolysis cell, using the anode as electron acceptor (Ruiz-Urigüen et al., 2022). This reactor eliminated the need of dosing high quantities of ferric iron. Optimization and scale-up are required to assess if bioelectrochemical reactors are suitable for degrading PFAA in contaminated water. Until now, the degradation capacity of A6 has only been tested using relatively pure cultures, on lab scale, under well-controlled conditions and at high PFAA concentrations of up to 100 mg L^{-1}. Nonetheless, scale-up of biodegradation by A6 bacteria to environmentally relevant remediation applications may be possible.

In addition to bacteria, fungi are exceptionally good at breaking down complex products (Harms et al., 2011). However, successful fungal mineralization of PFAA has never been reported in academic literature. Wood-decaying fungal strains were shown to degrade 6:2 fluorotelomer alcohol (6:2 FTOH), with 5:3 fluorotelomer carboxylic acid (5:3 FTCA) as

primary metabolite (Merino et al., 2018; Tseng et al., 2014). While not a PFAA, 5:3 FTCA is still considered a PFAS, and no complete mineralization was achieved.

1.2.3 Comparison of degradation technologies

Energy use of degradation technologies for liquid waste

The energy use is the most important variable when comparing the different degradation technologies. Unfortunately, estimations of energy use are rarely reported in peer-reviewed studies describing PFAS degradation technologies. Moreover, there is no standardized way of reporting energy requirements. In most literature, it has become conventional to report energy use as the electrical energy required for one order of magnitude degradation (EE/O, kWh m^{-3}). However, energy use is sometimes also reported as kWh m^{-3}, without any normalization to the amount of degradation. Another metric for energy use is as kWh per mass of PFAS destroyed, but this has a strong bias towards high-concentration matrices.

Another aspect that complicates direct comparisons between degradation technologies is that not all papers analyse the same PFAS. Most often, energy metrics are based on the degradation of PFOS and/or PFOA. However, when it is instead calculated based on the degradation of ΣPFAS or short-chain PFAA, higher energy requirements are found. Finally, the matrix plays a role in the energy demand, and stronger matrices will typically result in a higher energy use per order of degradation.

Table 2 gives an overview of the EE/O ranges reported for the aforementioned degradation technologies for PFAS in aqueous matrices. When possible, only studies treating real water matrices, preferably at pilot-scale were included, but such studies were not available for all technologies. It is important to realize that, despite its name, EE/O is not always directly proportional to order of magnitude degradation, so calculated values depend on the degradation range that was achieved in each study.

Table 2: Electrical energy required per order of magnitude degradation (EE/O; kWh m^{-3}) of PFAS for different technologies. For sources indicated with *, EE/O values were calculated based on data from the paper, instead of taken directly from the text. IDW = investigation derived waste, GW = groundwater, NF = nanofiltration, WW = wastewater.

Technology	**Source**	**EE/O (kWh m^{-3})**	**Compound**	**Water type**	**Initial conc. (µg L^{-1})**
Plasma degradation	(Singh et al., 2019)	1.7-56	Sum PFOS + PFOA	IDW	28-737
	(Nau-Hix et al., 2021)	4.6-9.2	Sum PFOS + PFOA	AFFF-impacted GW	1.7-4.6
	(Singh et al., 2021)	20-36	Sum PFOS + PFOA	Landfill leachate	2.7
	(Singh et al., 2020)	380-830	Sum PFOS + PFOA	AIX still-bottom	151,000-253,000
Supercritical water oxidation	(McDonough et al., 2022)*	310-320	PFOA	Diluted AFFF	72-83
	(Pinkard et al., 2021)*	1600	PFOS	Stock solution	30,000
Sono-chemical degradation	(Rodriguez-Freire et al., 2016)*	15-83	Total organic fluorine	Diluted AFFF	28,500-70,300
	(Wood et al., 2020)*	530	PFOS	Stock solution	9420
	(Kulkarni et al., 2022)	230-1400	PFOA	AFFF-impacted GW	39.5
		1300-3500	PFOS		70.4
Photo-degradation	(Qanbarzadeh et al., 2021)	51	PFOA	Spiked tap water	53,820
		85	PFBA		27,560
	(C. J. Liu et al., 2021)	64	PFOA	NF conc. from GW	0.02
		71	PFOS		0.19
Electro-chemical oxidation	(Soriano et al., 2017)	15-21	PFHxA	NF conc. from industrial WW	774,000-870,000
	(Maldonado et al., 2021)*	18	Sum PFOS + PFOA	Landfill leachate	3.9
	(Gomez-Ruiz et al., 2017)*	90-99	ΣPFAS	Industrial WW	1652
	(Pierpaoli et al., 2021)	130-160	PFOA	Landfill leachate	1.35
		180	PFOS		3.28
	(Schaefer et al., 2018)*	180-230	PFOA	AFFF-impacted GW	15-58
		95-610	PFOS		22-300
		350-380	PFHpA		2.6-12

Energy use of thermal PFAS degradation in spent GAC

For the production of GAC or its thermal regeneration in furnaces, the energy use is not limited to electrical energy. Instead, it also includes the energy required for heating the reactor, obtained by burning (fossil) fuels. Therefore, its climatic impact is often reported as kg CO_2-eqv. emitted per kg GAC, instead of kWh per kg GAC. Table 3 presents an overview of the estimated climatic impact of GAC regeneration. These calculations were done under the assumptions that:

i. the GAC is regenerated after treating 20,000 bed volumes, corresponding to approximately 10% breakthrough of PFOA for treatment of contaminated groundwater (C. J. Liu et al., 2019)
ii. the density of the GAC is 0.54 kg L^{-1} (C. J. Liu et al., 2019)
iii. the GAC is regenerated three times, after which all GAC is replaced by virgin GAC (Contactica et al., 2018)
iv. the regeneration yield is 90%, i.e. 10% supplementation of virgin GAC is required after each regeneration cycle (Bayer et al., 2005; Contactica et al., 2018)
v. The conversion factor from kg CO_2-eqv. to kWh equals 0.09 kg CO_2-eqv./kWh (Svenska MiljöEmissionsData (SMED), 2021)

Table 3: Rough estimations of the climatic impacts associated with GAC regeneration

Source	**kg CO_2 / kg virgin GAC**	**kg CO_2 / kg regenerated GAC**	**kg CO_2 / m^3 water**	**kWh / m^3 water**
(Bayer et al., 2005)	11	1.3	0.12	1.3
(Contactica et al., 2018)	13	2.6	0.16	1.8
(Emery et al., 2019)	N/A, based on kg CO_2 m^{-3} data directly (for drinking water)		0.33-2.7	3.7-30

Byproduct formation

In addition to the energy requirements, the formation of byproducts is an important factor. In many degradation technologies, PFAS are converted into shorter-chain PFAA prior to complete mineralization. Additionally, the formation of oxyhalide anions such as chlorate, perchlorate and bromate may pose an issue in advanced oxidation processes. Perchlorate can be removed with post-treatment steps such as biological sand-filtration (Schaefer et al.,

2017), but preventing its formation should be preferred. Table 4 summarizes the byproduct formation potential of the different treatment technologies.

Table 4: Overview of byproduct formation risk for each degradation technology

Technology	Short-chain PFAA	Oxyhalide anions	Sources
Thermal GAC regeneration	Possibly, more research needed	No	(Sonmez Baghirzade et al., 2021)
Plasma degradation	Yes	Yes	(Palma et al., 2022; Singh et al., 2021)
Supercritical water oxidation	Yes, but typically very low	Unlikely	(J. Li et al., 2022; McDonough et al., 2022)
Sonochemical degradation	Yes, when using oxidative additives	No	(Kulkarni et al., 2022; Sidnell et al., 2022)
Photo-degradation	Yes	Yes, in photo-oxidation	(Qanbarzadeh et al., 2021; Qian et al., 2016)
Electrochemical oxidation	Yes	Yes	(Maldonado et al., 2021; Radjenovic et al., 2020)

A final consideration is the technology readiness level and process safety of each degradation technology. While plasma degradation has the lowest energy use, scale-up and process safety may be an issue (Aggelopoulos, 2022). Supercritical water oxidation has not yet been tested on strong matrices, and has high energy requirements. Sonochemical- and photodegradation can be energy-efficient, but particularly photodegradation is hampered by matrix effects. Electrochemical oxidation has been applied successfully to a wide range of matrices at comparatively low EE/O, making it one of the most promising technologies, but can lead to significant byproduct formation.

1.2.4 Treatment train approaches

Combining two technologies in a treatment train is an effective PFAS-remediation strategy (Lu et al., 2020). Most commonly, a removal technology is coupled to a degradation technology. Combining a relatively low-energy removal technology with an energy-intensive degradation

technology for the PFAS-rich waste harnesses efficiency from the degradation step. This strategy is often referred to as 'concentrate-and-destroy'. Alternatively, combinations of two removal technologies to achieve high PFAS removal levels or to concentrate the waste stream even further have also been implemented.

Various examples of combinations of removal technologies exist. Foam fractionation has been combined with AIX polishing of the effluent (Burns et al., 2021). NF concentrate has been treated further with foam fractionation (McCleaf et al., 2023), GAC and AIX (Franke et al., 2021). Electrocoagulation has been integrated with foam fractionation (Shi et al., 2021), as well as followed by reverse osmosis (Baudequin et al., 2011).

Concentrate and destroy approaches have also been investigated extensively (Lu et al., 2020), for example by applying EO on NF concentrate. The aforementioned study into the removal and degradation of PFHxA by Soriano et al. (2017) found an optimal EE/O for the electrochemical step of 15 kWh m^{-3} concentrate. Since the concentrate volume was only 20% of the original volume, the EE/O over the entire treatment train is likely to be lower. A follow-up study mimicking this same treatment with artificial water found an EE/O of 3.1 kWh m^{-3} over the entire treatment train, i.e. including the energy use of the NF (Soriano et al., 2019). A similar increase in energy efficiency was found for a NF + EO system treating contaminated groundwater (Soriano et al., 2020). Another destructive technology used on NF concentrate is UV/sulfite photoreduction, which was reported to have treatment train EE/O values of approximately 14 kWh m^{-3} for PFOS and PFOA, but > 100 kWh m^{-3} for short-chain PFSA (C. J. Liu et al., 2021).

PFAS removal from contaminated groundwater using regenerable AIX resins has been combined with destructive treatment of the concentrated regenerant still-bottom, using EO or plasma treatment. For EO, the EE/O of the electrochemical step was 0.13–0.16 kWh m^{-3} for PFOA, 0.07–0.09 kWh m^{-3} for PFOS (Liang et al., 2022) and 0.83-1.0 kWh m^{-3} for different perfluoroalkyl ether carboxylic acids (Fang et al., 2023). For plasma treatment, the EE/O of the plasma step was roughly 0.01-0.03 kWh m^{-3} for the sum of PFOS and PFOA (Singh et al., 2020). Overall, these EE/O values of concentrate and destroy approaches are lower than those reported for stand-alone degradation technologies (Table 2).

For treatment trains with AIX, various life cycle analyses have been carried out (Boyer et al., 2021; Emery et al., 2019; G. Li et al., 2022). Similar

to GAC regeneration, the climatic impact over such treatment trains is reported in kg CO_2 m^{-3}. Table 5 gives an overview of the climatic impact for treatment train systems that include AIX removal of PFAS; regenerating the AIX resin with a solution containing methanol, water and salts; recovery of the methanol via distillation and subsequent treatment of the still-bottom with the option given in the table. For the still-bottom treatment with EO, exact values depended strongly on the EE/O of the EO step (G. Li et al., 2022).

Table 5: Overview of climatic impact over entire treatment train for different options for treating still-bottoms from AIX regeneration solutions, after methanol recovery by distillation. For conversion of kg CO_2 to kWh, the aforementioned conversion factor of 0.09 kg CO_2 kWh^{-1} was used.

Source	**Treatment of still-bottom**	**Compound**	**kg CO_2 / m^3 water**	**kWh / m^3 water**
(Emery et al., 2019)	GAC → incineration	ΣPFAS	0.32-0.50	3.6-5.6
(Boyer et al., 2021)	Incineration	PFOA + PFOS	0.89	10
	GAC → incineration		0.62	7.0
(G. Li et al., 2022)	EO	PFOS	0.04	0.41
		PFBA	0.22	2.5

An important consideration in the conversion of kg CO_2 to kWh is the source of electricity. The assumed value of 0.09 kg CO_2 kWh^{-1} used in Sweden is quite low compared to the rest of the world, leading to higher kWh m^{-3} values. Nonetheless, it should be realized that using electricity-based technologies such as electrochemical degradation, photodegradation or plasma treatment *can* be done with completely renewable energy. Conversely, thermal regeneration of GAC or heat distillation of AIX regenerant still use fossil fuels. The cleaner the electrical energy, the more sustainable it will be to switch to advanced electricity-based treatments.

2. Objective and research questions

The overall goal of this PhD research was to evaluate the potential of foam fractionation and electrochemical oxidation for the treatment of PFAS-contaminated water. As outlined in Chapter 1, both these technologies have advantages in terms of energy efficiency, scalability and use of consumables. However, up-scaled studies using real matrices and thorough analysis strategies were lacking. In this project, four papers (I-IV) were published to answer the following research questions:

1) Which factors affect the removal and mass balance recovery of PFAS from contaminated water using foam fractionation and how? (I & II)
2) How do the degradation efficiency and kinetics of electrochemical oxidation for the destruction of PFAS differ between contaminated water and concentrated foam? (III)
3) How do the aforementioned treatment technologies affect the biological activity of PFAS-contaminated groundwater and landfill leachate? (III)
4) Can the concept of foam fractionation be integrated with existing water treatment technologies? (IV)

3. Methodology

All papers included in this thesis were based on pilot- or full-scale treatment systems. Paper **I** explored the potential of removing PFAS with FF in continuous mode, instead of the thus-far commonly used batch mode. Additionally, it investigated the effect of various operating parameters on the removal of PFAS. This study identified gaps in the mass balance over the FF system, so paper **II** assessed if PFAS emissions to air could explain this loss of PFAS. Paper **III** evaluated the use of EO for degrading PFAS in the foam produced with the optimized system from paper **I**, as well as in natural groundwater and landfill leachate. Finally, paper **IV** explored if the concept of foam fractionation could be integrated with existing water treatment processes. Detailed methods are given in each paper separately, but a general overview of the methodology is given below.

3.1 Water treatment technologies

3.1.1 Foam fractionation

In Paper **I**, a pilot-scale continuous FF system was used on-site to treat landfill leachate from Hovgården municipal solid waste landfill in Uppsala, Sweden. The polypropylene (PP) FF column had a diameter of 19 cm, the water surface was at 1.63 m, and the foam was extracted directly above the water surface. A peristaltic pump supplied a steady flow of leachate. Air was dispersed at the bottom of the column using four brass diffusers and the air flow was controlled with a rotameter. The residence time, foam fraction and air flow rate were varied to evaluate their effect on the PFAS removal efficiency and find optimal treatment parameters.

In paper **II**, a pilot-scale continuous FF system designed by ECT2 (Emerging Compounds Treatment Technologies, Sweden) was used to treat PFAS-contaminated industrial water at Cytiva, Uppsala, Sweden. Water continuously entered the FF column (Ø 49 cm, water level at 109 cm) at a height of 92 cm above the column bottom. Air was introduced at the bottom using a venturi blower. Unlike the leachate from paper **I**, the industrial water did not foam readily, so a constant flow of dish soap was supplied with a peristaltic pump to enhance foaming. The foam was forced to collapse under warm air at a height of approximately 60 cm above the water level, from where the liquid foamate flowed down into a collection tank. The residence time was varied between experiments, with values ranging from 13 to 60 min.

3.1.2 Electrochemical oxidation

In paper **III**, a pilot-scale EO system was used to treat groundwater and landfill leachate, as well as fractionated foam from both water types at the Hovgården landfill. The foam fractionation system from paper **I** was used to produce foam, which was subjected to EO treatment in batch tests at 50 L volume. For the EO experiments with the natural waters, batch tests were done at two different treatment volumes (50 and 150 L). The EO parallel plate flow-through cell had a total active electrode area of 4600 cm^2 for both the stainless steel cathodes and the BDD anodes, and was operated galvanostatically at a current of 231 A for 9 h. Samples for PFAS analysis were collected at 9 time points during the EO treatment, and samples for extractable organofluorine (EOF) analysis, total oxidizable precursor (TOP) assays, effect-based bioassays and general chemistry were taken before and after each run.

3.1.3 Integrated foam fractionation

Paper **IV** scoped the potential of exploiting foam formation for the removal of PFAS in existing water treatment plants. In treatment plants that use aeration as part of their processes, foam formation can occur. Influent, effluent, foam and water under the foam were sampled from ten full-scale treatment plants where foaming was observed. The treatment processes included activated sludge, moving bed biofilm reactor (MBBR), electrocoagulation and ozonation. Water types included municipal wastewater, landfill leachate, industrial process water and stormwater runoff.

One influent sample from each plant was analysed for general chemistry parameters.

3.2 Chemical analysis methods

3.2.1 Target PFAS analysis

For papers **I**, **III** and **IV**, PFAS concentrations in the water samples were measured in the laboratory at SLU, Uppsala, Sweden. This method included 29 different PFAS: PFBA, PFPeA, PFHxA, PFHpA, PFOA, PFNA, PFDA, PFUnDA, PFDoDA, PFTriDA, PFTeDA, PFBS, PFPeS, PFHxS, PFHpS, PFOS, PFNS, PFDS, NaDONA, HFPO-DA, 4:2 FTSA, 6:2 FTSA, 8:2 FTSA, Me-FOSAA, Et-FOSAA, FOSA, PFECHS, 9Cl-PF3ONS and 11Cl-PF3OUdS. For full names of these PFAS, see paper **I**, **III** or **IV.** Twenty mass-labeled internal standards (IS) were used (Wellington Laboratories, MPFAC-24ES mixture with $^{13}C_3$-HFPO-DA added individually) and quantification was based on isotope dilution analysis.

Samples were filtered through 47 mm glass fiber filters (pore size 0.7 µm, Whatman, China), spiked with 5 ng of each IS, and solid phase extracted using Oasis® WAX cartridges (6 mL, 150 mg, 30 µm, Waters, Ireland). Extracts were concentrated to 1 mL under nitrogen and analysed on a SCIEX Triple Quad 3500 UPLC-MS/MS system. Optimal ion source parameters were determined for each compound according to the standard method optimization protocol of SCIEX and are given in paper **I**, together with details on the extraction and LC methods. For compounds with branched and linear isomers, only summed concentrations were measured.

For paper **II**, the water samples were sent to ALS Scandinavia for PFAS analysis. The ALS method included a total of 32 PFAS, which included PFDoDS, Me-FOSA, Et-FOSA, Me-FOSE, Et-FOSE, FOSAA, HPFHpA and PF37DMOA (for full names, see paper **II**) in addition to all PFAS in the SLU method except NaDONA, HFPO-DA, PFECHS, 9Cl-PF3ONS and 11Cl-PF3OUdS.

3.2.2 Air analysis

In papers **II** and **III**, aerosols were collected from the air exiting the FF and EO systems, respectively, using pre-combusted quartz microfiber filters (Ø 11 cm, pore size 2.2 µm, QM-A, Whatman). These filters had been used

previously for PFAS analysis in aerosols (Casas et al., 2020). Two filters were stacked in an aluminium holder, which was placed on top of the respective air outlet. These filters were analysed in the laboratory at SLU, and the method included the same 29 PFAS as the SLU method for water samples. Each filter was spiked with 2.5 ng IS, extracted with methanol, and the extracts were analysed on the aforementioned SCIEX UPLC-MS/MS system.

Paper **II** also included whole air sampling using sorbent-impregnated polyurethane foam discs (SIPs), which is a well-established method for PFAS detection in air (Ahrens et al., 2013). Four SIPs were employed in the same room as the FF system, at different distances from the air outlet. Additionally, one SIP was placed in the staircase of the same building, to serve as reference sample for the background PFAS concentration. SIPs were cleaned thoroughly using Soxhlet extraction prior to employment, and were Soxhlet extracted in cleaned extraction thimbles with methanol after their use. Extracts were again analysed on the same SCIEX UPLC-MS/MS system for concentrations of the aforementioned 29 PFAS.

3.2.3 Total oxidizable precursor (TOP) assay

The TOP assay is a method for converting oxidizable PFAS precursors into PFAA, which can subsequently be measured using a targeted analysis method (Ateia et al., 2023). It was originally developed by Houtz and Sedlak (2012), but has since been used in many studies. A TOP assay does not give information on the structure of the precursors, but it provides a more comprehensive quantification of total PFAS levels.

TOP assays were included in papers **III** and **IV**. 125 mL aqueous samples were amended with 2 g potassium persulfate and 1.9 mL 10 N NaOH, heated in a water bath to 80-85 °C for 6 h, cooled in an ice bath and adjusted to a pH of 6-8 by adding 30% HCl (Houtz & Sedlak, 2012). Samples were subsequently extracted and analysed using the normal protocol for target PFAS analysis, and PFAS concentrations were compared to the original samples for quantification of the precursor concentrations.

3.2.4 Extractable organofluorine (EOF)

EOF analysis is another method for a more complete quantification of PFAS compared to targeted analysis, at the cost of losing all structural information (Kärrman et al., 2021). In EOF analysis, organofluorine is extracted from

water and measured using combustion ion chromatography. EOF concentrations are expressed in ng L^{-1} F and can be compared to the fluorine equivalent concentration of target PFAS, before and/or after TOP assays.

EOF analysis was included in paper **III**. 750 mL sample was filtered and extracted using the same method as for the target PFAS analysis. Extracts were concentrated to 0.2 mL under nitrogen and analysed on a Thermo-Mitsubishi combustion ion chromatograph. Aliquots of 50 µL of extracts were combusted in ceramic boats at 1100 °C, combustion gases were absorbed in MilliQ water, and 200 µL aliquots of the absorption solution were injected onto the ion chromatograph and analysed for fluoride.

3.2.5 Bioassays

Effect-based bioassays were used to evaluate the toxic potency of water before and after treatment. Two bioassays were included in paper **III**: the transthyretin (TTR) binding assay and the *A. fischeri* bioluminescence assay. The TTR-binding assay measures the competition with thyroxine (T_4), a thyroid hormone, for binding to the distributor protein TTR (Weiss et al., 2009). The bioluminescence assay measures the inhibition of bacterial metabolism, indicating the general toxicity (Hamers et al., 2001).

Extracts from the EOF analysis were used for both bioassays and dilution curves were prepared in 96-well plates. For the TTR binding assay, TTR and a fluorescent conjugate of T_4 were added to each well, and the fluorescence was measured after 5 min. For the bioluminescence assay, an *A. fischeri* suspension was added to each well, and the luminescence was measured after 30 min exposure. The fluorescence and luminescence data were fitted to dose response curves, to derive the concentration of extract causing 50% inhibition (EC_{50}) of TTR-binding and bioluminescence, respectively. These EC_{50} values were subsequently expressed in PFOS- and triclosan-equivalent concentrations, to compare toxic potency before and after treatment.

3.2.6 General chemistry

Each study included the analysis of certain general chemistry parameters. These analyses were always conducted by ALS Scandinavia. Parameters included the concentrations of total organic carbon (TOC), DOC, nitrogen and phosphorus species, metals and salts, in addition to the turbidity, chemical oxygen demand (COD), pH, alkalinity and conductivity. Which

parameters were included differed for each study, and detailed information is given in each paper.

3.3 Quality control

All glassware was burned at 400 °C overnight and rinsed with methanol prior to use. PP and high-density polyethylene sample bottles were rinsed with methanol before sample collection. In paper **I**, samples were collected in quadruplicate. In paper **II**, experiments were done in duplicate, and influent samples for PFAS analysis were collected before and after each experiment. In paper **III**, experiments were done in duplicate, as were the bioassays and target PFAS analyses. Sampling for target PFAS analysis in paper **IV** was done in triplicate, but TOP assays were done only once for each sample type. Laboratory, Milli-Q or field blanks were included in all studies, also for the air and aerosol analyses, TOP assays, EOF analyses and bioassays. Papers **I**, **III** and **IV** included the analysis of samples spiked with native PFAS, to calculate and verify analytical recoveries.

3.4 Data analysis

Each paper assessed the PFAS removal or degradation efficiency (E), defined in Equation 1, with C_{Ef} and C_{In} the effluent and influent PFAS concentrations, respectively. Data analysis and visualization was always done in Matlab™, version 2017b (paper **I**) or 2020b (papers **II**-**IV**). In papers **I** and **III**, PFAS concentrations below the limit of quantification (LOQ) were set to zero, because the contribution of these PFAS to the ΣPFAS concentration was always below 0.4% (paper **I**) or 1.6% (paper **III**), which was deemed negligible. In papers **II** and **IV**, concentrations below LOQ were set to 0, 0.5 and 1 times the LOQ to compare the effect of these assumptions. Censored statistics were not used to calculate non-detect concentrations because the independent sample sizes were too small.

$$E = \left(1 - \frac{C_{Ef}}{C_{In}}\right) \cdot 100\%$$

Equation 1

3.5 Mass balance calculations

All papers included mass balance calculations. Equation 2 gives the general equation for a mass balance over a system. Here, *V* is the volume of the system, *C* the concentration of the compound of interest in the system, *t* the time, $\sum(\varphi_{In} \cdot C_{In})$ the sum over the product of all ingoing flow rates (φ) and corresponding concentrations (*C*), $\sum(\varphi_{Out} \cdot C_{Out})$ the same for all outgoing flows, and *R* the sum of all reaction terms. For a FF system, reactive transformation of PFAS is commonly excluded, i.e. *R* = 0. Assuming PFAS concentrations in the air are zero, the influent is the only relevant ingoing flow into an FF system. The two outgoing flows are the effluent (*Ef*) and the foam. Accordingly, the mass balance over a continuous foam fractionation system can be given as per Equation 3.

$$\frac{dV \cdot C}{dt} = \sum(\varphi_{In} \cdot C_{In}) - \sum(\varphi_{Out} \cdot C_{Out}) + R \cdot V$$

Equation 2: General mass balance

$$\frac{dV \cdot C}{dt} = \varphi_{In} \cdot C_{In} - \varphi_{Ef} \cdot C_{Ef} - \varphi_{Foam} \cdot C_{Foam} \overset{Steady\ state}{=} 0$$

Equation 3: Mass balance over continuous FF

At steady state, Equation 3 equals zero, so when the mass balance (MB) closes, Equation 4 should equal 100%. If the MB < 100%, there are gaps in the mass balance, i.e. less PFAS are recovered in the effluent and foam than there were in the influent. Conversely, if the MB > 100%, more PFAS are recovered in the effluent and foam than there were in the influent, which can happen if precursors are oxidized to PFAA during FF treatment. Equation 4 was used in all four papers, and Equation 3 was used in paper **II**, since steady state conditions were not always valid**.**

$$MB\ (\%) = \frac{\varphi_{Ef} \cdot C_{Ef} + \varphi_{Foam} \cdot C_{Foam}}{\varphi_{In} \cdot C_{In}} \cdot 100\ \%$$

Equation 4

The mass balance over the EO system in paper **III** included reactive transformation of PFAS and was operated in batch mode, i.e. it was never at

steady state. Moreover, since the electrochemical cell is more similar to a plug-flow rather than an ideally mixed system, the PFAS concentration depended on place in the reactor as well as time. Accordingly, a flux balance was used to derive the differential equation describing the PFAS concentration over space (z) and time as Equation 5, with v the superficial velocity of the flow. From Equation 5, a discretized numerical model was developed in Matlab™ that coupled the electrochemical degradation kinetics of ten PFAA.

$$\frac{\delta C(t,z)}{\delta t} = -v \cdot \frac{\delta C(t,z)}{\delta z} + R$$

Equation 5

4. Results and discussion

4.1 Foam fractionation (papers **I**, **II** & **III**)

4.1.1 PFAS removal – papers **I** & **III**

Early research on FF for the removal of PFAS focused exclusively on batch-mode operation. In paper **I**, it was shown that continuous FF could remove PFAS to a similar extent as batch. The optimal contact time in the continuous FF was found to be approximately 20 min, at constant air flow as well as at constant air ratio. The air ratio is the ratio of the air flow to the influent water flow, which determines the relative bubble surface area available for PFAS adsorption. The ΣPFAS removal was further shown to decrease for a foam fraction below 10% and an airflow below 7.5 L min^{-1}.

The highest ΣPFAS removal achieved in continuous mode in paper **I** was 63%, but removal of most individual long-chain PFAS exceeded 90%. The comparatively low ΣPFAS removal could be explained by the high mean contribution of short-chain PFCA to the ΣPFAS concentrations of 46%. Short-chain PFCA are removed far less efficiently in FF than other PFAS, e.g. PFBA had a mean removal of 0%. Figure 2 shows the contribution of each PFAS class to the influent, effluent and foam, and clearly illustrates the comparatively low removal of short-chain PFCA.

Paper **III** used the continuous FF system from paper **I** with a contact time of 20 min, airflow rate of 10 L min^{-1} and foam fraction of 10% to produce foam for electrochemical treatment. Both groundwater and leachate were subjected to FF treatment. The ΣPFAS removal from groundwater was 60% (Figure 2c), which is comparable to the 63% achieved in paper **I**. Conversely, the removal from leachate was only 51% (Figure 2b). This might be partially

caused by the higher fraction of short-chain PFCA in the leachate used in paper **III** (Figure 2b) of 49%, compared to 43% for the experiment shown in Figure 2a and 40% for the groundwater (Figure 2c).

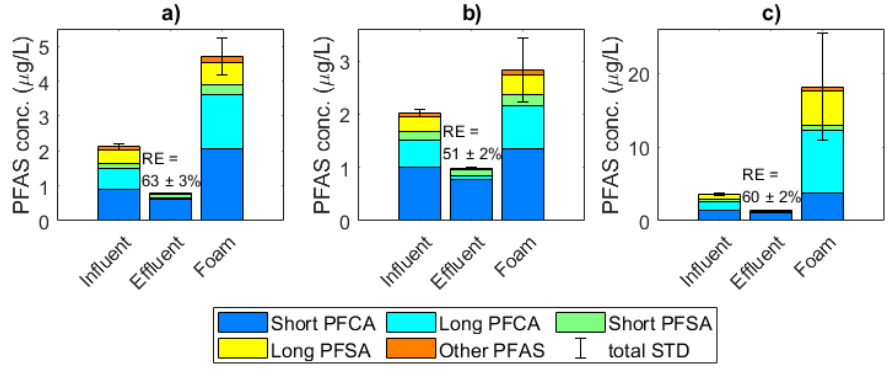

Figure 2: Average PFAS concentrations in influent, effluent and foam for a) the continuous experiment with the highest removal from leachate (paper **I**), at a contact time of 30 min, foam fraction of 20% and airflow of 13 L min^{-1}, b) the production of foam from leachate, and c) the production of foam from groundwater, both at a contact time of 20 min, foam fraction of 10% and airflow of 10 L min^{-1} (paper **III**). RE = ΣPFAS removal efficiency. Figure adapted from papers **I** and **III**, reprinted with permission from ACS.

4.1.2 PFAS removal – paper **II**

Paper **II** used a different continuous FF system to treat industrial water contaminated with AFFF. Compared to the results of papers **I** and **III**, a higher ΣPFAS removal of up to 84% was achieved with this system (Figure 3). The fraction short-chain PFCA in the influent industrial water was only 13%, which probably contributed to the higher removal efficiencies. Additionally, the dosing of surfactant may have increased the PFAS removal even further. Similar to papers **I** and **III**, the removal of short-chain PFCA was much lower than that of long-chain PFAS.

The concentration factors achieved in paper **II** were much higher than those in papers **I** and **III**. Removal efficiencies around 80% were achieved at foam fractions as low as 0.07%, i.e. concentration factors of up to 1400, compared to 10% (a factor 10) for papers **I** and **III**. A higher concentration factor means a lower volume of concentrated waste is generated that requires destructive treatment. This lower volume is beneficial from a treatment train perspective, where higher concentrations and lower volumes result in higher energy efficiencies of degradative technologies.

The much lower foam fraction of paper **II** was probably a result of the foam collection method. The system used in papers **I** and **III** collected the foam under gravity directly at the air/water interface, and the foam fraction was controlled by changing the height of the effluent tube. Conversely, the system from paper **II** used a fan and hot air to collect the foam from approximately 0.6 m above the water surface, and immediately collapse it into liquid foamate. The bubble size distribution in a foam changes with height, leading to a lower liquid fraction higher up in the column, so the foam collected in paper **II** was much drier. The foam fraction was not controlled directly, but was increased in some experiments by dosing higher concentrations of surfactant. Possibly, this dosing of surfactants in paper **II** also assisted in the generation of drier foam without compromising the PFAS removal efficiency.

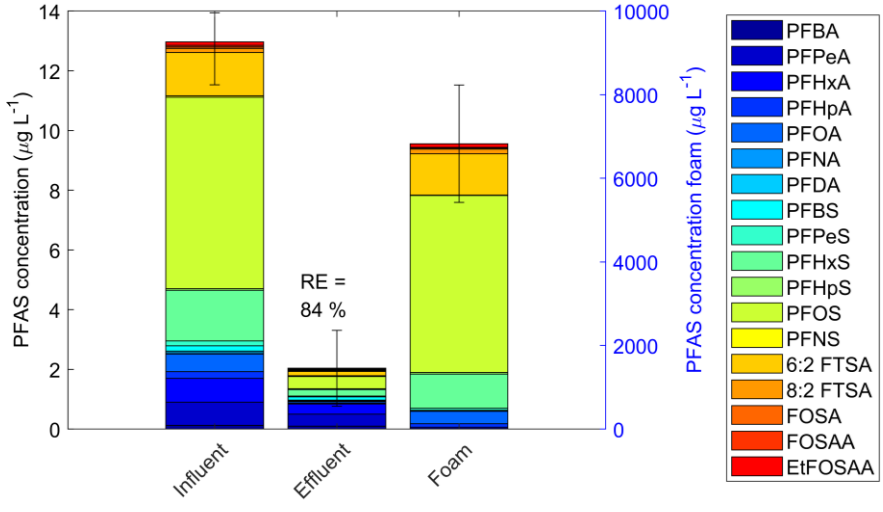

Figure 3: Average PFAS concentrations in influent, effluent and foam from industrial water at the highest removal efficiency (RE), at a contact time of 30 min and a foam fraction of 0.24%. Note that the foam concentration is given on the blue y-axis on the right. Figure adapted from paper **II**.

4.1.3 Mass balance (MB) closure – papers **I** & **III**

Over all experiments of paper **I**, the MB ranged from 66 ± 7% to 104 ± 10%, with a mean of 80 ± 12%. In paper **III**, the MB over the FF on leachate and groundwater closed for 58 ± 12% and 87 ± 35%, respectively. For individual

PFAS, the mass balance was found to close better for PFAS that were removed less efficiently, i.e. short-chain compounds. This observation lead to the hypothesis that PFAS may escape the FF system with the air, since particularly long-chain PFAS are susceptible to enrichment in aerosols (Casas et al., 2020; Ebersbach et al., 2016). Paper **II** aimed to investigate this theory further.

4.1.4 MB closure – paper **II**

In paper **II**, the mean ΣPFAS MB closure was 120 ± 40%. This high MB may have been caused by precursor degradation, leading to the formation of additional PFAA. Measurement uncertainties and flushing out PFAS that had adsorbed to the foam pipe in earlier experiments may have also contributed to high MB closures. The MB correlated negatively with turbidity, indicating that PFAS may have adsorbed to suspended solids that settled in the reactor and were lost from the MB.

While considerable PFAS emissions to air were detected, PFAS levels in the aerosol filters correlated *positively* with MB closure, i.e. higher PFAS emissions to aerosols were measured for experiments with higher MBs. Possibly, this was because higher precursor concentrations caused increased formation of PFAA in both the water and aerosol phase. Alternatively, higher suspended solids concentrations may have altered the collapse process of the foam and thereby lowered the aerosol emissions, in addition to causing a lower MB by adsorbing PFAS.

In this study, losses of PFAS to the air did not contribute significantly to the MB. However, PFAS emissions to the air were found to be a potential health risk for personnel working with the FF reactor. The measured concentrations could cause a PFAS exposure that exceeded the EFSA recommendation by a factor 15. Safety concerns may be less severe for full scale plants, since those typically vent their air to the outside. Nonetheless, the study demonstrated a need for further research into PFAS concentrations in the air around full scale FF reactors, to verify that the health of operating personnel is protected sufficiently.

4.1.5 Removal of TOP, EOF and toxicity – paper **III**

In paper **III**, the TOP assay did not result in increased PFAA concentrations, so concentrations of oxidizable precursors in the water were negligible. Conversely, higher than expected EOF concentrations demonstrated the

presence of additional organofluorines. EOF removal was on average 45% lower than target PFAS removal in the FF step, indicating that this additional portion of organofluorines was not susceptible to removal by FF. Therefore, it most likely consisted of ultrashort-chain PFAA or non-amphiphilic fluorinated compounds that do not degrade to target PFAS in the TOP assay.

FF treatment did not result in major changes in activity as measured by the effect-based bioassays. For groundwater and leachate, mean TTR-binding PFOS-equivalent concentrations decreased by 9 and 32%, respectively, and bioluminescence triclosan-equivalent concentrations by 10 and 21%. Probably, the decrease in toxicity was comparatively low because compounds other than PFAS were the main driver of the response in both assays, and these other compounds were not removed effectively with FF.

4.2 Electrochemical oxidation – paper **III**

4.2.1 Degradation of target PFAS

In both groundwater and leachate, a ΣPFAS degradation of approximately 80% was achieved after 9 h of EO treatment at 50 L volume, see Figure 4. Short-chain PFAA, most notably PFPeS and PFBA, were formed as degradation products from long-chain PFAA. The final degradation was higher for PFCA than for PFSA, and higher for long-chain PFAA than for short-chain. At 150 L volume, the PFAS degradation remained lower, because of the inverse relationship between volume and specific charge.

4.2.2 Degradation of EOF and toxicity

The electrochemical degradation of EOF was similar to that of ΣPFAS, indicating that the unknown organofluorine was susceptible to degradation by EO and that full mineralization of PFAS occurred. Similarly, the response in both of the effect-based bioassays decreased steeply after EO. The reduction in bioassay activity was often higher than the PFAS degradation, demonstrating the presence of active compounds other than PFAS that were also destroyed successfully by EO. Oxyhalide anion formation was not measured in this paper, but the disappearance of chloride indicated the formation of oxidized chlorine species. Nonetheless, the highly reduced activity in the bioassays implied a low formation of other toxic byproducts.

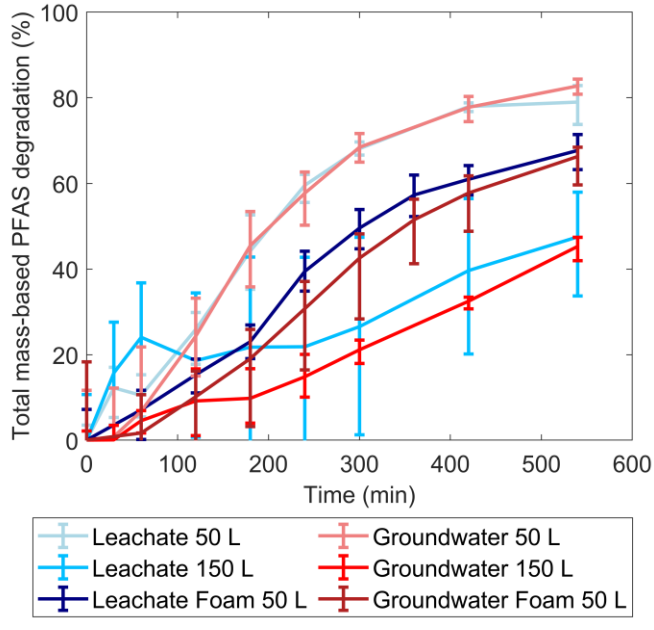

Figure 4: ΣPFAS degradation over time in EO experiments. Error bars represent min and max values based on the experimental and analytical duplicates (i.e., $n = 4$); lines connect the means. Figure reproduced from paper **III**, copyright 2023 ACS.

4.2.3 Coupled numerical model

After calibration of the rate constants, the coupled numerical model was able to reproduce the experimental results well, as exemplified in Figure 5. These rate constants depend on the concentrations of matrix compounds, as well as on the current intensity, intrinsic molecular properties and mass transfer limitations. A separate set of rate constants was calibrated for the fractionated foams, to account for the different matrix. Benefits of this model are its capability of simultaneously accounting for degradation and formation reactions and its adaptability for different reactor dimensions and treatment volumes.

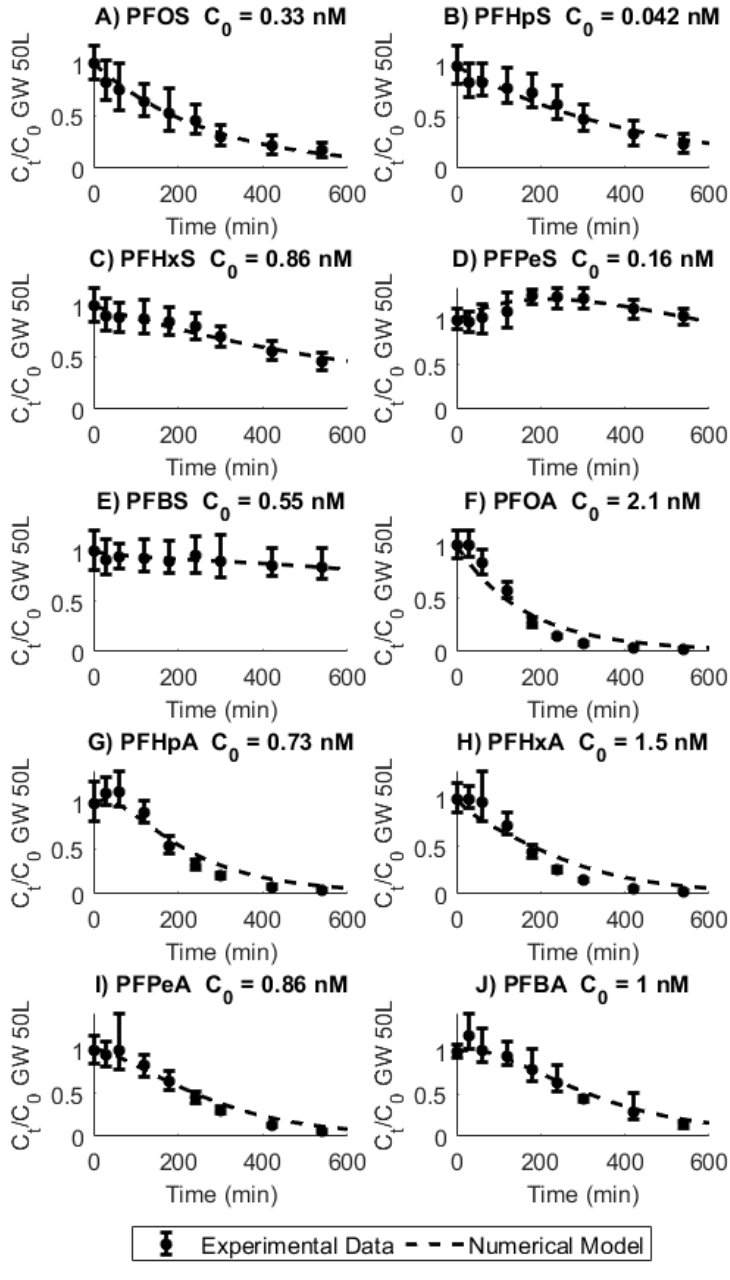

Figure 5: Individual degradation of PFAA for the EO run with 50 L groundwater, including the results of the numerical model. The headings state the initial concentration of each PFAA. Error bars represent min and max values based on the experimental and analytical duplicates (i.e., $n = 4$). Figure adapted from paper **III**, copyright 2023 ACS.

4.3 Treatment train: FF + EO – paper **III**

4.3.1 Degradation performance

Figure 6 shows the degradation efficiency over the entire FF + EO treatment train for all analysed variables. The treatment train was most effective for long-chain PFAS, due to their high removal in the FF and high degradation in the EO. PFSA degradation in the EO on foam was very low, e.g. < 15% in both groundwater and leachate foam for PFHxS. What caused this low degradation of PFSA in foam is unclear, but it could limit the full-scale application of the treatment train.

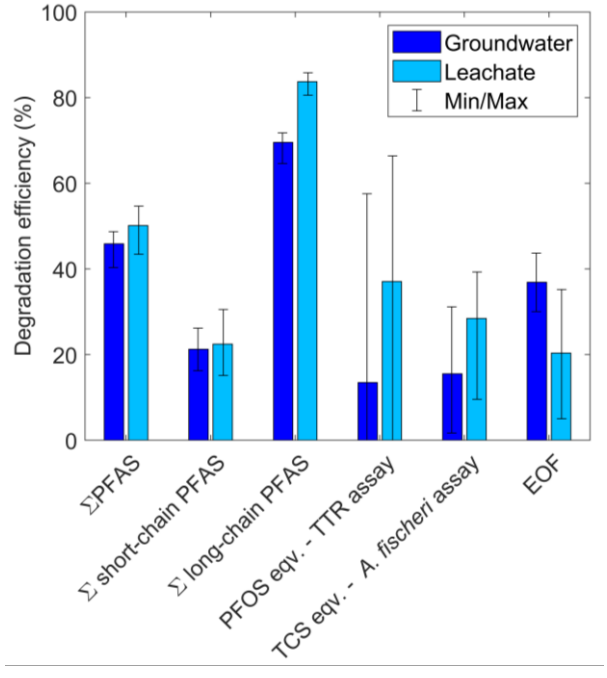

Figure 6: Degradation efficiency of the EO + FF treatment train, in terms of target PFAS, bioassay response and EOF. Error bars represent the min and max degradation based on all measurements per variable. TTR: transthyretin, TCS: triclosan, EOF: extractable organofluorine. Figure reproduced from paper **III**, copyright 2023 ACS.

4.3.2 Energy requirements

The energy requirements of the EO and FF + EO are summarized in Table 6. The degradation for FF + EO was based on the influent concentration of the original water, rather than that of the foam. In the calculation of the energy requirement for the FF + EO treatment train, the energy required for FF was ignored, because this was negligible compared to that of the EO (Burns et al., 2022). Overall, these values are higher than the energy requirements reported for other concentrate-and-destroy approaches (see section 1.2.4). Probably, the energy efficiency of the FF + EO treatment train can be reduced further by including secondary and tertiary foam fractionation steps, and by optimizing the EO reactor to reduce mass transfer limitations.

Table 6: Energy required for one order of magnitude degradation (EE/O) of PFOS and PFOA. For PFOS, energy requirements over the treatment train could not be determined reliably, due to its low degradation in the fractionated foam.

	PFAS	**EE/O (kWh m^{-3})**	
		Groundwater	**Leachate**
EO only	PFOA	160	240
	PFOS	350	410
EO + FF	PFOA	53	76

4.4 Integrated FF – paper **IV**

Paper **IV** aimed to investigate the potential of integrating FF with existing water treatment processes. While ΣPFAS enrichment factors (EF) from the influent to the foam reached up to 10^5, this did not result in considerable ΣPFAS removal at any of the sites (n = 10). A reason for this lack of PFAS removal could be that the foam was not actually removed at any of the plants, but instead left to collapse back into the effluent. Additionally, the total amount of foam compared to the volume of influent water was probably negligible, since foam has a very low density.

Nonetheless, long-chain PFAA were removed for up to 46% from influent to effluent, and up to 74% from influent to the water under the foam. Therefore, stimulating foam formation may lead to higher PFAS removal efficiencies, particularly considering the high EF in the foam. From a rough mass balance calculation, it was approximated that a foam fraction of 3%

may already result in a Σlong-chain PFAA removal of > 99% at one of the sites.

Similar to conventional foam fractionation, the enrichment of individual PFAS in the foam depended on the perfluorocarbon chain length. Figure 7 illustrates the wide range in EF obtained at the different sites, and demonstrates that enrichment factors were generally higher for longer chain lengths. The high variability in EF was unsurprising considering the wide variety of water matrices, treatment processes and plant designs included in the study. Based on ΣPFAS enrichment factors, MBBRs were most effective for enriching PFAS in foam, possibly because they do not contain suspended sludge that interferes with foam formation.

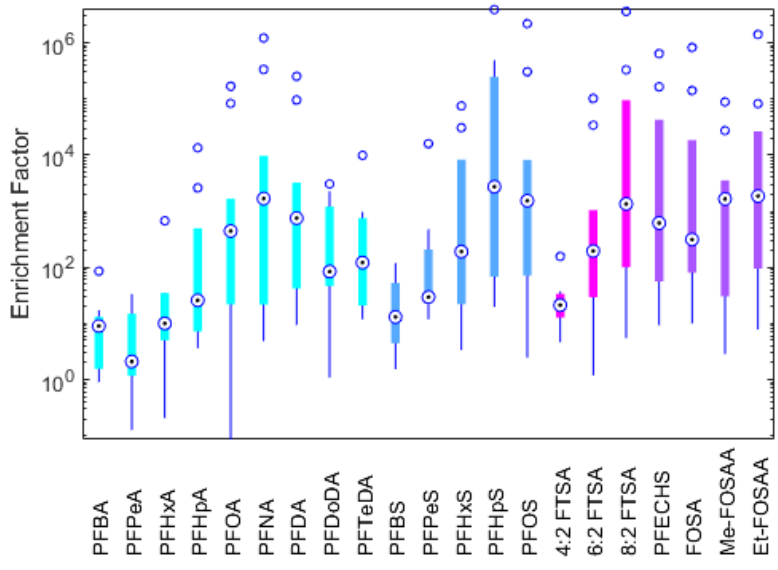

Figure 7: Box plot of enrichment factors across the different sites for individual PFAS. PFCA are colored light blue, PFSA dark blue, FTSA magenta and the other PFAS purple. Compounds of the same class have an increasing molecular weight from left to right. Only PFAS that were detected at at least eight of the sites were included, i.e. $8 \leq n \leq 10$. The bottom and top of each box represent the 25th to the 75th percentile, respectively. The black dot encircled in blue represents the median, and whiskers go to the most extreme data points, excluding outliers. Outliers (blue circles) are values more than 1.5 interquartile range from the bottom or top of the box. Figure reproduced from paper **IV**, copyright 2023 ACS.

5. Conclusions and outlook

This thesis evaluated the potential of foam fractionation and electrochemical oxidation for the treatment of PFAS-contaminated water in four papers. Brief answers to the research questions described in chapter 2 are given below.

1. *Which factors affect the removal and mass balance recovery of PFAS from contaminated water using foam fractionation and how?*

Papers **I** and **II** found that the removal of PFAS with FF was affected by the contact time in the column, the air flow rate and the concentration of dissolved salts. In paper **I**, the removal also decreased at lower foam fractions, but this effect was not reproduced in paper **II**. In paper **I**, it was hypothesized that mass balance closures < 100% were caused by loss of PFAS to the air. However, paper **II** did not find lower MBs at higher PFAS emissions to the air, despite the high airborne concentrations that were measured.

2. *How do the degradation efficiency and kinetics of electrochemical oxidation for the destruction of PFAS differ between contaminated water and concentrated foam?*

In paper **III**, it was shown that both the PFAS degradation efficiency and the kinetic rate constants were higher in contaminated groundwater and landfill leachate than in fractionated foam from these water types. Nonetheless, the energy use in terms of kWh per order of magnitude PFOA degradation was lower when applying EO to the foam rather than directly to the raw water.

3. *How do the aforementioned treatment technologies affect the biological activity of PFAS-contaminated groundwater and landfill leachate?*

Paper **III** applied the TTR-binding assay and a bacterial bioluminescence assay to influent and effluent from FF and EO. Here, FF was shown to only slightly reduce the biological activity of the water. Conversely, EO treatment caused a considerable decrease in both assay responses, indicating a lower toxicity in the effluent than the influent water. This result was particularly important considering the high byproduct formation potential of EO, which could also lead to higher toxic potencies in the effluent instead.

4. *Can the concept of foam fractionation be integrated with existing water treatment technologies?*

Paper **IV** showed that PFAS enrichment factors in foam occurring naturally on the surface of full-scale water treatment processes could exceed those in engineered foam fractionation systems. However, this high PFAS enrichment in foam did not lead to ΣPFAS removal from influent to effluent. Possibly, stimulating foam formation or actually removing the foam from the water surface could lead to PFAS removal. In some treatment plants, removal of long-chain PFAA was measured, indicating that integrated foam fractionation has potential as a treatment technology for PFAS.

Altogether, the work presented in this thesis demonstrates the high potential of FF and EO for treatment of PFAS in water. It has provided a deeper insight into the strengths and limitations of both technologies, but has also given rise to additional questions for further research.

In the field of FF, the low mass balance closure measured in papers **I** and **III** remains an open question. Since this FF system differed from that of paper **II**, air emissions might still have been a significant PFAS sink, possibly contributing to global PFAS accumulation by long range transport. More work on air emissions is also crucial from a human health perspective, as it should be ensured that PFAS concentrations in air do not exceed safe levels. Finally, the fate of precursors or EOF in FF has not been thoroughly assessed yet. Paper **III** identified a lower removal of EOF than target PFAS in FF, the cause of which remains to be determined.

A fruitful area of further work related to EO is the reactor design. Mass transfer limitations were found to limit the degradation efficiency in paper **III**, but these could potentially be reduced by optimizing the hydrodynamics

of the flow-through cell. Additionally, the use of innovative electrodes may increase the mass transfer while also diminishing byproduct formation. Finally, EO should be tested on more highly concentrated foam, obtained from secondary or tertiary FF steps, as well as on water types containing more novel and precursor-type PFAS than the leachate water from the Hovgården landfill.

One of the most exciting aspects of this thesis was the work on integrated FF. Paper **IV** was only a scoping study, but it created many opportunities for further research. In follow-up studies, it would be interesting to focus exclusively on one reactor, and try to obtain PFAS removal with foam by tweaking operating parameters. Alternatively, the broad sampling from paper **IV** could be repeated with additional treatment plants, but including more foam parameters and more thorough sampling strategies. Finally, it would be interesting to investigate more treatment processes, such as aerobic granular sludge or membrane bioreactors, or to investigate the removal of other contaminants than PFAS.

References

Aggelopoulos, C. A. (2022). Recent advances of cold plasma technology for water and soil remediation: A critical review. *Chemical Engineering Journal*, *428*(2), 131657. https://doi.org/10.1016/j.cej.2021.131657

Ahrens, L., & Bundschuh, M. (2014). Fate and effects of poly- and perfluoroalkyl substances in the aquatic environment: A review. *Environmental Toxicology and Chemistry*, *33*(9), 1921–1929. https://doi.org/10.1002/etc.2663

Ahrens, L., Harner, T., Shoeib, M., Koblizkova, M., & Reiner, E. J. (2013). Characterization of two passive air samplers for per- and polyfluoroalkyl substances. *Environmental Science and Technology*, *47*(24), 14024–14033. https://doi.org/10.1021/es4048945

Anderson, J. K., Brecher, R. W., Cousins, I. T., DeWitt, J., Fiedler, H., Kannan, K., Kirman, C. R., Lipscomb, J., Priestly, B., Schoeny, R., Seed, J., Verner, M., & Hays, S. M. (2022). Grouping of PFAS for human health risk assessment: Findings from an independent panel of experts. *Regulatory Toxicology and Pharmacology*, *134*, 105226. https://doi.org/10.1016/j.yrtph.2022.105226

Ankley, G. T., Cureton, P., Hoke, R. A., Houde, M., Kumar, A., Kurias, J., Lanno, R., McCarthy, C., Newsted, J., Salice, C. J., Sample, B. E., Sepúlveda, M. S., Steevens, J., & Valsecchi, S. (2021). Assessing the Ecological Risks of Per- and Polyfluoroalkyl Substances: Current State-of-the Science and a Proposed Path Forward. *Environmental Toxicology and Chemistry*, *40*(3), 564–605. https://doi.org/10.1002/etc.4869

Appleman, T. D., Dickenson, E. R. V., Bellona, C., & Higgins, C. P. (2013). Nanofiltration and granular activated carbon treatment of perfluoroalkyl acids. *Journal of Hazardous Materials*, *260*, 740–746. https://doi.org/10.1016/j.jhazmat.2013.06.033

Arp, H. P. H., Aurich, D., Schymanski, E. L., Sims, K., & Hale, S. E. (2023). Avoiding the Next Silent Spring: Our Chemical Past, Present, and Future. *Environmental Science & Technology*, *57*(16), 6355–6359. https://doi.org/10.1021/acs.est.3c01735

Ateia, M., Chiang, D., Cashman, M., & Acheson, C. (2023). Total Oxidizable Precursor (TOP) Assay - Best Practices , Capabilities and Limitations for PFAS Site Investigation and Remediation. *Environmental Science & Technology Letters*, *10*(4), 292–301. https://doi.org/10.1021/acs.estlett.3c00061

Australian Government - NHMRC; NRMMC. (2018). *Australian Drinking Water Guidelines 6 Version 3.5* (Issue December). https://www.nhmrc.gov.au/sites/default/files/documents/reports/aust-drinking-water-guidelines.pdf

Banayan Esfahani, E., Asadi Zeidabadi, F., Zhang, S., & Mohseni, M. (2022). Photochemical/catalytic oxidative/reductive decomposition of per- and polyfluoroalkyl substances (PFAS), decomposition mechanisms and effects of key factors: a review. *Environmental Science: Water Research and Technology*, *8*(4), 698–728. https://doi.org/10.1039/d1ew00774b

Bao, J., Yu, W. J., Liu, Y., Wang, X., Liu, Z. Q., & Duan, Y. F. (2020). Removal of perfluoroalkanesulfonic acids (PFSAs) from synthetic and natural groundwater by electrocoagulation. *Chemosphere*, *248*, 125951. https://doi.org/10.1016/j.chemosphere.2020.125951

Barbo, N., Stoiber, T., Naidenko, O. V., & Andrews, D. Q. (2023). Locally caught freshwater fish across the United States are likely a significant source of exposure to PFOS and other perfluorinated compounds. *Environmental Research*, *220*, 115165. https://doi.org/10.1016/j.envres.2022.115165

Barisci, S., & Suri, R. (2020). Electrooxidation of short and long chain perfluorocarboxylic acids using boron doped diamond electrodes. *Chemosphere*, *243*, 125349. https://doi.org/10.1016/j.chemosphere.2019.125349

Barjasteh, A., Dehghani, Z., Lamichhane, P., Kaushik, N., & Choi, E. H. (2021). Recent Progress in Applications of Non-Thermal Plasma for Water Purification, Bio-Sterilization, and Decontamination. *Applied Sciences*, *11*(8), 3372. https://doi.org/https://doi.org/10.3390/app11083372

Baudequin, C., Couallier, E., Rakib, M., Deguerry, I., Severac, R., & Pabon, M. (2011). Purification of firefighting water containing a fluorinated surfactant by reverse osmosis coupled to electrocoagulation-filtration. *Separation and Purification Technology*, *76*(3), 275–282. https://doi.org/10.1016/j.seppur.2010.10.016

Bayer, P., Heuer, E., Karl, U., & Finkel, M. (2005). Economical and ecological comparison of granular activated carbon (GAC) adsorber refill strategies. *Water Research*, *39*(9), 1719–1728. https://doi.org/10.1016/j.watres.2005.02.005

Belkouteb, N., Franke, V., McCleaf, P., Köhler, S., & Ahrens, L. (2020). Removal of per- and polyfluoroalkyl substances (PFASs) in a full-scale drinking water treatment plant: Long-term performance of granular activated carbon (GAC) and influence of flow-rate. *Water Research*, *182*, 115913. https://doi.org/10.1016/j.watres.2020.115913

Boyer, T. H., Ellis, A., Fang, Y., Schaefer, C. E., Higgins, C. P., & Strathmann, T. J. (2021). Life cycle environmental impacts of regeneration options for anion exchange resin remediation of PFAS impacted water. *Water Research*, *207*, 117798. https://doi.org/10.1016/j.watres.2021.117798

Brusseau, M. L., & Van Glubt, S. (2019). The influence of surfactant and solution composition on PFAS adsorption at fluid-fluid interfaces. *Water Research*, *161*, 17–26. https://doi.org/10.1016/j.watres.2019.05.095

Buck, R. C., Franklin, J., Berger, U., Conder, J. M., Cousins, I. T., Voogt, P. De, Jensen, A. A., Kannan, K., Mabury, S. A., & van Leeuwen, S. P. J. (2011).

Perfluoroalkyl and polyfluoroalkyl substances in the environment: Terminology, classification, and origins. *Integrated Environmental Assessment and Management*, *7*(4), 513–541. https://doi.org/10.1002/ieam.258

Buckley, T., Karanam, K., Han, H., Vo, H. N. P., Shukla, P., Firouzi, M., & Rudolph, V. (2023). Effect of different co-foaming agents on PFAS removal from the environment by foam fractionation. *Water Research*, *230*, 119532. https://doi.org/10.1016/j.watres.2022.119532

Buckley, T., Karanam, K., Xu, X., Shukla, P., Firouzi, M., & Rudolph, V. (2022). Effect of mono- and di-valent cations on PFAS removal from water using foam fractionation – A modelling and experimental study. *Separation and Purification Technology*, *286*, 120508. https://doi.org/10.1016/j.seppur.2022.120508

Buckley, T., Xu, X., Rudolph, V., Firouzi, M., & Shukla, P. (2021). Review of foam fractionation as a water treatment technology. *Separation Science and Technology*, *57*(6), 929–958. https://doi.org/10.1080/01496395.2021.1946698

Burns, D. J., Hinrichsen, H. M., Stevenson, P., & Murphy, P. J. C. (2022). Commercial-scale remediation of per- and polyfluoroalkyl substances from a landfill leachate catchment using Surface-Active Foam Fractionation (SAFF®). *Remediation*, *32*(2), 139–150. https://doi.org/10.1002/rem.21720

Burns, D. J., Stevenson, P., & Murphy, P. J. C. (2021). PFAS removal from groundwaters using Surface-Active Foam Fractionation. *Remediation*, *31*(4), 19–33. https://doi.org/10.1002/rem.21694

Cao, H., Zhang, W., Wang, C., & Liang, Y. (2020). Sonochemical degradation of poly- and perfluoroalkyl substances – A review. *Ultrasonics Sonochemistry*, *69*, 105245. https://doi.org/10.1016/j.ultsonch.2020.105245

Carson, R. (1962). *Silent Spring*. Houghton Mifflin.

Casas, G., Martínez-Varela, A., Roscales, J. L., Vila-Costa, M., Dachs, J., & Jiménez, B. (2020). Enrichment of perfluoroalkyl substances in the sea-surface microlayer and sea-spray aerosols in the Southern Ocean. *Environmental Pollution*, *267*, 115512. https://doi.org/10.1016/j.envpol.2020.115512

Chen, Y. C., Lo, S. L., & Lee, Y. C. (2012). Distribution and fate of perfluorinated compounds (PFCs) in a pilot constructed wetland. *Desalination and Water Treatment*, *37*(1–3), 178–184. https://doi.org/10.1080/19443994.2012.661270

Cheng, J., Vecitis, C. D., Park, H., Mader, B. T., & Hoffmann, M. R. (2008). Sonochemical degradation of perfluorooctane sulfonate (PFOS) and perfluorooctanoate (PFOA) in landfill groundwater: Environmental matrix effects. *Environmental Science and Technology*, *42*(21), 8057–8063. https://doi.org/10.1021/es8013858

Cheng, J., Vecitis, C. D., Park, H., Mader, B. T., & Hoffmann, M. R. (2010). Sonochemical degradation of perfluorooctane sulfonate (PFOS) and perfluorooctanoate (PFOA) in groundwater: Kinetic effects of matrix inorganics. *Environmental Science and Technology*, *44*(1), 445–450.

https://doi.org/10.1021/es902651g
Chetverikov, S. P., Sharipov, D. A., Korshunova, T. Y., & Loginov, O. N. (2017). Degradation of perfluorooctanyl sulfonate by strain Pseudomonas plecoglossicida 2.4-D. *Applied Biochemistry and Microbiology*, *53*(5), 533–538. https://doi.org/10.1134/S0003683817050027
Contactica, EMIVASA, & PORTABLECRAC. (2018). *LCA & LCCA of acquiring Virgin AC and of thermal regeneration* (Issue D6.1). https://www.spire2030.eu/sites/default/files/users/user735/Deliverables/WP6/D6 1_Virgin activated carbon Thermal regeneration_v4_FINAL.pdf
Cousins, I. T., Dewitt, J. C., Glüge, J., Goldenman, G., Herzke, D., Lohmann, R., Ng, C. A., Scheringer, M., & Wang, Z. (2020). The high persistence of PFAS is sufficient for their management as a chemical class. *Environmental Science: Processes and Impacts*, *22*(12), 2307–2312. https://doi.org/10.1039/d0em00355g
Cousins, I. T., Johansson, J. H., Salter, M. E., Sha, B., & Scheringer, M. (2022). Outside the Safe Operating Space of a New Planetary Boundary for Per- and Polyfluoroalkyl Substances (PFAS). *Environmental Science and Technology*, *56*(16), 11172–11179. https://doi.org/10.1021/acs.est.2c02765
Cousins, I. T., Ng, C. A., Wang, Z., & Scheringer, M. (2019). Why is high persistence alone a major cause of concern? *Environmental Science: Processes and Impacts*, *21*(5), 781–792. https://doi.org/10.1039/c8em00515j
Danish EPA. (2021). *Skærpede krav til PFAS-stoffer i drikkevand*. https://mst.dk/service/nyheder/nyhedsarkiv/2021/jun/skaerpede-krav-til-pfas-stoffer-i-drikkevand/
De Silva, A. O., Armitage, J. M., Bruton, T. A., Dassuncao, C., Heiger-Bernays, W., Hu, X. C., Kärrman, A., Kelly, B., Ng, C., Robuck, A., Sun, M., Webster, T. F., & Sunderland, E. M. (2021). PFAS Exposure Pathways for Humans and Wildlife: A Synthesis of Current Knowledge and Key Gaps in Understanding. *Environmental Toxicology and Chemistry*, *40*(3), 631–657. https://doi.org/10.1002/etc.4935
DeLuca, N. M., Minucci, J. M., Mullikin, A., Slover, R., & Cohen Hubal, E. A. (2022). Human exposure pathways to poly- and perfluoroalkyl substances (PFAS) from indoor media: A systematic review. *Environment International*, *162*, 107149. https://doi.org/10.1016/j.envint.2022.107149
Dixit, F., Dutta, R., Barbeau, B., Berube, P., & Mohseni, M. (2021). PFAS removal by ion exchange resins: A review. *Chemosphere*, *272*, 129777. https://doi.org/10.1016/j.chemosphere.2021.129777
Duinslaeger, N., & Radjenovic, J. (2022). Electrochemical degradation of per- and polyfluoroalkyl substances (PFAS) using low-cost graphene sponge electrodes. *Water Research*, *213*, 118148. https://doi.org/10.1016/j.watres.2022.118148
Ebersbach, I., Ludwig, S. M., Constapel, M., & Kling, H. W. (2016). An alternative treatment method for fluorosurfactant-containing wastewater by aerosol-mediated separation. *Water Research*, *101*, 333–340.

https://doi.org/10.1016/j.watres.2016.05.063
EFSA. (2020). *PFAS in food: EFSA assesses risks and sets tolerable intake*. https://www.efsa.europa.eu/en/news/pfas-food-efsa-assesses-risks-and-sets-tolerable-intake
Emery, I., Kempisty, D., Fain, B., & Mbonimpa, E. (2019). Evaluation of treatment options for well water contaminated with perfluorinated alkyl substances using life cycle assessment. *International Journal of Life Cycle Assessment*, *24*(1), 117–128. https://doi.org/10.1007/s11367-018-1499-8
European Chemicals Agency. (2023a). *ANNEX XV RESTRICTION REPORT - Per- and polyfluoroalkyl substances*. https://echa.europa.eu/documents/10162/f605d4b5-7c17-7414-8823-b49b9fd43aea
European Chemicals Agency. (2023b). *ECHA publishes PFAS restriction proposal*. https://echa.europa.eu/-/echa-publishes-pfas-restriction-proposal
Fang, Y., Meng, P., Schaefer, C., & Knappe, D. R. U. (2023). Removal and destruction of perfluoroalkyl ether carboxylic acids (PFECAs) in an anion exchange resin and electrochemical oxidation treatment train. *Water Research*, *230*, 119522. https://doi.org/10.1016/j.watres.2022.119522
Fenton, S. E., Ducatman, A., Boobis, A., DeWitt, J. C., Lau, C., Ng, C., Smith, J. S., & Roberts, S. M. (2021). Per- and Polyfluoroalkyl Substance Toxicity and Human Health Review: Current State of Knowledge and Strategies for Informing Future Research. *Environmental Toxicology and Chemistry*, *40*(3), 606–630. https://doi.org/10.1002/etc.4890
Franke, V., Ullberg, M., McCleaf, P., Wålinder, M., Köhler, S. J., & Ahrens, L. (2021). The Price of Really Clean Water: Combining Nanofiltration with Granular Activated Carbon and Anion Exchange Resins for the Removal of Per- And Polyfluoralkyl Substances (PFASs) in Drinking Water Production. *ACS ES&T Water*. https://doi.org/10.1021/acsestwater.0c00141
Göckener, B., Weber, T., Rüdel, H., Bücking, M., & Kolossa-Gehring, M. (2020). Human biomonitoring of per- and polyfluoroalkyl substances in German blood plasma samples from 1982 to 2019. *Environmental International*, *145*, 106123. https://doi.org/10.1016/j.envint.2020.106123
Gole, V. L., Sierra-Alvarez, R., Peng, H., Giesy, J. P., Deymier, P., & Keswani, M. (2018). Sono-chemical treatment of per- and poly-fluoroalkyl compounds in aqueous film-forming foams by use of a large-scale multi-transducer dual-frequency based acoustic reactor. *Ultrasonics Sonochemistry*, *45*, 213–222. https://doi.org/10.1016/j.ultsonch.2018.02.014
Gomez-Ruiz, B., Gómez-Lavín, S., Diban, N., Boiteux, V., Colin, A., Dauchy, X., & Urtiaga, A. (2017). Efficient electrochemical degradation of poly- and perfluoroalkyl substances (PFASs) from the effluents of an industrial wastewater treatment plant. *Chemical Engineering Journal*, *322*, 196–204. https://doi.org/10.1016/j.cej.2017.04.040
Hamers, T., Smit, M. G. D., Murk, A. J., & Koeman, J. H. (2001). Biological and chemical analysis of the toxic potency of pesticides in rainwater.

Chemosphere, *45*(4–5), 609–624. https://doi.org/10.1016/S0045-6535(01)00017-0

Harms, H., Schlosser, D., & Wick, L. Y. (2011). Untapped potential: Exploiting fungi in bioremediation of hazardous chemicals. *Nature Reviews Microbiology*, *9*(3), 177–192. https://doi.org/10.1038/nrmicro2519

Horst, J., McDonough, J., Ross, I., & Houtz, E. (2020). Understanding and Managing the Potential By-Products of PFAS Destruction. *Groundwater Monitoring and Remediation*, *40*(2), 17–27. https://doi.org/10.1111/gwmr.12372

Houtz, E. F., & Sedlak, D. L. (2012). Oxidative conversion as a means of detecting precursors to perfluoroalkyl acids in urban runoff. *Environmental Science and Technology*, *46*(17), 9342–9349. https://doi.org/10.1021/es302274g

Huang, S., & Jaffé, P. R. (2019). Defluorination of Perfluorooctanoic Acid (PFOA) and Perfluorooctane Sulfonate (PFOS) by Acidimicrobium sp. Strain A6. *Environmental Science and Technology*, *53*, 11410–11419. https://doi.org/10.1021/acs.est.9b04047

Huang, S., Sima, M., Long, Y., Messenger, C., & Jaffé, P. R. (2022). Anaerobic degradation of perfluorooctanoic acid (PFOA) in biosolids by Acidimicrobium sp. strain A6. *Journal of Hazardous Materials*, *424*, 127699. https://doi.org/10.1016/j.jhazmat.2021.127699

Ji, B., Kang, P., Wei, T., & Zhao, Y. (2020). Challenges of aqueous per- and polyfluoroalkyl substances (PFASs) and their foreseeable removal strategies. *Chemosphere*, *250*, 126316. https://doi.org/10.1016/j.chemosphere.2020.126316

Kärrman, A., Yeung, L. W. Y., Spaan, K. M., Lange, F. T., Nguyen, M. A., Plassmann, M., De Wit, C. A., Scheurer, M., Awad, R., & Benskin, J. P. (2021). Can determination of extractable organofluorine (EOF) be standardized? First interlaboratory comparisons of EOF and fluorine mass balance in sludge and water matrices. *Environmental Science: Processes and Impacts*, *23*(10), 1458–1465. https://doi.org/10.1039/d1em00224d

Kirk, M., Smurthwaite, K., Bräunig, J., Trevenar, S., Lucas, R., Lal, A., Korda, R., Clements, A., Mueller, J., & Armstrong, B. P. (2018). *The PFAS Health Study: Systematic Literature Review*. *The Australian National University*. http://nceph.anu.edu.au/

Krause, M. J., Thoma, E., Sahle-Damesessie, E., Crone, B., Whitehill, A., Shields, E., & Gullett, B. (2022). Supercritical Water Oxidation as an Innovative Technology for PFAS Destruction. *Journal of Environmental Engineering*, *148*(2), 1–8. https://doi.org/10.1061/(asce)ee.1943-7870.0001957

Kulkarni, P. R., Richardson, S. D., Nzeribe, B. N., Adamson, D. T., Kalra, S. S., Mahendra, S., Blotevogel, J., Hanson, A., Dooley, G., Maraviov, S., & Popovic, J. (2022). Field Demonstration of a Sonolysis Reactor for Treatment of PFAS-Contaminated Groundwater. *Journal of Environmental Engineering*, *148*(11), 1–12. https://doi.org/10.1061/(asce)ee.1943-7870.0002064

Kwon, B. G., Lim, H. J., Na, S. H., Choi, B. I., Shin, D. S., & Chung, S. Y. (2014).

Biodegradation of perfluorooctanesulfonate (PFOS) as an emerging contaminant. *Chemosphere*, *109*, 221–225. https://doi.org/10.1016/j.chemosphere.2014.01.072

Lau, C., Anitole, K., Hodes, C., Lai, D., Pfahles-Hutchens, A., & Seed, J. (2007). Perfluoroalkyl acids: A review of monitoring and toxicological findings. *Toxicological Sciences*, *99*(2), 366–394. https://doi.org/10.1093/toxsci/kfm128

Lee, T., Speth, T. F., & Nadagouda, M. N. (2022). High-pressure membrane filtration processes for separation of Per- and polyfluoroalkyl substances (PFAS). *Chemical Engineering Journal*, *431*(P2), 134023. https://doi.org/10.1016/j.cej.2021.134023

Lemal, D. M. (2004). Perspective on Fluorocarbon Chemistry. *Journal of Organic Chemistry*, *69*(1), 1–11. https://doi.org/10.1021/jo0302556

Lenka, S. P., Kah, M., & Padhye, L. P. (2021). A review of the occurrence, transformation, and removal of poly- and perfluoroalkyl substances (PFAS) in wastewater treatment plants. *Water Research*, *199*, 117187. https://doi.org/10.1016/j.watres.2021.117187

Li, G., Dunlap, J., Wang, Y., Huang, Q., & Li, K. (2022). Environmental Life Cycle Assessment (LCA) of Treating PFASs with Ion Exchange and Electrochemical Oxidation Technology. *ACS ES&T Water*, *2*(9), 1555–1564. https://doi.org/10.1021/acsestwater.2c00196

Li, J., Pinkard, B. R., Wang, S., & Novosselov, I. V. (2022). Review: Hydrothermal treatment of per- and polyfluoroalkyl substances (PFAS). *Chemosphere*, *307*(P2), 135888. https://doi.org/10.1016/j.chemosphere.2022.135888

Li, P., Zhi, D., Zhang, X., Zhu, H., Li, Z., Peng, Y., He, Y., Luo, L., Rong, X., & Zhou, Y. (2019). Research progress on the removal of hazardous perfluorochemicals: A review. *Journal of Environmental Management*, *250*, 109488. https://doi.org/10.1016/j.jenvman.2019.109488

Liang, S., Mora, R., Huang, Q., Casson, R., Wang, Y., Woodard, S., & Anderson, H. (2022). Field demonstration of coupling ion-exchange resin with electrochemical oxidation for enhanced treatment of per- and polyfluoroalkyl substances (PFAS) in groundwater. *Chemical Engineering Journal Advances*, *9*, 100216. https://doi.org/10.1016/j.ceja.2021.100216

Liang, S., Pierce, R., Lin, H., Chiang, S. Y. D., & Huang, Q. (2018). Electrochemical oxidation of PFOA and PFOS in concentrated waste streams. *Remediation*, *28*(2), 127–134. https://doi.org/10.1002/rem.21554

Lin, H., Wang, Y., Niu, J., Yue, Z., & Huang, Q. (2015). Efficient Sorption and Removal of Perfluoroalkyl Acids (PFAAs) from Aqueous Solution by Metal Hydroxides Generated in Situ by Electrocoagulation. *Environmental Science and Technology*, *49*(17), 10562–10569. https://doi.org/10.1021/acs.est.5b02092

Liu, C. J., McKay, G., Jiang, D., Tenorio, R., Cath, J. T., Amador, C., Murray, C. C., Brown, J. B., Wright, H. B., Schaefer, C., Higgins, C. P., Bellona, C., & Strathmann, T. J. (2021). Pilot-scale field demonstration of a hybrid

nanofiltration and UV-sulfite treatment train for groundwater contaminated by per- and polyfluoroalkyl substances (PFASs). *Water Research*, *205*, 117677. https://doi.org/10.1016/j.watres.2021.117677

Liu, C. J., Werner, D., & Bellona, C. (2019). Removal of per- And polyfluoroalkyl substances (PFASs) from contaminated groundwater using granular activated carbon: A pilot-scale study with breakthrough modeling. *Environmental Science: Water Research and Technology*, *5*(11), 1844–1853. https://doi.org/10.1039/c9ew00349e

Liu, S., Jin, B., Arp, H. P. H., Chen, W., Liu, Y., & Zhang, G. (2022). The Fate and Transport of Chlorinated Polyfluorinated Ether Sulfonates and Other PFAS through Industrial Wastewater Treatment Facilities in China. *Environmental Science & Technology*, *56*(5), 3002–3010. https://doi.org/10.1021/acs.est.1c04276

Liu, X., Huang, X., Wei, X., Zhi, Y., Qian, S., Li, W., Yue, D., & Wang, X. (2023). Occurrence and removal of per- and polyfluoroalkyl substances (PFAS) in leachates from incineration plants: A full-scale study. *Chemosphere*, *313*, 137456. https://doi.org/10.1016/j.chemosphere.2022.137456

Liu, Y., Hu, X. M., Zhao, Y., Wang, J., Lu, M. X., Peng, F. H., & Bao, J. (2018). Removal of perfluorooctanoic acid in simulated and natural waters with different electrode materials by electrocoagulation. *Chemosphere*, *201*, 303–309. https://doi.org/10.1016/j.chemosphere.2018.02.129

Lu, D., Sha, S., Luo, J., Huang, Z., & Zhang Jackie, X. (2020). Treatment train approaches for the remediation of per- and polyfluoroalkyl substances (PFAS): A critical review. *Journal of Hazardous Materials*, *386*, 121963. https://doi.org/10.1016/j.jhazmat.2019.121963

Maldonado, V. Y., Landis, G. M., Ensch, M., Becker, M. F., Witt, S. E., & Rusinek, C. A. (2021). A flow-through cell for the electrochemical oxidation of perfluoroalkyl substances in landfill leachates. *Journal of Water Process Engineering*, *43*, 102210. https://doi.org/10.1016/j.jwpe.2021.102210

Mayakaduwage, S., Ekanayake, A., Kurwadkar, S., Upamali, A., & Vithanage, M. (2022). Phytoremediation prospects of per- and polyfluoroalkyl substances : A review. *Environmental Research*, *212*, 113311. https://doi.org/10.1016/j.envres.2022.113311

McCleaf, P., Englund, S., Östlund, A., Lindegren, K., Wiberg, K., & Ahrens, L. (2017). Removal efficiency of multiple poly- and perfluoroalkyl substances (PFASs) in drinking water using granular activated carbon (GAC) and anion exchange (AE) column tests. *Water Research*, *120*, 77–87. https://doi.org/10.1016/j.watres.2017.04.057

McCleaf, P., Kjellgren, Y., & Ahrens, L. (2021). Foam fractionation removal of multiple per- and polyfluoroalkyl substances from landfill leachate. *AWWA Water Science*, *3*(5), 1–14. https://doi.org/https://doi.org/10.1002/aws2.1238

McCleaf, P., Stefansson, W., & Ahrens, L. (2023). Drinking water nanofiltration with concentrate foam fractionation—A novel approach for removal of per- and polyfluoroalkyl substances (PFAS). *Water Research*, *232*, 119688.

https://doi.org/10.1016/j.watres.2023.119688
McDonough, J. T., Kirby, J., Bellona, C., Quinnan, J. A., Welty, N., Follin, J., & Liberty, K. (2022). Validation of supercritical water oxidation to destroy perfluoroalkyl acids. *Remediation*, *32*(1–2), 75–90. https://doi.org/10.1002/rem.21711
McNamara, J. D., Franco, R., Mimna, R., & Zappa, L. (2017). Comparison of Activated Carbons for Removal of Perfluorinated Compounds From Drinking Water. *Journal - American Water Works Association*, *110*, E1–E14. https://doi.org/https://doi.org/10.5942/jawwa.2018.110.0003
Mei, W., Sun, H., Song, M., Jiang, L., Li, Y., Lu, W., Ying, G. G., Luo, C., & Zhang, G. (2021). Per- and polyfluoroalkyl substances (PFASs) in the soil–plant system: Sorption, root uptake, and translocation. *Environment International*, *156*, 106642. https://doi.org/10.1016/j.envint.2021.106642
Mejia Avendaño, S., Zhong, G., & Liu, J. (2015). Comment on "Biodegradation of perfluorooctanesulfonate (PFOS) as an emerging contaminant." *Chemosphere*, *138*, 1037–1038. https://doi.org/10.1016/j.chemosphere.2015.03.022
Meng, P., Deng, S., Maimaiti, A., Wang, B., Huang, J., Wang, Y., Cousins, I. T., & Yu, G. (2018). Efficient removal of perfluorooctane sulfonate from aqueous film-forming foam solution by aeration-foam collection. *Chemosphere*, *203*, 263–270. https://doi.org/10.1016/j.chemosphere.2018.03.183
Merino, N., Wang, M., Ambrocio, R., Mak, K., O'Connor, E., Gao, A., Hawley, E. L., Deeb, R. A., Tseng, L. Y., & Mahendra, S. (2018). Fungal biotransformation of 6:2 fluorotelomer alcohol. *Remediation*, *28*(2), 59–70. https://doi.org/10.1002/rem.21550
Moussa, D. T., El-Naas, M. H., Nasser, M., & Al-Marri, M. J. (2017). A comprehensive review of electrocoagulation for water treatment: Potentials and challenges. *Journal of Environmental Management*, *186*, 24–41. https://doi.org/10.1016/j.jenvman.2016.10.032
Mudumbi, J. B. N., Ntwampe, S. K. O., Muganza, M., & Okonkwo, J. O. (2014). Susceptibility of Riparian Wetland Plants to Perfluorooctanoic Acid (PFOA) Accumulation. *International Journal of Phytoremediation*, *16*(9), 926–936. https://doi.org/10.1080/15226514.2013.810574
Murray, C. C., Marshall, R. E., Liu, C. J., Vatankhah, H., & Bellona, C. L. (2021). PFAS treatment with granular activated carbon and ion exchange resin: Comparing chain length, empty bed contact time, and cost. *Journal of Water Process Engineering*, *44*, 102342. https://doi.org/10.1016/j.jwpe.2021.102342
National Institute for Public Health and the Environment (RIVM). (2022). *Risicogrenzen voor PFAS in oppervlaktewater*.
Nau-Hix, C., Multari, N., Singh, R. K., Richardson, S., Kulkarni, P., Anderson, R. H., Holsen, T. M., & Thagard, S. M. (2021). Field Demonstration of a Pilot-Scale Plasma Reactor for the Rapid Removal of Poly- and Perfluoroalkyl Substances in Groundwater. *ACS ES&T Water*, *1*(3), 680–687. https://doi.org/10.1021/acsestwater.0c00170

Nienhauser, A. B., Ersan, M. S., Lin, Z., Perreault, F., Westerhoff, P., & Garcia-Segura, S. (2022). Boron-doped diamond electrodes degrade short- and long-chain per- and polyfluorinated alkyl substances in real industrial wastewaters. *Journal of Environmental Chemical Engineering*, *10*(2), 107192. https://doi.org/10.1016/j.jece.2022.107192

Nriagu, J. O. (1990). The rise and fall of leaded gasoline. *Science of the Total Environment*, *92*, 13–28. https://doi.org/10.1016/0048-9697(90)90318-O

Palma, D., Richard, C., & Minella, M. (2022). State of the art and perspectives about non-thermal plasma applications for the removal of PFAS in water. *Chemical Engineering Journal Advances*, *10*, 100253. https://doi.org/10.1016/j.ceja.2022.100253

Paul, A. G., Jones, K. C., & Sweetman, A. J. (2009). A first global production, emission, and environmental inventory for perfluorooctane sulfonate. *Environmental Science and Technology*, *43*(2), 386–392. https://doi.org/10.1021/es802216n

Pierpaoli, M., Szopińska, M., Wilk, B. K., Sobaszek, M., Łuczkiewicz, A., Bogdanowicz, R., & Fudala-Książek, S. (2021). Electrochemical oxidation of PFOA and PFOS in landfill leachates at low and highly boron-doped diamond electrodes. *Journal of Hazardous Materials*, *403*, 123606. https://doi.org/10.1016/j.jhazmat.2020.123606

Pinkard, B. R., Shetty, S., Stritzinger, D., Bellona, C., & Novosselov, I. V. (2021). Destruction of perfluorooctanesulfonate (PFOS) in a batch supercritical water oxidation reactor. *Chemosphere*, *279*, 130834. https://doi.org/10.1016/j.chemosphere.2021.130834

Post, G. B. (2021). Recent US State and Federal Drinking Water Guidelines for Per- and Polyfluoroalkyl Substances. *Environmental Toxicology and Chemistry*, *40*(3), 550–563. https://doi.org/10.1002/etc.4863

Prevedouros, K., Cousins, I. T., Buck, R. C., & Korzeniowski, S. H. (2006). Sources, fate and transport of perfluorocarboxylates. *Environmental Science and Technology*, *40*(1), 32–44. https://doi.org/10.1021/es0512475

Qanbarzadeh, M., Wang, D., Ateia, M., Sahu, S. P., & Cates, E. L. (2021). Impacts of Reactor Configuration, Degradation Mechanisms, and Water Matrices on Perfluorocarboxylic Acid Treatment Efficiency by the UV/Bi 3 O(OH)(PO 4) 2 Photocatalytic Process . *ACS ES&T Engineering*, *1*(2), 239–248. https://doi.org/10.1021/acsestengg.0c00086

Qian, Y., Guo, X., Zhang, Y., Peng, Y., Sun, P., Huang, C. H., Niu, J., Zhou, X., & Crittenden, J. C. (2016). Perfluorooctanoic Acid Degradation Using UV-Persulfate Process: Modeling of the Degradation and Chlorate Formation. *Environmental Science and Technology*, *50*(2), 772–781. https://doi.org/10.1021/acs.est.5b03715

Radjenovic, J., Duinslaeger, N., Avval, S. S., & Chaplin, B. P. (2020). Facing the Challenge of Poly- and Perfluoroalkyl Substances in Water: Is Electrochemical Oxidation the Answer? *Environmental Science & Technology*, *54*, 14815–14829. https://doi.org/10.1021/acs.est.0c06212

Radjenovic, J., & Sedlak, D. L. (2015). Challenges and Opportunities for Electrochemical Processes as Next-Generation Technologies for the Treatment of Contaminated Water. *Environmental Science and Technology*, *49*(19), 11292–11302. https://doi.org/10.1021/acs.est.5b02414

Rayne, S., Forest, K., & Friesen, K. J. (2008). Congener-specific numbering systems for the environmentally relevant C4 through C8 perfluorinated homologue groups of alkyl sulfonates, carboxylates, telomer alcohols, olefins, and acids, and their derivatives. *Journal of Environmental Science and Health - Part A Toxic/Hazardous Substances and Environmental Engineering*, *43*(12), 1391–1401. https://doi.org/10.1080/10934520802232030

Rickard, B. P., Rizvi, I., & Fenton, S. E. (2022). Per- and poly-fluoroalkyl substances (PFAS) and female reproductive outcomes: PFAS elimination, endocrine-mediated effects, and disease. *Toxicology*, *465*, 153031. https://doi.org/10.1016/j.tox.2021.153031

RIVM. (2021). *Analyse bijdrage drinkwater en voedsel aan blootstelling EFSA-4 PFAS in Nederland en advies drinkwaterrichtwaarde*. https://www.rivm.nl/documenten/analyse-bijdrage-drinkwater-en-voedsel-aan-blootstelling-efsa-4-pfas-in-nederland

Rodowa, A. E., Knappe, D. R. U., Chiang, S. Y. D., Pohlmann, D., Varley, C., Bodour, A., & Field, J. A. (2020). Pilot scale removal of per- and polyfluoroalkyl substances and precursors from AFFF-impacted groundwater by granular activated carbon. *Environmental Science: Water Research and Technology*, *6*(4), 1083–1094. https://doi.org/10.1039/c9ew00936a

Rodriguez-Freire, L., Abad-Fernández, N., Sierra-Alvarez, R., Hoppe-Jones, C., Peng, H., Giesy, J. P., Snyder, S., & Keswani, M. (2016). Sonochemical degradation of perfluorinated chemicals in aqueous film-forming foams. *Journal of Hazardous Materials*, *317*, 275–283. https://doi.org/10.1016/j.jhazmat.2016.05.078

Ruiz-Urigüen, M., Shuai, W., Huang, S., & Jaffé, P. R. (2022). Biodegradation of PFOA in microbial electrolysis cells by Acidimicrobiaceae sp. strain A6. *Chemosphere*, *292*, 133506. https://doi.org/10.1016/j.chemosphere.2021.133506

Savage, P. E. (1999). Organic Chemical Reactions in Supercritical Water. *Chemical Reviews*, *99*(2), 603–621. https://doi.org/10.1021/cr9700989

Schaefer, C. E., Andaya, C., Burant, A., Condee, C. W., Urtiaga, A., Strathmann, T. J., & Higgins, C. P. (2017). Electrochemical treatment of perfluorooctanoic acid and perfluorooctane sulfonate: Insights into mechanisms and application to groundwater treatment. *Chemical Engineering Journal*, *317*, 424–432. https://doi.org/10.1016/j.cej.2017.02.107

Schaefer, C. E., Andaya, C., Maizel, A., & Higgins, C. P. (2019). Assessing Continued Electrochemical Treatment of Groundwater Impacted by Aqueous Film-Forming Foams. *Journal of Environmental Engineering*, *145*(12), 06017009. https://doi.org/10.1061/(ASCE)EE.1943-7870.0001605

Schaefer, C. E., Choyke, S., Ferguson, P. L., Andaya, C., Burant, A., Maizel, A.,

Strathmann, T. J., & Higgins, C. P. (2018). Electrochemical Transformations of Perfluoroalkyl Acid (PFAA) Precursors and PFAAs in Groundwater Impacted with Aqueous Film Forming Foams. *Environmental Science and Technology*, *52*(18), 10689–10697. https://doi.org/10.1021/acs.est.8b02726

Secretariat of the Stockholm Convention. (2022). *PFASs listed under the Stockholm Convention*. http://chm.pops.int/Implementation/IndustrialPOPs/PFAS/Overview/tabid/5221/Default.aspx

Shahsavari, E., Rouch, D., Khudur, L. S., Thomas, D., Aburto-Medina, A., & Ball, A. S. (2021). Challenges and Current Status of the Biological Treatment of PFAS-Contaminated Soils. *Frontiers in Bioengineering and Biotechnology*, *8*, 602040. https://doi.org/10.3389/fbioe.2020.602040

Sharma, S., Shetti, N. P., Basu, S., Nadagouda, M. N., & Aminabhavi, T. M. (2022). Remediation of per- and polyfluoroalkyls (PFAS) via electrochemical methods. *Chemical Engineering Journal*, *430*(P2), 132895. https://doi.org/10.1016/j.cej.2021.132895

Shi, H., Chiang, S. Y. (Dora), Wang, Y., Wang, Y., Liang, S., Zhou, J., Fontanez, R., Gao, S., & Huang, Q. (2021). An electrocoagulation and electrooxidation treatment train to remove and degrade per- and polyfluoroalkyl substances in aqueous solution. *Science of the Total Environment*, *788*, 147723. https://doi.org/10.1016/j.scitotenv.2021.147723

Shi, H., Wang, Y., Li, C., Pierce, R., Gao, S., & Huang, Q. (2019). Degradation of Perfluorooctanesulfonate by Reactive Electrochemical Membrane Compose of Magnéli Phase Titanium Suboxie. *Environmental Science and Technology*, *53*(24), 14528–14537. https://doi.org/10.1021/acs.est.9b04148

Sidnell, T., Wood, R. J., Hurst, J., Lee, J., & Bussemaker, M. J. (2022). Sonolysis of per- and poly fluoroalkyl substances (PFAS): A meta-analysis. *Ultrasonics Sonochemistry*, *87*, 105944. https://doi.org/10.1016/j.ultsonch.2022.105944

Singh, R. K., Brown, E., Mededovic Thagard, S., & Holsen, T. M. (2021). Treatment of PFAS-containing landfill leachate using an enhanced contact plasma reactor. *Journal of Hazardous Materials*, *408*(November 2020), 124452. https://doi.org/10.1016/j.jhazmat.2020.124452

Singh, R. K., Multari, N., Nau-Hix, C., Anderson, R. H., Richardson, S. D., Holsen, T. M., & Mededovic Thagard, S. (2019). Rapid Removal of Poly- and Perfluorinated Compounds from Investigation-Derived Waste (IDW) in a Pilot-Scale Plasma Reactor. *Environmental Science and Technology*, *53*(19), 11375–11382. https://doi.org/10.1021/acs.est.9b02964

Singh, R. K., Multari, N., Nau-Hix, C., Woodard, S., Nickelsen, M., Mededovic Thagard, S., & Holsen, T. M. (2020). Removal of Poly- And Per-Fluorinated Compounds from Ion Exchange Regenerant Still Bottom Samples in a Plasma Reactor. *Environmental Science and Technology*, *54*(21), 13973–13980. https://doi.org/10.1021/acs.est.0c02158

Siriwardena, D. P., James, R., Dasu, K., Thorn, J., Iery, R. D., Pala, F., Schumitz, D., Eastwood, S., & Burkitt, N. (2021). Regeneration of per- and

polyfluoroalkyl substance-laden granular activated carbon using a solvent based technology. *Journal of Environmental Management*, *289*, 112439. https://doi.org/10.1016/j.jenvman.2021.112439

Sonmez Baghirzade, B., Zhang, Y., Reuther, J. F., Saleh, N. B., Venkatesan, A. K., & Apul, O. G. (2021). Thermal Regeneration of Spent Granular Activated Carbon Presents an Opportunity to Break the Forever PFAS Cycle. *Environmental Science and Technology*, *55*(9), 5608–5619. https://doi.org/10.1021/acs.est.0c08224

Soriano, Á., Gorri, D., & Urtiaga, A. (2017). Efficient treatment of perfluorohexanoic acid by nanofiltration followed by electrochemical degradation of the NF concentrate. *Water Research*, *112*, 147–156. https://doi.org/10.1016/j.watres.2017.01.043

Soriano, Á., Gorri, D., & Urtiaga, A. (2019). Membrane preconcentration as an efficient tool to reduce the energy consumption of perfluorohexanoic acid electrochemical treatment. *Separation and Purification Technology*, *208*, 160–168. https://doi.org/10.1016/j.seppur.2018.03.050

Soriano, Á., Schaefer, C., & Urtiaga, A. (2020). Enhanced treatment of perfluoroalkyl acids in groundwater by membrane separation and electrochemical oxidation. *Chemical Engineering Journal Advances*, *4*, 100042. https://doi.org/10.1016/j.ceja.2020.100042

Sunderland, E. M., Hu, X. C., Dassuncao, C., Tokranov, A. K., Wagner, C. C., & Allen, J. G. (2019). A review of the pathways of human exposure to poly- and perfluoroalkyl substances (PFASs) and present understanding of health effects. *Journal of Exposure Science and Environmental Epidemiology*, *29*(2), 131–147. https://doi.org/10.1038/s41370-018-0094-1

Svenska MiljöEmissionsData (SMED). (2021). *Emissionsfaktor för nordisk elmix med hänsyn till import och export*. Rapport Nr. 4 2021. https://smed.se/luft-och-klimat/4708

Swedish Agency for Marine and Water Management. (2019). *Havs- och vattenmyndighetens föreskrifter om klassificering och miljökvalitetsnormer avseende ytvatten - HVMFS 2019:25*. https://viss.lansstyrelsen.se/ReferenceLibrary/55035/HVMFS 2019-25-ev.pdf

Swedish Food Agency. (2022). *Livsmedelsverkets föreskrifter om dricksvatten*. https://www.livsmedelsverket.se/globalassets/om-oss/lagstiftning/dricksvatten---naturl-mineralv---kallv/livsfs-2022-12_web_t.pdf

The European Parliament and the Council of the European Union. (2020). Directive (EU) 2020/2184 of the European Parliament and of the Council of 16 December 2020 on the quality of water intended for human consumption. *Official Journal of the European Union*, *435*, 1–62. http://data.europa.eu/eli/dir/2020/2184/oj

Tow, E. W., Ersan, M. S., Kum, S., Lee, T., Speth, T. F., Owen, C., Bellona, C., Nadagouda, M. N., Mikelonis, A. M., Westerhoff, P., Mysore, C., Frenkel, V. S., Desilva, V., Walker, W. S., Safulko, A. K., & Ladner, D. A. (2021).

Managing and treating per-and polyfluoroalkyl substances (PFAS) in membrane concentrates. *AWWA Water Science*, *3*(5), 1–23. https://doi.org/10.1002/aws2.1233

Trautmann, A. M., Schell, H., Schmidt, K. R., Mangold, K. M., & Tiehm, A. (2015). Electrochemical degradation of perfluoroalkyl and polyfluoroalkyl substances (PFASs) in groundwater. *Water Science and Technology*, *71*(10), 1569–1575. https://doi.org/10.2166/wst.2015.143

Tröger, R., Köhler, S. J., Franke, V., Bergstedt, O., & Wiberg, K. (2020). A case study of organic micropollutants in a major Swedish water source – Removal efficiency in seven drinking water treatment plants and influence of operational age of granulated active carbon filters. *Science of the Total Environment*, *706*, 135680. https://doi.org/10.1016/j.scitotenv.2019.135680

Tseng, N., Wang, N., Szostek, B., & Mahendra, S. (2014). Biotransformation of 6:2 Fluorotelomer alcohol (6:2 FTOH) by a wood-rotting fungus. *Environmental Science and Technology*, *48*(7), 4012–4020. https://doi.org/10.1021/es4057483

Ullberg, M., Lavonen, E., Köhler, S. J., Golovko, O., & Wiberg, K. (2021). Pilot-scale removal of organic micropollutants and natural organic matter from drinking water using ozonation followed by granular activated carbon. *Environmental Science: Water Research and Technology*, *7*(3), 535–548. https://doi.org/10.1039/d0ew00933d

Urtiaga, A., Gómez-Lavín, S., & Soriano, A. (2022). Electrochemical treatment of municipal landfill leachates and implications for poly- and perfluoroalkyl substances (PFAS) removal. *Journal of Environmental Chemical Engineering*, *10*(3), 107900. https://doi.org/10.1016/j.jece.2022.107900

US EPA. (2022a). *Draft Aquatic Life Ambient Water Quality Criteria for Perfluorooctane Sulfonate (PFOS)*. https://www.epa.gov/wqc/aquatic-life-criteria-perfluorooctane-sulfonate-pfos

US EPA. (2022b). *Draft Aquatic Life Ambient Water Quality Criteria for Perfluorooctanoic Acid (PFOA)*. https://www.epa.gov/wqc/aquatic-life-criteria-perfluorooctanoic-acid-pfoa

US EPA. (2023). *Proposed PFAS National Primary Drinking Water Regulation*. https://www.epa.gov/sdwa/and-polyfluoroalkyl-substances-pfas

Uwayezu, J. N., Carabante, I., Lejon, T., van Hees, P., Karlsson, P., Hollman, P., & Kumpiene, J. (2021). Electrochemical degradation of per- and poly-fluoroalkyl substances using boron-doped diamond electrodes. *Journal of Environmental Management*, *290*, 112573. https://doi.org/10.1016/j.jenvman.2021.112573

Vo, P. H. N., Buckley, T., Xu, X., Nguyen, T. M. H., Rudolph, V., & Shukla, P. (2023). Foam fractionation of per- and polyfluoroalkyl substances (PFASs) in landfill leachate using different cosurfactants. *Chemosphere*, *310*, 136869. https://doi.org/10.1016/j.chemosphere.2022.136869

Wang, J., Lin, Z., He, X., Song, M., Westerho, P., Doudrick, K., & Hanigan, D. (2022). Critical Review of Thermal Decomposition of Per- and

Polyfluoroalkyl Substances : Mechanisms and Implications for Thermal Treatment Processes. *Environmental Science & Technology*, *56*(9), 5355–5370. https://doi.org/10.1021/acs.est.2c02251

Wang, Y., Ji, Y., Tishchenko, V., & Huang, Q. (2023). Removing per- and polyfluoroalkyl substances (PFAS) in water by foam fractionation. *Chemosphere*, *311*(P2), 137004. https://doi.org/10.1016/j.chemosphere.2022.137004

Wang, Z., Buser, A. M., Cousins, I. T., Demattio, S., Drost, W., Johansson, O., Ohno, K., Patlewicz, G., Richard, A. M., Walker, G. W., White, G. S., & Leinala, E. (2021). A New OECD Definition for Per- And Polyfluoroalkyl Substances. *Environmental Science and Technology*, *55*(23), 15575–15578. https://doi.org/10.1021/acs.est.1c06896

Wang, Z., Dewitt, J. C., Higgins, C. P., & Cousins, I. T. (2017). A Never-Ending Story of Per- and Polyfluoroalkyl Substances (PFASs)? *Environmental Science and Technology*, *51*(5), 2508–2518. https://doi.org/10.1021/acs.est.6b04806

Wei, Z., Xu, T., & Zhao, D. (2019). Treatment of per- And polyfluoroalkyl substances in landfill leachate: Status, chemistry and prospects. *Environmental Science: Water Research and Technology*, *5*(11), 1814–1835. https://doi.org/10.1039/c9ew00645a

Weiss, J. M., Andersson, P. L., Lamoree, M. H., Leonards, P. E. G., Van Leeuwen, S. P. J., & Hamers, T. (2009). Competitive binding of poly- and perfluorinated compounds to the thyroid hormone transport protein transthyretin. *Toxicological Sciences*, *109*(2), 206–216. https://doi.org/10.1093/toxsci/kfp055

Wofsy, S. C., McElroy, M. B., & Sze, N. D. (1975). Freon consumption: Implications for atmospheric Ozone. *Science*, *187*(4176), 535–537. https://doi.org/10.1126/science.187.4176.535

Wood, R. J., Sidnell, T., Ross, I., McDonough, J., Lee, J., & Bussemaker, M. J. (2020). Ultrasonic degradation of perfluorooctane sulfonic acid (PFOS) correlated with sonochemical and sonoluminescence characterisation. *Ultrasonics Sonochemistry*, *68*, 105196. https://doi.org/10.1016/j.ultsonch.2020.105196

Woodard, S., Berry, J., & Newman, B. (2017). Ion exchange resin for PFAS removal and pilot test comparison to GAC. *Remediation*, *27*(3), 19–27. https://doi.org/10.1002/rem.21515

Xiao, F., Sasi, P. C., Yao, B., Kubátová, A., Golovko, S. A., Golovko, M. Y., & Soli, D. (2020). Thermal Stability and Decomposition of Perfluoroalkyl Substances on Spent Granular Activated Carbon. *Environmental Science and Technology Letters*, *7*(5), 343–350. https://doi.org/10.1021/acs.estlett.0c00114

Xiao, X., Ulrich, B. A., Chen, B., & Higgins, C. P. (2017). Sorption of Poly- and Perfluoroalkyl Substances (PFASs) Relevant to Aqueous Film-Forming Foam (AFFF)-Impacted Groundwater by Biochars and Activated Carbon. *Environmental Science and Technology*, *51*(11), 6342–6351.

https://doi.org/10.1021/acs.est.7b00970

Yang, B., Han, Y., Yu, G., Zhuo, Q., Deng, S., Wu, J., & Zhang, P. (2016). Efficient removal of perfluoroalkyl acids (PFAAs) from aqueous solution by electrocoagulation using iron electrode. *Chemical Engineering Journal*, *303*, 384–390. https://doi.org/10.1016/j.cej.2016.06.011

Yi, L. B., Chai, L. Y., Xie, Y., Peng, Q. J., & Peng, Q. Z. (2016). Isolation, identification, and degradation performance of a PFOA-degrading strain. *Genetics and Molecular Research*, *15*(2), 1–12. https://doi.org/10.4238/gmr.15028043

Yin, T., Chen, H., Reinhard, M., Yi, X., He, Y., & Gin, K. Y. H. (2017). Perfluoroalkyl and polyfluoroalkyl substances removal in a full-scale tropical constructed wetland system treating landfill leachate. *Water Research*, *125*, 418–426. https://doi.org/10.1016/j.watres.2017.08.071

Zhang, C., Peng, Y., Ning, K., Niu, X., Tan, S., & Su, P. (2014). Remediation of Perfluoroalkyl Substances in Landfill Leachates by Electrocoagulation. *Clean - Soil, Air, Water*, *42*(12), 1740–1743. https://doi.org/10.1002/clen.201300563

Zhang, Z., Sarkar, D., Biswas, J. K., & Datta, R. (2022). Biodegradation of per- and polyfluoroalkyl substances (PFAS): A review. *Bioresource Technology*, *344*(PB), 126223. https://doi.org/10.1016/j.biortech.2021.126223

Zhi, Y., & Liu, J. (2015). Adsorption of perfluoroalkyl acids by carbonaceous adsorbents: Effect of carbon surface chemistry. *Environmental Pollution*, *202*, 168–176. https://doi.org/10.1016/j.envpol.2015.03.019

Popular science summary

PFAS, or per- and polyfluoroalkyl substances, are a useful group of chemicals. They make non-stick pans non-sticky and fabrics water repellent, and they are used to produce electronics, firefighting foams, industrial lubricants and all other sorts of products. A large part of the usefulness of PFAS comes from the fact that they are persistent, meaning that it is very difficult to destroy them. However, this persistency also has a downside: once PFAS end up in the environment, they tend to stay there. Combined with the fact that PFAS can also be very mobile, it has now become virtually impossible to find anything in the environment that is not contaminated with these chemicals.

This widespread occurrence of PFAS is a problem, because some PFAS are known to cause a range of health problems in humans. The same PFAS for which these effects have been shown most extensively are often also bioaccumulative, which means that concentrations of some PFAS in your body can increase during your lifetime. It is thus extremely important to prevent human exposure to these chemicals. An important pathway by which PFAS reach the environment is through the discharge of PFAS-contaminated water. Treating these types of water before they reach the environment is thus essential to ensure that human food or drinking water stay PFAS-free, or at least contain as low concentrations of PFAS as possible.

PFAS are often found in industrial or municipal wastewater and in the wastewater that originates from landfills (leachate). The methods that are generally used to treat these kinds of water were not designed to remove PFAS, so they have very low removal efficiencies. In my studies, I looked into two alternative treatment methods, called foam fractionation and electrochemical oxidation. Foam fractionation is a method that can remove PFAS as a concentrated foam, but it does not destroy the PFAS.

Electrochemical oxidation uses electricity to actually destroy the PFAS, but it requires a lot more energy than foam fractionation.

Foam fractionation works by adsorbing PFAS from the water on rising air bubbles, followed by the formation of foam on the surface of the water. By removing this foam, the remaining water becomes relatively PFAS-free. I started with optimizing a foam fractionation system for the removal of PFAS from landfill leachate. Here, up to 60 % of the total PFAS content was removed, but not all of the removed PFAS was found back in the foam. In a follow-up study on PFAS-contaminated industrial water, I investigated if these disappearing PFAS were emitted to the air instead. In this study, the total PFAS removal reached up to 84%, and most of the removed PFAS was found back in the foam. However, we also found high PFAS emissions to the air, so it is important to install filters on the air outlet of foam fractionation reactors.

Electrochemical oxidation could destroy PFAS in landfill leachate and in groundwater from below the same landfill. Additionally, it could also destroy PFAS in the foam from the foam fractionation on both of these water types. The total PFAS degradation was higher when treating the contaminated water directly than when treating the foam. On the other hand, the energy use was much lower for treatment of the foam, so combining foam fractionation with electrochemical oxidation could be a good way to destroy PFAS in water.

Foam formation on the water surface of existing wastewater treatment plants is quite common. In the final part of this thesis, I thus investigated if this type of foam formation could be combined with removal of PFAS. PFAS concentrations in the foam from existing treatment processes were up to 100,000 times higher than concentrations in the influent to the process, but this did not lead to measurable PFAS removal from influent to effluent. However, it is possible that implementing process changes and removal of the foam could lead to considerable PFAS removal in existing wastewater treatment plants. Altogether, this thesis contributes to an increased understanding of treatment options for PFAS-contaminated water, with a particular focus on FF and EO.

Populärvetenskaplig sammanfattning

PFAS, eller per- och polyfluoralkylämnen, är en användbar grupp av kemikalier. De finns i teflonpannornas non-stick-beläggning, gör tyger vattenavvisande och används för att producera elektronik, brandskum, industriella smörjmedel och många andra produkter. En stor del av nyttan med PFAS kommer från det faktum att de är långlivade, vilket innebär att de är mycket svårt att förstöra. Men denna uthållighet har också en baksida: när PFAS väl hamnat i miljön kommer de att stanna där. I kombination med att PFAS sprids lätt i miljön har det nu blivit så gott som omöjligt att hitta något alls som inte är förorenat med dessa kemikalier.

Denna omfattande förekomst av PFAS är ett problem, eftersom vissa PFAS är kända för att orsaka en rad hälsoproblem hos människor. Samma PFAS som orsakar dessa effekter är ofta också bioackumulerande, vilket innehåller att koncentrationerna av vissa PFAS i din kropp kan öka under din livstid. Det är därför mycket viktigt att förhindra människors exponering för dessa kemikalier. En viktig väg för PFAS att nå miljön är genom utsläpp av PFAS-förorenat vatten. Att behandla dessa typer av vatten innan de når miljön är därför angeläget, för att säkerställa att mat och dricksvatten förblir PFAS-fritt, eller åtminstone har låga halter.

PFAS finns ofta i industriellt eller kommunalt avloppsvatten och i lakvatten från avfallsdeponier. De metoder som vi vanligtvis behandlar förorenat vatten med är inte utformade för att ta bort PFAS, så reningseffektiviteten är låg. I mina studier utforskade jag två alternativa metoder, så kallad skumfraktionering och elektrokemisk oxidation. Skumfraktionering kan ta bort PFAS som ett koncentrerat skum, men bryter inte ner PFAS. Elektrokemisk oxidation använder elektricitet för att ta bort PFAS genom att bryta ner molekylerna, men kräver mycket mer energi än skumfraktionering.

Skumfraktionering fungerar genom att adsorbera PFAS från vattnet på stigande luftbubblor, följt av skumbildning på vattenytan. Genom att ta bort detta skum blir det kvarvarande vattnet relativt PFAS-fritt. Jag började med att undersöka ett skumfraktioneringssystem för att ta bort PFAS från lakvatten från en deponi. Upp till 60 % av den totala PFAS-halten togs bort, men all borttagen PFAS återfanns inte i skummet. I en uppföljande studie av PFAS-förorenat industrivatten undersökte jag om förluster av PFAS vid skumfraktionering kunde bero på avgång till luft. I den här studien renades PFAS bort med upp till 84 %, och det mesta av det borttagna PFAS hittades i skummet. Men jag fann även höga PFAS-halter i omgivande luft, och det visar att det är viktigt att installera filter på luftutflöden från skumfraktioneringsreaktorer.

Elektrokemisk oxidation kunde bryta ner PFAS i lakvatten från en deponi och i grundvatten från samma deponi. Dessutom kunde denna metod också förstöra PFAS i skummet från skumfraktioneringen för båda dessa vattentyper. Den totala PFAS-nedbrytningen var högre vid direkt behandling av det förorenade vattnet än vid behandling av skummet. Å andra sidan var energianvändningen mycket lägre för behandling av skummet, så att kombinera skumfraktionering med elektrokemisk oxidation kan vara ett bra sätt att ta bort PFAS från förorenat vatten.

Skumbildning på vattenytan i befintliga avloppsreningsverk är ganska vanligt. Jag undersökte därför om denna typ av skumbildning kunde kombineras med avlägsnande av PFAS. PFAS-koncentrationerna i skummet från befintliga reningsprocesser var upp till 100 000 gånger högre än koncentrationerna i inflödet till processen, men detta ledde inte till mätbar PFAS-rening från inflöde till utflöde. Det är dock möjligt att införandet av processförändringar och borttagning av skummet kan leda till betydande PFAS-borttagning i befintliga avloppsreningsverk. Sammantaget bidrar denna avhandling till en ökad förståelse för behandlingsalternativ för PFAS-förorenat vatten, med särskilt fokus på FF och EO.

Acknowledgements

Thank you to **Karin Wiberg**, for always making time to understand my projects, thoroughly edit my manuscripts and talk to me about all aspects of life. I will miss your enthusiasm, dedication and our discussions about volleyball ;) Thanks also to **Lutz Ahrens, Hans Peter Arp** and **Philip McCleaf**, for sharing your expertise and helping me organize, operate and model my pilot systems.

Björn and Malin: I probably would have quit in my first year if it wasn't for the two of you. Thank you so much for everything. **Paul**: Thanks for all our runs and gym-sessions, the stimulating discussions and for believing so strongly in me. **Svante**: If I ever fail at avoiding analytical chemistry for the rest of my career, I'll know where to find you. Thanks for your help, and your patience. **Michel**: Thank you for always being positive, interested in everyone and a joy to work with. **Valentina**: Thanks for being a great Sciex buddy, for sharing my frustration about many things, and for so actively trying to fix them.

Everyone else at SLU: Thank you for the pubs, the fikas, the dinners, the parties, and for always listening to me complaining about Sweden in general and its winters in particular…

The PERFORCE3 ESRs: It was truly wonderful to share this experience with you. I love how close we have gotten, and I hope we can make yearly reunions a tradition!

Thank you to the rest of my co-authors and co-workers: **Sofia Bjälkefur Seroka** for the rides to Hovgården and your endless patience with my ever-changing plans; **Timo Hamers, Peter Cenijn** and everyone else at the VU for welcoming me and teaching me about bioassays, **Mélanie Lauria** for doing such an excellent job on the EOF analyses; **Patrik Hollman** for the construction of the BDD EO cell and all your help with fixing its leaks;

Jeffrey Lewis for your refreshing no-nonsense approach that is often difficult to find in academia, as well as everyone else at ECT2 for creating such an inspiring company; **Erik Wall** and **Svante Skarpås** for all the help and excellent organization at Cytiva; **Chantal Keane** and everyone else who contributed to paper IV for sending samples and checking the manuscript; **Elin Eriksson** for answering all my questions and for the outstanding lab organization; **Theo Kalogeropoulos** and everyone at Sciex for all the long hours assisting me with fixing our instrument; and **John Smit** for introducing me to the world of PFAS in landfill leachate, lending me Afvalzorg's potentiostat and always being available for help.

Finally, a big thank you to my family and friends back home, for putting things into perspective, providing me with much-needed mental sanity, always being available for skype sessions and (**Dad & Geranne**) for hosting me during all my secondments to the NL. **Gianno**: thank you for joining me in this forlorn country, listening to me talk about foam for hours on end, pretending to read my papers and letting me practice all my presentations on you. You have been so much more important than you realize.

This project was funded by the European Union's Horizon 2020 programme as part of the PERFORCE3 international training network (grant agreement 860665).

I

ACS ES&T Water

pubs.acs.org/estwater

Article

Pilot-Scale Continuous Foam Fractionation for the Removal of Per- and Polyfluoroalkyl Substances (PFAS) from Landfill Leachate

Sanne J. Smith,* Karin Wiberg, Philip McCleaf, and Lutz Ahrens

Cite This: *ACS EST Water* 2022, 2, 841−851

Read Online

ACCESS | Metrics & More | Article Recommendations | Supporting Information

ABSTRACT: Per- and polyfluoroalkyl substances (PFAS) are of concern for their ubiquity in the environment combined with their persistent, bioaccumulative, and toxic properties. Landfill leachate is often contaminated with these chemicals, and therefore, the development of cost-efficient water treatment technologies is urgently needed. The present study investigated the applicability of a pilot-scale foam fractionation setup for the removal of PFAS from natural landfill leachate in a novel continuous operating mode. A benchmark batch test was also performed to compare treatment efficiency. The ΣPFAS removal efficiency plateaued around 60% and was shown to decrease for the investigated process variables air flow rate (Q_{air}), collected foam fraction ($\%_{foam}$) and contact time in the column (t_c). For individual long-chain PFAS, removal efficiencies above 90% were obtained, whereas the removal for certain short-chain PFAS was low (<30%). Differences in treatment efficiency between enriching mode versus stripping mode as well as between continuous versus batch mode were negligible. Taken together, these findings suggest that continuous foam fractionation is a highly applicable treatment technology for PFAS contaminated water. Coupling the proposed cost- and energy-efficient foam fractionation pretreatment to an energy-intensive degradative technology for the concentrated foam establishes a promising strategy for on-site PFAS remediation.

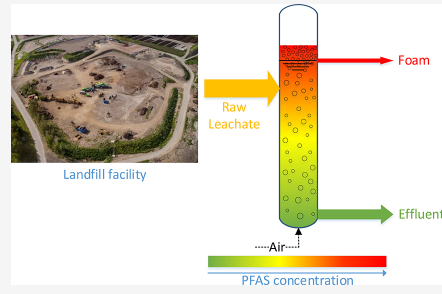

KEYWORDS: *per- and polyfluoroalkyl substances, water treatment, foam fractionation, landfill leachate, pilot-scale*

1. INTRODUCTION

Per- and polyfluoroalkyl substances (PFAS) are a class of persistent, bioaccumulative, and toxic chemicals that have become widespread in the environment.[1] They are used in consumer products, industrial applications, and firefighting foams for their high water and oil resistance, as well as for their surfactant properties.[2−4] An increasing amount of research continues to show their extensive prevalence in the environment as well as their toxicity to both humans and animals.[5,6] The most well-known class of PFAS are the perfluoroalkyl acids (PFAA), which encompass the perfluoroalkyl carboxylates (PFCA) and perfluoroalkanesulfonates (PFSA).[7] These types of PFAS are commonly used as surfactants and can also be classified on the basis of the length of their hydrophobic perfluoroalkyl tail, with a total perfluorocarbon chain length below six for PFSA and seven for PFAA generally being considered short-chained (PFSA: $C_nF_{2n+1}SO_3H$, $n \leq 5$; PFCA: $C_nF_{2n+1}COOH$, $n \leq 6$).[7,8]

Point sources of contaminated water are an important contributor to the origin of PFAS in the environment,[2] implying that further pollution can be partially prevented by installing appropriate treatment technologies. Examples of such point sources include discharged leachate water from landfills, with total aqueous concentrations ranging from 100 to >100 000 ng L^{-1}.[2,9,10] PFAS in landfills originate from discarded consumer and industrial waste or PFAS-contaminated biosolids. Moreover, landfilled bottom ash from waste incinerators may still contain incompletely combusted PFAS. Biological leaching and physicochemical desorption of these PFAS result in their release to the landfill leachate, leading to high aqueous PFAS concentrations.[9,11] Although the production and use of increasingly many PFAS are banned or restricted,[12,13] landfills store previously produced waste over large timespans; hence, PFAS release from landfills is expected to remain a problem for the foreseeable future.[11]

With PFAS under widespread international scrutiny, limit values for discharge to the environment are becoming more stringent. In 2020, the European Food Safety Authority (EFSA) introduced a tolerably weekly intake of 4.4 ng of perfluorohexanesulfonic acid (PFHxS), perfluorooctanesulfonic acid (PFOS), perfluorooctanoic acid (PFOA), and

Received: January 20, 2022
Revised: March 28, 2022
Accepted: April 22, 2022
Published: May 4, 2022

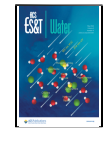

https://doi.org/10.1021/acsestwater.2c00032
ACS EST Water 2022, 2, 841−851

perfluorononanoic acid (PFNA) per kilogram body weight per week.[14] Consequently, to protect drinking water sources, many countries are starting to define concentration limits in environmental waters and hence enforcing treatment of contaminated effluents.[15−17] Common wastewater treatment technologies, such as activated sludge or coagulation, are ineffective toward the removal of most PFAS.[18,19] The current state of the art for PFAS removal from water is adsorption to granular activated carbon (GAC),[20] but GAC needs to be regenerated often, is sensitive to matrix effects, and is less effective in the removal of short-chained PFAS.[21,22] Hence, the development of alternative methods for the treatment of PFAS contaminated water is urgently needed.

Treatment methodologies can be broadly divided into removal and degradation techniques. Where removal technologies aim to concentrate PFAS into a waste fraction that is sent to further treatment, degradation technologies aim to mineralize the PFAS.[23] Examples of removal methods include adsorption, membrane filtration, reverse osmosis, and ion exchange.[20,24−29] Degradation methods include electrochemical oxidation, ultrasonication, advanced reduction processes, plasma treatment, and biological treatment.[20,24−31] Degradation methods have the obvious advantage that the PFAS are destroyed rather than concentrated, but the formation of persistent transformation products can be an issue.[31] Combining multiple removal and degradation approaches into a treatment train process is generally considered the most promising approach for future on-site PFAS remediation.[23]

A removal method that could be highly suitable as a first step in such a treatment train process is foam fractionation, which exploits the surfactant properties of common PFAS and has been applied successfully in full scale for the remediation of PFAS-contaminated groundwater.[32−34] In foam fractionation, PFAS are adsorbed on the surface of gas bubbles rising through water. At the air−water interface, these bubbles form a foam that is enriched in PFAS, so separation and collapse of the foam results in a concentrated foamate and a relatively PFAS-free retentate.[35] The process can be carried out in both batch and continuous operation. In continuous operation, stripping mode refers to operation with the liquid feed stream located above the liquid surface, whereas the feed enters below the foam/water interface in enriching mode.[35,36]

Foam fractionation is a suitable water treatment technology for dilute solutions using only air, thereby eliminating the need for chemicals, solvents, filter material, and adsorbents.[37] Leachate water is a particularly complex matrix to treat, requiring extensive pretreatment before conventional PFAS treatment, such as GAC, ion exchange, or membrane filtration, can be applied successfully.[29] These matrix effects are less problematic in the case of foam fractionation due to a beneficial effect of high ionic strength on the process performance and no risks of clogging or fouling of filter or membrane materials.[3,38,39] Hence, foam fractionation has received increasing attention as a successful technology for PFAS removal from landfill leachate.[36,40,41] However, its applicability is not limited to leachate water but extends to PFAS-contaminated groundwater, process water, and wastewater.[33,34,36,40,42]

An important limitation of foam fractionation is the low removal efficiency of short-chain PFAS.[3,33,38,40−42] Metal cation activators can be used to increase the removal, but this effect has not been shown for short-chain substances.[38,40,43] ΣPFAS removal has further been shown to increase for increasing aeration time,[3,38,40,42] gas flow rate,[3,32,33,40] and ionic strength[3,38,42] and for decreasing initial PFAS concentration.[3,42,43] However, for low initial PFAS concentrations (<50 ng L^{-1}), removal was instead observed to increase at increasing concentration for a wide range of compounds.[40] The effect of pH is ambiguous, with some studies reporting more efficient treatment at low pH,[43] others at intermediate pH,[3] and others at high pH.[32] Most probably, this is because other operating conditions are more influential than pH. Finally, the PFAS concentration in the foam has been shown to depend on the collected foam volume.[3,41]

Reported removal efficiencies strongly depend on the types of PFAS and water matrices under investigation but generally range between 0 and <50% for short-chain PFCA,[33,34,38,40−42] while for long-chain PFAS, efficiencies can reach up to >99%.[3,34,38,40−43] Most work on PFAS removal with foam fractionation has been done in batch mode, with easy control of contact time and effluent quality.[3,32,40−43] However, recent exploratory work by McCleaf et al.[40] has indicated that similar removal efficiencies can be reached in continuous operation, which comes with operational advantages in larger scale applications, but until now no pilot-scale results have been presented in academic literature.

The present study aimed to assess the effect of operational parameters on PFAS removal from landfill leachate with continuous pilot-scale foam fractionation. The specific objectives were to (i) determine the effectiveness of this technology in a continuous setup, (ii) for the first time, systematically evaluate the effect of different operating parameters on this continuous pilot scale process, and (iii) test real landfill leachate on-site and thereby avoid effects of sedimentation and chemical or microbiological changes during transport. The findings advance the understanding of the opportunities provided by the use of foam fractionation for PFAS removal from contaminated water.

2. MATERIALS AND METHODS

2.1. Treatment setup. A 19 cm diameter polypropylene (PP) column was used for all experiments with the water surface at 1.63 m height above the column bottom. Leachate water from the Hovgården landfill in Uppsala, Sweden was collected in real time from the inflow to the on-site water treatment plant. The influent vessel (PP, 300 L) was mixed by the inflow of leachate. All leachate originated from the same pumping station, thus excluding leachate from an area of the landfill where sludge from a municipal wastewater treatment plant is stored. All tests were done on days with similar weather profiles to exclude effects due to fluctuations in water quality as much as possible. A peristaltic pump with variable flow rate (Watson Marlow, 630SN/RE with Pureweld Xl 12.7 mm tubing) supplied a steady leachate flow to the column. The leachate entered the column under the water surface in enriching mode, at a height of 1.43 m above the column bottom (Figure 1). In stripping mode, the influent entered above the water surface at a height of 1.83 m above the column bottom. All experiments were done at room temperature.

Air was dispersed at the bottom of the column using four brass diffusers, each with 18 mm diameter and 30 mm length, attached to a stainless steel manifold. The airflow was controlled with a rotameter (0−20 L min^{-1}, ZYIA instrument company, FL3-1). The column top was sealed and nearly airtight so all inlet air exited the column at the foam exit surface, carrying with it foam accumulated at the water surface.

https://doi.org/10.1021/acsestwater.2c00032
ACS EST Water 2022, 2, 841−851

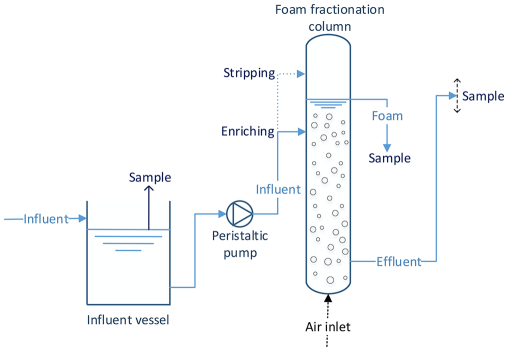

Figure 1. Process flow diagram of the continuous foam fractionation treatment. Column ø: 19 cm, water surface 1.63 m above column bottom. The height of the effluent hose was adaptable, which was used to control the foam and effluent flow rates. In enriching mode, the influent entered the column below the water surface (solid line). In stripping mode, the influent entered above the water surface (dotted line).

The foam collection was optimized by changing the height of the effluent outlet, thereby controlling the effluent flow as well. The foam flow was measured at least every 30 min with a PP volumetric flask. A process overview of the treatment setup is given in Figure 1.

The independent variables in all experiments were contact time (t_c, min), air flow (Q_{air}, L min^{-1}), and foam fraction ($\%_{foam}$, %). The t_c was assessed at both constant Q_{air} and at constant air-to-feed ratio (AR). The t_c and AR were not entirely independent, since both are functions of the water flow rate (Q_W), as given in eqs 1 and 2, with V_{column} as the water volume in the column. The foam fraction was defined as in eq 3, with Q_F as the foam flow (L min^{-1}).

$$t_c = \frac{V_{column}}{Q_W} \quad (1)$$

$$AR = \frac{Q_{air}}{Q_W} \quad (2)$$

$$\%_{foam} = \frac{Q_F}{Q_W} \quad (3)$$

2.2. Experimental Approach. To confirm the independence of sampling time on the removal in continuous operation shown by McCleaf et al.,[40] a 30 min continuous initial experiment was performed in triplicate at 10 min t_c, 10 L min^{-1} Q_{air}, and 30% foam. In these tests, approximately 250 mL of influent from the influent vessel was collected in clean PP bottles initially, 150 mL of foam and 250 mL of effluent were sampled after both 15 and 30 min treatment time from their respective exit hoses (without the use of a vacuum pump), and 250 mL of water from directly under the air/water interface was sampled after 30 min with a vacuum pump (GAST, DOA-P704-AA) connected to a PVC hose that was inserted approximately 5 cm below the water surface.

In this initial experiment, no significant differences between the effluent at 15 min and the effluent at 30 min were found in the concentrations of individual compounds as well as groups (paired t test, all $p > 0.05$). Detailed results, including the difference between sampling the effluent from the bottom as compared to the top of the column, are given in the Supporting Information (SI) Section A (Figure S1). On the basis of this stability in effluent over time, all subsequent continuous experiments (Table 1, all except Exp. 0 and 15) were run once for a total duration of 2 h, with replicate influent, effluent, and foam samples taken at four different time points (30, 60, 90, and 120 min) instead of in experimental triplicates. Approximately 250 mL of influent and effluent and 150 mL of foam were collected in clean PP bottles at each sampling time point. Average influent, effluent, and foam concentrations were calculated from the four different samples

Table 1. Overview of All Experiments[a]

Exp.	contact time (min)	air flow (L min^{-1})	targeted foam fraction (%)	water flow rate in (L min^{-1})	foam flow rate (L min^{-1})	effluent flow rate (L min^{-1})	air ratio	operating mode
0	10	10	30	4.6	0.46	4.2	2.2	enriching
1	10	20	10	4.6	0.46	4.2	4.3	enriching
2	30	6.7	10	1.5	0.15	1.4	4.3	enriching
3	10	20	10	4.6	0.46	4.2	4.3	stripping
4	30	13	20	1.5	0.31	1.2	8.7	stripping
5	30	13	20	1.5	0.31	1.2	8.7	enriching
6	20	20	10	2.3	0.23	2.1	8.7	enriching
7	20	10	10	2.3	0.23	2.1	4.3	enriching
8	20	10	20	2.3	0.46	1.8	4.3	enriching
9	20	10	30	2.3	0.69	1.6	4.3	enriching
10	20	5.0	20	2.3	0.46	1.8	2.2	enriching
11	20	20	20	2.3	0.46	1.8	8.7	enriching
12	30	20	10	1.5	0.15	1.4	13	enriching
13	15	13	10	3.1	0.31	2.8	4.3	enriching
14	20	10	5	2.3	0.12	2.2	4.3	enriching
15	20	20	3		batch mode - not applicable			
16	15	20	10	3.1	0.31	2.8	6.5	enriching
17	20	7.5	20	2.3	0.46	1.8	3.2	enriching

[a]See Figure 1 for the difference between stripping and enriching modes.

https://doi.org/10.1021/acsestwater.2c00032
ACS EST Water 2022, 2, 841−851

per type for each experiment to assess the effects of t_c, Q_{air} and $\%_{foam}$. A detailed overview of all experiments is given in Table 1, and the dates on which the experiments were performed are given in Table S1.

Additionally, a set of triplicate batch experiments was carried out (Table 1, Exp. 15) to investigate the difference between continuous and batch operation. Here, the column was filled up to 1.57 m height and an air flow of 20 L/min was applied for 20 min contact time. During the first 15 min, foam collection was identical to the continuous tests, but during the final 5 min, foam was also collected with a vacuum pump to increase the collected foam fraction. Effluent samples were taken from sampling points on both the bottom and the top of the column, to compare the effect of sampling height.

2.3. PFAS Analysis. In total, 29 PFAS were included in analytical method, namely, 11 PFCA (PFBA, PFPeA, PFHxA, PFHpA, PFOA, PFNA, PFDA, PFUnDA, PFDoDA, PFTriDA, PFTeDA), 7 PFSA (PFBS, PFPeS, PFHxS, PFHpS, PFOS, PFNS, PFDS), 3 fluorotelomer sulfonates (4:2 FTSA, 6:2 FTSA, 8:2 FTSA), the two components of F-53B (9Cl-PF3ONS and 11Cl-PF3OUdS),[44] HFPO-DA (trade name GenX), FOSA, MeFOSAA, EtFOSAA, NaDONA, and PFECHS. Twenty mass-labeled internal standards (IS) were used, which were spiked to the samples before extraction (Wellington Laboratories, MPFAC-24ES mixture with $^{13}C_3$-HFPO-DA added individually): $^{13}C_4$-PFBA, $^{13}C_5$-PFPeA, $^{13}C_5$-PFHxA, $^{13}C_4$-PFHpA, $^{13}C_8$-PFOA, $^{13}C_9$-PFNA, $^{13}C_6$-PFDA, $^{13}C_7$-PFUnDA, $^{13}C_3$-PFDoDA, $^{13}C_2$-PFTeDA, $^{13}C_3$-PFBS, $^{13}C_3$-PFHxS, $^{13}C_8$-PFOS, $^{13}C_2$-4:2 FTSA, $^{13}C_2$-6:2 FTSA, $^{13}C_2$-8:2 FTSA, $^{13}C_3$-HFPO-DA, $^{13}C_8$-FOSA, D_3-MeFOSAA, and D_5-EtFOSAA (for full names and other details of the native PFAS and IS see Tables S3 and S4).

The collected samples were filtered through glass microfiber filters (47 mm diameter, Whatman, China), weighed, and subsequently analyzed for PFAS concentration using solid phase extraction (SPE) followed by ultraperformance liquid chromatography tandem mass-spectrometry (UPLC−MS/MS) analysis. The SPE method has been described previously[22,45] (see also Section C in the Supporting Information).

A SCIEX Triple Quad 3500 UPLC−MS/MS system was used for PFAS analysis. Twenty microliters of extract was injected on a Phenomenex Gemini 1.7 μm C18 HPLC column with a Phenomenex KJ0-4282 analytical guard column and a Phenomenex Kinetix 1.7 μm C18 precolumn, all at 40 °C. A gradient of 0.6 mL/min 10 mM ammonium acetate in Milli-Q water and methanol was used for a total duration of 9 min per run. The initial gradient was set to 5% methanol, which was increased to 55% within the first 0.1 min. Then, it was further increased to 99% over 4.4 min, held there for 3.5 min, after which it was decreased again to 5% over 0.5 min and held there for another 0.5 min. The MS/MS was operated in scheduled multiple reaction monitoring (MRM) mode with negative electrospray ionization. For compounds with branched as well as linear isomers, only summed concentrations were reported. Details and quality control data on the analytical method are given in Tables S2−S4 in the SI Section C.

2.4. General Chemistry Analysis. For one continuous experiment and the batch experiment, 1 L influent, effluent, and foam samples were taken and shipped to ALS Scandinavian, Stockholm, Sweden for general chemistry analysis. For the preliminary triplicate continuous experiment and another continuous experiment, only influent and effluent were sampled and analyzed. The parameters were included in the analysis, and the results are given in Table S5.

2.5. Data Treatment. For each continuous test, mean concentrations of the four collected influent, effluent, and foam samples were calculated. The removal efficiency (RE) was calculated as in eq 4, with the standard deviation (σ_{RE}) calculated as in eq 5. Here, C_{EF}, C_{IN}, σ_{EF}, and σ_{IN} refer to the effluent and influent mean PFAS concentrations and corresponding standard deviations, respectively. The removal efficiency as a function of the independent variables (x) was fitted to eq 6 using the unweighted *fit* function in Matlab (version R2017B), with k and RE_{Max} as dependent empirical variables. This equation was selected because it converges to a horizontal asymptote and proved suitable for fitting the data, but other equations may be appropriate as well.

$$RE = \left(1 - \frac{C_{EF}}{C_{IN}}\right)\cdot 100\% \tag{4}$$

$$\sigma_{RE} = RE\cdot\sqrt{\left(\frac{\sigma_{IN}}{C_{IN}}\right)^2 + \left(\frac{\sigma_{EF}}{C_{EF}}\right)^2} \tag{5}$$

$$RE(x) = RE_{max} - RE_{max}\cdot e^{-k\cdot x} \tag{6}$$

For PFCA and PFSA, the mean RE as a function of perfluoroalkyl chain length (N_c) was fitted to eq 7, with a as the dependent empirical variable. Furthermore, a mass balance (MB) and its corresponding standard deviation (σ_{MB}) were calculated for each experiment as per eqs 8 and 9, respectively, with C_{Foam} the mean concentration in the foam and σ_{Foam} the corresponding standard deviation. All statistical analyses, curve fitting, and plotting were done in Matlab, version R2017b.

$$RE(N_c) = 100/(1 + e^{-N_c+4})^a \tag{7}$$

$$MB = \frac{\left(1 - \frac{\%_{foam}}{100}\right)\cdot C_{EF} + \frac{\%_{foam}}{100}\cdot C_{foam}}{C_{IN}}\cdot 100\% \tag{8}$$

$$\sigma_{MB} = MB\cdot\sqrt{\left(\frac{\sigma_{IN}}{C_{IN}}\right)^2 + \left(\frac{\sigma_{EF}}{C_{EF}}\right)^2 + \left(\frac{\sigma_{foam}}{C_{foam}}\right)^2} \tag{9}$$

Values below the limit of quantification were taken as zero, which is acknowledged to introduce an error. However, substituting a fraction of the detection limit is known to introduce an equal level of inaccuracy.[46] In all analyzed samples, the highest possible concentration of nondetect PFAS would contribute at most 0.4% to the ΣPFAS concentration (see SI Section C for details). This fraction was deemed negligible; hence, nondetect concentrations were set to zero. Some samples were contaminated or lost during the analysis, in which case the results were based on the remaining three samples. An overview of all tests for which samples were excluded is given in Table S6.

3. RESULTS AND DISCUSSION

3.1. Leachate Characteristics. The average ΣPFAS concentration in the influent leachate was 2400 ± 400 ng L^{-1}. Because the untreated leachate was collected from the influent of an operating treatment plant and the tests were carried out over different days, this level of variability falls

https://doi.org/10.1021/acsestwater.2c00032
ACS EST Water 2022, 2, 841−851

within the expectations. The influent ΣPFAS consisted of 46 ± 10% short-chain PFCA, 27 ± 6% long-chain PFCA, 7 ± 1% short-chain PFSA, 15 ± 3% long-chain PFSA, and 4 ± 1% other types of PFAS (for details on the PFAS classification see Table S7). The influent ΣPFAS concentration was not found to affect the removal efficiency (Pearson's $r = -0.23$ (95% CI: −0.71−0.40), $p > 0.05$). Of all PFAS included in the analysis, a statistically significant correlation between RE and influent concentration was only found for PFECHS, with the RE increasing at higher influent concentrations (Pearson's $r = 0.74$ (95% CI: 0.28−0.92), $p < 0.05$). All PFAS included in the method were detected in at least one of the samples.

For leachate samples taken on testing dates, average influent dissolved organic carbon (DOC), conductivity, ammonium, and bicarbonate alkalinity were 36 mg L^{-1}, 440 mS m^{-1}, 59 mg L^{-1}, and 1300 mg L^{-1}, respectively. A selective overview of the mean general chemistry characteristics of the influent, effluent, and foam is given in Table 2, with the complete data set given in Table S5. DOC, iron, and aluminum were enriched in the foam, but otherwise no effects of the treatment on the general chemistry were found. Samples were not taken for each test, but the leachate composition from this pumping station at Hovgården is known to be very stable in terms of general chemistry characteristics. On the basis of 15 regularly distributed measurements in 2021, relative variations of the mean iron concentration (5.7 mg L^{-1}), conductivity (510 mS m^{-1}), pH (7.6), and total organic carbon (43 mg L^{-1}) were only 15, 11, 3, and 10%, respectively.

Table 2. Overview of General Chemistry Data[a]

	influent ($n = 4$)	effluent ($n = 4$)	foam ($n = 2$)
DOC (mg L^{-1})	36	36	45
phosphor (μg L^{-1})	140	120	190
calcium (mg L^{-1})	150	150	150
manganese (μgL^{-1})	520	530	610
sodium (mg L^{-1})	710	710	740
potassium (mg L^{-1})	240	240	260
iron (mg L^{-1})	5.3	4.8	9.7
aluminum (μg L^{-1})	27	25	44
copper (μg L^{-1})	54	28	77
magnesium (mg L^{-1})	56	57	60
COD-Mn (mg L^{-1})	27	29	31
ammonium (mg L^{-1})	59	60	61
nitrate (mg L^{-1})	18	18	17
chloride (mg L^{-1})	920	910	950
sulfate (mg L^{-1})	130	120	95
conductivity (mS m^{-1})	440	450	440
pH	7.9	8.0	8.0
alkalinity (mg L^{-1})	1300	1300	1400
TOC (mg L^{-1})	36	34	48

[a]For the complete dataset, see Table S5.

3.2. Effect of Process Variables. The effect of all investigated process variables on the ΣPFAS removal is shown in Figure 2. Both at constant air-to-feed ratio (AR) and at constant air flow (Q_{air}), decreasing the contact time (t_c) below 20 min was shown to decrease the ΣPFAS removal efficiency (RE). Importantly, it was found that t_c also limits the removal while the AR is kept constant, although the effect may be different at higher AR values. This result indicates that increasing the Q_{air} cannot make up for a too short t_c. These results are in good agreement with the results of Meng et al.,[3] who found total aeration time to be one of the most influential variables in the performance of foam fractionation for PFAS removal from aqueous firefighting foam concentrate.

Altogether, the results strongly indicate that RE is negatively impacted by t_c values below 15 min, but the extent of decrease in RE is uncertain. The initial experiment at 10 min t_c (Exp. 0, Table 1, SI Section A) showed a higher RE of 47 ± 3% as compared to the RE found in Exp. 1 of 42 ± 1%, which indicates that higher ΣPFAS removal efficiencies may be achievable at a short t_c than is now shown in Figure 2A, B. Nonetheless, for the experiment in stripping mode at 10 min t_c (Exp. 3, Table 1), an even lower RE of 29 ± 4.7% was observed (Section 3.4), confirming the limited RE at low t_c values.

Collecting lower foam fractions lead to higher foam concentrations, as found from one-way ANOVA over the ΣPFAS concentration of all collected foam samples divided into groups based on their $\%_{foam}$ ($F(4, 61) = 3.8$, $p < 0.05$), which has also been found previously.[3,41] Differences in foam concentration were only statistically significant between 30% foam as compared to 3% and 5% ($p < 0.05$) but statistically insignificant between the other groups. Decreasing the $\%_{foam}$ only affected the removal at fractions below 10%, which corresponds to Robey et al.'s[41] finding that most of the removal occurs in the first 14% of volume removed. This is beneficial from a process design perspective, since achieving the same removal at a low $\%_{foam}$ leads to a lower volume of concentrated foam that needs secondary treatment. Since the $\%_{foam}$ is controlled by changing the effluent flow and the foam outlet is directly above the water−air surface, the collected foam was relatively wet. Strictly speaking, this mode of operation is a mix of bubble fractionation and foam fractionation, as explained by Lemlich.[35] However, since foaming was observed in all tests, foam fractionation was chosen as terminology.

Q_{air} was shown to limit the removal at values below 7.5 L min^{-1} (Figure 2D). Since the removal is highly dependent on the surface area available for sorption, air flow is considered a very influential process variable.[35] The air−liquid surface area further relates to the size of the introduced air bubbles.[35,42] In the current study, the diffusers used generated relatively large air bubbles (up to approximately 5 mm diameter). Instead, the use of a membrane, glass frit, electrochemical bubble generation, or other technologies may increase the available surface area and thereby improve the removal.[40,42]

For all process parameters, their effect on the ΣPFAS RE fits well with the empirical model given by eq 6. For each run, the ΣPFAS removal was shown to plateau around 60%, with fitted RE_{max} values ranging between 56% and 61% for the effect of Q_{air} (Figure 2D) and the effect of t_c at constant Q_{air} (Figure 2B), respectively. The ΣPFAS RE is thus affected by all these variables, but the effect is limited and RE_{Max} does not reach 100%. Instead, it is also limited by the PFAS composition of the inlet water. The leachate water used in this study contained on average 46% short-chain PFCA, which were only marginally removed in the foam fractionation process. Therefore, the ΣPFAS removal reached a plateau at approximately 60%. It should be realized that the fitted RE_{Max} and k parameters obtained for each variable, given in Table S8, probably depend strongly on the inlet water composition and parameters such as PFAS composition and DOC concentration.

3.3. Effect of PFAS Composition and Chain Length. On the basis of the results presented in Figure 2, all

https://doi.org/10.1021/acsestwater.2c00032
ACS EST Water 2022, 2, 841−851

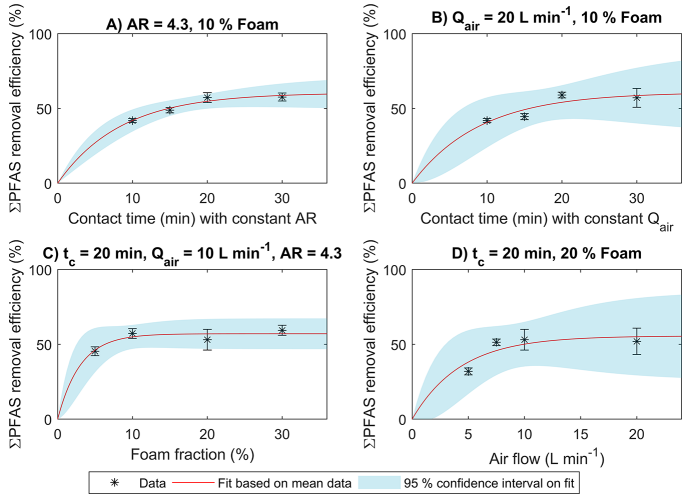

Figure 2. Effect of (A) contact time (t_c) at a constant air ratio (AR) of 4.3, 10% foam; (B) t_c at a constant air flow (Q_{air}) of 20 L min^{-1}, 10% foam; (C) foam fraction ($\%_{foam}$) at constant t_c = 20 min, Q_{air} = 10 L min^{-1}; AR = 4.3 and (D) Q_{air} at constant t_c = 20 min, 20% foam on the total PFAS removal. The red lines and blue shading represent a least-squares fit of the mean data to eq 6 with the corresponding 95% confidence interval of the fit, respectively. The experiments included in each plot in order of increasing x-value were (A) 1, 13, 7, and 2; (B) 1, 16, 6, and 12; (C) 14, 7, 8, and 9; and (D) 10, 17, 8, and 11 (Table 1).

experiments representing the lowest removal efficiencies in Figure 2A−D were deemed process-limited. Therefore, 12 continuous experiments without process-induced limitations on the RE were selected for statistical analysis (experiments 2, 4−9, 11−13, 16, and 17 in Table 1). All these 12 experiments have a t_c, $\%_{foam}$, and Q_{air} of at least 15 min, 10%, and 7.5 L min^{-1}, respectively.On the basis of these experiments, a significant negative correlation (Pearson's r = −0.63 (95% CI: −0.88 to −0.09), $p < 0.05$) between the fraction short-chain PFCA in the influent ΣPFAS and the ΣPFAS RE was found, as illustrated in Figure 3. Hence, water types with a high fraction of long-chain compounds may thus be more suitable for foam fractionation treatment than the leachate water used in the current study. Even commercially available batch foam fractionation processes have a lower removal of short-chain PFAS in comparison to long-chain PFAS.[36,47]

The relationship between perfluorocarbon chain length and RE is further illustrated in Figure 4. These results confirm the literature finding that PFAS removal efficiencies decrease exponentially with perfluoroalkyl chain length in foam fractionation,[3,33,40−42] with a fit as given in eq 7. For readability, only PFCA and PFSA were included in Figure 4, but a more complete plot is given in Figure S2. Although the comparatively low influent concentrations of most non-PFAA PFAS causes high variability in some of the results, similar dependencies on perfluorocarbon chain length were found for the RE of 4:2 FTSA, 6:2 FTSA, 8:2 FTSA, FOSA, MeFOSAA, and EtFOSAA, as also shown in Figure S2.

PFOS and PFOA had average removal efficiencies of 95 ± 2% and 92 ± 3%, at mean influent concentrations of 230 ± 110 and 630 ± 150 ng L^{-1}, respectively. The REs for other C_8 PFAS (8:2 FTSA, FOSA, MeFOSAA, and EtFOSAA) were similarly high. PFNS was only detected at quantifiable concentrations in two influent and 28 foam samples but not in any effluent samples and was thus assumed to have a

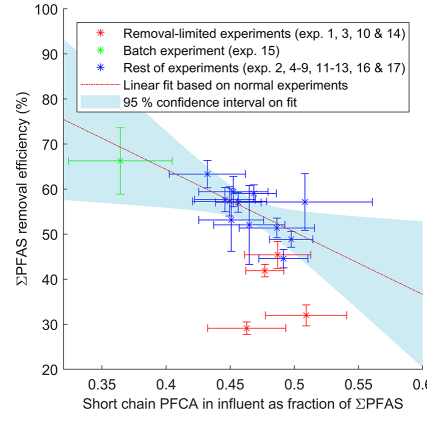

Figure 3. ΣPFAS removal efficiency (%) as a function of fraction short-chain PFCA in total influent PFAS. The correlation fit is only based on experiments without process limitations on the removal, represented in blue in this plot (see Table 1). Horizontal error bars represent the standard deviation of the short-chain PFCA fraction, and vertical error bars represent the standard deviation of ΣPFAS removal efficiency.

removal efficiency of 100%. These results correspond well with the literature findings in other foam fractionation studies of >90% removal for long-chain PFCA and PFSA but lower or no removal of short-chain compounds.[33,36,40,42] PFCA of the same carbon number were removed to a lower extent than their PFSA equivalent, which has also been shown previously.[33,34,40,42] This phenomenon is due to PFSA having higher adsorption coefficients to water−air interfaces because

https://doi.org/10.1021/acsestwater.2c00032
ACS EST Water 2022, 2, 841−851

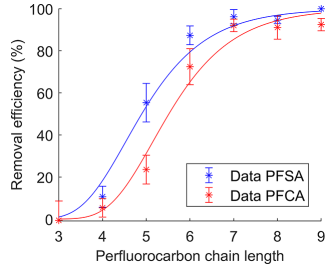

Figure 4. PFCA and PFSA removal as a function of perfluorocarbon chain length. Only the results from experiments without process-induced limitations were included in this plot (i.e., Exp. 2, 4–9, 11–13, 16, and 17, Table 1). The solid lines are model fits to eq 7, with the optimized parameter a at 9400 and 5100 for PFCA and PFSA, respectively. Error bars represent the standard deviation between experiments.

of their higher hydrophobicity.[33,34] This effect was more pronounced for shorter chain lengths, as visible in Figure 4.

3.4. Enriching versus Stripping Modes. Two experiments were carried out in stripping mode, i.e., with the water influent above the air/water interface, as well as in enriching mode under otherwise identical conditions (experiments 3 and 4 (stripping) and 1 and 5 (enriching) in Table 1). In both comparisons, the mean ΣPFAS removal was higher in enriching mode than in stripping mode (Figure 5). These differences are not in accordance with the literature, which predicts a higher removal of contaminants in stripping mode compared to enriching mode, because the liquid between the foam bubbles has a higher PFAS concentration in stripping mode.[35,36] In the current system, the foam layer was not sufficiently stable, so introduction of the influent above the foam surface lead to an observable collapse of the foam. Improvements of the column, such as introducing an inlet valve higher above the interface on the opposite side of the foam outlet and a foam outlet above this inlet valve, may prevent the foam from collapsing and result in improved

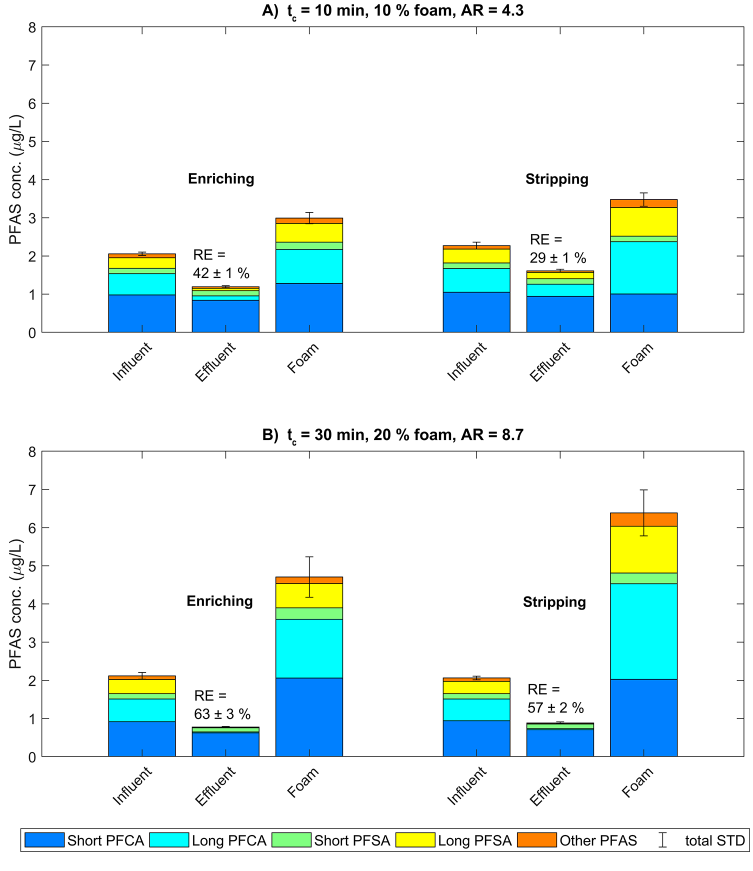

Figure 5. Comparison between experiments in enriching (A) Exp. 1 and (B) Exp. 5, Table 1)) and stripping (A) Exp. 3 and (B) Exp 4, Table 1)) modes under otherwise identical conditions. (A): 10 min contact time (t_c), 10% foam, air ratio (AR) 4.3. (B): 30 min t_c, 20% foam, AR 8.7. Error bars represent the standard deviation of the ΣPFAS concentration. For the classification of all PFAS, see SI Section F.

https://doi.org/10.1021/acsestwater.2c00032
ACS EST Water 2022, 2, 841–851

performance in stripping mode. Moreover, introducing a vacuum pump for continuous foam collection may also increase the removal, as shown by McCleaf et al.[40]

3.5. Batch Mode. The ΣPFAS RE of the benchmark test in batch mode was 66 ± 7%, as shown in Figure 6. This result was not significantly different from the continuous test with the highest removal (Figure 5B, $p > 0.05$, Welch t test). Furthermore, as shown in Figure 3, the fraction short-chain PFAS was lowest of all experiments in the batch test, which may have increased the ΣPFAS RE. Moreover, the removal in batch mode strongly depended on where the effluent samples are taken. After turning off the air flow, effluent taken from the bottom of the column had lower PFAS concentrations than effluent taken from the top of the column, which only had a removal of 48 ± 14%. It may thus be possible to increase the batch-mode removal by collecting a higher foam fraction, but the limitation of low short-chain PFCA removal was not reduced in batch operation.

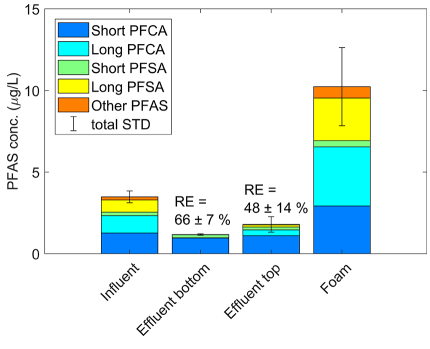

Figure 6. Removal efficiency in batch test (t_c 20 min, Q_{air} 20 L min^{-1}, 3% foam). Error bars represent the standard deviation of the ΣPFAS concentration. For the classification of all PFAS, see SI Section F.

3.6. Mass Balance. The mass balance did not close for all experiments. The mass balance for the continuous tests ranged from 66 ± 7% to 104 ± 10%, for experiments 12 and 10 (Table 1), respectively. For the batch experiment, the mass balance only closed to 42 ± 15% when considering the bottom effluent samples or 59 ± 22% when considering the top effluent samples. The preliminary continuous experiment showed an enrichment of some PFAS in the water layer at the top of the column relative to the effluent, as shown in Figure S1. These PFAS will not show up in the mass balance, since they are neither in the foam nor in the effluent, and their accumulation may thus lead to a lower mass balance closure. It could be hypothesized that collecting higher foam fractions would thus improve the mass balance closure, but no significant effect of the $\%_{foam}$ on the mass balance was found (one-way ANOVA, $p > 0.05$), and in the batch test, the mass balance did not close either when only considering the top layer concentrations.

The overall mass balance did not correlate with ΣPFAS removal either, but individual balances closed significantly better for compounds with a lower removal, i.e., short-chain compounds (Pearson's $r = -0.95$ (95% CI: -0.96 – -0.94), $p < 0.05$). For perfluorocarbon chain lengths up to 10 for PFCA and up to 8 for PFSA, one-way ANOVA showed a statistically significant difference in mass balance closure with increasing chain length ($F(7,88) = 14$ for PFCA, $F(4,55) = 21$ for PFSA, $p < 0.05$ for both). PFAS with perfluorocarbon chain lengths above the specified numbers were excluded because of their relatively low influent concentrations of <5 ng L^{-1}, and only the results from experiments without process-induced limitations (Exp. 2, 4–9, 11–13, 16, and 17, Table 1) were included in these calculations. Box plots and details on the statistical calculations are given in SI Section I.

Since long-chain PFAS were removed better and were thus more enriched at the air–water surface, these strong correlations indicate that PFAS accumulating at the air–water interface may also escape to the air as aerosols rather than being captured in the foam. This hypothesis is supported by the work of Ebersbach et al.,[42] who demonstrated the aerosol-mediated removal of 6:2 FTSA, PFOS, and PFOA from concentrated water. Moreover, aerosol enrichment with PFAS is a well-documented phenomenon, both in nature and in engineered systems.[48−50] The presence of aerosols in the current system was visible from the bursting of foam bubbles, leading to the formation of droplets and bubbles on the lid and upper walls of the column. However, McCleaf et al.[40] found no significant PFAS concentrations in their aerosol trap after foam fractionation, which may be related to their use of a vacuum pump for foam collection. In addition to loss of PFAS in aerosols, the complex water matrix may have caused transformation of certain compounds as a result of oxidation, which could have further skewed the mass balance.

4. CONCLUSIONS

This study set out to examine the applicability of pilot-scale continuous foam fractionation for treatment of PFAS-contaminated leachate water. It was shown that treatment efficiency decreased with decreasing contact time, air flow rate and collected foam fraction. Long-chain compounds were removed better than short-chain PFAS, and PFSA were removed more efficiently than PFCA. PFOS and PFOA had average removal efficiencies of 95% and 92%, but no removal of PFBA and only 10% removal of PFBS were found. No improvement in treatment efficiency was found when operating in batch mode, which indicates that continuous operation is a viable alternative for commercially available batch systems. Despite the relatively low ΣPFAS removal of approximately 60%, the results indicate a high applicability of continuous foam fraction, especially for treatment of water types contaminated with mainly long-chain PFAS. Further research is required to confirm if the high long-chain PFAS removal extends to water types with different water quality matrixes and PFAS concentrations than the investigated leachate.

Currently, most regulations for aqueous PFAS emissions to the environment still include almost exclusively long-chain PFAS. For example, the European Water Framework Directive defined an average annual PFOS concentration in inland surface water of 0.65 ng L^{-1} as the environmental quality limit.[51] In The Netherlands, soil-washing facilities are allowed to discharge 4000 m^3 of wastewater containing at most 500 ng L^{-1} PFOS, 500 ng L^{-1} PFOA, and 1000 ng L^{-1} HFPO–DA (GenX) annually.[52] In the United States, efforts are underway to enforce remediation of PFOS and PFOA releases into the environment.[16] In the most effective continuous experiment presented in this study, mean PFOS and PFOA concentrations decreased from 230 and 580 to 7 and 20 ng L^{-1}, respectively, which falls well within the Dutch standards for soil washing

https://doi.org/10.1021/acsestwater.2c00032
ACS EST Water 2022, 2, 841–851

wastewater. However, landfill facilities often have specific individual discharge permits for PFAS, so drawing generalized conclusions on the treatment performance with respect to regulatory limits is difficult.

The greatest advantage of the presented technology is its simplicity. Aeration is common in most wastewater treatment facilities, and for plants, treating PFAS contaminated water introducing a foam fractionation process is thus an easily implemented and economical way to decrease PFAS emissions to the environment. Possibly, this technology can even be integrated with aeration steps that are already applied on-site, by installing an appropriate foam collection system. Naturally, the collected foam would need further treatment, where the reduced volume of approximately 10% of the total inlet volume allows relatively smaller on-site degradative treatment of the coalesced foam, as exemplified in previous studies.[32,33]

Two of the most promising degradative treatment technologies for PFAS-contaminated water are plasma treatment and electrochemical oxidation.[53] Both these technologies have been applied successfully to leachate water matrices similar to the foam produced in this study, with ΣPFAS concentrations in the low $\mu g\ L^{-1}$ range, albeit at higher TOC concentrations and conductivities.[54,55] Both these destructive technologies were more effective for the removal of long-chain as compared to short-chain PFAS. A drawback of electrochemical degradation was the formation of short-chain compounds as degradation products, which was not observed in plasma treatment. These results indicate that degradative treatment of the foam produced, as described here, will most probably be possible.

Further research should focus on improving the removal of short-chain compounds in the foam fractionation process. Alternative methods for the introduction of air bubbles, such as electrochemical bubble formation, may lead to higher available surface area and thus higher removal. Possibly, this will increase the removal of short-chain compounds. The use of image processing technologies for determining the size distributions in bubbly flows could enhance the understanding of the effect of bubble size on removal.[56,57] Alternatively, additives such as metal activators may be tested, which have been shown to increase the removal of long-chain compounds.[40,43] Enhanced foam collection, for example with a vacuum pump, may also improve the removal of short-chain PFAS, as may combining several foam fractionation steps in a row.

Another area for future work would be the variation in mass balance closure that was found. Introducing air as well as aerosol sampling and analyzing the PFAS concentrations in the exhaust air may be beneficial toward closing the mass balance and could indicate if any PFAS escape the system. Finally, testing other water matrixes with a higher fraction of long-chain compounds could confirm the presented limitation of low short-chain removal.

■ ASSOCIATED CONTENT

Supporting Information

The Supporting Information is available free of charge at https://pubs.acs.org/doi/10.1021/acsestwater.2c00032.

Figures of overview of results of preliminary experiment, PFAS removal as a function of chain length, and boxplots for the different individual PFAS included in the ANOVA analysis for the effect of chain length on mass balance, tables of dates of experiments, scheduled multiple reaction monitoring transitions for LC−MS/MS analysis of PFAS concentrations, internal standards used for compounds without a corresponding mass labeled internal standard in the IS mixture, overview of instrument parameters for quantification of PFAS, general chemistry results of analyzed samples, legitimization of sample exclusion, overview of PFAS designation into groups, and fitted parameters for the effect of process variables on ΣPFAS removal, and discussion of analytical method (PDF)

■ AUTHOR INFORMATION

Corresponding Author

Sanne J. Smith − *Department of Aquatic Sciences and Assessment, Swedish University of Agricultural Sciences (SLU), SE-750 07 Uppsala, Sweden;* orcid.org/0000-0002-3487-0528; Email: sanne.smith@slu.se

Authors

Karin Wiberg − *Department of Aquatic Sciences and Assessment, Swedish University of Agricultural Sciences (SLU), SE-750 07 Uppsala, Sweden*

Philip McCleaf − *Uppsala Water and Waste AB, SE-751 44 Uppsala, Sweden*

Lutz Ahrens − *Department of Aquatic Sciences and Assessment, Swedish University of Agricultural Sciences (SLU), SE-750 07 Uppsala, Sweden;* orcid.org/0000-0002-5430-6764

Complete contact information is available at: https://pubs.acs.org/10.1021/acsestwater.2c00032

Notes

The authors declare no competing financial interest.

■ ACKNOWLEDGMENTS

This project received funding from the European Union's Horizon 2020 research and innovation program under the Marie Skłodowska-Curie grant agreement No. 860665 (PERFORCE3 Innovative Training Network). The authors would further like to thank Uppsala Water and Waste AB, especially the employees working at Hovgården and particularly Sofia Bjälkefur-Seroka, for their support. Finally, the authors acknowledge and thank Axel Krögelström for his MSc thesis work, which partly laid the foundation for the presented study.

■ REFERENCES

(1) Sunderland, E. M.; Hu, X. C.; Dassuncao, C.; Tokranov, A. K.; Wagner, C. C.; Allen, J. G. A Review of the Pathways of Human Exposure to Poly- and Perfluoroalkyl Substances (PFASs) and Present Understanding of Health Effects. *J. Expo. Sci. Environ. Epidemiol* **2019**, *29* (2), 131−147.

(2) Ahrens, L. Polyfluoroalkyl Compounds in the Aquatic Environment: A Review of Their Occurrence and Fate. *J. Environ. Monit* **2011**, *13* (1), 20−31.

(3) Meng, P.; Deng, S.; Maimaiti, A.; Wang, B.; Huang, J.; Wang, Y.; Cousins, I. T.; Yu, G. Efficient Removal of Perfluorooctane Sulfonate from Aqueous Film-Forming Foam Solution by Aeration-Foam Collection. *Chemosphere* **2018**, *203*, 263−270.

(4) Lemal, D. M. Perspective on Fluorocarbon Chemistry. *J. Org. Chem.* **2004**, *69* (1), 1−11.

(5) Lau, C.; Anitole, K.; Hodes, C.; Lai, D.; Pfahles-Hutchens, A.; Seed, J. Perfluoroalkyl Acids: A Review of Monitoring and Toxicological Findings. *Toxicol. Sci.* **2007**, *99* (2), 366−394.
(6) Fenton, S. E.; Ducatman, A.; Boobis, A.; DeWitt, J. C.; Lau, C.; Ng, C.; Smith, J. S.; Roberts, S. M. Per- and Polyfluoroalkyl Substance Toxicity and Human Health Review: Current State of Knowledge and Strategies for Informing Future Research. *Environ. Toxicol. Chem.* **2021**, *40* (3), 606−630.
(7) Buck, R. C.; Franklin, J.; Berger, U.; Conder, J. M.; Cousins, I. T.; Voogt, P. De; Jensen, A. A.; Kannan, K.; Mabury, S. A.; van Leeuwen, S. P. J. Perfluoroalkyl and Polyfluoroalkyl Substances in the Environment: Terminology, Classification, and Origins. *Integr. Environ. Assess. Manag.* **2011**, *7* (4), 513−541.
(8) Rayne, S.; Forest, K.; Friesen, K. J. Congener-Specific Numbering Systems for the Environmentally Relevant C 4 through C8 Perfluorinated Homologue Groups of Alkyl Sulfonates, Carboxylates, Telomer Alcohols, Olefins, and Acids, and Their Derivatives. *J. Environ. Sci. Heal. - Part A Toxic/Hazardous Subst. Environ. Eng.* **2008**, *43* (12), 1391−1401.
(9) Hamid, H.; Li, L. Y.; Grace, J. R. Review of the Fate and Transformation of Per- and Polyfluoroalkyl Substances (PFASs) in Landfills. *Environ. Pollut.* **2018**, *235*, 74−84.
(10) Benskin, J. P.; Li, B.; Ikonomou, M. G.; Grace, J. R.; Li, L. Y. Per- and Polyfluoroalkyl Substances in Landfill Leachate: Patterns, Time Trends, and Sources. *Environ. Sci. Technol.* **2012**, *46* (21), 11532−11540.
(11) Stoiber, T.; Evans, S.; Naidenko, O. V. Disposal of Products and Materials Containing Per- and Polyfluoroalkyl Substances (PFAS): A Cyclical Problem. *Chemosphere* **2020**, *260*, 127659.
(12) Stockholm Convention. SC UNEP.POPS-COP.4-SC-4−17 Listing of perfluorooctaine sulfonic acid, its salts and perfluorooctaine sulfonyl fluoride. http://chm.pops.int/Portals/0/Repository/COP4/UNEP-POPS-COP.4-17.English.PDF (accessed 2022-03-17).
(13) European Chemicals Agency. Scientific committees support further restrictions of PFAS. https://echa.europa.eu/-/scientific-committees-support-further-restrictions-of-pfas (accessed 2022-03-17).
(14) EFSA. PFAS in food: EFSA assesses risks and sets tolerable intake. https://www.efsa.europa.eu/en/news/pfas-food-efsa-assesses-risks-and-sets-tolerable-intake (accessed 2022-03-17).
(15) *Havs- Och Vattenmyndighetens Föreskrifter Om Klassificering Och Miljökvalitetsnormer Avseende Ytvatten - HVMFS 2019:25*; Swedish Agency for Marine and Water Management, 2019.
(16) US Congress. H.R.2467 - PFAS Action Act of 2021. https://www.congress.gov/bill/117th-congress/house-bill/2467# (accessed 2022-03-17).
(17) The National Institute for Public Health and the Environment (RIVM). Nieuwe risicogrenzen voor PFAS in grond en grondwater. https://www.rivm.nl/pfas/nieuwe-risicogrenzen-voor-pfas-in-grond-en-grondwater (accessed 2022-03-17).
(18) Yu, J.; Hu, J.; Tanaka, S.; Fujii, S. Perfluorooctane Sulfonate (PFOS) and Perfluorooctanoic Acid (PFOA) in Sewage Treatment Plants. *Water Res.* **2009**, *43* (9), 2399−2408.
(19) Bao, Y.; Niu, J.; Xu, Z.; Gao, D.; Shi, J.; Sun, X.; Huang, Q. Removal of Perfluorooctane Sulfonate (PFOS) and Perfluorooctanoate (PFOA) from Water by Coagulation: Mechanisms and Influencing Factors. *J. Colloid Interface Sci.* **2014**, *434*, 59−64.
(20) Arias Espana, V. A.; Mallavarapu, M.; Naidu, R. Treatment Technologies for Aqueous Perfluorooctanesulfonate (PFOS) and Perfluorooctanoate (PFOA): A Critical Review with an Emphasis on Field Testing. *Environ. Technol. Innov* **2015**, *4*, 168−181.
(21) Xiao, F. Emerging Poly- and Perfluoroalkyl Substances in the Aquatic Environment: A Review of Current Literature. *Water Res.* **2017**, *124*, 482−495.
(22) Belkouteb, N.; Franke, V.; McCleaf, P.; Köhler, S.; Ahrens, L. Removal of Per- and Polyfluoroalkyl Substances (PFASs) in a Full-Scale Drinking Water Treatment Plant: Long-Term Performance of Granular Activated Carbon (GAC) and Influence of Flow-Rate. *Water Res.* **2020**, *182*, 115913.
(23) Lu, D.; Sha, S.; Luo, J.; Huang, Z.; Zhang Jackie, X. Treatment Train Approaches for the Remediation of Per- and Polyfluoroalkyl Substances (PFAS): A Critical Review. *J. Hazard. Mater.* **2020**, *386*, 121963.
(24) Banks, D.; Jun, B. M.; Heo, J.; Her, N.; Park, C. M.; Yoon, Y. Selected Advanced Water Treatment Technologies for Perfluoroalkyl and Polyfluoroalkyl Substances: A Review. *Sep. Purif. Technol.* **2020**, *231*, 115929.
(25) Merino, N.; Qu, Y.; Deeb, R. A.; Hawley, E. L.; Hoffmann, M. R.; Mahendra, S. Degradation and Removal Methods for Perfluoroalkyl and Polyfluoroalkyl Substances in Water. *Environ. Eng. Sci.* **2016**, *33* (9), 615−649.
(26) Horst, J.; McDonough, J.; Ross, I.; Dickson, M.; Miles, J.; Hurst, J.; Storch, P. Water Treatment Technologies for PFAS: The Next Generation. *Groundw. Monit. Remediat* **2018**, *38* (2), 13−23.
(27) Li, P.; Zhi, D.; Zhang, X.; Zhu, H.; Li, Z.; Peng, Y.; He, Y.; Luo, L.; Rong, X.; Zhou, Y. Research Progress on the Removal of Hazardous Perfluorochemicals: A Review. *J. Environ. Manage.* **2019**, *250*, 109488.
(28) Mahinroosta, R.; Senevirathna, L. A Review of the Emerging Treatment Technologies for PFAS Contaminated Soils. *J. Environ. Manage.* **2020**, *255*, 109896.
(29) Wei, Z.; Xu, T.; Zhao, D. Treatment of Per- And Polyfluoroalkyl Substances in Landfill Leachate: Status, Chemistry and Prospects. *Environ. Sci. Water Res. Technol.* **2019**, *5* (11), 1814−1835.
(30) Nzeribe, B. N.; Crimi, M.; Mededovic Thagard, S.; Holsen, T. M. Physico-Chemical Processes for the Treatment of Per- And Polyfluoroalkyl Substances (PFAS): A Review. *Crit. Rev. Environ. Sci. Technol.* **2019**, *49* (10), 866−915.
(31) Horst, J.; McDonough, J.; Ross, I.; Houtz, E. Understanding and Managing the Potential By-Products of PFAS Destruction. *Groundw. Monit. Remediat* **2020**, *40* (2), 17−27.
(32) Lyu, X. J.; Liu, Y.; Chen, C.; Sima, M.; Lyu, J. F.; Ma, Z. Y.; Huang, S. Enhanced Use of Foam Fractionation in the Photodegradation of Perfluorooctane Sulfonate (PFOS). *Sep. Purif. Technol.* **2020**, *253* (May), 117488.
(33) Dai, X.; Xie, Z.; Dorian, B.; Gray, S.; Zhang, J. Comparative Study of PFAS Treatment by UV, UV/Ozone, and Fractionations with Air and Ozonated Air. *Environ. Sci. Water Res. Technol.* **2019**, *5* (11), 1897−1907.
(34) Burns, D. J.; Stevenson, P.; Murphy, P. J. C. PFAS Removal from Groundwaters Using Surface-Active Foam Fractionation. *Remediation* **2021**, *31* (4), 19−33.
(35) Lemlich, R. Adsorptive Bubble Separation Methods: Foam Fractionation and Allied Techniques. *Ind. Eng. Chem.* **1968**, *60* (10), 16−29.
(36) Buckley, T.; Xu, X.; Rudolph, V.; Firouzi, M.; Shukla, P. Review of Foam Fractionation as a Water Treatment Technology. *Sep. Sci. Technol.* **2022**, *57*, 929.
(37) Burghoff, B. Foam Fractionation Applications. *J. Biotechnol.* **2012**, *161* (2), 126−137.
(38) Buckley, T.; Karanam, K.; Xu, X.; Shukla, P.; Firouzi, M.; Rudolph, V. Effect of Mono- and Di-Valent Cations on PFAS Removal from Water Using Foam Fractionation − A Modelling and Experimental Study. *Sep. Purif. Technol.* **2022**, *286*, 120508.
(39) Tow, E. W.; Ersan, M. S.; Kum, S.; Lee, T.; Speth, T. F.; Owen, C.; Bellona, C.; Nadagouda, M. N.; Mikelonis, A. M.; Westerhoff, P.; Mysore, C.; Frenkel, V. S.; Desilva, V.; Walker, W. S.; Safulko, A. K.; Ladner, D. A. Managing and Treating Per-and Polyfluoroalkyl Substances (Pfas) in Membrane Concentrates. *AWWA Water Sci.* **2021**, *3* (5), No. e1233.
(40) McCleaf, P.; Kjellgren, Y.; Ahrens, L. Foam Fractionation Removal of Multiple Per- and Polyfluoroalkyl Substances from Landfill Leachate. *AWWA Water Sci.* **2021**, *3* (5), 1−14.
(41) Robey, N. M.; da Silva, B. F.; Annable, M. D.; Townsend, T. G.; Bowden, J. A. Concentrating Per- and Polyfluoroalkyl Substances (PFAS) in Municipal Solid Waste Landfill Leachate Using Foam Separation. *Environ. Sci. Technol.* **2020**, *54*, 12550−12559.

(42) Ebersbach, I.; Ludwig, S. M.; Constapel, M.; Kling, H. W. An Alternative Treatment Method for Fluorosurfactant-Containing Wastewater by Aerosol-Mediated Separation. *Water Res.* **2016**, *101*, 333−340.
(43) Lee, Y. C.; Wang, P. Y.; Lo, S. L.; Huang, C. P. Recovery of Perfluorooctane Sulfonate (PFOS) and Perfluorooctanoate (PFOA) from Dilute Water Solution by Foam Flotation. *Sep. Purif. Technol.* **2017**, *173*, 280−285.
(44) Wang, S.; Huang, J.; Yang, Y.; Hui, Y.; Ge, Y.; Larssen, T.; Yu, G.; Deng, S.; Wang, B.; Harman, C. First Report of a Chinese PFOS Alternative Overlooked for 30 Years: Its Toxicity, Persistence, and Presence in the Environment. *Environ. Sci. Technol.* **2013**, *47* (18), 10163−10170.
(45) Ahrens, L.; Taniyasu, S.; Yeung, L. W. Y.; Yamashita, N.; Lam, P. K. S.; Ebinghaus, R. Distribution of Polyfluoroalkyl Compounds in Water, Suspended Particulate Matter and Sediment from Tokyo Bay, Japan. *Chemosphere* **2010**, *79* (3), 266−272.
(46) Helsel, D. R. Fabricating Data: How Substituting Values for Nondetects Can Ruin Results, and What Can Be Done about It. *Chemosphere* **2006**, *65* (11), 2434−2439.
(47) Nelson, C. System and Method for Treatment of Soil and Groundwater Contaminated with PFAS. WO 2017/218335 A1, 2017.
(48) Casas, G.; Martínez-Varela, A.; Roscales, J. L.; Vila-Costa, M.; Dachs, J.; Jiménez, B. Enrichment of Perfluoroalkyl Substances in the Sea-Surface Microlayer and Sea-Spray Aerosols in the Southern Ocean. *Environ. Pollut.* **2020**, *267*, 115512.
(49) Cao, Y.; Lee, C.; Davis, E. T. J.; Si, W.; Wang, F.; Trimpin, S.; Luo, L. 1000-Fold Preconcentration of Per- And Polyfluorinated Alkyl Substances within 10 minutes via Electrochemical Aerosol Formation. *Anal. Chem.* **2019**, *91* (22), 14352−14358.
(50) Sha, B.; Johansson, J. H.; Benskin, J. P.; Cousins, I. T.; Salter, M. E. Influence of Water Concentrations of Perfluoroalkyl Acids (PFAAs) on Their Size-Resolved Enrichment in Nascent Sea Spray Aerosols. *Environ. Sci. Technol.* **2021**, *55* (14), 9489−9497.
(51) European Parliament and the Council of the European Union. Directive 2013/11/EU of the European Parliament and of the Council of 12 August 2013 Amending Directives 2000/60/EC and 2008/105/EC as Regards Priority Substances in the Field of Water Policy. *Off. J. Eur. Union* **2013**, *226*, 1−17.
(52) *IENW/BSK-2020/117392: Uniforme Voorwaarden Lozingen Gronddepots En Grondreinigers*; Ministry of Infrastructure and Water Management: The Netherlands, 2020.
(53) Verma, S.; Varma, R. S.; Nadagouda, M. N. Remediation and Mineralization Processes for Per- and Polyfluoroalkyl Substances (PFAS) in Water: A Review. *Sci. Total Environ.* **2021**, *794*, 148987.
(54) Singh, R. K.; Brown, E.; Mededovic Thagard, S.; Holsen, T. M. Treatment of PFAS-Containing Landfill Leachate Using an Enhanced Contact Plasma Reactor. *J. Hazard. Mater.* **2021**, *408*, 124452.
(55) Maldonado, V. Y.; Landis, G. M.; Ensch, M.; Becker, M. F.; Witt, S. E.; Rusinek, C. A. A Flow-through Cell for the Electrochemical Oxidation of Perfluoroalkyl Substances in Landfill Leachates. *J. Water Process Eng.* **2021**, *43* (June), 102210.
(56) Lau, Y. M.; Deen, N. G.; Kuipers, J. A. M. Development of an Image Measurement Technique for Size Distribution in Dense Bubbly Flows. *Chem. Eng. Sci.* **2013**, *94*, 20−29.
(57) Fu, Y.; Liu, Y. Development of a Robust Image Processing Technique for Bubbly Flow Measurement in a Narrow Rectangular Channel. *Int. J. Multiph. Flow* **2016**, *84*, 217−228.

https://doi.org/10.1021/acsestwater.2c00032
ACS EST Water 2022, 2, 841−851

Supplementary Information to *Pilot-scale continuous foam fractionation for the removal of per- and polyfluoroalkyl substances (PFAS) from landfill leachate*

Sanne Smith[1], Karin Wiberg[1], Philip McCleaf[2]and Lutz Ahrens[1]

[1]Department of Aquatic Sciences and Assessment, Swedish University of Agricultural Sciences (SLU), P.O. Box 7050, SE-750 07, Uppsala, Sweden
[2]Uppsala Water and Waste AB, P.O. Box 1444, SE-751 44, Uppsala, Sweden
E-mail contact: sanne.smith@slu.se

A. Results preliminary experiment

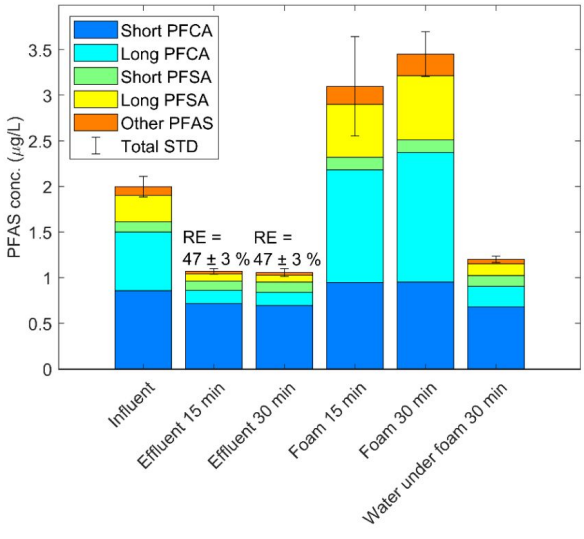

Figure SI. 1: Overview of results of preliminary experiment (t_c = 10 min, 30 % foam, AR 2.16, Q_{air} 10 L min^{-1}). Error bars represent the standard deviation on the ΣPFAS concentration.

Figure SI. 1 summarizes the results of the preliminary triplicate experiments at 10 minutes contact time (t_c), air flow 10 L min^{-1} (Q_{air}) and 30 % foam. For details on the experimental approach, see main text section 2.2. PFHxA, PFOA, PFDA, PFPeS, PFHxS, PFHpS, PFOS, PFECHS, FOSA, MeFOSAA and EtFOSAA concentrations were significantly higher directly under the air/water surface than in the effluent samples for at least one of the time points. However, since the effluent quality remained constant, this was deemed not to affect treatment performance in continuous mode. Moreover, ΣPFAS removal directly

under the air/water surface was 40 ± 2.5 %, indicating that removal already takes place in the top part of the column. Hence, further tests were carried out as described in main text section 2.2, with replicate samples taken at four different time points instead of in experimental triplicates.

B. Overview of experiments

Table SI. 1: Dates of experiments. Experiments that were deemed process-limited are indicated with an asterisk.

Exp.	Date
0	2021-04-12
1*	2022-03-11
2	2021-08-24
3*	2021-08-24
4	2021-08-30
5	2021-08-30
6	2021-08-30
7	2021-09-09
8	2021-09-09
9	2021-09-09
10*	2021-09-14
11	2021-09-14
12	2021-09-14
13	2021-09-27
14*	2021-09-27
15	2021-09-27
16	2021-10-13
17	2021-10-13

C. Analytical Method

Water samples were sonicated for 5 min before filtration. After filtration, 100 µL of the IS mixture (main text Section 2.2) at 50 ng mL^{-1} concentration for individual IS in methanol was added to each sample, the samples were then vigorously mixed and sonicated again for 5 min. Oasis® WAX cartridges (6 mL, 150 mg, 30 µm, Waters) were preconditioned with 4 mL 0.1 % ammonium hydroxide in methanol, followed by 4 mL methanol and 4 mL Milli-Q water. After sample loading at approximately one drop per second, the cartridges were washed with 4 mL 25 mM ammonium acetate buffer in Milli-Q water. The cartridges were dried under vacuum and eluted with 4 mL methanol and 4 mL 0.1% ammonium hydroxide in methanol. The extracts were concentrated to 1 mL volume under nitrogen. A lab blank of 150 mL Milli-Q water was included in each run.

The limit of quantification (LOQ) was 0.33 ng L^{-1} for the foam samples (150 mL analyzed) and 0.2 ng L^{-1} for the influent and effluent samples (250 mL analyzed). The LOQ was set to the lowest concentration of the calibration curve with a consistent signal-to-noise ratio of 10. As explained in the main text, concentrations below the LOQ were taken as zero, which introduces an error. The lowest ΣPFAS concentration found in any of the samples was 750 ng L^{-1}, with 15 of the PFAS in the method being non-detects. The maximum concentration of the non-detects in this effluent sample thus contributed 0.4 % to

the total PFAS concentration, which was deemed negligible; hence non-detect concentrations were set to zero.

120 mL Milli-Q samples spiked with 6.25, 12.5 and 25 ng of each native PFAS included in the analysis were extracted and analyzed for their recovery. For all compounds, the mean and median absolute deviation from the spiked concentrations were 9.0 % and 5.7 %, respectively. The only compounds with mean absolute deviations higher than 15 % were HFPO-DA, PFECHS, PFDS, 11Cl-PF3OUdS and PFTriDA, of which only PFDS and PFTriDA were above 20 % (-26 % and 39 % mean deviation, respectively). The maximum contribution of these compounds to the ΣPFAS concentrations in all samples were only 0.004 % and 3 %, respectively, but nonetheless, the concentrations of these compounds should be considered to have a lower degree of accuracy.

Table SI. 2: Scheduled multiple reaction monitoring transitions for LC-MS/MS analysis of PFAS concentrations. The compounds are ordered on precursor mass.

Compound	Precursor mass (Q1, m/z)	Product mass (Q3, m/z)	Retention time (min)	Declustering potential (V)	Collision energy (V)	Collision cell exit potential (V)
Perfluorobutanoic acid (PFBA)	213.0	168.9	1.06	-20	-12	-5
$^{13}C_4$-PFBA	217.0	172.0	1.06	-25	-14	-9
Perfluoropentanoic acid (PFPeA)	262.9	218.9	1.27	-5	-12	-11
$^{13}C_5$-PFPeA	268.0	223.0	1.27	-30	-12	-9
Perfluorobutane sulfonate (PFBS)	299.0	80.0	1.30	-90	-64	-7
PFBS	299.0	99.0	1.30	-90	-50	-9
$^{13}C_3$-PFBS	302.0	80.0	1.30	-90	-70	-5
Perfluorohexanoic acid (PFHxA)	313.0	268.9	1.56	-35	-10	-14
PFHxA	313.0	118.9	1.56	-35	-26	-9
$^{13}C_5$-PFHxA	318.0	273.0	1.56	-35	-14	-13
4:2 Fluorotelomer sulfonic acid (4:2 FTSA)	327.0	307.0	1.53	-75	-28	-11
4:2 FTSA	327.0	287.0	1.53	-75	-28	-11
hexafluoropropylene oxide dimer acid (HFPO-DA)	328.9	284.9	1.66	-20	-8	-13
HFPO-DA	328.9	169.0	1.66	-20	-8	-13
$^{13}C_2$-4:2 FTSA	329.0	309.0	1.53	-5	-28	-13
$^{13}C_3$-HFPO-DA	332.0	287.0	1.66	-15	-8	-9
Perfluoropentane sulfonate (PFPeS)	349.0	80.0	1.57	-100	-76	-7
PFPeS	349.0	99.0	1.57	-100	-66	-7
Perfluoroheptanoic acid (PFHpA)	362.9	318.9	1.93	-40	-14	-11

PFHpA	362.9	169.0	1.93	-40	-24	-5
$^{13}C_4$-PFHpA	367.0	172.0	1.93	-40	-24	-7
4,8-dioxa-3H-perfluorononanoic acid (NaDONA)	376.9	250.9	1.96	-45	-18	-9
NaDONA	376.9	84.9	1.96	-45	-54	-7
Perfluorohexane sulfonate (PFHxS)	399.0	79.9	1.92	-95	-82	-5
PFHxS	399.0	99.0	1.92	-115	-70	-7
$^{13}C_3$-PFHxS	402.0	80.0	1.92	-105	-86	-7
Perfluorooctanoic acid (PFOA)	413.0	369.1	2.32	-45	-16	-15
PFOA	413.0	169.1	2.32	-40	-24	-5
$^{13}C_8$-PFOA	421.0	376.0	2.32	-45	-16	-17
6:2 Fluorotelomer sulfonate (6:2 FTSA)	427.0	81.0	2.28	-85	-72	-7
$^{13}C_2$-6:2 FTSA	429.0	81.0	2.28	-90	-70	-7
Perfluoroheptane sulfonate (PFHpS)	448.9	80.0	2.32	-130	-90	-7
PFHpS	448.9	99.0	2.32	-125	-80	-7
Perfluoroethyl-cyclohexane sulfonate (PFECHS)	461.0	381.0	2.26	-90	-38	-13
PFECHS	461.0	99.0	2.26	-95	-68	-7
Perfluorononanoic acid (PFNA)	463.0	219.0	2.71	-50	-24	-9
PFNA	463.0	168.9	2.71	-45	-26	-9
$^{13}C_9$-PFNA	472.0	172.0	2.71	-50	-26	-9
Perfluorooctane sulfonamide (FOSA)	498.0	78.0	2.91	-105	-86	-7
Perfluorooctane sulfonate (PFOS)	499.2	80.0	2.71	-130	-110	-7
PFOS	499.2	98.9	2.71	-115	-94	-9
$^{13}C_8$-FOSA	506.0	77.9	2.91	-110	-82	-7
$^{13}C_8$-PFOS	507.0	80.0	2.71	-135	-108	-7
Perfluorodecanoic acid (PFDA)	513.0	268.9	3.09	-55	-26	-11
PFDA	513.0	218.9	3.09	-50	-26	-9
$^{13}C_6$-PFDA	519.0	474.0	3.09	-75	-14	-19
8:2 Fluorotelomer sulfonate (8:2 FTSA)	527.2	506.9	3.08	-125	-38	-15
8:2 FTSA	527.2	81.0	3.08	-110	-88	-7
$^{13}C_2$-8:2 FTSA	529.0	81.0	3.08	-120	-86	-7
9-chloro-hexadecafluoro-3-oxanonane sulfonate	531.0	351.0	2.92	-110	-36	-13

(9Cl-PF3ONS)						
9Cl-PF3ONS	531.0	83.0	2.92	-105	-78	-7
Perfluorononane sulfonate (PFNS)	549.0	80.0	3.07	-140	-110	-7
PFNS	549.0	99.0	3.07	-135	-92	-7
Perfluoroundecanoic acid (PFUnDA)	563.0	519.0	3.43	-60	-18	-9
PFUnDA	563.0	268.9	3.43	-55	-26	-11
N-methyl-perfluorooctane sulfonamido acetic acid (MeFOSAA)	569.9	418.9	3.26	-90	-28	-21
MeFOSAA	569.9	482.9	3.26	-90	-22	-21
$^{13}C_7$-PFUnDA	570.0	525.0	3.43	-90	-18	-9
D_3-MeFOSAA	573.0	419.0	3.26	-80	-28	-19
N-ethyl-perfluorooctane sulfonamido acetic acid (EtFOSAA)	584.0	419.0	3.44	-85	-28	-17
EtFOSAA	584.0	219.0	3.44	-85	-36	-9
D_5-EtFOSAA	589.0	419.0	3.44	-85	-30	-15
Perfluorodecane sulfonate (PFDS)	598.9	80.0	3.41	-150	-120	-7
PFDS	598.9	99.0	3.41	-155	-114	-7
Perfluorododecanoic acid (PFDoDA)	613.0	569.0	3.74	-60	-18	-11
PFDoDA	613.0	318.9	3.74	-65	-28	-13
$^{13}C_3$-PFDoDA	615.0	570.0	3.74	-65	-18	-11
11-chloro-eicosafluoro-3-oxaundecane-1-sulfonic acid (11Cl-PF3OUdS)	630.9	450.9	3.59	-115	-42	-19
11Cl-PF3OUdS	630.9	83.0	3.59	-120	-80	-7
Perfluorotridecanoic acid (PFTriDA)	662.9	618.9	4.03	-70	-18	-11
PFTriDA	662.9	319.0	4.03	-70	-32	-11
Perfluorotetradecanoic acid (PFTeDA)	713.0	668.9	4.29	-75	-20	-9
PFTeDA	713.0	368.8	4.29	-75	-30	-13
$^{13}C_2$-PFTeDA	715.0	670.0	4.29	-75	-20	-13

Table SI. 3: Internal standards used for compounds without a corresponding mass labeled internal standard in the IS mixture.

Compound	IS used
PFPeS	$^{13}C_3$-PFHxS
NaDONA	$^{13}C_3$-HFPO-DA
PFHpS	$^{13}C_8$-PFOS
PFECHS	$^{13}C_8$-PFOS
9Cl-PF3ONS	IS_FOSA
PFNS	$^{13}C_8$-PFOS
PFDS	$^{13}C_8$-PFOS
11Cl-PF3OUdS	$^{13}C_8$-FOSA
PFtriDA	$^{13}C_2$-PFTeDA

Table SI. 4: Overview of instrument parameters for quantification of PFAS

Instrument	Sciex Triple Quad™ 3500 LC-MS/MS (USA)		
Guard column	Phenomenex KJ0-4282		
Precolumn	Phenomenex Kinetix® 1.7 µm C18 100 Å		
Analytical column	Phenomenex Gemini® 3 µm C18 110 Å		
Autosampler temperature	15 °C		
Injection volume	10 µL		
Flow rate	0.6 mL min^{-1}		
Column oven temperature	40 °C		
Mobile phase	A: 10 mM ammonium acetate in MilliQ water; B: 100 % methanol		
Gradient program	Time (min)	%A	%B
	0	95	5
	0.1	45	55
	4.5	1	99
	8	1	99
	8.5	95	5
	9	95	5
Ionization	Heated electrospray ionization in negative mode		
Negative ion spray voltage	-3000 V		
Curtain gas pressure	35 psi		
Collision gas pressure	8 psi		
Gas temperature	600 °C		
Ion source gas 1 pressure	30 psi		
Ion source gas 2 pressure	40 psi		
Run time	9 min		
Calibration curve concentrations	0.01, 0.05, 0.1, 0.5, 1, 5, 10, 50 & 100 ng mL^{-1}		

D. General Chemistry

Table SI. 5: General chemistry results of analyzed samples

	Influent				Effluent				Foam	
Experiment	**0**	**1**	**13**	**15**	**0**	**1**	**13**	**15**	**13**	**15**
DOC (mg L^{-1})	36	35	37	36	36	33	38	39	42	49
Phosphor (µg L^{-1})	200	117	132	96	200	76	104	104	173	202
Calcium (mg L^{-1}	156	150	154	149	157	137	155	153	154	151
Manganese (µg L^{-1})	442	487	636	526	432	351	646	681	633	586
Sodium (mg L^{-1})	640	702	743	759	647	697	751	754	730	746
Potassium (mg L^{-1})	222	222	251	264	224	220	276	258	266	257
Iron (mg L^{-1})	5.1	5.8	5.3	5.2	4.5	3.6	5.9	5.4	9.2	10
Aluminum (µg L^{-1})	63	14	21	9.4	59	14	16	10	26	61
Copper (µg L^{-1})	26	13	15	161	28	15	53	16	76	78
Magnesium (mg L^{-1})	50	57	59	60	50	57	61	60	59	60
Hardness (°dH)	33	34	35	35	34	32	36	35	35	35
NO_2 (mg L^{-1})	0.65	0.37	0.76	0.68	0.76	0.39	0.68	0.66	0.69	0.71
COD-Mn (mg L^{-1})	38	19	25	27	46	19	28	25	31	31
Ammonium (mg L^{-1})	62	56	58	60	62	55	61	61	61	60
Phosphate (mg L^{-1})	0.15	0.06	<0.04	<0.04	0.18	0.06	<0.04	<0.04	<0.04	<0.04
Nitrate (mg L^{-1})	16	21	17	20	17	21	17	17	17	17
Fluoride (mg L^{-1})	<0.5	<0.5	<0.5	<0.5	<0.5	<0.5	<0.5	<0.5	<0.5	<0.5
Chloride (mg L^{-1})	818	909	909	1050	834	915	950	950	950	948
Sulphate (mg L^{-1})	202	111	121	99	199	112	93	89	98	92
Turbidity (FNU)	56	27	32	24	41	37	59	51	55	106
Conductivity (mS m^{-1})	403	484	430	436	425	477	446	450	441	443
pH	7.7	8.0	7.7	8.0	8.0	8.1	8.0	7.7	8.0	8.0
Alkalinity (mg L^{-1})	1280	1330	1370	1260	1260	1230	1380	1480	1410	1390
TOC (mg L^{-1})	26	45	38	37	26	33	39	39	43	52
Uranium (µg L^{-1})	26	43	30	29	26	43	30	30	29	30

E. Overview of excluded data

Table SI. 6: Legitimization of sample exclusion. In addition to these samples, some foam extracts had too high concentrations of PFOA (>> 100 ng mL^{-1}), which made quantification with a quadratic calibration curve impossible. For these samples, the PFOA calibration curve was changed to linear. Unrealistically high values indicate a value that is at least a factor 5 or 400 ng L^{-1} higher than the mean concentration of the remaining three samples of the same type.

Experiment number	Excluded sample	Reason of exclusion
4	Foam 2 hr	Lost during collection due to human error
10	Influent 2 hr	Lost during analysis due to a production error in the polypropylene tube used for collection after extraction
	Effluent 0.5 hr	Contaminated in lab – unrealistically high PFNA, FOSA, PFOS, PFDA, PFUnDA and PFDoDA concentrations
	PFBA in effluent 1 hr	Unrealistically high value - replaced by concentration of 0.5 hr sample (which was otherwise excluded)
	PFBA in foam 2 hr	Unrealistically high value - excluded
11	Effluent 2 hr	Contaminated in lab – unrealistically high PFOA, PFNA, FOSA, PFOS, PFDA, PFUnDA and PFDoDA concentrations
	PFTeDA in effluent 1 hr	Unrealistically high value – replaced by concentration of 2 hr sample (which was otherwise excluded)
15	Bottom effluent r2	Not spiked with IS prior to extraction

In total, 204 PFAS samples were analyzed for the study, of which five have been excluded completely and three have one excluded compound.

F. Classification of PFAS

Table SI. 7: Overview of PFAS designation into groups

Group	Compounds
Short carboxylates	PFBA, PFPeA, PFHxA, PFHpA
Long carboxylates	PFOA, PFNA, PFUnDA, PFDoDA, PFTriDA, PFTeDA
Short sulfonates	PFBS, PFPeS
Long sulfonates	PFHxS, PFHpS, PFOS, PFNS, PFDS
Rest	4:2 FTSA, 6:2 FTSA, 8:2 FTSA, FOSA, HFPO-DA, NaDONA, PFECHS, 9Cl-PF3ONS, 11ClPF3OUdS, Me-FOSAA, Et-FOSAA

G. Fitted parameters

Table SI. 8: Fitted parameters for the effect of process variables on ΣPFAS removal, Equation 6 in the main text.

Process variable	*k*	RE_{Max} (%)
Contact time at constant AR	0.12 min^{-1}	60.5
Contact time at constant AF	0.11 min^{-1}	60.9

Foam fraction	0.33	57.1
Air flow	0.23 min L^{-1}	56.7

H. PFAS removal as a function of chain length

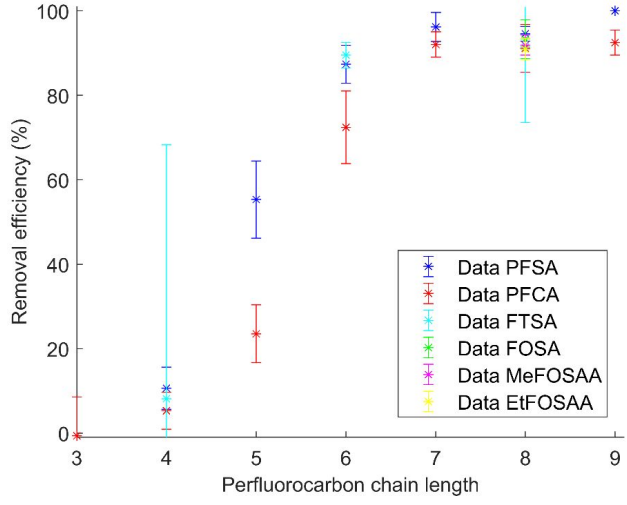

Figure SI. 2: PFAS removal as a function of chain length. Note that PFNA, PFOS, 8-2 FTSA, FOSA, MeFOSAA and EtFOSAA all have a perfluorocarbon chain length of 8. The mean influent concentration of 4-2 FTSA was only 0.8 ng L^{-1}, which caused a high standard deviation in the results as compared to compounds with higher initial concentrations.

I. Mass balance for individual compounds

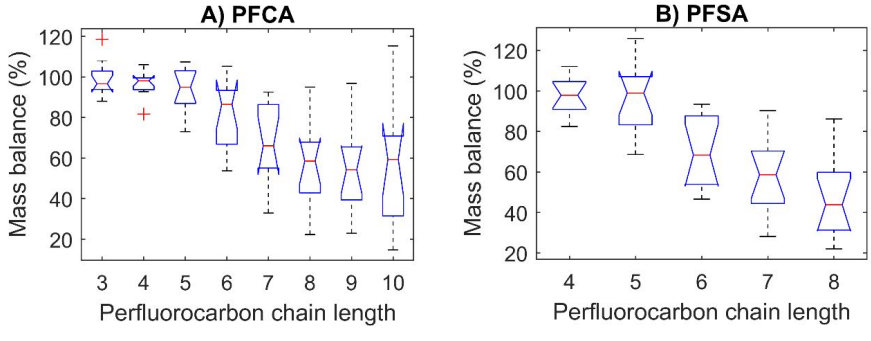

Figure SI. 3: Boxplots for the different individual PFAS included in the Anova analysis for the effect of chain length on mass balance. Note that the red lines represent medians, whereas the statistical analysis is based on mean values. The groups include the mean individual mass balances from experiments 2, 4-9, 11-13, 16 and 17, e.g. n = 12 for each group.

Based on the Anova results outlined in the main text, a statistically significant difference was found with at least 3 other groups for each PFCA group and at least 2 other groups for each PFSA group (Tukey's honestly significant difference procedure).

II

Science of the Total Environment 871 (2023) 162050

Contents lists available at ScienceDirect

Science of the Total Environment

journal homepage: www.elsevier.com/locate/scitotenv

Foam fractionation for removal of per- and polyfluoroalkyl substances: Towards closing the mass balance

Sanne J. Smith [a,*], Jeffrey Lewis [b], Karin Wiberg [a], Erik Wall [c], Lutz Ahrens [a]

[a] Department of Aquatic Sciences and Assessment, Swedish University of Agricultural Sciences (SLU), P.O. Box 7050, SE-750 07 Uppsala, Sweden
[b] ECT2, Lärlingsgatan 14b, SE-90422 Umeå, Sweden
[c] Cytiva, Björkgatan 30, SE-75323 Uppsala, Sweden

HIGHLIGHTS

- Foam fractionation could remove PFAS from industrial water on pilot-scale.
- Air emissions were high, but no major contributor to low mass-balance closures.
- Airborne PFAS caused an occupational exposure that exceeds the EFSA recommendation.
- Removal correlated positively with total element concentration and conductivity.

GRAPHICAL ABSTRACT

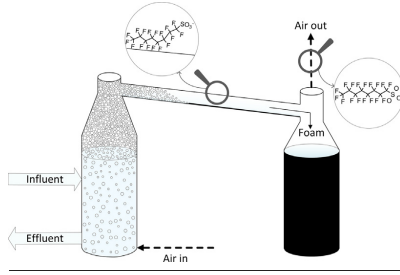

ARTICLE INFO

Guest Editor: Vitor Vilar

Keywords:
Per- and polyfluoroalkyl substances (PFAS)
Water treatment
Air emissions
Foam fractionation
Pilot-scale
Remediation

ABSTRACT

Foam fractionation has recently attracted attention as a low-cost and environmentally benign treatment technology for water contaminated with per- and polyfluoroalkyl substances (PFAS). However, data on the mass balance over the foam fractionation process are scarce and when available, gaps in the mass balance are often identified. This study verified the high treatment efficiency of a pilot-scale foam fractionation system for removal of PFAS from industrial water contaminated with aqueous film-forming foam. ΣPFAS removal reached up to 84 % and the removal of perfluorooctane sulfonic acid (PFOS) up to 97 %, but the short-chain perfluorobutanoic acid (PFBA) was only removed with a mean efficiency of 1.5 %. In general, mobile short-chain PFAS were removed less efficiently when the perfluorocarbon chain length was below six for carboxylic acids and below five for sulfonic acids. Fluctuations in treatment efficiency due to natural variations in the chemistry of the influent water were minor, confirming the robustness of the technology, but significant positive correlations between PFAS removal and influent metal concentration and conductivity were observed. Over all experiments, the mass balance closure did not differ significantly from 100 %. Nonetheless, PFAS sorption to the walls of the reactor was measured, as well as high PFAS emissions by the air exiting the reactor. PFAS emissions in aerosols correlated positively with mass balance closure. The elevated aerial PFAS concentrations measured in the experimental facility have implications for worker safety and prevention of PFAS-emissions to the atmosphere, and demonstrate the importance of installing appropriate filters on the air outlet of foam fractionation systems.

1. Introduction

Per- and polyfluoroalkyl substances (PFAS) are exceptionally stable anthropogenic chemicals with versatile applications as lubricants, coatings and surfactants (Buck et al., 2011; Evich et al., 2022). The widespread

* Corresponding author.
E-mail address: sanne.smith@slu.se (S.J. Smith).

http://dx.doi.org/10.1016/j.scitotenv.2023.162050
Received 18 August 2022; Received in revised form 1 February 2023; Accepted 2 February 2023
Available online 7 February 2023

use, high mobility and persistent nature of PFAS has caused their ubiquitous presence in the environment, ultimately leading to human exposure to these chemicals via contaminated air, water or food (Sunderland et al., 2019). The toxicology of most PFAS is still poorly understood, although numerous health impacts have been demonstrated for legacy compounds such as perfluoroalkyl carboxylic acids (PFCA) and perfluorosulfonic acids (PFSA) (Fenton et al., 2020). Because of these findings, health-based guidelines for PFAS exposure have been introduced in e.g. the U.S. and Europe (EFSA, 2020; US EPA, 2016).

To adequately limit human exposure to PFAS, the development of cost-efficient remediation technologies for contaminated sources is urgently needed. The use of PFAS-containing aqueous film-forming foams (AFFF) constitutes an important source of these chemicals, causing contamination of soil, groundwater and surface water (Ahrens, 2011; Lenka et al., 2021; Sunderland et al., 2019). Treating AFFF-contaminated water before discharge is hence crucial towards preventing the spread of PFAS in the environment. Numerous treatment methods exist that are being applied on full-scale, of which adsorption to granular activated carbon (GAC) (Belkouteb et al., 2020), ion exchange resins (IEX) (Dixit et al., 2021) or foam fractionation (Burns et al., 2021) are used most often.

Of these three treatment technologies, foam fractionation has the advantage that no consumables are used during the process, generating very low operating expenses (Burns et al., 2021). Moreover, since no regeneration of sorbent materials using thermal treatment or organic solvents is necessary, the treatment can be considered environmentally benign. The process has been well-described in academic literature for the removal of PFAS (Buckley et al., 2022, 2021; Burns et al., 2021; Lee et al., 2017; McCleaf et al., 2021; Meng et al., 2018; Smith et al., 2022). In essence, it is similar to conventional sorption processes, but the sorbent consists of rising air bubbles that are introduced at the bottom of a water column. Because most PFAS are amphiphilic, they adsorb to the surface of these air bubbles, with their polar parts remaining in the water phase and their apolar tails inside the air bubble. If enough surfactant molecules are present, a PFAS-enriched foam will form on top of the water, which can be harvested as foamate and treated further separately. Conversely, the bulk water phase will be depleted of PFAS.

The effectiveness of foam fractionation towards the removal of long-chain PFAS (i.e. PFSA: $C_nF_{2n+1}SO_3H$, $n > 5$; PFCA: $C_nF_{2n+1}COOH$, $n > 6$) has been documented extensively, with removal efficiencies generally exceeding 95 % (Buckley et al., 2022; Burns et al., 2021; Lee et al., 2017; McCleaf et al., 2021; Meng et al., 2018). However, foam fractionation is less suitable for the removal of the more mobile short-chain PFAS, because these compounds have lower air-water sorption coefficients (Buckley et al., 2022; Burns et al., 2021). Moreover, various studies report a loss of PFAS in the overall mass balance, with up to 36 % less PFAS measured in the foamate than was removed from the water phase (McCleaf et al., 2021; Smith et al., 2022). It is unclear whether these missing PFAS are emitted to the air, adsorb to the reactor walls or are transformed during the treatment process. Finally, effects of natural variations in the chemistry of the influent water are still poorly understood.

To assess these knowledge gaps, the current study aimed to investigate the mass balance of the foam fractionation process, as well as verify the performance of the treatment. Specifically, objectives were to *i)* explore the effect of residence time, surfactant dosage, conductivity and metal and total organic carbon (TOC) concentration on the PFAS removal using a pilot-scale continuous foam fractionation reactor treating an industrial AFFF-contaminated water stream with highly variable composition, *ii)* comprehensively examine the PFAS mass balance over the influent, effluent and foam and *iii)* evaluate whether PFAS are present in the air and aerosols that exit this pilot-scale foam fractionation reactor and if this could explain any gaps in the mass balance.

2. Methods

The brands and purity grades of all chemicals can be found in Table SI 1. All glassware was burned at 400 °C overnight and all glass or plastic containers were rinsed three times with the appropriate solvent before use. Full names of all PFAS compounds are given in Tables SI 2 and SI 3.

2.1. Experimental approach

A pilot-scale continuous foam fractionation system designed by ECT2 (Emerging Compounds Treatment Technologies, Sweden) was used in all experiments to treat PFAS-contaminated industrial water at Cytiva, Uppsala, Sweden. This water consisted of a mixture of AFFF-contaminated surface runoff, groundwater and process water with a variable composition, collected continuously in a 12 m^3 storage filled to 50 % capacity prior to entering the on-site water treatment system. The water was pumped directly from this tank into the foam fractionating system, so PFAS concentrations and other chemical parameters in the influent varied over time. A schematic overview of the process is given in Fig. 1. Water continuously entered the foam fractionation column (Ø 49.4 cm, water level at 108.5 cm) at a height of 92 cm above the column bottom and exited the column at the bottom. A venturi blower was used for introducing air bubbles to the water in a recirculation loop. To enhance foaming, a constant flow of soap (Neutral® Hand Dishwash, Unilever, ingredients: 5–15 % anionic surfactants, <5 % amphoteric surfactants, non-ionic surfactants, sodium benzoate) solution in influent water was supplied to the venturi system using a peristaltic pump (Masterflex L/S with neoprene tubing). Once the foam rose to the top of the system at approximately 60 cm above the water level, it was forced to collapse under warm air that entered the system through a heater. The liquid foamate then flowed down a pipe into a foam collection vessel. A fan blowing air out of the system was placed on top of the foam vessel, to improve the foam flow.

Duplicate foam fractionation runs at various residence times (13, 20, 30 and 60 min) and soap ratios (21, 62 and 125 ppmv) were carried out to assess the PFAS removal efficiency of the system, see Table 1 for details. The soap ratio is the ratio between the pure soap dosage rate to the venturi and the influent water flow rate. For each experiment, the system was run for 1 h after the foam flow started, except for the experiments at 60 min residence time, which were run for 2 h. The foam flow rate was observed to remain relatively constant over the duration of each experiment. 250 mL influent was collected before and after each run in clean polypropylene (PP) bottles from a valve in the influent hose for determination of PFAS concentrations, pH and conductivity, to correct for the variability of the influent during the experiment. 250 mL effluent and foam were collected for PFAS analysis at the end of each run. Moreover, 500 mL influent was collected at the end of each experiment for determination of the TOC and metal concentrations.

All experimental duplicates were carried out directly after each other, to minimize variations in the influent. Two of the experiments were repeated in duplicate one week later, to assess the effect of differences in influent water characteristics. Before each experiment, the column was flushed with at least three column volumes of influent water in the absence of air flow to clean the system. After each experiment, all foam was pumped out of the foam collection vessel with a peristaltic pump (Watson Marlow, 630SN/RE with Pureweld Xl 12.7 mm tubing) and weighed to determine the amount of foam produced. Foam samples were taken from this bulk foam. At the end of the experimental period, the pipe through which the foam flowed to the collection vessel was rinsed with MilliQ water and ethanol, which was combined and sent in for PFAS analysis to check for PFAS sorption to the pipe walls.

2.2. Air and aerosol sampling

An aluminum air sampler holder (Tisch Environmental, pre-cleaned with acetone) containing two pre-combusted stacked quartz microfiber filters (⌀ 11 cm, pore size 2.2 μm, QM-A, Whatman) was placed above the fan (see Fig. 1), to collect aerosols in the air exiting the system. To ensure detectable PFAS concentrations, the filters were only replaced after each set of duplicates rather than between duplicates as well. There was a space of approximately 5 mm between the sampler and the air exit, so not all air

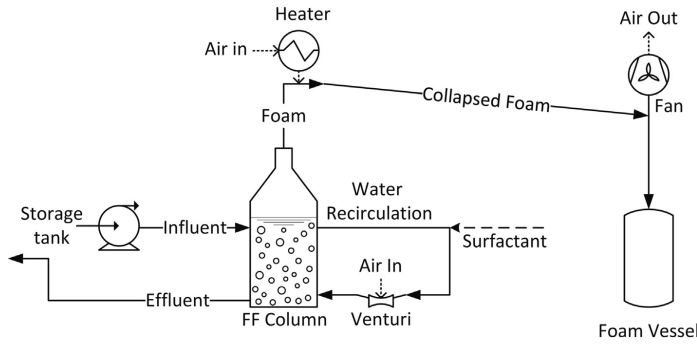

Fig. 1. Process overview of the single-stage pilot-scale continuous foam fractionation reactor employed in this study. The conical-shaped top part of the column filled up with foam, which subsequently flowed down into the foam collection vessel.

passed through the filters, because otherwise the air flow through the fan was inhibited too much. The minimum air flow was found by detecting the point where foam collection system did not work properly anymore, causing low foam flows and incomplete collapse of the foam. In the repeated run of experiment 1, the aerosol sampler was placed upside down, such that the distance between the air outlet and the filter was decreased from approximately 9 cm to 4 cm.

To sample the PFAS content in the air around the foam fractionation reactor, four passive air samplers (PAS; Tisch Environmental) containing sorbent-impregnated polyurethane foam discs (SIPs) were employed in the same room as the reactor during all experiments, over a total duration of eleven days. The approximate placement of these four PAS-SIPs is shown in Fig. SI 1. The use of SIPs for PFAS detection in air is a well-established method that has been developed and verified extensively in earlier studies (Ahrens et al., 2013; Shoeib et al., 2008; Winkens et al., 2017). An additional PAS-SIP was employed in the staircase of the same building as a reference location for the background indoor environment. A field blank was collected by placing a SIP inside the PAS housing for one minute on-site, after which the SIP was treated as all other samples. All PAS housings had been cleaned with tap water followed by thorough rinsing with acetone prior to employment and SIPs were only handled using acetone-rinsed tweezers.

The SIPs were prepared according to the protocol by Ahrens et al. (2013). In brief, polyurethane foam discs (PUFs, Tisch Environmental, 0.5 × 5.5″) were cleaned by Soxhlet extraction with acetone for 24 h, followed by petroleum ether for 17 h and fresh petroleum ether for 7 h. Finely ground XAD-4 resin was Soxhlet extracted with methanol for 17 h, followed by dichloromethane for 24 h and hexane for 6 h. The clean XAD-4 was kept in a beaker at −20 °C, while the PUFs were dried in a pre-cleaned vacuum desiccator for approximately 72 h. After drying, the PUFs were impregnated by dipping them in a XAD-4 in hexane slurry (approximately 6.4 g L^{-1}) three times for 30 s and subsequent drying on a heating plate, both repeated twice. After the second drying step, the SIPs were dried further in a vacuum desiccator again for 72 h. Prior to transport, the SIPs were wrapped in pre-cleaned aluminum foil and stored in individual airtight zip-lock bags.

2.3. Chemical analyses

All water samples were shipped to ALS Scandinavia for PFAS (n = 32, *Table SI 2*), TOC, turbidity and metal and element content analysis. For the PFAS analysis, a laboratory blank of 250 mL MilliQ water, a field blank of 250 mL MilliQ water, which was opened on-site for 1 min, and a surfactant blank of approximately 5 g/L surfactant in MilliQ water were sent in as well. Limits of quantification (LOQ) of individual PFAS in the analytical method varied between 0.01 and 25 μg L^{-1}, depending on the PFAS compound and the matrix, and are given in Table SI 2. An overview of the metals and elements included in the analysis with their quantification limits is given in Table SI 4. pH and conductivity of the influent were measured on-site using a Knick Memosens 555 pH sensor and Hach CDC401 conductivity probe, respectively.

The quartz microfiber filters used for aerosol collection and the PAS-SIPs were analyzed in the laboratory at the Department of Aquatic Sciences and Assessment, Swedish University of Agricultural Sciences. The extraction was carried out according to a modified protocol described by Casas et al. (2020). One blank without filter and one blank with a clean filter were included in addition to the field blank. Each filter was transferred to a 50 mL PP vial and spiked with 50 μL of an internal standard (IS) mixture containing 50 ng mL^{-1} of each individual compound (Smith et al., 2022). 15 mL of methanol was added, after which the tubes were vortexed and sonicated for 20 min. The methanol was decanted into a second tube, and the extraction was repeated twice with 5 mL of methanol. The combined methanol fractions were concentrated to 0.5 mL under a gentle stream of N_2 and transferred to 1.5 mL Eppendorf tubes. The PP tubes were rinsed

Table 1
Overview of experimental parameters. Experiments 1 and 2 (E1 and E2) were repeated twice (R1 and R2), one week apart, to assess the effect of a different influent water quality. In E1 R2, the distance between the air outlet and the aerosol filters was decreased. The soap ratio is the ratio between the volumetric dish-soap dosage rate and the influent water flow rate. Since the surfactant concentration of the dish-soap was 5–15 %, the pure soap ratio was between 1.05 and 3.15 ppmv for a soap ratio of 21 ppmv, between 3.1 and 9.3 ppmv for a soap ratio of 62 and between 6.25 and 18.8 for a soap ratio of 125.

Experiment ID	Contact time (min)	Water flow rate (L/min)	Soap dilution factor	Soap solution flow rate (mL/min)	Soap ratio (ppmv)	Run time (h)
E1 R1, E1 R2	30	6.9	250	36	21	1
E2 R1, E2 R2	20	10	250	54	21	1
E3	13	16	250	83	21	1
E4	60	3.5	83	18	62	2
E5	20	10	83	54	62	1
E6	20	10	42	54	125	1

three times with methanol, which was added to the same Eppendorf tubes, and the extracts were concentrated to 0.5 mL again. Then, the tubes were centrifuged for 15 min at 4000 rpm (Eppendorf centrifuge 5424R) and 150 μL supernatant was transferred to an analytical PP insert vial.

Prior to the extraction of the SIPs (Ahrens et al., 2013), extraction thimbles (Munktell Ahlstrom, ET/MG 160, 33 × 80 mm) were cleaned by Soxhlet extraction with 350 mL methanol for 18 h, followed by 350 mL of a 1:1 acetone:diethyl ether mixture for 24 h. Then, each SIP was added into a cleaned extraction thimble and Soxhlet extracted with 330 mL methanol for 24 h. A solvent blank without thimble and SIP was included in addition to the field blank. Each extract was concentrated to approximately 4 mL using rotary evaporation and transferred to a pre-cleaned 15 mL PP tube. The round-bottomed flask used during the Soxhlet extraction followed by rotary evaporation was rinsed three times with methanol, which was added to the extract, and the extracts were concentrated to 0.5 mL under N_2. Subsequently, the tubes were centrifuged for 20 min at 3900 rpm (Eppendorf centrifuge 5810R) and 150 μL supernatant was transferred to an analytical PP insert vial. Finally, the filter and SIP extracts were analyzed for 29 PFAS on a Sciex 3500 UPLC-MS/MS system according a modified method described previously (Smith et al., 2022) and in the SI (page 3).

2.4. Data handling

Concentrations of individual PFAS and elements that were not detected in any of the samples were set to zero. Other non-detect compounds, i.e. PFAS or elements that were present above the LOQ in at least one sample, were given a concentration equal to half their LOQ. For the water samples, LOQs of individual PFAS varied depending on the water matrix and were occasionally higher in the influent as compared to the effluent samples. In this case, the removal would increase by as much as 10 % points if non-detect concentrations were set equal to their LOQ. On the other end, setting all non-detect PFAS concentrations to zero was also deemed unrealistic, hence a factor 0.5 was chosen. Nonetheless, it should be acknowledged that this choice affects the results, and a sensitivity analysis in the form of repeated plots for factors 0 and 1 is given in the SI. Furthermore, most important statistical relationships are based on ΣPFAS concentrations as well as PFOS concentrations, since PFOS was the only PFAS present above the LOQ in all samples and thus unaffected by this choice. LOQs in the air and aerosol samples were set to the maximum concentration recovered in any of the field or lab blanks and are given in Table SI 3. For compounds that were not detected in any blanks, the instrument LOQ of 0.1 ng per filter or SIP was used. SIP and aerosol filter concentrations were not blank-corrected and values below the LOQ were set to half the LOQ. Air concentrations were estimated by assuming a common linear air sampling rate of 4 $m^3\ d^{-1}$, as described in Ahrens et al. (2013), resulting in a total air volume sampled of 44 m^3 per SIP.

Mean removal efficiencies (RE) for each experiment were calculated as per Eq. (1), with C_{Ef} the mean effluent PFAS water concentration over both duplicates (n = 2) and C_{In} the mean of the influent water concentrations measured before and after the experiment for both duplicates (n = 4). Similarly, mean mass balance closures (MB) were calculated as per Eq. (2), with C_{Foam} the mean foam PFAS concentration over both duplicates (n = 2) and $\%_{Foam}$ the mean foam fraction (%). The foam fraction was calculated by dividing the total mass of collapsed foam collected at the end of each experiment by the total volume of water treated. It should be acknowledged that this calculation is an approximation, because the foam concentration was based on a time-integrated sample over the entire experiment, whereas the effluent concentration was only measured at the end during steady-state operation. Moreover, the measurement uncertainties in the influent flow rate as well as the foam volume deserve consideration. An unsteady state analysis over the foam concentration is provided in SI Section 2 (p. 5–7), which showed that although the mean theoretical error caused by sampling the bulk foam was 30 %, the magnitude of this error did not correlate significantly with the mass balance. Hence, the combined effect of analytical uncertainty in PFAS concentrations, uncertainty in the measured flows and degradation of precursors contributed more to the mass balance uncertainty than this theoretical error. All data analysis and plotting were done in Matlab™, version R2020b.

$$RE\ (\%) = 100 - \frac{C_{Ef}}{C_{In}} \cdot 100 \tag{1}$$

$$MB\ (\%) = \frac{\frac{\%_{Foam}}{100} \cdot C_{Foam} + \left(1 - \frac{\%_{Foam}}{100}\right) \cdot C_{Ef}}{C_{In}} \cdot 100 \tag{2}$$

3. Results and discussion

3.1. Characteristics of influent water

The mean influent ΣPFAS concentration with corresponding standard deviation was 15 ± 3.9 μg L^{-1}, with PFOS (7.6 ± 2.6 μg L^{-1}), PFHxS (1.7 ± 0.51 μg L^{-1}) and 6:2 FTSA (1.3 ± 0.41 μg L^{-1}) as major components. A complete overview of the mean influent concentrations of all detected compounds is given in Table SI 5. Mean TOC, turbidity, pH, conductivity, aluminum and iron concentrations were 8.5 ± 0.6 mg L^{-1}, 21 ± 24 FNU, 7.4 ± 0.1, 1300 ± 190 μS cm^{-1}, 150 ± 97 μg L^{-1} and 790 ± 560 μg L^{-1}, with a complete overview given in Table SI 5. These values show the high variation in the quality of the industrial water stream under investigation, with relative errors exceeding 100 % for certain parameters.

Based on the mean influent concentrations of all eight experiments, significant positive correlations between influent ΣPFAS as well as PFOS concentration and aluminum (Al), boron (B), barium (Ba), calcium (Ca), iron (Fe), potassium (K), lithium (Li), magnesium (Mg), silicon (Si) and strontium (Sr) were found, with Pearson r values ranging from 0.74 (Sr) to 0.85 (Ba) for PFOS and from 0.73 (Al) to 0.93 (Si and Ba) for ΣPFAS. Conversely, both influent ΣPFAS and PFOS concentrations significantly correlated negatively ($p < 0.05$, $r = -0.90$ and -0.78, respectively) with P concentration. P and Zn correlated positively with each other, but negatively with B, Ca, Li, Mg, Si and Sr. An overview of all correlation coefficients is given in Fig. SI 4. These trends indicate that at least two distinct sources contributed to the process water, one with higher P and Zn, lower PFAS and lower other metal concentrations compared to the other, and the overall composition of the influent water depends on the ratio of these two contributing flows.

3.2. PFAS removal in different experiments

Between experiments, the ΣPFAS removal efficiency (RE) ranged from 63 to 84 %, as illustrated in Fig. 2. Increasing the relative surfactant dosage lead to higher foam fractions, with mean foam fractions of 0.17 %, 1.1 % and 7.1 % at soap ratios of 21, 62 and 125 ppmv, respectively (only significant between ratios of 62 and 125 ppmv, 1-way ANOVA, $F(2,5) = 82.53$, $p = 0.0001$). However, higher foam fractions did not correlate significantly with higher ΣPFAS or PFOS removal and ΣPFAS removal efficiencies above 80 % were already achieved at foam fractions below 0.5 %, see Fig. 2A), B) and F). This result is extremely relevant for practical applications of the foam fractionation technology, because it means that competitive PFAS removal can be achieved with up to 1400-fold reductions in water volume. Certain commercial applications of foam fractionation for PFAS remediation use a multistage treatment (Burns et al., 2021), where the foam undergoes subsequent foam fractionation to achieve higher concentration factors. Depending on the costs for foam treatment, including additional foam fractionation stages could be worthwhile for the current system as well.

The RE was significantly higher at 20, 30 and 60 min contact time (t_c) as compared to 13 min, but no significant differences in RE between 20, 30 and 60 min t_c were found (one-way ANOVA, $F(3,4) = 25.55$, $p = 0.005$ followed by Tukey's hsd procedure). This result is in accordance with

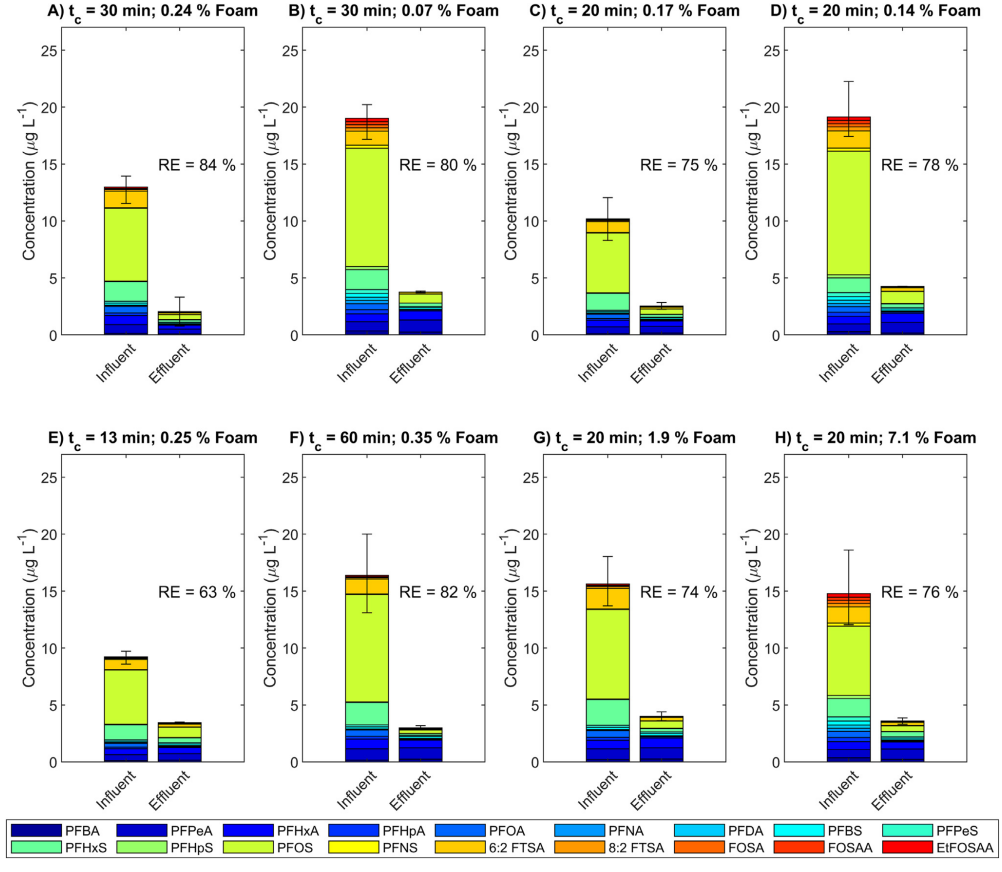

Fig. 2. Influent and effluent PFAS concentrations in different experiments, with non-detect concentrations set to 50 % of the LOQ. The repeated runs of experiments 1 (A): E1 R1 and B): E1 R2) and 2 (C): E2 R1 and D): E2 R2, see Table 1) one week in between are shown in separate subplots. Experiments 3, 4, 5 and 6 are shown in E), F), G) and H), respectively. Plot headings give the experimental t_c, which was a set variable, and the mean measured foam fraction. Plots with non-detect concentrations set to 0 and 100 % of the LOQ are given in Figs. SI 5 and 6. Error bars represent the minimum and maximum ΣPFAS concentrations found in any of the corresponding samples.

previous studies that have found optimal removal starting at contact times around 20 min (Buckley et al., 2022; Burns et al., 2021; Smith et al., 2022). Nonetheless, the mean RE increased from 76 to 82 % upon increasing the t_c from 20 to 30 min, so a positive effect of operating at higher t_c cannot be excluded. Moreover, when considering only PFOS instead of ΣPFAS in the ANOVA analysis to exclude any effects related to PFAS concentrations below the LOQ, a significant difference between the RE at 20 and 60 min t_c was found, strengthening the hypothesis that increasing the t_c above 20 min may cause a higher PFAS removal. More replicated experiments would be needed to confirm this hypothesis.

3.3. Effect of chain length and functional group on PFAS removal

The PFAS removal increased with chain length and PFSA were removed more efficiently than PFCA, as illustrated in Fig. 3. This phenomenon has been documented extensively previously (Buckley et al., 2022; Burns et al., 2021; McCleaf et al., 2021; Smith et al., 2022) and is due to a higher sorption affinity to the air-water interface of longer chain compounds and of PFSA compared to PFCA. Other long-chain PFAS such as 6:2 FTSA, 8:2 FTSA, FOSA and EtFOSAA were also removed at high efficiencies. PFNA, PFDA, PFHpS, PFNS and FOSAA were only present above the LOQ in foam samples, but not in any influent or effluent samples. Their reported removal was thus entirely based on sporadic lower LOQ values in the effluent than in the influent and is probably no accurate representation of their true removal. PFOS, PFOA, 6:2 FTSA and PFHxS had the highest mean removal efficiencies of 91 ± 5 %, 89 ± 4 %, 84 ± 7 % and 81 ± 8 %, respectively. The removal efficiency was below 30 % for PFCA with a perfluoroalkyl chain length below six and PFSA with a chain length below five. Because of this, the mean fraction of short-chain PFAS increased from 16 to 42 % from influent to effluent (min – max: 14–19 % to 26–54 %).

3.4. Effects of variations in influent water chemistry on PFAS removal

Over all eight experiments, the ΣPFAS as well as the PFOS removal efficiency correlated significantly with the influent conductivity and total elements concentration, as illustrated in Fig. 4 ($r = 0.80$, $p = 0.02$ for all). Similarly, both ΣPFAS and PFOS RE correlated significantly with the individual concentrations of Ba, K, Na and Sr ($r > 0.71$, $p < 0.05$). Expectedly, the total elements concentration and conductivity also correlated strongly with each other ($r = 0.99$, $p \approx 10^{-7}$). These results confirm

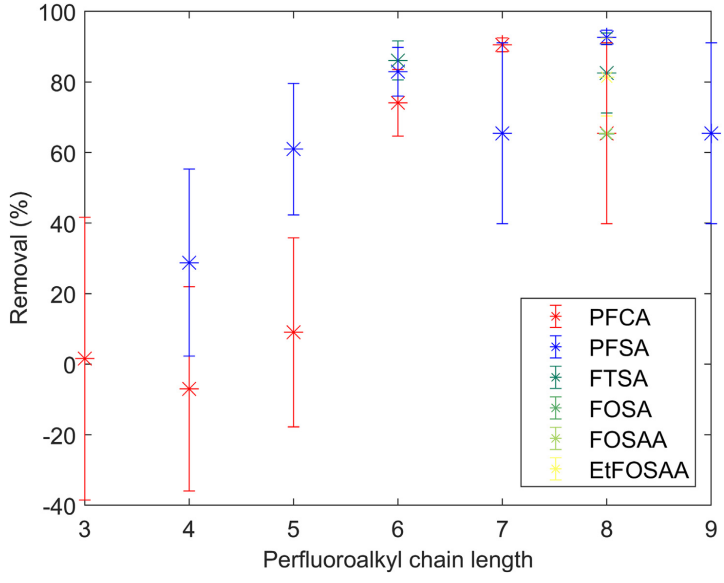

Fig. 3. Removal efficiency versus perfluoroalkyl chain length, with concentrations below the LOQ set to 50 % of the LOQ. Plots with non-detect concentrations set to 1 and 100 % of the LOQ are given in Fig. SI 7A and B. Error bars represent the standard deviation between experiments. E3 (Table 1) was excluded because of the noticeable effect of the short t_C of 13 min on the removal efficiency.

literature findings that the removal efficiency of PFAS in foam fractionation can be improved by dosing metal cation activators or increasing the ionic strength (Buckley et al., 2022; Meng et al., 2018). Moreover, they show that these effects also occur due to unintentional variations in influent water chemistry, instead of intentional dosing of metal salts. The experiment at 13 min residence time had the lowest removal efficiency as well as the lowest conductivity and total elements concentration (Fig. 4). This low removal efficiency may have been caused by a combination of these two factors, but it is not possible with our data to separate and apportion their respective effects. No significant correlations between RE and turbidity, TOC concentration or pH were found.

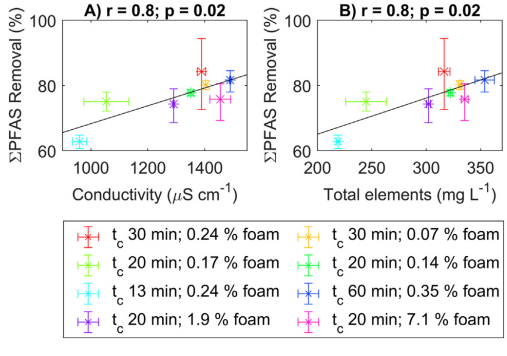

Fig. 4. ΣPFAS removal efficiency vs. conductivity and total dissolved element concentration. Horizontal error bars represent the standard deviation of A) conductivity and B) total elements concentration between experiments; vertical error bars represent the standard deviation of ΣPFAS removal between experiments.

No major differences in RE were found between the two experiments that were repeated one week apart (E1 and E2), despite higher PFAS concentrations and higher turbidity in the influent of the second runs, see Fig. 2A to D and Table SI 6. Notwithstanding the fact that dissolved elements and TOC concentrations stayed relatively similar, these minor changes in RE confirm the robustness of the treatment performance against natural variations in water quality. Conversely, the total mass balance closure decreased from 140 % in the first run to 58 % in the second run for E1, and from 98 % to 90 % for E2. These decreases in mass balance may be explained by the increased turbidity (i.e. increased adsorption to particulate matter) and the decreased foam fraction in the second runs, as outlined in Section 3.5 below.

3.5. Mass balance

The mean ΣPFAS mass balance over all experiments was 120 ± 40 % and did not differ significantly from 100 % (one-sample *t*-test), irrespective of how non-detect concentrations were handled. For non-detect concentrations set to half the LOQ, none of the mass balances for individual PFAS differed significantly from 100 % either (one-sample *t*-tests), as shown in Fig. 5. However, this conclusion changed when non-detects were handled differently, as illustrated in Fig. SI 8. Despite most mean mass balances not differing significantly from 100 %, those for certain individual compounds were below 100 % (e.g. PFBS: 86 %, PFPeS: 89 % and PFHpA: 91 %). Moreover, two experiments (E1 R2 and E2 R2, Table 1) had ΣPFAS mass balances below 100 %.

Another explanation for these low mass balance closures may be the loss of PFAS via adsorption to particulate matter. A significant negative correlation between turbidity and ΣPFAS mass balance closure was found ($r = -0.76$, $p = 0.03$. Insignificant for PFOS: $r = -0.70$, $p = 0.054$). This indicates that PFAS may have adsorbed to suspended solids in the water samples, which may have settled somewhere in the system and were thus lost from the mass balance. Turbidity further correlated with iron and aluminum content ($r = 0.97$ and 0.94, respectively, both $p < 0.0005$), which

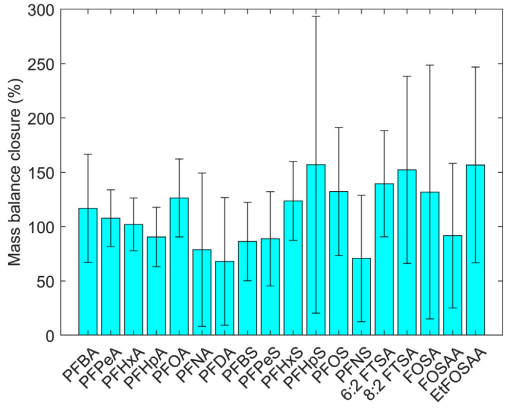

Fig. 5. Mass balance closure (%) for individual PFAS. Error bars represent the standard deviation over all experiments (n = 8).

form minerals that have a high PFAS adsorption capacity (Campos-Pereira et al., 2020; Wang and Shih, 2011; Zhang et al., 2021), further strengthening the hypothesis that PFAS may have adsorbed to suspended matter that was lost from the mass balance.

The solution used for rinsing the foam pipe after all experiments contained high PFOS, 6:2 FTSA, PFHxS and PFOA concentrations of 5700, 600, 540 and 240 μg L^{-1}, respectively. Notably, the sample also contained PFUnDA, PFDoDA, PFDS and EtFOSE (1.5, 1.1, 4.0 and 3.3 μg L^{-1}, respectively), which were not quantifiably detected in any of the other water or foam samples. Since all these four compounds are long-chained, they have high sorption coefficients (Campos-Pereira et al., 2022) and thus stick to the reactor walls rather than being transported with the foam. The full composition of this sample is given in Table SI 7. Because only one sample was collected after all tests, which probably did not contain all PFAS that were adsorbed to the pipe walls, no quantitative conclusions can be drawn on the percentage of PFAS that adsorbed to the foam pipe. Nonetheless, the high concentrations in this sample indicate that sorption to reactor parts may be an important PFAS sink.

PFOS mass balance closure correlated positively with foam fraction ($r = 0.83$, $p = 0.01$). Based on the high PFOS concentrations in the rinsing solution sample, PFOS that adsorbed to the foam pipe in experiments at low foam fractions may have been flushed out of the foam pipe at higher foam fractions. However, this correlation was not found for ΣPFAS. These results indicate that at high foam fractions, mass balance closures exceeding 100 % for especially long-chain PFAS with high sorption affinities may be caused by this rinsing effect.

For most compounds and experiments, mean mass balance closures were above 100 %, i.e. on average more PFAS was present in the foam and effluent than in the influent water. This excess of PFAS could possibly be explained by oxidative transformation of PFAS precursors that were not included in the analysis method (Houtz et al., 2016, 2013). PFCA, PFSA, FOSA and FTSA can be formed from precursors that are typically present in AFFF (Choi et al., 2022; Houtz et al., 2013), whereas EtFOSAA is generally considered a precursor compound itself (Choi et al., 2022; Houtz and Sedlak, 2012). The mean mass balance closure of EtFOSAA also exceeded 100 % (Fig. 5), which accordingly cannot be explained by precursor transformation. Probably, mass balance closures exceeding 100 % are thus also due to measurement uncertainties.

The measurement uncertainty in the PFAS concentrations reported by ALS was high, up to 40 %. When this measurement uncertainty results in reported underestimated influent concentrations or overestimated foam concentrations, the mass balance closure exceeds 100 %. A multivariable plot visualizing the sensitivity of the mass balance to these uncertainties in reported concentrations is given in Fig. SI 9. Moreover, the fluctuations in influent PFAS concentrations contributed to uncertainties in the mass balance. Nonetheless, despite these considerable measurement uncertainties, no significant differences in overall mass balance closure from 100 % were found based on all replicate analyses done in this study.

3.6. PFAS emissions to air and aerosols

The extraordinarily high recovered PFAS masses in both aerosol filters and SIP discs (see Fig. 6) clearly indicate that aerial PFAS concentrations around the reactor were much higher than normal levels in indoor air (Shoeib et al., 2008; Winkens et al., 2017). Extremely high mean ΣPFAS concentrations of 98 ng m^{-3} were measured in the air surrounding the foam fractionation reactor (sample locations 1–4, Fig. SI 1). The highest concentration of 140 ng m^{-3} was measured in the SIP disc located closest to the air outlet of the reactor (sample 4, Fig. SI 1). For comparison, the air at the reference site in the staircase of the same building had a ΣPFAS concentration of 3.6 ng m^{-3}. It should be noted that these concentrations are rough estimations based on a previously determined sampling rate (Ahrens et al., 2013), since no calibration was done in the present study.

Breakthrough through the bottom aerosol filters was low, i.e. the ΣPFAS mass measured in the top filter ranged between 0.1 % and 5 % of that in the bottom filter. The PFAS mass measured in the bottom filter clearly depended on the distance between the air outlet and the filters. 46 μg of ΣPFAS was found in the filter from the experiment in which the distance between the aerosol filter and the air outlet was decreased (E1 R2, Table 1). In comparison, over all other experiments the highest ΣPFAS mass found was only 7 μg. Based on the influent concentration of the water during each corresponding run, the highest loss of PFAS in aerosols corresponded to only 0.3 % of the entire aqueous ΣPFAS mass treated during the operation of the foam fractionation system. However, since not all air that exited the reactor passed through the filters, the actual amounts of PFAS leaving the reactor with the air were probably higher than what was caught in the aerosol filters.

The mean PFAS composition of the foam, aerosols and air was very similar, as illustrated in Fig. SI 8. For all three matrices, the main component was PFOS, at a mass-based fraction between 66 % (foam) and 77 % (aerosols), followed by PFHxS (5–13 %) and 6:2 FTSA (4–12 %). Conversely, the fraction of short-chain PFAS was only 0.7–2.6 %. In comparison, the composition of the reference air sample was slightly different, with only 43 % PFOS and 15 % short-chain PFAS. This indicates that either the

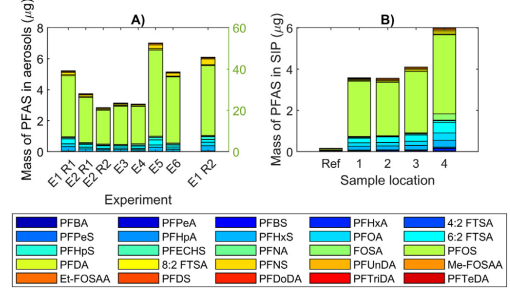

Fig. 6. Measured PFAS quantities in A) the bottom aerosol filters and B) the SIP discs. The result for the aerosol filter from experiment 1, run 2 (E1 R2) is shown on a different scale, represented by the y-axis in green on the right-side of A), to ensure readability of the data. This was the experiment during which the distance between the aerosol filter and the air outlet was decreased, causing much higher PFAS concentrations in the aerosol filter. Note that aerosol concentrations were not time-normalized, and that the duration of E4 was twice as long as the other experiments.

PFAS in the air at the reference site did not originate from the foam fractionation reactor, or that short-chain PFAS are more susceptible to transport through air than long-chain PFAS (Wong et al., 2018).

A hypothesis of this study was that high PFAS emissions in air and aerosols could explain loss of PFAS from the mass balance. Surprisingly, however, a strong positive correlation between mass balance closure and PFAS levels in the aerosol filters was found. Because of the aforementioned effect of the decreased distance between the air outlet and the filters, the results from E1 R2 were excluded from this analysis. The correlation was significant for both ΣPFAS ($r = 0.93$, $p = 0.002$) and PFOS ($r = 0.79$, $p = 0.03$). As it is improbable that a causal relationship exists between higher mass balance closure over the water phase and higher PFAS emissions in aerosols, the correlation may be explained by a common cause of the two phenomena. Possibly, both were caused by higher initial PFAS precursor concentrations and thus increased formation of target PFAS in the water as well as the aerosols. Precursor concentrations were not measured in the current study, so this could not be confirmed.

An alternative explanation relates to the role of suspended solids. PFAS-enriched aerosols are formed by bubble bursting at the air-water interface (De Leeuw et al., 2011; Sha et al., 2022), which in the foam fractionation reactor occurs mostly at the surface of the foam layer. At high suspended solids concentration, the presence of particles may impact the stability of the foam and thereby alter the collapse process, as has been discussed widely in literature (Fameau and Salonen, 2014; Kaptay and Babcsán, 2012; Petrovski et al., 2011). This altered collapse process may have resulted in lower aerosol emissions. This hypothesis is strengthened by the positive correlation between turbidity and foam concentrations ($r = 0.90$, $p = 0.003$ for ΣPFAS; $r = 0.90$, $p = 0.002$ for PFOS). An overview of these correlations is given in Fig. 7. Hence, the aforementioned positive correlation between mass balance closure and aerosol concentration was possibly caused by two separate effects at higher suspended solids concentrations: a decreased formation of PFAS-enriched aerosols and a lower mass balance closure because of PFAS loss due to sorption. However, the negative correlations of aerosol concentrations with foam concentrations and turbidity were not significant, so more research would be required to test this hypothesis.

3.6.1. Implications for worker safety

The high estimated PFAS concentrations in the air around the reactor have important implications for worker protection. The European Food Safety Authority (EFSA) includes PFOA, PFOS, PFNA and PFHxS in their recommended group tolerable weekly intake of 4.4 ng kg bodyweight^{-1} week^{-1} (EFSA, 2020). The EFSA further recommends assuming a body weight of 60 kg and an inhalation rate of 1.25 m^3 hr^{-1} for the assessment of operator exposure to plant protection products (Charistou et al., 2022). Using these same assumptions and the mean measured PFAS concentrations, an operator working a 40-h week in the room with the pilot-scale foam fractionation reactor is exposed to roughly 66 ng kg bodyweight^{-1} week^{-1} of the four PFAS included in the EFSA guidelines. This already exceeds the EFSA recommendation by a factor 15, and does not yet include PFAS exposure through diet or drinking water. On the other hand, the American Conference for Governmental Industrial Hygienists (ACGIH) has defined an occupational exposure limit for the ammonium salt of PFOA in air of 0.01 mg m^{-3} (ACGIH, 2020). The highest concentration of PFOA measured in this study was 8 ng m^{-3}, which is orders of magnitude below this limit. Nonetheless, guideline concentrations for PFAS are decreasing rapidly (Cousins et al., 2022; Post, 2021), so minimizing exposure where possible is advisable. Hence, to ensure worker safety, appropriate filters must be installed on the air outlet of pilot-scale foam fractionation reactors.

In most full-scale foam fractionation systems, the air is vented to the outside, usually already through activated carbon filters. Additionally, since the control of full-scale systems is more automated, workers are not expected to spend 40 h per week near the reactor. Accordingly,

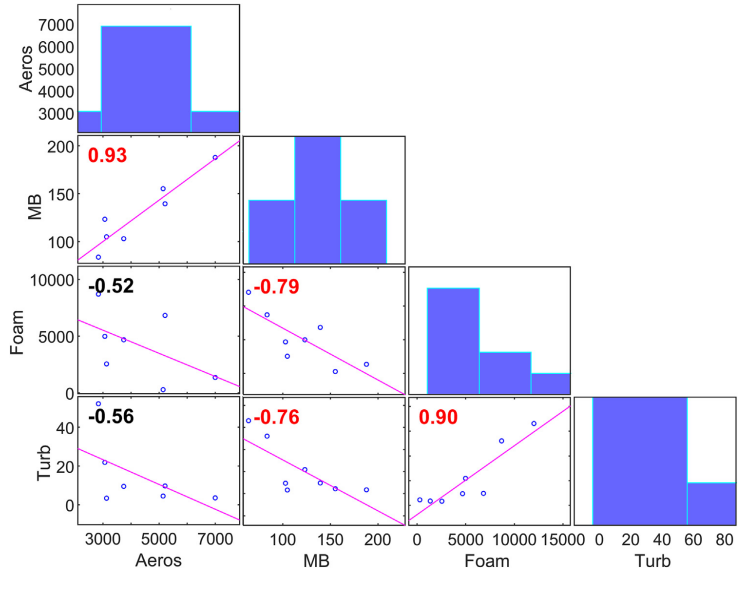

Fig. 7. Correlation matrix between aerosol concentration (Aeros, ng filter^{-1}), mass balance (MB, %), foam concentration (Foam, μg L^{-1}) and turbidity (Turb, FNU). Each data point represents the mean of one experiment. E1 R2 was excluded from the correlations with aerosol concentration, due to the strong effect of sampling aerosols closer to the air outlet. Numbers represent Pearson's correlation coefficient and are significant ($p < 0.05$) when shown in red.

the health risks demonstrated in this study are likely to be less severe for full-scale plants. Nonetheless, further research should look into the PFAS concentrations in the air around full-scale foam fractionation systems, to confirm that the safety measures are appropriate.

4. Conclusion

This study verified the high PFAS removal efficiency of a pilot scale foam fractionation system treating AFFF-contaminated industrial water. Effects of the highly variable water composition on the treatment efficiency were minimal, confirming the robustness of the technology. Nonetheless, removal efficiencies were shown to increase at higher conductivity and metal concentrations. Removal of long-chain PFAS was much higher than that of short-chain PFAS, which implies that the applicability of the technology depends on which compounds are included in guidelines and regulations. The four PFAS included in the EFSA tolerable weekly intake guideline (PFOA, PFOS, PFNA and PFHxS; EFSA, 2020) had a high combined mean removal efficiency of 90 %. Nonetheless, their mean total effluent concentration was still 1 μg L^{-1}, indicating that either a second foam fractionation step or other polishing treatments may be necessary to adequately limit human exposure to these compounds. For example, ion exchange may be used if further removal of mobile short-chain PFAS is required (Dixit et al., 2021).

There were no statistically significant differences from 100 % for individual or ΣPFAS mass balances. Nonetheless, PFAS adsorption to the walls of the reactor was found after all experiments. PFAS emissions from the air outlet of the reactor were also considerable, although they correlated positively rather than negatively with mass balance closure. These high PFAS emissions to air have important implications for the safety of operating personnel, since someone who works full-time in the room with the pilot-scale foam fractionation equipment would already have a PFAS exposure that is approximately 15 times higher than the EFSA recommendation. Moreover, PFAS that are emitted to the air rather than captured in the foam may still end up in the environment by means of long-range transport. Therefore, this study demonstrated the importance of installing adequate filters on the air outlet of foam fractionation systems.

CRediT authorship contribution statement

Sanne J. Smith: Conceptualization, Methodology, Investigation, Formal analysis, Visualization, Writing – original draft. **Jeffrey Lewis:** Conceptualization, Methodology, Resources, Writing – review & editing. **Karin Wiberg:** Writing – review & editing, Supervision, Project administration, Funding acquisition. **Erik Wall:** Writing – review & editing, Project administration. **Lutz Ahrens:** Conceptualization, Resources, Writing – review & editing, Supervision, Project administration, Funding acquisition.

Data availability

Data will be made available on request.

Declaration of competing interest

The authors declare that they have no known competing financial interests or personal relationships that could have appeared to influence the work reported in this paper.

Acknowledgements

This project has received funding from the European Union's Horizon 2020 research and innovation program under the Marie Skłodowska-Curie grant agreement No 860665 (PERFORCE3 innovative training network). We would further like to thank Svante Skarpås from Cytiva and Daniel Eriksson from ECT2 for their help with setting up the pilot system. Lastly, we thank Michael McLachlan (Stockholm University) and Angela Perez (ECT2) for their valuable comments.

Appendix A. Supplementary data

Supplementary data to this article can be found online at https://doi.org/10.1016/j.scitotenv.2023.162050.

References

ACGIH, 2020. American Conference for Governmental Industrial Hygienists TLV-TWA for Ammonium Perfluorooctanoate.
Ahrens, L., 2011. Polyfluoroalkyl compounds in the aquatic environment: a review of their occurrence and fate. J. Environ. Monit. 13, 20–31. https://doi.org/10.1039/c0em00373e.
Ahrens, L., Harner, T., Shoeib, M., Koblizkova, M., Reiner, E.J., 2013. Characterization of two passive air samplers for per- and polyfluoroalkyl substances. Environ. Sci. Technol. 47, 14024–14033. https://doi.org/10.1021/es4048945.
Belkouteb, N., Franke, V., McCleaf, P., Köhler, S., Ahrens, L., 2020. Removal of per- and polyfluoroalkyl substances (PFASs) in a full-scale drinking water treatment plant: long-term performance of granular activated carbon (GAC) and influence of flow-rate. Water Res. 182, 115913. https://doi.org/10.1016/j.watres.2020.115913.
Buck, R.C., Franklin, J., Berger, U., Conder, J.M., Cousins, I.T., Voogt, P.De, Jensen, A.A., Kannan, K., Mabury, S.A., van Leeuwen, S.P.J., 2011. Perfluoroalkyl and polyfluoroalkyl substances in the environment: terminology, classification, and origins. Integr. Environ. Assess. Manag. 7, 513–541. https://doi.org/10.1002/ieam.258.
Buckley, T., Xu, X., Rudolph, V., Firouzi, M., Shukla, P., 2021. Review of foam fractionation as a water treatment technology. Sep. Sci. Technol., 1–30 https://doi.org/10.1080/01496395.2021.1946698.
Buckley, T., Karanam, K., Xu, X., Shukla, P., Firouzi, M., Rudolph, V., 2022. Effect of mono- and di-valent cations on PFAS removal from water using foam fractionation – a modelling and experimental study. Sep. Purif. Technol. 286, 120508. https://doi.org/10.1016/j.seppur.2022.120508.
Burns, D.J., Stevenson, P., Murphy, P.J.C., 2021. PFAS removal from groundwaters using surface-active foam fractionation. Remediation 31, 19–33. https://doi.org/10.1002/rem.21694.
Campos-Pereira, H., Kleja, D.B., Sjöstedt, C., Ahrens, L., Klysubun, W., Gustafsson, J.P., 2020. The adsorption of per- and polyfluoroalkyl substances (PFASs) onto ferrihydrite is governed by surface charge. Environ. Sci. Technol. 54, 15722–15730. https://doi.org/10.1021/acs.est.0c01646.
Campos-Pereira, H., Makselon, J., Kleja, D.B., Prater, I., Kögel-Knabner, I., Ahrens, L., Gustafsson, J.P., 2022. Binding of per- and polyfluoroalkyl substances (PFASs) by organic soil materials with different structural composition – charge- and concentration-dependent sorption behavior. Chemosphere 297, 134167. https://doi.org/10.1016/j.chemosphere.2022.134167.
Casas, G., Martínez-Varela, A., Roscales, J.L., Vila-Costa, M., Dachs, J., Jiménez, B., 2020. Enrichment of perfluoroalkyl substances in the sea-surface microlayer and sea-spray aerosols in the Southern Ocean. Environ. Pollut. 267, 115512. https://doi.org/10.1016/j.envpol.2020.115512.
Charistou, A., Coja, T., Craig, P., Hamey, P., Martin, S., Sanvido, O., Chiusolo, A., Colas, M., Istace, F., 2022. Guidance on the assessment of exposure of operators, workers, residents and bystanders in risk assessment of plant protection products. EFSA J. 20, 1–134. https://doi.org/10.2903/j.efsa.2022.7032.
Choi, Y.J., Helbling, D.E., Liu, J., Olivares, C.I., Higgins, C.P., 2022. Microbial biotransformation of aqueous film-forming foam derived polyfluoroalkyl substances. Sci. Total Environ. 824. https://doi.org/10.1016/j.scitotenv.2022.153711.
Cousins, I.T., Johansson, J.H., Salter, M.E., Sha, B., Scheringer, M., 2022. Outside the safe operating space of a new planetary boundary for per- and polyfluoroalkyl substances (PFAS). Environ. Sci. Technol. 56, 11172–11179. https://doi.org/10.1021/acs.est.2c02765.
De Leeuw, G., Andreas, E.L., Anguelova, M.D., Fairall, C.W., Lewis, E.R., O'Dowd, C., Schulz, M., Schwartz, S.E., 2011. Production flux of sea spray aerosol. Rev. Geophys. 49, 1–39. https://doi.org/10.1029/2010RG000349.
Dixit, F., Dutta, R., Barbeau, B., Berube, P., Mohseni, M., 2021. PFAS removal by ion exchange resins: a review. Chemosphere 272, 129777. https://doi.org/10.1016/j.chemosphere.2021.129777.
EFSA, 2020. PFAS in food: EFSA assesses risks and sets tolerable intake [WWW Document]. URL https://www.efsa.europa.eu/en/news/pfas-food-efsa-assesses-risks-and-sets-tolerable-intake (accessed 3.17.22).
Evich, M.G., Davis, M.J.B., McCord, J.P., Acrey, B., Awkerman, J.A., Knappe, D.R.U., Lindstrom, A.B., Speth, T.F., Tebes-Stevens, C., Strynar, M.J., Wang, Z., Weber, E.J., Henderson, W.M., Washington, J.W., 2022. Per- and polyfluoroalkyl substances in the environment. Science, 375 https://doi.org/10.1126/science.abg9065.
Fameau, A.L., Salonen, A., 2014. Effect of particles and aggregated structures on the foam stability and aging. C. R. Phys. 15, 748–760. https://doi.org/10.1016/j.crhy.2014.09.009.
Fenton, S.E., Ducatman, A., Boobis, A., DeWitt, J.C., Lau, C., Ng, C., Smith, J.S., Roberts, S.M., 2020. Per- and polyfluoroalkyl substance toxicity and human health review: current state of knowledge and strategies for informing future research. Environ. Toxicol. Chem. 40, 606–630. https://doi.org/10.1002/etc.4890.
Houtz, E.F., Sedlak, D.L., 2012. Oxidative conversion as a means of detecting precursors to perfluoroalkyl acids in urban runoff. Environ. Sci. Technol. 46, 9342–9349. https://doi.org/10.1021/es302274g.
Houtz, E.F., Higgins, C.P., Field, J.A., Sedlak, D.L., 2013. Persistence of perfluoroalkyl acid precursors in AFFF-impacted groundwater and soil. Environ. Sci. Technol. 47, 8187–8195. https://doi.org/10.1021/es4018877.
Houtz, E.F., Sutton, R., Park, J.S., Sedlak, M., 2016. Poly- and perfluoroalkyl substances in wastewater: significance of unknown precursors, manufacturing shifts, and likely AFFF impacts. Water Res. 95, 142–149. https://doi.org/10.1016/j.watres.2016.02.055.

Kaptay, G., Babcsán, N., 2012. Particle stabilized foams. In: Stevenson, P. (Ed.), Foam Engineering: Fundamentals and Applications. John Wiley & Sons Ltd, Chichester, UK, pp. 121–143 https://doi.org/10.1002/9781119954620.ch7.

Lee, Y.C., Wang, P.Y., Lo, S.L., Huang, C.P., 2017. Recovery of perfluorooctane sulfonate (PFOS) and perfluorooctanoate (PFOA) from dilute water solution by foam flotation. Sep. Purif. Technol. 173, 280–285. https://doi.org/10.1016/j.seppur.2016.09.012.

Lenka, S.P., Kah, M., Padhye, L.P., 2021. A review of the occurrence, transformation, and removal of poly- and perfluoroalkyl substances (PFAS) in wastewater treatment plants. Water Res. 199, 117187. https://doi.org/10.1016/j.watres.2021.117187.

McCleaf, P., Kjellgren, Y., Ahrens, L., 2021. Foam fractionation removal of multiple per- and polyfluoroalkyl substances from landfill leachate. AWWA Water Sci. 3, 1–14. https://doi.org/10.1002/aws2.1238.

Meng, P., Deng, S., Maimaiti, A., Wang, B., Huang, J., Wang, Y., Cousins, I.T., Yu, G., 2018. Efficient removal of perfluorooctane sulfonate from aqueous film-forming foam solution by aeration-foam collection. Chemosphere 203, 263–270. https://doi.org/10.1016/j.chemosphere.2018.03.183.

Petrovski, S., Dyson, Z.A., Quill, E.S., McIlroy, S.J., Tillett, D., Seviour, R.J., 2011. An examination of the mechanisms for stable foam formation in activated sludge systems. Water Res. 45, 2146–2154. https://doi.org/10.1016/j.watres.2010.12.026.

Post, G.B., 2021. Recent US state and federal drinking water guidelines for per- and polyfluoroalkyl substances. Environ. Toxicol. Chem. 40, 550–563. https://doi.org/10.1002/etc.4863.

Sha, B., Johansson, J.H., Tunved, P., Bohlin-Nizzetto, P., Cousins, I.T., Salter, M.E., 2022. Sea spray aerosol (SSA) as a source of perfluoroalkyl acids (PFAAs) to the atmosphere: field evidence from long-term air monitoring. Environ. Sci. Technol. 56, 228–238. https://doi.org/10.1021/acs.est.1c04277.

Shoeib, M., Harner, T., Sum, C.L., Lane, D., Zhu, J., 2008. Sorbent-impregnated polyurethane foam disk for passive air sampling of volatile fluorinated chemicals. Anal. Chem. 80, 675–682. https://doi.org/10.1021/ac701830s.

Smith, S.J., Wiberg, K., McCleaf, P., Ahrens, L., 2022. Pilot-scale continuous foam fractionation for the removal of per- and polyfluoroalkyl substances (PFAS) from landfill leachate. ACS ES&T Water 2, 841–851. https://doi.org/10.1021/acsestwater.2c00032.

Sunderland, E.M., Hu, X.C., Dassuncao, C., Tokranov, A.K., Wagner, C.C., Allen, J.G., 2019. A review of the pathways of human exposure to poly- and perfluoroalkyl substances (PFASs) and present understanding of health effects. J. Expo. Sci. Environ. Epidemiol. 29, 131–147. https://doi.org/10.1038/s41370-018-0094-1.

US EPA, 2016. Drinking Water Health Advisories for PFOA and PFOS [WWW Document]. URL (accessed 4.14.22) https://www.epa.gov/ground-water-and-drinking-water/drinking-water-health-advisories-pfoa-and-pfos.

Wang, F., Shih, K., 2011. Adsorption of perfluorooctanesulfonate (PFOS) and perfluorooctanoate (PFOA) on alumina: influence of solution pH and cations. Water Res. 45, 2925–2930. https://doi.org/10.1016/j.watres.2011.03.007.

Winkens, K., Koponen, J., Schuster, J., Shoeib, M., Vestergren, R., Berger, U., Karvonen, A.M., Pekkanen, J., Kiviranta, H., Cousins, I.T., 2017. Perfluoroalkyl acids and their precursors in indoor air sampled in children's bedrooms. Environ. Pollut. 222, 423–432. https://doi.org/10.1016/j.envpol.2016.12.010.

Wong, F., Shoeib, M., Katsoyiannis, A., Eckhardt, S., Stohl, A., Bohlin-Nizzetto, P., Li, H., Fellin, P., Su, Y., Hung, H., 2018. Assessing temporal trends and source regions of per- and polyfluoroalkyl substances (PFASs) in air under the Arctic Monitoring and Assessment Programme (AMAP). Atmos. Environ. 172, 65–73. https://doi.org/10.1016/j.atmosenv.2017.10.028.

Zhang, Z., Sarkar, D., Datta, R., Deng, Y., 2021. Adsorption of perfluorooctanoic acid (PFOA) and perfluorooctanesulfonic acid (PFOS) by aluminum-based drinking water treatment residuals. J. Hazard. Mater. Lett. 2, 100034. https://doi.org/10.1016/j.hazl.2021.100034.

Supplementary Information - *Foam fractionation for removal of per- and polyfluoroalkyl substances: Towards closing the mass balance*

Sanne J. Smith[1*], Jeffrey Lewis[2], Karin Wiberg[1], Erik Wall[3], Lutz Ahrens[1]

[1]Department of Aquatic Sciences and Assessment, Swedish University of Agricultural Sciences (SLU), P.O. Box 7050, SE-750 07, Uppsala, Sweden
[2]ECT2, Lärlingsgatan 14b, SE-90422 Umeå, Sweden
[3]Cytiva, Björkgatan 30, SE-75323 Uppsala, Sweden

1. Supplementary Methods

Table SI 1: Brands and purity levels of used chemicals

Chemical	**Brand**	**Purity grade**
Acetone	Merck Suprasolv®	GC-grade
Petroleum ether	VWR Chemicals	Technical grade
Methanol	Merck LiChrosolv®	Hypergrade for LC-MS
Dichloromethane	Merck SupraSolv®	GC-grade
Hexane	Merck SupraSolv®	GC-grade
Ammonium acetate	Sigma Aldrich LiChropur®	LC-grade
Diethyl ether	VWR Chemicals AnalaR NORMAPUR®	ACS/Reag.

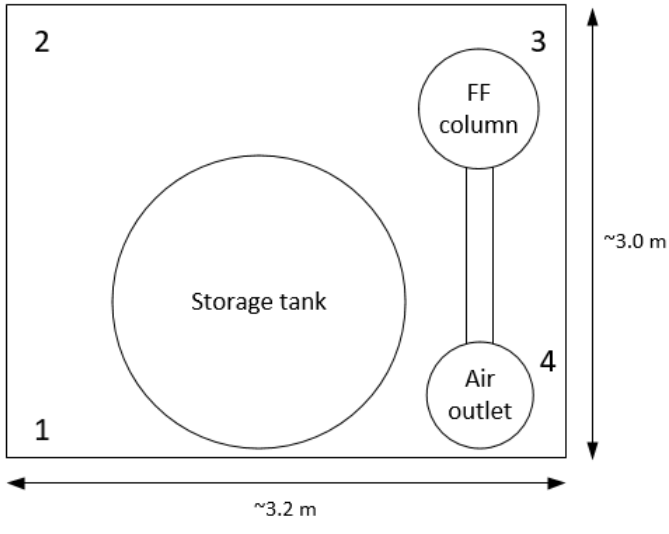

Figure SI 1: Schematic overview from above of the placement of PAS-SIP samplers in the pilot scale experimental room

Table SI 2: Reported LOQ ranges of PFAS in water samples. Compounds indicated with an asterisk were not detected in any of the samples and thus excluded from the data analysis.

Compound	Limit of quantification (min – max; µg L^{-1})
Perfluorobutanoic acid (PFBA)	0.01-10
Perfluoropentanoic acid (PFPeA)	0.01-10
Perfluorohexanoic acid (PFHxA)	0.01-10
Perfluoroheptanoic acid(PFHpA)	0.01-10
Perfluorooctanoic acid (PFOA)	0.1- 1
Perfluorononanoic acid (PFNA)	0.01-10
Perfluorodecanoic acid (PFDA)	0.01-10
Perfluoroundecanoic acid (PFUnDA)*	0.01-10
Perfluorododecanoic acid (PFDoDA)*	0.01-10
Perfluorotridecanoic acid (PFTriDA)*	0.025-25
Perfluorotetradecanoic acid (PFTeDA)*	0.025-25
Perfluorobutane sulfonic acid (PFBS)	0.01-10
Perfluoropentane sulfonic acid (PFPeS)	0.01-10
Perfluorohexane sulfonic acid (PFHxS)	1
Perfluoroheptane sulfonic acid (PFHpS)	0.01-10
Perfluorooctane sulfonic acid (PFOS)	NA – always present above LOQ
Perfluorononane sulfonic acid (PFNS)	0.01-10
Perfluorodecane sulfonic acid (PFDS)*	0.01-10
Perfluorododecane sulfonic acid (PFDoDS)*	0.025-25
4:2 fluorotelomer sulfonate (4:2 FTSA)*	0.01-10
6:2 fluorotelomer sulfonate (6:2 FTSA)	0.1-10
8:2 fluorotelomer sulfonate (8:2 FTSA)	0.01-10
Perfluorooctane sulfonamide (FOSA)	0.01-10
N-methyl- perfluorooctane sulfonamide (MeFOSA)*	0.05-50
N-ethyl- perfluorooctane sulfonamide (EtFOSA)*	0.05-50
N-Methyl-perfluorooctane sulfonamidoethanol (MeFOSE)*	0.025-25
N-Ethyl-perfluorooctane sulfonamidoethanol (EtFOSE)*	0.025-25
Perfluorooctane sulfonamido acetic acid (FOSAA)	0.01-50
N-methyl-perfluorooctane sulfonamido acetic acid (MeFOSAA)*	0.01-10
N-ethyl-perfluorooctane sulfonamido acetic acid (EtFOSAA)	0.01-10
7H-perfluoroheptanoic acid (HPFPpA)*	0.01-10
Perfluoro-3,7-dimethyloctanoic acid (PF37DMOA)*	0.01-10

Blank concentrations were all below LOQ, which varied between 0.3 and 2 ng L^{-1} for the blank samples. As the only exception, PFOS was found in the field blank at a concentration of 0.7 ng L^{-1}, which was 0.2 % of the lowest PFOS concentration in all other samples and thus deemed negligible.

Table SI 3: LOQs in aerosol filters and SIP discs. Compounds indicated with an asterisk were not detected in any of the samples and thus excluded from the data analysis.

Compound	LOQ in aerosol filter (ng filter^{-1})	LOQ in SIP (ng SIP^{-1})
PFBA	2.1	2.3
PFPeA	0.1	1.7
PFHxA	0.1	0.7
PFHpA	0.1	1.8
PFOA	0.3	1.6
PFNA	0.2	0.8
PFDA	0.3	3.2
PFUnDA	0.5	0.8
PFDoDA	0.2	0.5
PFTriDA	0.2	0.6
PFTeDA	1.8	0.3
PFBS	0.2	0.3
PFPeS	0.1	0.2
PFHxS	0.4	0.4
PFHpS	0.1	0.1
PFOS	7.0	1.1
PFNS	0.1	0.1
PFDS	0.1	0.1
4:2 FTSA	0.2	0.2
6:2 FTSA	1.2	1.0
8:2 FTSA	0.4	1.4
FOSA	0.2	0.4
MeFOSAA	0.1	0.1
EtFOSAA	0.2	0.1
Hexafluoropropylene oxide dimer acid (HFPO-DA)*	0.1	0.1
4,8-dioxa-3H-perfluorononanoic acid (NaDONA)*	0.1	0.1
Perfluoroethyl-cyclohexane sulfonate (PFECHS)	0.1	0.1
9-chloro-hexadecafluoro-3-oxanonane sulfonate (9Cl-PF3ONS)*	0.1	0.1
11-chloro-eicosafluoro-3-oxaundecane-1-sulfonic acid (11Cl-PF3OUdS)*	0.1	0.1

In the UPLC-MS/MS analysis, background PFAS from the mobile phases were trapped on a Phenomenex Kinetix® 1.7 µm C18 pre-column. For analysis, a Phenomenex Gemini® 3 µm C18 HPLC analytical column with a Phenomenex KJ0-4282 analytical guard column were used. A gradient of methanol and 10 mM ammonium acetate in HPLC-grade MilliQ water was run for 11 minutes, with the fraction of methanol starting at 5 %, increased to 55 % in 0.1 min, increased to 99 % over 4.4 min, kept there for 3.5 min, then decreased again to 5 % over 0.5 min and kept there for 2.5 min. Scheduled MRM mode with negative

electrospray ionization was used for MS/MS operation. Compounds with different isomers were reported as their summed concentrations. For further details on the analytical method, see Smith et al. (2022).

Table SI 4: Reported LOQ values for elements, metals and TOC concentrations and turbidity.

Al, aluminum (µg L^{-1})	200
As, arsenic (µg L^{-1})	100
B, boron (µg L^{-1})	20
Ba, barium (µg L^{-1})	10
Ca, calcium (mg L^{-1})	0.2
Cd, cadmium (µg L^{-1})	20
Co, cobalt (µg L^{-1})	20
Cr, chromium (µg L^{-1})	20
Cu, copper (µg L^{-1})	10
Fe, iron (mg L^{-1})	0.02
K, potassium (mg L^{-1})	0.5
Li, lithium (µg L^{-1})	10
Mg, magnesium (mg L^{-1})	0.09
Mn, manganese (µg L^{-1})	10
Mo, molybdenum (µg L^{-1})	20
Na, sodium (mg L^{-1})	0.2
Ni, nickel (µg L^{-1})	40
P, phosphorus (µg L^{-1})	200
Pb, lead (µg L^{-1})	100
Si, silica (mg L^{-1})	0.04
Sr, strontium (µg L^{-1})	10
V, vanadium (µg L^{-1})	10
Zn, zinc (µg L^{-1})	10
Turbidity (NTU)	1
Total organic carbon, TOC (mg L^{-1})	0.5

2. Unsteady State Analysis

List of symbols

V: Volume of tank
C_{In}: Influent concentration
C_{Ef}: Effluent concentration
C_F: Foam concentration
φ_{In}: Influent flow rate
φ_{Ef}: Effluent flow rate
φ_F: Foam flow rate
f_F: Dimensionless foam flow rate as fraction of influent flow rate
f_E: Dimensionless effluent flow rate as fraction of influent flow rate
K: Dimensionless equilibrium constant for foam concentration as fraction of effluent concentration
x_R: Dimensionless C_{Ef} as fraction of C_{In} ***at steady state*** (i.e. steady state removal $= (1 - x_R) \cdot 100\ \%$)
t_c: Contact time ($t_c = \frac{V}{\varphi_{In}}$)

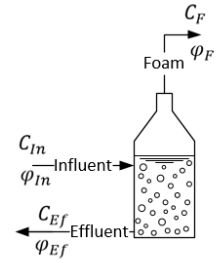

Figure SI 1: Diagram of mass balance unit

Derivation of mass balance and assumptions:

The derivation of the foam concentration as a function of time during unsteady state operation (Equation SI 1) relies on three crucial assumptions. The validity of these assumptions is arguable, so the calculations below should be considered as approximations. Nonetheless, the calculation is useful to estimate the significance of the error in the foam concentrations caused by sampling the bulk foam, compared to the other measurement uncertainties outlined in the main text. Any reactive formation or degradation of PFAS in the foam fractionation reactor was ignored in this derivation.

Assumption 1: C_{Ef} is always homogeneous in the entire liquid bulk (ideally stirred reactor, i.e. no plug-flow behaviour). Then, the mass balance (see Figure SI 2) can be derived as:

$$V\frac{\partial C_{Ef}}{\partial t} = \varphi_{In}C_{In} - \varphi_{Ef}C_{Ef} - \varphi_F C_F$$

Assumption 2: The flow rates are constant from the start, i.e. also during unsteady state conditions:

$$\varphi_F = f_F\varphi_{In}; \qquad \varphi_{Ef} = f_{Ef}\varphi_{In}; \qquad f_{Ef} + f_F = 1$$

Assumption 3: The foam concentration is always in equilibrium with the effluent concentration:

$$C_F = KC_{Ef}$$

Derivation of equilibrium constant as function of foam fraction and removal at steady state:

We introduce a constant x_R that gives the removal ***at steady state***. This is not a variable, i.e. it does not vary with time, but purely describes the relationships between effluent and influent at steady state for given flow rates. The subscript *ss* is added to the concentrations to denote that these are concentrations at steady state. We use x_R to calculate *K* based on the measured foam fraction and steady state removal. Because *K* is constant, this equation for *K* is valid under unsteady state conditions as well.

$$C_{Ef,ss} = x_R C_{In}; \quad RE = (1 - x_R) \cdot 100\ \%$$ *(e.g. at removal of 80 %, x_R = 0.2)*

$$V\frac{\partial C_{Ef,ss}}{\partial t} = 0 \rightarrow \text{Steady state} \qquad \varphi_{Ef} = f_{Ef}\varphi_{In};\ \varphi_F = f_F\varphi_{In};\ C_{Ef,ss} = x_R C_{In};\ C_{F,ss} = K x_R C_{In}$$

$$\varphi_{In}C_{In} - \varphi_{Ef}C_{Ef,ss} - \varphi_F C_{F,ss} = 0$$

$$\varphi_{In}C_{In} - f_{Ef}\varphi_{In}x_R C_{In} - f_F\varphi_{In}K x_R C_{In} = 0$$

$$K = \frac{\varphi_{In}C_{In} - f_{Ef}\varphi_{In}x_R C_{In}}{f_F\varphi_{In}x_R C_{In}} = \frac{1 - f_{Ef}x_R}{f_F x_R}$$

Derivation of relative foam concentration as function of time:
We now consider the situation **at unsteady state:**

$$V\frac{\partial C_{Ef}}{\partial t} = \varphi_{In}C_{In} - f_{Ef}\varphi_{In}C_{Ef} - f_F\varphi_{In}KC_{Ef} \qquad t_c = \frac{V}{\varphi_{In}};\ K = \frac{1 - f_{Ef}x_R}{f_F x_R}$$

$$\frac{\partial C_{Ef}}{\partial t} = \frac{1}{t_c}\left(C_{In} - f_{Ef}C_{Ef} - f_F\frac{1 - f_{Ef}x_R}{f_F x_R}C_{Ef}\right)$$

$$\frac{\partial C_{Ef}}{\partial t} = \frac{1}{t_c}\left(C_{In} - f_{Ef}C_{Ef} - \frac{1}{x_R}C_{Ef} + f_{Ef}C_{Ef}\right) = \frac{1}{t_c}\left(C_{In} - \frac{C_{Ef}}{x_R}\right)$$

$$\frac{\partial C_{Ef}}{C_{In} - \frac{C_{Ef}}{x_R}} = \frac{1}{t_c}\partial t \qquad \text{At } t = 0,\ C_{Ef} = C_{In}$$

$$\int_{C_{Ef} = C_{In}}^{C_{Ef}(t)} \frac{\partial C_{Ef}}{C_{In} - \frac{C_{Ef}}{x_R}} = \frac{1}{t_c}\int_{t=0}^{t}\partial t$$

$$-x_R \cdot \ln\left(\frac{C_{In} - \frac{C_{Ef}(t)}{x_R}}{C_{In} - \frac{C_{In}}{x_R}}\right) = \frac{1}{t_c}\cdot t$$

$$\frac{C_{In} - \frac{C_{Ef}(t)}{x_R}}{C_{In} - \frac{C_{In}}{x_R}} = e^{-\frac{t}{t_c x_R}}$$

$$1 - \frac{C_{Ef}(t)}{C_{In}x_R} = \left(1 - \frac{1}{x_R}\right)e^{-\frac{t}{t_c x_R}}$$

$$\frac{C_{Ef}(t)}{C_{In}x_R} = 1 + \left(\frac{1}{x_R} - 1\right)e^{-\frac{t}{t_c x_R}}$$

$$\frac{C_{Ef}(t)}{C_{In}} = x_R + (1 - x_R)e^{-\frac{t}{t_c x_R}} \qquad C_F = KC_{Ef};\ K = \frac{1 - f_{Ef}x_R}{f_F x_R}$$

$$\frac{C_F(t)}{C_{In}} = K \cdot \frac{C_{Ef}(t)}{C_{In}} = \frac{1 - f_{Ef}x_R}{f_F x_R}\cdot\left(x_R + (1 - x_R)e^{-\frac{t}{t_c x_R}}\right)$$

Equation SI 1: Relative foam concentration over time

Equation SI 1 can be used to plot the relative foam concentration over time as function of the removal efficiency at steady state, the contact time and the foam fraction. From the ratio between the integral of

this function and the integral of the relative steady state foam concentration over time, the theoretical error in foam concentration can be calculated for each experiment, as shown graphically in Figure SI 3.

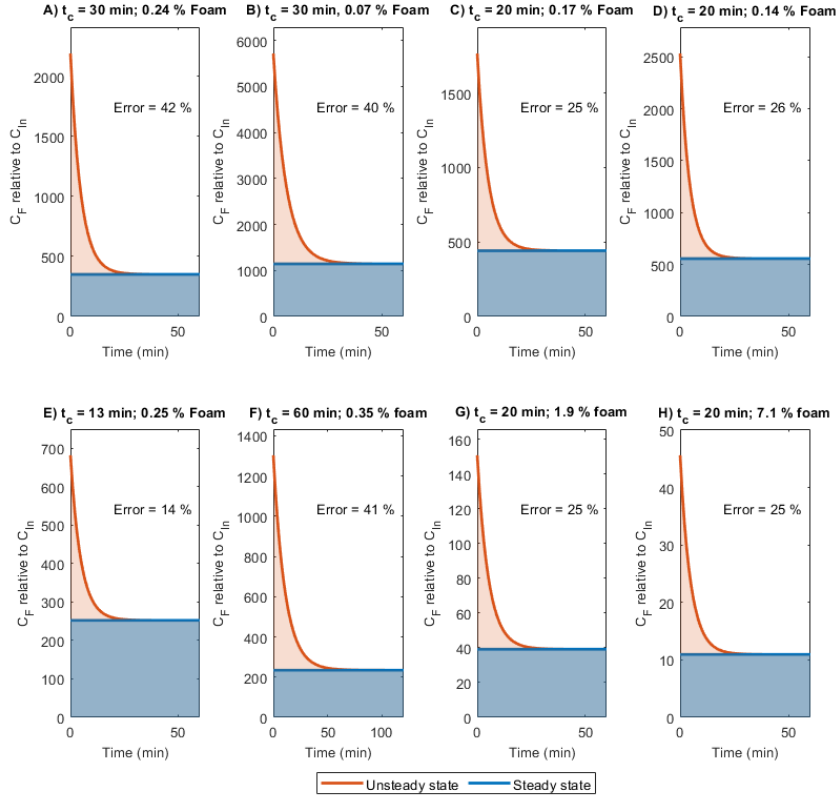

Figure SI 3: Theoretical error caused by sampling the bulk foam for each experiment. See Figure 2 in the main text for the removal efficiency of each experiment.

No significant correlations between the theoretical error and the ΣPFAS (*r = -0.12, p = 0.*78) or PFOS (*r = -0.06, p = 0.*88) mass balance, or between the theoretical error and the ΣPFAS (*r = 0.58, p = 0.*13) or PFOS (*r = 0.59, p = 0.*12) foam concentrations were found. While counterintuitive, this indicates that the error caused by sampling the bulk foam is not significant compared to the measurement uncertainties in PFAS concentrations, flow rates and the other reasons for variations in the mass balance outlined in the main text. The significant negative correlation between foam concentration and mass balance closure (main text Figure 7) strengthens this hypothesis further. Hence, foam concentrations were not corrected for this theoretical error, to prevent an unintentional increase in the uncertainty in the foam concentrations. The assumptions made in the calculation of these errors may not be valid, so the calculated errors are approximations in themselves. Using them to correct the foam concentrations may thus lead to even higher uncertainties, rather than lower.

3. Supplementary Results

Table SI 5: Mean and corresponding standard deviation of the influent PFAS and element concentrations. Only concentrations of compounds that were detected above the LOQ in at least one of the water samples are reported. Compounds that were only detected in foam samples are indicated with an asterisk.

PFAS	Concentration (µg L^{-1})	Parameter	Concentration/Value
PFBA	0.21 ± 0.16	Al, aluminum (µg L^{-1})	150 ± 97
PFPeA	0.76 ± 0.22	B, boron (µg L^{-1})	120 ± 20
PFHxA	0.70 ± 0.17	Ba, barium (µg L^{-1})	64 ± 11
PFHpA	0.26 ± 0.12	Ca, calcium (mg L^{-1})	130 ± 22
PFOA	0.50 ± 0.11	Cu, copper (µg L^{-1})	5.9 ± 2.4
PFNA*	0.13 ± 0.18	Fe, iron (µg L^{-1})	790 ± 560
PFDA*	0.13 ± 0.18	K, potassium (mg L^{-1})	15 ± 1.8
PFBS	0.23 ± 0.14	Li, lithium (µg L^{-1})	15 ± 2.5
PFPeS	0.22 ± 0.14	Mg, magnesium (mg L^{-1})	25 ± 4.2
PFHxS	1.7 ± 0.51	Mn, manganese (µg L^{-1})	230 ± 78
PFHpS*	0.13 ± 0.18	Na, sodium (mg L^{-1})	120 ± 21
PFOS	7.6 ± 2.6	P, phosphorus (mg L^{-1})	1.1 ± 0.93
PFNS	0.13 ± 0.18	Si, silica (mg L^{-1})	9.1 ± 1.4
6:2 FTSA	1.3 ± 0.41	Sr, strontium (µg L^{-1})	330 ± 54
8:2 FTSA	0.19 ± 0.16	Zn, zinc (µg L^{-1})	190 ± 98
FOSA*	0.13 ± 0.18	Turbidity (NTU)	21 ± 24
FOSAA*	0.13 ± 0.18	TOC (mg L^{-1})	8.5 ± 0.60
EtFOSAA	0.18 ± 0.16	pH	7.4 ± 0.13
		Conductivity (µS cm^{-1})	1300 ± 190

B	Ba	Ca	Cu	Fe	K	Li	Mg	Mn	Na	P	Si	Sr	Zn	Turb	TOC	pH	Cond	ΣPFAS	PFOS	
0.42	0.58	0.41	0.73	0.93	0.37	0.45	0.39	-0.15	0.09	-0.45	0.50	0.37	0.00	0.93	0.02	0.58	0.24	0.73	0.78	**Al**
	0.93	1.00	0.27	0.53	0.99	1.00	1.00	0.52	0.80	-0.93	0.99	0.99	-0.72	0.49	-0.40	0.79	0.95	0.89	0.76	**B**
		0.93	0.34	0.73	0.94	0.94	0.93	0.39	0.84	-0.83	0.94	0.93	-0.56	0.69	-0.29	0.79	0.91	0.93	0.85	**Ba**
			0.24	0.52	0.99	1.00	1.00	0.53	0.82	-0.93	0.99	1.00	-0.72	0.47	-0.42	0.77	0.96	0.88	0.75	**Ca**
				0.62	0.21	0.29	0.23	-0.16	0.02	-0.30	0.31	0.21	0.29	0.51	0.24	0.59	0.11	0.49	0.55	**Cu**
					0.51	0.55	0.51	-0.03	0.35	-0.46	0.58	0.49	-0.09	0.97	0.10	0.69	0.43	0.76	0.83	**Fe**
						0.99	0.99	0.58	0.86	-0.89	0.98	1.00	-0.7	0.45	-0.35	0.78	0.98	0.86	0.72	**K**
							1.00	0.49	0.80	-0.95	1.00	0.99	-0.71	0.51	-0.43	0.78	0.95	0.91	0.78	**Li**
								0.53	0.82	-0.93	0.99	1.00	-0.73	0.46	-0.42	0.77	0.97	0.88	0.74	**Mg**
									0.41	-0.28	0.44	0.52	-0.20	-0.15	0.16	0.27	0.57	0.23	0.02	**Mn**
										-0.67	0.78	0.85	-0.64	0.28	-0.3	0.64	0.93	0.62	0.55	**Na**
											-0.95	-0.92	0.78	-0.48	0.65	-0.68	-0.83	-0.9	-0.78	**P**
												0.99	-0.71	0.56	-0.45	0.78	0.93	0.93	0.81	**Si**
													-0.74	0.45	-0.43	0.76	0.98	0.87	0.74	**Sr**
														-0.17	0.79	-0.39	-0.72	-0.53	-0.41	**Zn**
															-0.09	0.56	0.36	0.77	0.84	**Turb**
																0.02	-0.34	-0.41	-0.33	**TOC**
																	0.76	0.72	0.66	**pH**
																		0.77	0.63	**Cond**
																			0.95	**ΣPFAS**

Figure SI 4: Pearson's r correlation coefficients between all influent variables. Significant correlations are indicated in red ($p < 0.05$). Turb = turbidity; TOC = total organic carbon; Cond = conductivity.

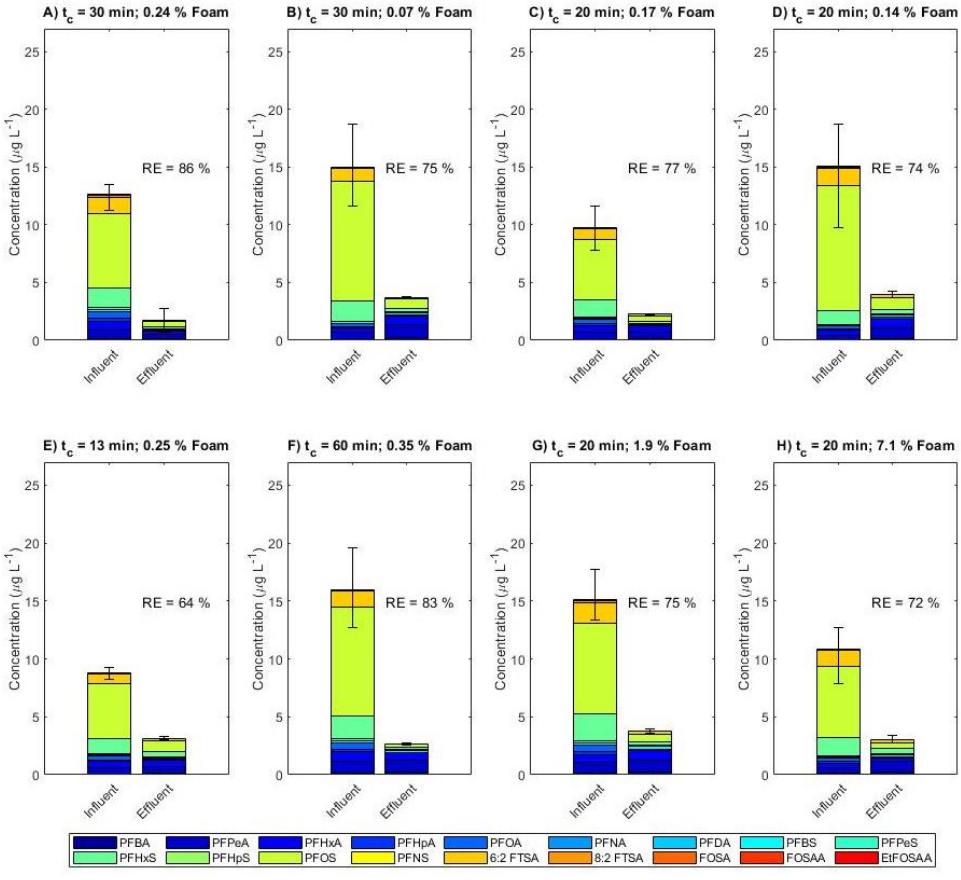

Figure SI 5: Influent and effluent PFAS concentrations in different experiments, with non-detect concentrations set to zero. Error bars represent the minimum and maximum ΣPFAS concentrations found in any of the corresponding samples.

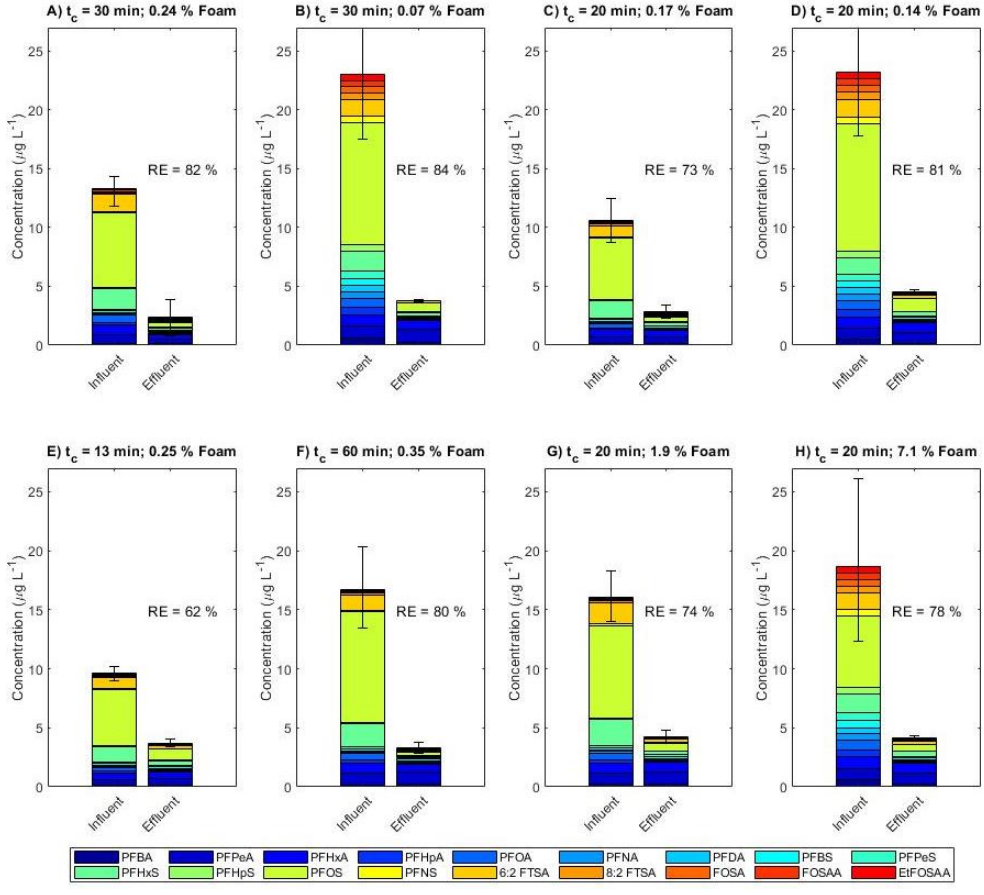

Figure SI 6: Influent and effluent PFAS concentrations in different experiments, with non-detect concentrations set to 100 % of the LOQ. Error bars represent the minimum and maximum ΣPFAS concentrations found in any of the corresponding samples.

Table SI 6: Mean influent characteristics of each experiment. See main text Table 1 for experimental details.

Experiment	Mean total metal and elements concentration (mg L^{-1})	Mean turbidity (NTU)	Mean TOC concentration (mg L^{-1})
1, run 1	320	9.7	9.4
1, run 2 (one week later)	330	66	8.1
2, run 1	240	9.5	9.2
2, run 2 (one week later)	320	52	8.8
3	220	3.4	8.4
4	350	22	7.9
5	300	3.5	7.9
6	340	4.5	8.1

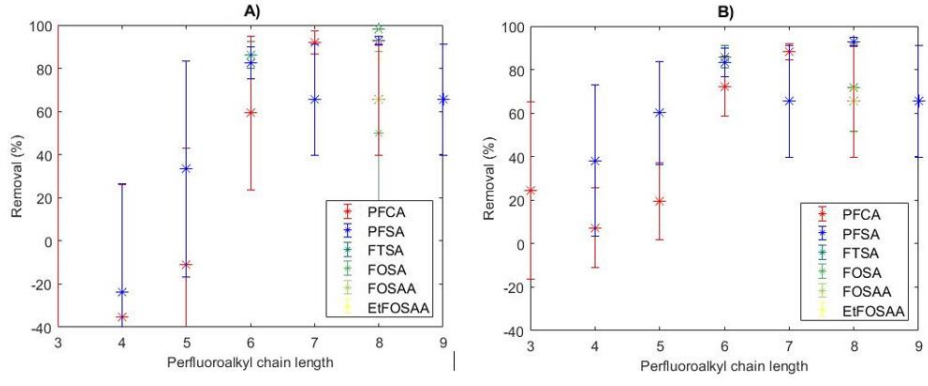

Figure SI 7: Removal efficiency versus perfluoroalkyl chain length, with concentrations below the LOQ set to A) 1 % of the LOQ and B) 100 % of the LOQ. Error bars represent the standard deviation between experiments. Concentrations were set to 1 % rather than 0 % to prevent removal efficiencies from going to infinity when the influent concentrations were below the LOQ for all samples. For concentrations below the LOQ set to 1 % of the LOQ (A), mean PFBA removal was at – 400 % due to a higher frequency of non-detects in the influent than in the effluent.

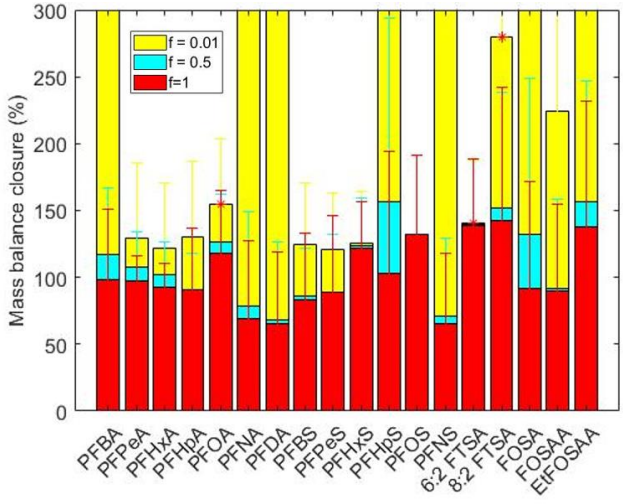

Figure SI 8: Mass balance closure (%) for individual PFAS with concentration below the LOQ set to 1 % (yellow), 50 % (blue) and 100 % (red) of the LOQ. Concentrations were set to 1 % rather than 0 % to prevent mass balance closures from going to infinity when the influent concentrations were below the LOQ for all samples. For PFOS, the result is the same irrespective of the choice in LOQ reporting, because PFOS was present above the LOQ in all samples. Error bars represent the positive standard deviation between experiments. Bars indicated with a red asterisk indicate a mass balance closure that is significantly different from 100 % (one-sided t-test, $p < 0.05$).

Table SI 7: PFAS concentrations in solution used to rinse the foam pipe after all experiments.

Compound	Concentration (µg L^{-1})
PFBA	<1
PFPeA	1.34
PFHxA	11.5
PFHpA	34
PFOA	236
PFNA	12.6
PFDA	7.61
PFUnDA	1.47
PFDoDA	1.06
PFTrDA	<2.5
PFTeDA	<2.5
PFBS	1.09
PFPeS	17.6
PFHxS	541
PFHpS	62.5
PFOS	5720
PFNS	4.92
PFDS	3.96
PFDoDS	<2.5
4:2 FTSA	<1
6:2 FTSA	601
8:2 FTSA	72.7
FOSA	53
MeFOSA	<5
EtFOSA	<5
MeFOSE	<2.5
EtFOSE	3.26
FOSAA	8.68
MeFOSAA	<1
EtFOSAA	124
HPFHpA	<1
PF37DMOA	<1

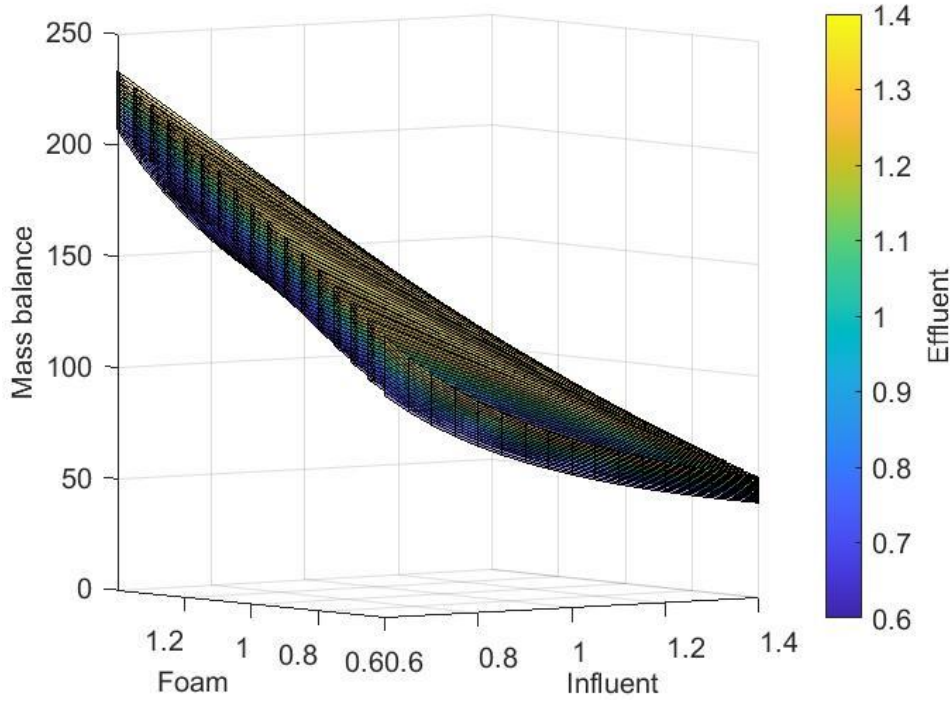

Figure SI 9: Multivariable plot showing the sensitivity of the mass balance at 80 % removal (z-axis) to the 40 % uncertainty in reported influent, foam (x and y axes) and effluent (coloring) concentration. The axes and color bar scale indicate the factor by which the reported concentration differs from the true concentration, with a mass balance closure of 100 % corresponding to the situation where all three factors are equal to 1 (i.e. the true concentrations are reported).

The mass balance exceeds 100 % for higher foam concentrations, higher effluent concentrations and lower influent concentrations. The effect of the uncertainty in the foam and influent concentrations (axes) is higher than that of the uncertainty in the effluent concentration (coloring), because of the comparatively low concentration of the effluent. Altogether, the combined uncertainties will lead to a too high mass balance closure approximately 6 % more often than to a too low mass balance closure.

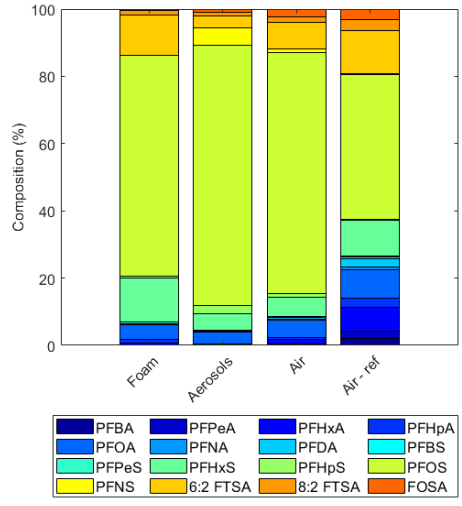

Figure SI 10: Composition profile of the foam, aerosol and air samples, including the reference air sample collected in the stairwell. Only compounds that were detected and included in the water as well as air analyses were considered.

III

ACS ES&T Water

pubs.acs.org/estwater

Article

Electrochemical Oxidation for Treatment of PFAS in Contaminated Water and Fractionated Foam—A Pilot-Scale Study

Sanne J. Smith,* Melanie Lauria, Lutz Ahrens, Philip McCleaf, Patrik Hollman, Sofia Bjälkefur Seroka, Timo Hamers, Hans Peter H. Arp, and Karin Wiberg

Cite This: *ACS EST Water* 2023, 3, 1201−1211

Read Online

ACCESS | Metrics & More | Article Recommendations | Supporting Information

ABSTRACT: Per- and polyfluoroalkyl substances (PFAS) are persistent synthetic contaminants that are present globally in water and are exceptionally difficult to remove during conventional water treatment processes. Here, we demonstrate a practical treatment train that combines foam fractionation to concentrate PFAS from groundwater and landfill leachate, followed by an electrochemical oxidation (EO) step to degrade the PFAS. The study combined an up-scaled experimental approach with thorough characterization strategies, including target analysis, PFAS sum parameters, and toxicity testing. Additionally, the EO kinetics were successfully reproduced by a newly developed coupled numerical model. The mean total PFAS degradation over the designed treatment train reached 50%, with long- and short-chain PFAS degrading up to 86 and 31%, respectively. The treatment resulted in a decrease in the toxic potency of the water, as assessed by transthyretin binding and bacterial bioluminescence bioassays. Moreover, the extractable organofluorine concentration of the water decreased by up to 44%. Together, these findings provide an improved understanding of a promising and practical approach for on-site remediation of PFAS-contaminated water.

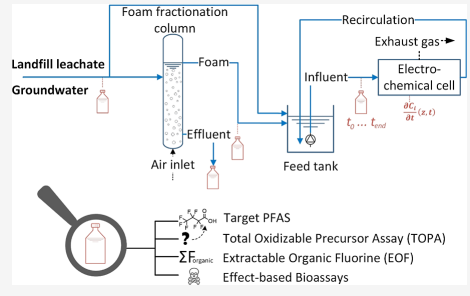

KEYWORDS: *foam fractionation, electrochemical oxidation, per- and polyfluoroalkyl substances, landfill leachate, groundwater, numerical modeling*

INTRODUCTION

The widespread presence of per- and polyfluoroalkyl substances (PFAS), particularly in the aquatic environment, has become a global cause for concern.[1−4] PFAS originate from various sources like the use of aqueous film-forming foam (AFFF), industrial releases, landfilling of PFAS-containing waste, and atmospheric deposition.[5−7] Additionally, the breakdown of less mobile perfluoroalkyl acid (PFAA) precursor compounds leads to increasing levels of mobile short-chain PFAS.[8] Commonly, perfluoroalkyl carboxylic acids (PFCA, $C_nF_{2n+1}COOH$) and perfluoroalkyl sulfonic acids (PFSA, $C_nF_{2n+1}SO_3H$) are considered short-chained for carbon chain lengths (n) below seven and six, respectively.[9] For the two most well-known PFAS, perfluorooctanoic acid (PFOA) and perfluorooctane sulfonic acid (PFOS), adverse health effects have been described extensively.[2,9] Among others, PFAS exposure is suspected of causing thyroid hormone system disruption, decreased immune function, and liver diseases.[10]

PFAS, particularly PFAA, are exceptionally inert toward chemical and biological degradation.[4] Many PFAS are highly soluble in water and are thus ineffectively removed with conventional wastewater treatment technologies.[1,4] For these reasons, reducing PFAS concentrations in contaminated water to below guideline levels[11] has proven extremely challenging.[12,13] To mitigate these difficulties, combining two or more technologies in a treatment train is considered a necessary approach for future PFAS mitigation.[14] Specifically, combining an appropriate preconcentration technology with an on-site degradation technology is of interest to harvest efficiency from the degradation step.[14−17]

Foam fractionation (FF) is an example of such a preconcentration technology.[18] Its suitability for the treatment of PFAS-contaminated water has been well described in academic literature.[19−25] FF exploits the surfactant properties of common PFAS by adsorbing the compounds on rising air bubbles. If the surfactant concentration of the feed water is sufficiently high, PFAS can be harvested as a concentrated foam from the top of the water and treated further. The resulting de-foamed effluent has substantially reduced PFAS concentrations and can either be discharged to the environment or subjected to further treatments.[20] The advantages of

Received: December 30, 2022
Revised: March 2, 2023
Accepted: March 3, 2023
Published: March 15, 2023

https://doi.org/10.1021/acsestwater.2c00660
ACS EST Water 2023, 3, 1201−1211

the FF technology compared to conventional preconcentration technologies, e.g., adsorption to activated carbon or membrane filtration, are its low use of consumables and its robustness against complex and variable water matrices.[20,22,25] A disadvantage is that it only works for surface-active PFAS and is thus less efficient for the removal of short-chain or non-amphiphilic PFAS.

A promising destructive technology for the resulting PFAS-enriched foam is electrochemical oxidation (EO). Remediation companies are starting to apply the FF-EO treatment train commercially,[26] but no systematic or modeling investigations have been described in academic literature yet. EO using anodes with a high O_2 evolution overpotential has been successfully applied for the degradation of inert organic water pollutants.[27] Specifically, boron-doped diamond (BDD) electrodes are often the material of choice for their excellent mechanical, chemical, and thermal stability, as well as their high electron transfer ability.[28] Effective PFAS degradation on BDD electrodes has been demonstrated on the laboratory scale.[29,30]

EO studies commonly use artificially increased PFAS concentrations in synthetic solutions and thereby likely overestimate the treatment efficiency due to negligible matrix effects.[31] In order to reach high PFAS degradation in environmental matrices, it is necessary to increase the total energy density by increasing either the total current or the total time. Otherwise, the presence of organic matter, scavenging compounds, and inorganic salts prevents efficient treatment.[32] Differences in treatment effectiveness upon switching from artificial to natural matrices have been extensively shown,[30,32−35] with decreased efficiencies especially noticeable for long-chain compounds[30] and at high chemical oxygen demand (COD) concentrations under current limiting conditions.[32]

Mass transfer limitations also complicate the large-scale application of electrochemical PFAS degradation. To minimize operational costs and maximize energy efficiency, it is important to remain in the reaction-limited operational regime.[27] Scale formation on electrode surfaces prevents the migration of PFAS to the electrode surface, thereby creating a mass transfer limitation that needs to be removed by acid rinsing.[36] Similarly, fluorination of the BDD surface after PFAS degradation causes lower degradation rates but can be reversed by UV irradiation.[37,38] Mass transfer limitations can also be reduced by keeping initial PFAS concentrations high[39] or by using innovative turbulence-enhancing reactor designs.[40,41] Finally, decreasing the current density over time can help to remain in the reaction-limited regime and thereby provide energy-efficient degradation at the cost of higher treatment times.[42]

The formation of toxic degradation byproducts forms a substantial obstacle for industrial applications of the electrochemical technology. If the total applied energy density is not sufficient, PFAS are merely degraded to shorter-chain compounds.[30] Additionally, in water containing chloride or bromide at relevant concentrations, the formation of perchlorate, bromate, and toxic organic halides is a concern.[35,41] It is therefore important to evaluate the toxicity of the electrochemically treated water. This assessment can be done using effect-based bioassays, as exemplified by other studies.[43−46]

The exact mechanism of PFAS degradation on BDD electrodes is still under discussion. However, there is a consensus that an initial direct electron transfer to the BDD surface is rate-limiting in the degradation of PFOA and PFOS.[31,40] This hypothesis is supported by PFAA being insusceptible to degradation by direct hydroxyl radical oxidation.[47] Moreover, the addition of a radical scavenger was shown not to affect PFAS removal rates by EO on BDD electrodes.[33] A proposed mechanism for the electro-oxidation of PFAS shows that secondary radicals are involved in the degradation after the rate-limiting step.[31] The presence of radical scavengers at high concentrations may therefore still prevent effective PFAS degradation in complex matrices.

Most studies conclude that PFOS oxidation follows the same pathway as PFOA oxidation. An initial electron transfer from the sulfate group to the anode leads to the formation of short-chain PFCA as intermediate degradation products, without the formation of any short-chain PFSA. However, in certain studies, the formation of perfluorobutane sulfonate (PFBS),[41,48] perfluorohexane sulfonate (PFHxS),[41] and perfluoroheptane sulfonate (PFHpS)[32] has been observed. An alternative degradation mechanism, in which PFOS degradation can lead to both PFCA and PFSA formation, is given in Pierpaoli et al. (2021).[32] Nonetheless, numerous studies, wherein increasing short-chain PFSA concentrations were not measured, exist as well.[29,34,36]

Here, we improve the understanding and demonstrate the high-technology readiness level of an FF−EO treatment train for the remediation of PFAS-contaminated groundwater and landfill leachate. Pilot-scale experiments were performed with real water matrices that were comprehensively analyzed for their general chemistry characteristics. EO was applied directly to the groundwater and leachate, as well as to collapsed foam produced in an on-site FF process from both water types. The objectives were to (i) evaluate the treatment effectiveness extensively using target and non-target methods, such as the total oxidizable precursor (TOP) assay and extractable organofluorine (EOF) analysis, (ii) assess the toxic potency of the water before and after treatment using two in vitro bioassays, and (iii) develop an extensive numerical model incorporating the coupled mass balances of 10 PFAS, enabling theoretical insights into the electrochemical degradation kinetics. The findings delineate both the potential of the FF-EO treatment train and limitations that need to be overcome to achieve industrial-scale on-site destructive PFAS treatment.

MATERIALS AND METHODS

Treatment Pilot. The treatment was carried out on-site at the Hovgården landfill in Uppsala, Sweden, which has been the subject of previous studies regarding PFAS treatment.[19,22] Leachate was collected directly from the influent to the on-site leachate water treatment plant, and groundwater was extracted from an observation well downgradient of the landfill from approximately an 8 m depth below ground surface and 7 m depth below the groundwater table. High-density polyethylene bottles were rinsed three times with methanol (LC-grade, Merck, Germany) prior to their use for sampling.

Foam Fractionation. A previously described and optimized FF setup was used for the production of foam from groundwater and leachate for the EO.[22] This system was run in continuous mode using a 19 cm diameter column with the liquid level at 1.63 m. The residence time, air flow rate, and collected foam fraction were 20 min, 10 L min^{-1}, and 10%, respectively. The foam fraction is the percentage of influent water that was taken from the reactor as foam. A schematic

https://doi.org/10.1021/acsestwater.2c00660
ACS EST Water 2023, 3, 1201−1211

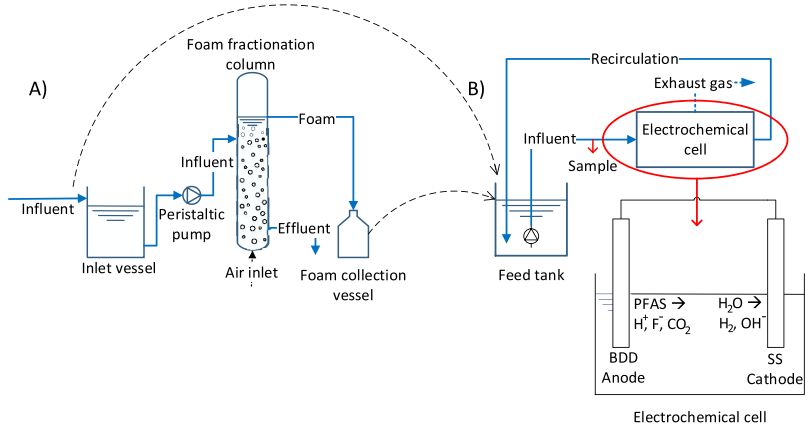

Figure 1. Schematic overview of (A) the FF (adapted from Smith et al. 2022)[22] and (B) the EO process. The FF was a continuous process, but the EO experiments were done batch-wise. During the EO experiments with fractionated foam, the exhaust gas outlet shown in (B) was closed, i.e., all gas and water was recirculated to the feed tank. Electrochemical degradation experiments were done with groundwater and leachate, as well as with foam produced from both water types, all in separate duplicate experiments. The influent to the FF (A) was groundwater or leachate. The influent to the EO (B) was groundwater, leachate, or fractionated foam produced from either groundwater or leachate.

overview of the test setup is given in Figure 1A. The system was left to run continuously for 9 h, with 250 mL of influent and effluent and 100 mL of foam collected after 2, 4, 6, and 8 h for PFAS analysis. Additionally, influent and effluent samples for organofluorine and bioassays (750 mL) and TOP assay analysis (200 mL) were collected after 2 and 6 h, and general chemistry samples of the influent and the effluent (1 L) were collected after 5 h.

Electrochemical Oxidation. Groundwater and leachate were subjected to EO treatment in separate batch tests at 50 and 150 L total volume. The produced foam from both water types was only tested at a volume of 50 L. For each of these experiments, 9 h batch tests were carried out in duplicate, using a 20 L flow-through cell with a total active BDD anodic and stainless-steel (SS; grade 304) cathodic surface area of 9 200 cm^2 each. The BDD electrodes were manufactured by Nova Diamant AB, had niobium as the base material, and were coated on both sides. Individual SS and BDD electrodes had a shape of 5 × 20 cm (total area of 200 cm^2 per electrode) and were mounted alternatingly with a spacing of 3 mm. 23 BDD and 24 SS electrodes were stacked in a package, giving an active area of 4600 cm^2 for each (the outside area of the two outermost SS electrodes was not considered part of the active electrode area). Two of these packages were used in series in the flow-through cell, with a diffusor between them to reduce mass flow limitations.

Power was supplied to this cell at a constant current of 231 A using an Agilent Technologies power supply (N8722A). The effluent from the flow-through cell was recycled to the inlet cell through steel spiral-reinforced PVC hoses with a 40 mm inner diameter at a flow rate of approximately 12 L min^{-1}. A schematic overview of the test setup is given in Figure 1B. For the tests with groundwater at 150 L, a portable stirrer (KGC, 1100W) was used to mix the inlet tank. In between each test, the system was rinsed with approximately 20 L ∼2.5 g L^{-1} (pH 2−3) of citric acid solution.

250 mL samples for target PFAS analysis were collected from a valve before the electrochemical cell at times 0, 0.5, 1, 2, 3, 4, 5, 7, and 9 h for tests with leachate and groundwater and at 0, 1, 2, 3, 4, 5, 6, 7, and 9 h for tests with fractionated foam. The pH and temperature of these samples were measured with a Hach pH meter (HQ40D multimeter with Intellical PHC101 electrode), and the voltage was read from the power supply. These results are given in Supporting Information Section 1. Additionally, samples for general water chemistry analysis (1 L), EOF, and bioassays (750 mL) and TOP assays (125 mL) were collected from the same valve at times 0 and 9 h, further referred to as, respectively, the "influent" and "effluent".

For the EO on the fractionated foam, the formation of foam in the gas outlet prevented an effective electrochemical treatment. Hence, this outlet was closed, and all the exhaust gas exited the reactor through the same recirculation hose as the water during these experiments. Foam formation occurred in the feed tank during the start of each EO experiment, but this had always mostly disappeared by the first sampling occasion. To assess the loss of PFAS in aerosols exiting the inlet tank, two stacked pre-combusted quartz microfiber filters (⌀ 11 cm, QM-A, Whatman) were placed in an aluminum holder (Tisch Environmental) on top of the inlet tank during each of the runs with foam. These filters have been used previously for sampling PFAS in aerosols with a size range between 0.1 and 2 μm,[49] see also Supporting Information Section 3. The system was otherwise entirely airtight, so all air exiting the system passed through these filters.

Analyses. *General Water Chemistry.* Selected water samples were sent to ALS Scandinavia, Danderyd, Stockholm, for the analysis of inorganic elements, dissolved organic carbon (DOC), total organic carbon (TOC), COD, nutrients, turbidity, conductivity, alkalinity, and pH. More details and results are presented in Supporting Information Section 2.

Target PFAS and TOP Assays. All target PFAS analyses (n = 29, full names of all PFAS compounds are given in Table S3) on groundwater, leachate, and collapsed foam for the electrochemical treatment were done in analytical duplicates, so each 250 mL sample was split in two samples of 125 mL, i.e., n = 4 for all time points (analytical duplicates +

https://doi.org/10.1021/acsestwater.2c00660
ACS EST Water 2023, 3, 1201−1211

experimental duplicates). The influent, effluent, and collapsed foam samples (n = 4 for each) from the FF were analyzed without analytical duplicates. The analytical methods for both the water samples and quartz microfiber filters are described in Supporting Information Sections 3 and 4 and have also been described in detail previously.[22,49] The influent and effluent samples of all electrochemical and FF tests were also analyzed with TOP assays, which aim to oxidize unknown PFAA precursors to PFCA to enable concentration measurements with targeted analysis. The TOP assay method is described in Supporting Information Section 5 and has been previously described by Houtz and Sedlak (2012).[50]

Extractable Organofluorine. EOF is a measurement of the entire organofluorine content of an extract, without giving any information on the molecular structure of individual organofluorine compounds. 750 mL of influent and effluent water from each treatment experiment were filtered and extracted using the same method as for the target PFAS analysis. Because these extracts were also used for bioassay analysis, extra rinsing steps that are normally included in extractions for EOF to remove fluoride ions[51] were omitted. Extracts were concentrated to 200 μL in methanol, i.e., the concentration factor was 3750. Measurements of EOF were carried out using a Thermo-Mitsubishi combustion ion chromatograph and a previously developed method,[52] see also Supporting Information Section 6. Extracts of the foam influent to the EO were diluted twice prior to EOF analysis.

Bioassays. To assess the effect of the evaluated PFAS treatment technologies on the toxic potency of the groundwater and leachate, two bioassays were carried out on the undiluted extracts from the EOF analysis. First, the transthyretin (TTR)-binding assay was used to assess the thyroid toxicity of the PFAS-contaminated water. TTR is a distributor protein that binds the TH-precursor thyroxine (T_4) and transports it to target tissues. PFAS can compete with T_4 for the binding to TTR, thereby preventing effective transport of TH.[44,53] Additionally, the more generic *Aliivibrio fischeri* bioluminescence assay was carried out to give information on the general toxic potency of the water.[43,54] Herein, exposure of the marine bioluminescent bacterium *A. fischeri* to toxic components in the extracts results in a decrease in bioluminescence compared to a blank caused by the inhibition of the bacterial metabolism.[43] This type of bioassay has been used previously to evaluate the effectiveness of water treatment with advanced oxidation.[45] Assay responses were expressed as PFOS-equivalent and triclosan-equivalent concentrations, respectively, and for the TTR assay also, the expected PFOS-equivalent concentration based on the measured target PFAS concentrations were calculated. Detailed methods for both bioassays, together with quality control data, are given in Supporting Information Section 7.

Data Treatment. All data analysis and plotting were done in MATLAB (R2020b). The treatment efficiency (E) was calculated as per eq 1, with C_{Ef} and C_{In} being the effluent and influent concentrations of the corresponding treatment process, respectively. The degradation efficiency of the entire treatment train (E_{tt}, Figure 6) was calculated as per eq 2, with $C_{Ef,FF}$ and $C_{In,FF}$ the effluent and influent concentrations from the FF, respectively, and $C_{Ef,EO\ on\ foam}$ being the effluent concentration of the EO on the foam produced in the FF. The factors 0.9 and 0.1 come from the fact that 90% of the FF influent exits the column as effluent and 10% as foam. The foam is subsequently electrochemically degraded to form EO effluents. Minimum efficiencies were determined based on the maximum effluent concentration and the minimum influent concentration, and vice versa for the maximum efficiencies.

$$E = \left(1 - \frac{C_{Ef}}{C_{In}}\right) \times 100\% \tag{1}$$

$$E_{tt} = \left(1 - \frac{0.9 \times C_{Ef,FF} + 0.1 \times C_{Ef,EO\ on\ foam}}{C_{In,FF}}\right) \times 100\% \tag{2}$$

PFAS Degradation Kinetics Model. A coupled ordinary differential equation (ODE) model to describe the degradation and formation of PFAS in an electrochemical flow cell was developed as a discretized 2D model along the axial position of the reactor. The model was developed using MATLAB (R2020b). It builds on a previous model for the degradation of PFOA developed by Urtiaga et al.,[39] but the current model removes the assumption that the variation with time of the PFOA concentration is negligible compared to its variation along the axial position of the reactor (i.e., $\frac{\partial C_{PFOA}}{\partial t} \ll \frac{\partial C_{PFOA}}{\partial z}$). Moreover, it coupled the degradation and formation of a total of 10 PFAS rather than only PFOA.

All PFCA and PFSA with perfluorocarbon chain lengths between four and eight were included in the model, which together made up over 95% of the influent total target PFAS concentration in all electrochemical experiments. The model couples all degradation reactions to each other by incorporating the co-occurring stepwise degradation mechanism to shorten perfluorinated chain lengths.[31,32] Hence, the degradation rate of the PFCA with a chain length of n is included as a formation rate of the PFCA with chain length $n - 1$. As explained in the introduction, the situation is more complex for PFSA, which can degrade to both PFCA and PFSA. For simplicity, PFOS and PFHpS were assumed to degrade only to PFCA since the clear formation of PFHpS or PFHxS was not observed. Contrarily, PFHxS and PFPeS were assumed to degrade only to PFSA. PFBS was assumed to degrade only to PFBA, which has been confirmed in at least two previous studies.[29,55] Degradation of precursors to PFOA and PFOS was included as well, but since the TOP assays did not indicate the presence of any PFAA precursors, PFOA and PFOS precursor concentrations and rate constants were set to zero. For the same reason, precursor degradation to any other PFAA was also not included.

A detailed description of the model equations is given in Supporting Information Section 8. In brief, for each compound, an ODE in the form of eq 3 was derived, combining all formation and degradation reactions as functions of axial position and time. Here, Q is the flow rate ($m^3\ min^{-1}$), A_{cell} is the cross-sectional area of the reactor (m^2), $C_{i,n}$ is the concentration of compound i at axial position n (M), z_n the axial position in the reactor at node n (m), and k_i the degradation rate constant of compound i (min^{-1}). The sum term includes all reactions that lead to the formation of compound i. This set of equations was solved using the MATLAB ode23 solver, which is a built-in software function.

$$\frac{\partial C_i}{\partial t}(z, t) = \frac{Q}{A_{cell}} \times \frac{C_{i,n} - C_{i,n-1}}{z_n - z_{n-1}} - k_i \times C_{i,n-1} + \sum k_{i+1} \times C_{i+1} \tag{3}$$

https://doi.org/10.1021/acsestwater.2c00660
ACS EST Water 2023, 3, 1201−1211

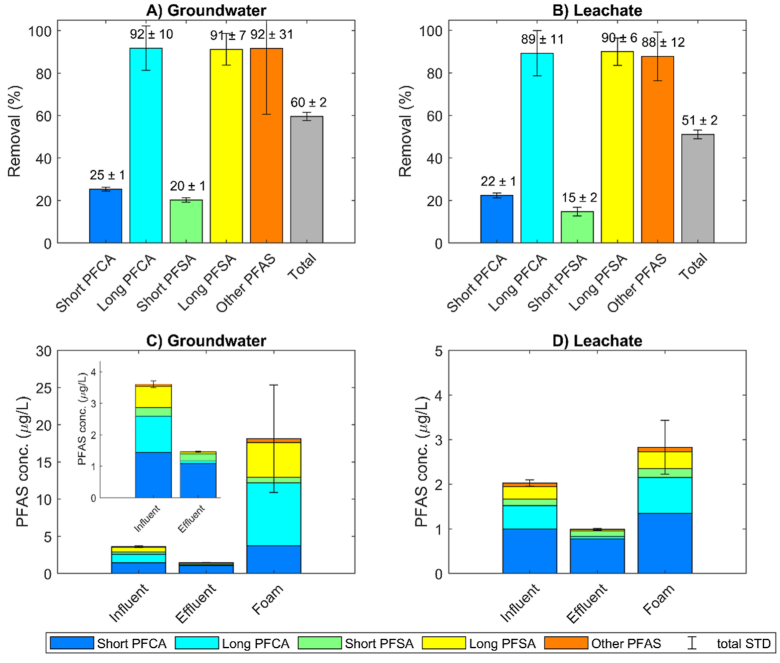

Figure 2. FF treatment effectiveness in terms of long-chain and short-chain PFAS removal [(A,B), %] and PFAS concentration [(C,D), $\mu g\ L^{-1}$] for groundwater (A,C) and leachate (B,D) before treatment and in the foam. Error bars represent the total standard deviation over the four samples taken during the FF treatment ($n = 4$). The foam concentrations also include the samples ($n = 4$) taken from the bulk foam prior to EO (i.e., total $n = 8$ for the foam). The insert in (C) shows the influent and effluent concentrations of the groundwater in more detail.

The values for the kinetic constants (Table S7) were found by minimizing the sum of squared errors between the model and experimental results from the 50 L groundwater tests. This calibration was done sequentially, in the order PFOS < PFHpS < PFHxS < PFPeS < PFBS < PFOA < PFHpA < PFHxA < PFPeA < PFBA, since the model results for shorter chain compounds depend on the degradation rates of long-chain compounds but not vice versa. To verify the model performance, the modeled degradation at a volume of 150 L using these same calibrated constants was then compared to the experimental results of the 150 L groundwater experiment. For simplicity, the degradation rate constants were assumed to be independent of concentration changes of any matrix compounds, such as TOC or chloride that may co-occur with PFAS degradation. Despite slight differences between the groundwater and leachate matrices (Tables S1 and S2), the constants calibrated using the 50 L groundwater results were able to predict the PFAS degradation in leachate reasonably accurately (as presented below). For the results of the experiments with fractionated foam, separate kinetic constants were calibrated.

RESULTS AND DISCUSSION

Mean Σ_{29}PFAS concentrations and the corresponding standard deviations prior to any treatment ($n = 12$) were 3.1 ± 0.4 $\mu g\ L^{-1}$ in the groundwater and 2.2 ± 0.2 $\mu g\ L^{-1}$ in the landfill leachate. The groundwater and leachate, respectively, had mean DOC concentrations of 34 and 43 mg L^{-1}, nitrate concentrations of 0.3 and 41 mg L^{-1}, iron concentrations of 2.1 and 2.7 mg L^{-1}, a pH of 7.5 and 7.8, and a conductivity of 450 and 470 mS m^{-1}. Detailed results of how each treatment step affected the general water chemistry are given in Supporting Information Section 2. Mean PFAS concentrations in the raw waters and after each treatment step are given in Tables S8 and S9.

Foam Fractionation. The mean ΣPFAS removal effectiveness for the FF treatment was 60% in the groundwater and 51% in the leachate. Because of their higher adsorption coefficients to the air−water interface, long-chain PFAS were removed better than short-chain PFAS. This is a well-known limitation of the FF technology for PFAS removal.[19−22,25] The higher ΣPFAS removal in the groundwater is caused by this same limitation since the groundwater contained a higher percentage of long-chain PFAA (50%) than the leachate (40%, Figures 2C and 1D). As illustrated in Figure 2A,B, the removal of these long-chain PFAA reached approximately 90% in both water types.

Average recoveries of the influent ΣPFAS in the effluent and the foam were 87 ± 35% and 58 ± 13% for groundwater and leachate, respectively. Explanations for the loss of PFAS from the mass balance have been investigated and discussed in previous work and are likely to include sorption to reactor walls and emissions to air.[19,22,56] For the system used in this study, the high variability in mass balance closure mostly originated from the highly variable foam concentrations, while the effluent concentrations were relatively constant (Figure 2C,D). The low ΣPFAS recovery for the leachate indicates that not all PFAS that were removed from the influent were

https://doi.org/10.1021/acsestwater.2c00660
ACS EST Water 2023, 3, 1201−1211

captured in the foam, which would imply that these PFAS were not degraded in the EO. Conversely, the mass balance for the groundwater closed considerably better. Mass balance closures for commercial FF systems have not yet been reported,[20,25] which is an important knowledge gap for this treatment technology.

Electrochemical Oxidation. Up to 84% ΣPFAS degradation was achieved after 540 min of EO (Figure 3). Unlike for the FF, the EO treatment effectiveness was similar for groundwater and leachate. For the experiments at 150 L volume, the recirculation was not sufficient to keep the inlet tank well-mixed, causing a high variability within the leachate results. A stirrer was installed for the groundwater tests at 150 L to prevent this issue, leading to more reproducible results. As expected,[32,42] the degradation was highly dependent on the specific charge Q (A h L^{-1}, eq S3). Because of the inverse relation between Q and treated volume, the PFAS degradation in both matrices remained lower at a higher volume. However, when plotted against the specific charge instead of time, the results were independent of volume, as illustrated in Figure S5.

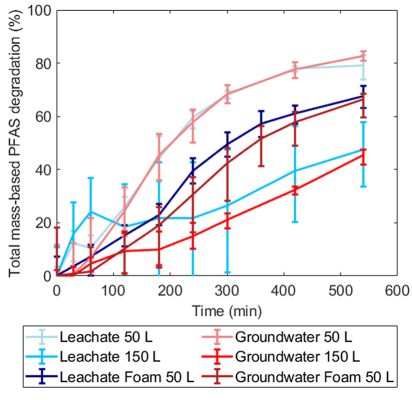

Figure 3. ΣPFAS degradation over time in all electrochemical experiments. Error bars represent min and max values based on the experimental and analytical duplicates (i.e., $n = 4$); lines connect the means.

A lower final degradation effectiveness of approximately 65% was achieved for the fractionated foam of both matrices, as could be expected based on the higher initial PFAS concentrations in the foam. ΣPFAS concentrations were 2.2 and 2.8 $\mu g\ L^{-1}$ in the leachate and groundwater, respectively, versus 3.6 and 19 $\mu g\ L^{-1}$ in the corresponding concentrated foams. The higher PFAS concentrations may have accelerated diffusive mass transfer from the bulk foam to the electrodes. Consequently, electron transfer at the BDD anodes became rate-limiting rather than mass transfer, making the degradation curve more linear[40] (Figures 3, S6 and S7). Conversely, the degradation in the unfractionated waters was still limited by mass transfer and could thus be made more energy-efficient by implementing turbulence-inducing reactor designs.[40,41] Additionally, electrode scaling (Tables S1 and S2) or fluorination may have contributed to lower degradation rates in the foam experiments.

Figure 4 shows the degradation of 10 individual PFAS during the experiments with groundwater at a 50 L volume, together with the kinetic model results at calibrated rate constants (Table S7). For PFSA, the final degradation decreased in the order of PFOS > PFHpS > PFHxS > PFBS > PFPeS, whereas the numerical rate constants decreased in the order of PFPeS > PFOS > PFHpS > PFBS > PFHxS. For PFCA, the final degradation decreased as PFOA > PFHxA > PFHpA > PFPeA > PFBA and the rate constants as PFPeA > PFBA > PFHpA > PFHxA > PFOA. Since short-chain PFAS were formed as degradation products, net short-chain degradation was lower than long-chain degradation, despite higher rate constants for certain short-chain compounds. The optimization of EO-based mineralization will need to account

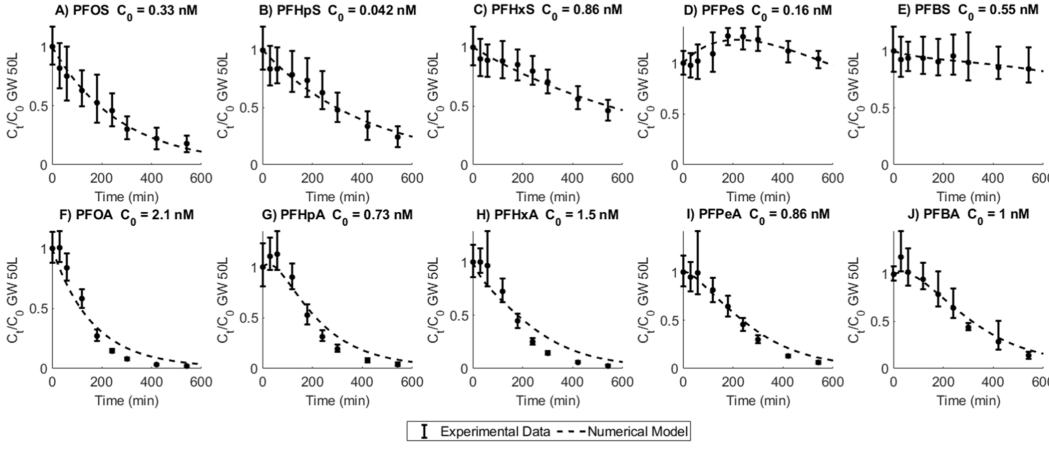

Figure 4. Individual degradation of PFAA with chain lengths up to 8 for the EO run with 50 L groundwater. The initial concentration of each PFAA is stated in the heading, and shorter-chain PFAS could be formed from the degradation of longer-chain PFAS. Error bars represent min and max values based on the experimental and analytical duplicates (i.e., $n = 4$); dots represent the mean, and the dotted line is the model prediction with calibrated kinetic constants, see Table S7.

https://doi.org/10.1021/acsestwater.2c00660
ACS EST Water 2023, 3, 1201−1211

for co-occurring short-chain PFAS formation and degradation. Earlier studies on the degradation of isolated PFAS found increased rate constants for higher chain lengths.[29,57] The higher hydrophobicity of long-chain compounds can lead to their easier adsorption onto the BDD anode, causing faster degradation. Conversely, in the current study, the unequal initial PFAS concentrations and matrix competition effects probably contributed to the observed trend in degradation rates.

The degradation of PFSA was slower than that of PFCA, both in terms of rate and final degradation, as reported previously.[29,31,33] This difference is attributable to the slower electron transfer from PFSA to BDD than from PFCA due to the higher electrophilicity and standard reduction potential of a sulfonic group as compared to a carboxyl group.[29,31] Additionally, PFSA adsorb more readily to suspended solids than PFCA,[58] which may have decreased the availability of PFSA for degradation on the BDD surface. Similar trends in the degradation were found for the remaining electrochemical experiments, with experimental and model results given in Figures S6−S10.

As visualized in Figures 4 and S6−S10, the PFAS degradation kinetics model was able to represent the EO results for leachate and groundwater well after calibration of the rate constants (Table S7). The 50 L groundwater experiments were used for this calibration, after which the model was able to adequately reproduce the degradation in leachate and groundwater at all volumes tested. A major benefit of this coupled numerical model is the capability of simultaneously accounting for formation and degradation rates of diverse PFAS, thereby eliminating the need to test individual compounds in isolated tests. The model is easily adaptable for other reactor dimensions and may be used to predict the degradation at varying treatment times or volumes.

The model, however, overestimated the PFAS degradation in the fractionated foam considerably (Figures S9 and S10). Pseudo-first-order degradation rate constants depend on matrix interferences and mass transfer limitations, in addition to intrinsic molecular properties.[31] Therefore, the calibrated constants are likely to be different for different water types. Since the groundwater foam had higher DOC and TOC concentrations than the original groundwater (Table S1), and the leachate foam also had different concentrations of certain ions than the original leachate (particularly iron and nitrogen species, Table S2), competition from co-solutes or the presence of radical scavengers may have affected the PFAS degradation rate constants.[32] Additionally, the high initial long-chain PFSA concentrations made the model assumptions regarding PFSA degradation pathways more influential. Implementing the wrong degradation pathway of a long-chain PFSA will have substantial effects on the modeled concentration of shorter PFAS. When calibrating the rate constants specifically for the fractionated foam, better fits were obtained (Figures S11 and S12), as discussed in detail in Supporting Information Section 8.

Figures S11 and S12 also show that PFSA degradation in the fractionated foams was very low. It is currently unclear what caused this low degradation efficiency, but it is nonetheless an important result. If EO would be used commercially for the degradation of fractionated foam, it is crucial that PFSA are degraded to a similar extent as PFCA. Particularly, PFOS is commonly included in regulations that stipulate maximum allowed concentrations in water,[1] and PFOS had a degradation efficiency of 0% in the leachate foam and only 36% in the groundwater foam in our study.

The estimated ΣPFAS concentrations in the gas exiting the electrochemical reactor during the degradation of groundwater and leachate foam were 5.0 and 1.7 $\mu g\ m^{-3}$, respectively. These concentrations are orders of magnitude higher than typical atmospheric PFAS levels,[59−61] stressing the need to install appropriate air filters on exhaust gas pipes from electrochemical treatment facilities. Alternatively, where possible, the air exhaust could be coupled to the FF unit to recirculate until degradation. This loss of PFAS corresponds to only ∼1% (leachate) and ∼0.6% (groundwater) of the influent foam concentrations, which is negligible compared to the measured degradation. Concentrations in the top aerosol filters were consistently lower than in the bottom filters (Figure S2), which indicates that the escape of PFAS through both filters was probably low. Calculation methods and complete results from the aerosol analysis are given in Supporting Information Section 2.

TOP Assay and EOF Analysis. PFCA concentrations did not increase after the TOP assay in groundwater and leachate compared to the target PFAS concentrations, indicating that oxidizable PFAA precursor concentrations were negligible.[50] This may be because all oxidizable PFAA precursors were already degraded in the landfill. Higher EOF concentrations than explained by the target PFAS concentrations were found in most samples, indicating that unknown PFAS may be present. Nevertheless, the decrease in EOF after EO was similar to the target PFAS degradation, as visualized in Figure S3. In the FF treatment, however, EOF removal was lower than the target PFAS removal, indicating the presence of non-standard PFAS that were not removed effectively. Further analytical work would be needed to identify these potential PFAS. With this one exception, the results of the TOP assays and EOF analysis are largely consistent in demonstrating the effectiveness of the treatment (see detailed results in Supporting Information Sections 5 and 6).

It is common practice that additional washing steps are included in the extraction procedure for EOF analysis to remove fluoride, with the drawback of increasing the loss of more polar and shorter PFAS.[51] Therefore, overall EOF recoveries might be lower in post-treatment samples, where the proportion of short-chain PFAS was higher than in pre-treatment samples. In this study, these extra washing steps were omitted, achieving nonetheless a good fluoride removal (>99%) and good overall EOF recoveries (70%) in quality control samples (which included short-chain PFAS, see Supporting Information Section 6). Accordingly, the possible overestimation of EOF removal due to PFAS recovery variability as a function of chain length is probably low.

Electrochemical treatment may result in the transformation of precursors that are not detected by the TOP assay.[34] Schaefer et al. (2018) found that while the TOP assay substantially underestimated the organic fluorine present in AFFF-contaminated water, this additional organic fluorine did not degrade to PFAA during either the EO or the TOP assay. Specifically, the degradation of organic fluorine compounds belonging to e.g., the AmPr-FASA (*N*-dimethyl ammonio propyl perfluoroalkyl sulfonamide) class was shown not to result in the formation of PFAA, although they were degraded during EO. Because our EOF results indicated the presence of unknown PFAS while no increased PFAA concentrations were measured in the TOP assay, it is plausible that compounds

https://doi.org/10.1021/acsestwater.2c00660
ACS EST Water 2023, 3, 1201−1211

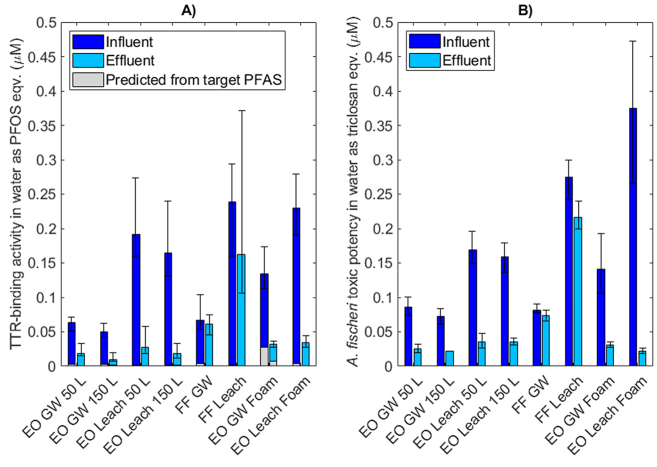

Figure 5. Effect of the EO and FF treatment of groundwater (GW) and leachate (leach) on (A) TTR-binding activity expressed as the mean PFOS-equivalent concentration and (B) the *A. fischeri* bioluminescence activity expressed as the mean triclosan equivalent concentration after 30 min exposure. Error bars represent min and max values based on the experimental and analytical duplicates (i.e., n = 4). See Supporting Information Section 7 for the calculation of the predicted TTR-binding activity of target PFAS, represented as light gray bars in (A). Significance was not calculated due to a too small independent sample size.

such as AmPr-FASA were present. EOF results do not give structural information, so verifying that this unknown organic fluorine did not degrade to PFAA during EO was not possible in this study. However, PFAA formation due to precursor degradation was nevertheless deemed negligible and thus left out of the model.

Bioassays. EO treatment resulted in a decreased capacity to compete with the thyroid hormone thyroxine (T_4) for TTR-binding as well as a decreased effect on bacterial respiration determined with the *A. fischeri* bioluminescence assay for all experiments, as illustrated in Figure 5. Assay responses from the influent to the electrochemical effluent decreased by up to 89% (leachate 150 L) and 94% (leachate foam) for the TTR-binding and bioluminescence assay, respectively. Conversely, for the FF treatment, no major changes in TTR-binding activity and cellular toxicity from the influent to effluent were evident. Here, mean TTR-binding PFOS equivalent concentrations decreased by 9 and 32% for groundwater and leachate, respectively, and bioluminescence triclosan equivalent concentrations by 10 and 21%.

The leachate had higher activities than groundwater in both assays, despite the higher target PFAS concentrations in groundwater, which was likely due to other substances present in the leachate. The predicted fraction of the TTR-binding activity that corresponded to the measured target PFAS concentrations varied between 0.21% (FF leachate effluent) and 21% (EO groundwater foam effluent), with mean resp. median values of 5.5 and 2.4%. This implies that there were other compounds present in the extracts with TTR-binding capacity but that these compounds were also destroyed effectively in the electrochemical treatment. The effective degradation of these unidentified compounds may also explain the higher decrease in bioassay activity than in target PFAS concentrations after EO treatment on the foam (Figures 2 and 4).

Energy Use. The energy consumption of EO can be calculated as described previously[15] and as presented in eq S18. Since the power usage was relatively similar for all EO experiments (Figure S1B), the energy consumption was mostly dependent on the treated volume, resulting in an energy consumption after 9 h of treatment of approximately 270 kW h m^{-3} for all 50 L experiments and 93 kW h m^{-3} for all 150 L experiments. This is comparable to values calculated based on literature descriptions of other EO systems used for PFAS degradation in heavy matrices with similar efficiencies.[17,48] Normalized energy consumptions were calculated as described by Sharma et al.[62] and in eq S19. The normalized energy consumption per log removal of PFOA was on average 240 and 160 kW h m^{-3} for leachate and groundwater and 410 and 350 kW h m^{-3} per log removal of PFOS, respectively.

The energy consumption of a full-scale FF plant described by Burns et al.[25] was 0.8 kW h m^{-3}. Although the energy use of our pilot-scale FF system may have been somewhat higher because of the smaller scale, it was probably still negligible compared to the energy consumption of the EO. Accordingly, since the removal of both PFOA and PFOS in the FF was approximately 90%, the energy consumption to reach one log removal of PFOA or PFOS in the entire treatment train depended only on the EO system. This can be estimated as described in Supporting Information Section 9 (eq S19) and was 76 and 53 kW h m^{-3} for one log removal of PFOA from leachate and groundwater, respectively. For PFOS, the energy consumption over the entire treatment train could not be determined reliably with the current data due to its low degradation in the fractionated foam.

CONCLUSIONS

Figure 6 summarizes the performance of the entire treatment train in terms of target PFAS and EOF degradation as well as reduction in bioassay activity. Due to the poor removal of short-chain PFAS in the FF step combined with their formation in the EO, the overall degradation of long-chain PFAS (mean 77%) was more than three times higher than that

https://doi.org/10.1021/acsestwater.2c00660
ACS EST Water 2023, 3, 1201−1211

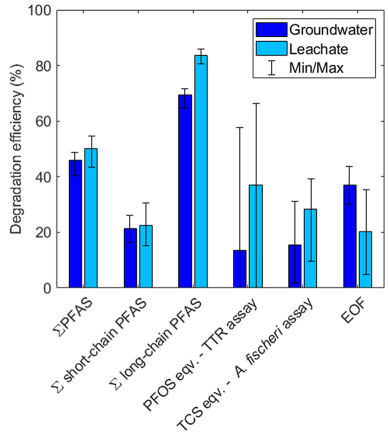

Figure 6. Degradation efficiency of the entire FF-EO treatment train, as defined by eq 2. Error bars represent the minimum and maximum degradation based on all respective measurements per variable, i.e., analytical and experimental duplicates for target PFAS in the EO experiments and bioassays, experimental quadruplicates for target PFAS in the FF experiments, and experimental duplicates for EOF analysis. TTR: transthyretin; TCS: triclosan; EOF: extractable organofluorine. See Supporting Information Section 2.3 for the calculation method of these efficiencies.

of short-chain PFAS (mean 22%). For all tested treatment outputs included in Figure 6, the treatment resulted in a mean reduction of at least 13% (TTR assay, groundwater), implying that degradation exceeds byproduct formation in the EO. When treating all the water directly with EO, degradation efficiencies were higher (Figure 3), but at the cost of a higher energy use due to the 10-fold larger volume requiring energy-intensive destructive treatment.

Our results indicate three main options for improving this treatment train, which may motivate further studies advancing the presented technologies. First, operating the FF system to produce lower foam volumes will generate foam at higher PFAS concentrations, as well as enable longer treatment times in the EO because of the lower foam volume. A longer treatment time corresponds to a higher total energy density, with the additional benefit of improved mass transfer rates because of the higher concentrations. To further concentrate the foam, secondary and tertiary FF steps can be included, as has been exemplified previously.[20,25] It should, however, be noted that the efficiency of the EO may decrease even further when more concentrated foam is treated, and that foaming in the EO may become an issue that prevents effective treatment. Second, the employment of auxiliary surfactants may lead to a higher removal of short-chain compounds in the FF. Finally, improving the mass transfer in the EO by employing innovative flow cell designs may increase the degradation rates and thereby enable complete degradation of short-chain as well as long-chain PFAS.

Other recommended areas for future research include following up on the low mass balance closure of the FF process and the low degradation of PFSA during EO treatment of the fractionated foam. If the proposed treatment train is implemented at full scale, it would be crucial to confirm that all PFAS that are removed from the influent in the FF end up in the foam, such that they are degraded with EO. Additionally, the low electrochemical degradation of PFSA in fractionated foam that was found in this study may challenge the applicability of EO as a destructive technology for PFAS-enriched foam. This low degradation may be due to artifacts or due to matrix-specific effects, but this should be confirmed by thoroughly testing and mechanistically characterizing EO on foam prior to the implementation of full-scale systems.

■ ASSOCIATED CONTENT

Supporting Information

The Supporting Information is available free of charge at https://pubs.acs.org/doi/10.1021/acsestwater.2c00660.

pH, voltage, and temperature results; general chemistry results; aerosol analysis—additional methods and results; analytical method—detailed methods and quality control results; TOP assays—additional methods and results; EOF analysis—additional methods and results; bioassays—additional methods and results; model—derivation of equations, calibrated rate constants and pseudocode; and additional EO results (PDF)

■ AUTHOR INFORMATION

Corresponding Author

Sanne J. Smith − *Department of Aquatic Sciences and Assessment, Swedish University of Agricultural Sciences (SLU), SE-750 07 Uppsala, Sweden;* orcid.org/0000-0002-3487-0528; Email: sanne.smith@slu.se

Authors

Melanie Lauria − *Department of Environmental Science, Stockholm University, 10691 Stockholm, Sweden;* orcid.org/0000-0002-5304-650X

Lutz Ahrens − *Department of Aquatic Sciences and Assessment, Swedish University of Agricultural Sciences (SLU), SE-750 07 Uppsala, Sweden;* orcid.org/0000-0002-5430-6764

Philip McCleaf − *Uppsala Water and Waste AB, SE-751 44 Uppsala, Sweden*

Patrik Hollman − *Nova Diamant AB, 75646 Uppsala, Sweden*

Sofia Bjälkefur Seroka − *Uppsala Water and Waste AB, SE-751 44 Uppsala, Sweden*

Timo Hamers − *Amsterdam Institute for Life and Environment (A-LIFE), Vrije Universiteit Amsterdam, 1081 HV Amsterdam, The Netherlands*

Hans Peter H. Arp − *Norwegian Geotechnical Institute (NGI), NO-0806 Oslo, Norway; Department of Chemistry, Norwegian University of Science and Technology (NTNU), NO-7491 Trondheim, Norway;* orcid.org/0000-0002-0747-8838

Karin Wiberg − *Department of Aquatic Sciences and Assessment, Swedish University of Agricultural Sciences (SLU), SE-750 07 Uppsala, Sweden*

Complete contact information is available at: https://pubs.acs.org/10.1021/acsestwater.2c00660

Notes

The authors declare no competing financial interest.

https://doi.org/10.1021/acsestwater.2c00660
ACS EST Water 2023, 3, 1201−1211

■ ACKNOWLEDGMENTS

This project received funding from the European Union's Horizon 2020 research and innovation program under the Marie Skłodowska-Curie grant agreement no 860665 (PERFORCE3 innovative training network). The authors would further like to thank Uppsala Water and Waste AB, particularly the employees working at Hovgården, for their support.

■ REFERENCES

(1) Lenka, S. P.; Kah, M.; Padhye, L. P. A Review of the Occurrence, Transformation, and Removal of Poly- and Perfluoroalkyl Substances (PFAS) in Wastewater Treatment Plants. *Water Res.* **2021**, *199*, 117187.

(2) Göckener, B.; Weber, T.; Rüdel, H.; Bücking, M.; Kolossa-Gehring, M. Human Biomonitoring of Per- and Polyfluoroalkyl Substances in German Blood Plasma Samples from 1982 to 2019. *Environ. Int.* **2020**, *145*, 106123.

(3) Falk, S.; Stahl, T.; Fliedner, A.; Rüdel, H.; Tarricone, K.; Brunn, H.; Koschorreck, J. Levels, Accumulation Patterns and Retrospective Trends of Perfluoroalkyl Acids (PFAAs) in Terrestrial Ecosystems over the Last Three Decades. *Environ. Pollut.* **2019**, *246*, 921−931.

(4) Evich, M. G.; Davis, M. J. B.; McCord, J. P.; Acrey, B.; Awkerman, J. A.; Knappe, D. R. U.; Lindstrom, A. B.; Speth, T. F.; Tebes-Stevens, C.; Strynar, M. J.; Wang, Z.; Weber, E. J.; Henderson, W. M.; Washington, J. W. Per- and Polyfluoroalkyl Substances in the Environment. *Science* **2022**, *375*, 887.

(5) Ahrens, L.; Bundschuh, M. Fate and Effects of Poly- and Perfluoroalkyl Substances in the Aquatic Environment: A Review. *Environ. Toxicol. Chem.* **2014**, *33*, 1921−1929.

(6) Benskin, J. P.; Li, B.; Ikonomou, M. G.; Grace, J. R.; Li, L. Y. Per- and Polyfluoroalkyl Substances in Landfill Leachate: Patterns, Time Trends, and Sources. *Environ. Sci. Technol.* **2012**, *46*, 11532−11540.

(7) Stoiber, T.; Evans, S.; Naidenko, O. V. Disposal of Products and Materials Containing Per- and Polyfluoroalkyl Substances (PFAS): A Cyclical Problem. *Chemosphere* **2020**, *260*, 127659.

(8) Li, F.; Duan, J.; Tian, S.; Ji, H.; Zhu, Y.; Wei, Z.; Zhao, D. Short-Chain per- and Polyfluoroalkyl Substances in Aquatic Systems: Occurrence, Impacts and Treatment. *Chem. Eng. J.* **2020**, *380*, 122506.

(9) Buck, R. C.; Franklin, J.; Berger, U.; Conder, J. M.; Cousins, I. T.; de Voogt, P. D.; Jensen, A. A.; Kannan, K.; Mabury, S. A.; van Leeuwen, S. P. J. Perfluoroalkyl and Polyfluoroalkyl Substances in the Environment: Terminology, Classification, and Origins. *Integr. Environ. Assess. Manage.* **2011**, *7*, 513−541.

(10) Fenton, S. E.; Ducatman, A.; Boobis, A.; DeWitt, J. C.; Lau, C.; Ng, C.; Smith, J. S.; Roberts, S. M. Per- and Polyfluoroalkyl Substance Toxicity and Human Health Review: Current State of Knowledge and Strategies for Informing Future Research. *Environ. Toxicol. Chem.* **2021**, *40*, 606−630.

(11) Cousins, I. T.; Johansson, J. H.; Salter, M. E.; Sha, B.; Scheringer, M. Outside the Safe Operating Space of a New Planetary Boundary for Per- and Polyfluoroalkyl Substances (PFAS). *Environ. Sci. Technol.* **2022**, *56*, 11172−11179.

(12) Verma, S.; Varma, R. S.; Nadagouda, M. N. Remediation and Mineralization Processes for Per- and Polyfluoroalkyl Substances (PFAS) in Water: A Review. *Sci. Total Environ.* **2021**, *794*, 148987.

(13) Li, P.; Zhi, D.; Zhang, X.; Zhu, H.; Li, Z.; Peng, Y.; He, Y.; Luo, L.; Rong, X.; Zhou, Y. Research Progress on the Removal of Hazardous Perfluorochemicals: A Review. *J. Environ. Manage.* **2019**, *250*, 109488.

(14) Lu, D.; Sha, S.; Luo, J.; Huang, Z.; Zhang Jackie, X. Treatment Train Approaches for the Remediation of Per- and Polyfluoroalkyl Substances (PFAS): A Critical Review. *J. Hazard. Mater.* **2020**, *386*, 121963.

(15) Soriano, Á.; Gorri, D.; Urtiaga, A. Efficient Treatment of Perfluorohexanoic Acid by Nanofiltration Followed by Electrochemical Degradation of the NF Concentrate. *Water Res.* **2017**, *112*, 147−156.

(16) Shi, H.; Chiang, S. Y.; Wang, Y.; Wang, Y.; Liang, S.; Zhou, J.; Fontanez, R.; Gao, S.; Huang, Q. An Electrocoagulation and Electrooxidation Treatment Train to Remove and Degrade Per- and Polyfluoroalkyl Substances in Aqueous Solution. *Sci. Total Environ.* **2021**, *788*, 147723.

(17) Liang, S.; Mora, R.; Huang, Q.; Casson, R.; Wang, Y.; Woodard, S.; Anderson, H. Field Demonstration of Coupling Ion-Exchange Resin with Electrochemical Oxidation for Enhanced Treatment of per- and Polyfluoroalkyl Substances (PFAS) in Groundwater. *Chem. Eng. J. Adv.* **2022**, *9*, 100216.

(18) Lemlich, R. Adsorptive Bubble Separation Methods: Foam Fractionation and Allied Techniques. *Ind. Eng. Chem.* **1968**, *60*, 16−29.

(19) McCleaf, P.; Kjellgren, Y.; Ahrens, L. Foam Fractionation Removal of Multiple Per- and Polyfluoroalkyl Substances from Landfill Leachate. *AWWA Water Sci.* **2021**, *3*, 1−14.

(20) Burns, D. J.; Stevenson, P.; Murphy, P. J. C. PFAS Removal from Groundwaters Using Surface-Active Foam Fractionation. *Remediation* **2021**, *31*, 19−33.

(21) Buckley, T.; Karanam, K.; Xu, X.; Shukla, P.; Firouzi, M.; Rudolph, V. Effect of Mono- and Di-Valent Cations on PFAS Removal from Water Using Foam Fractionation − A Modeling and Experimental Study. *Sep. Purif. Technol.* **2022**, *286*, 120508.

(22) Smith, S. J.; Wiberg, K.; McCleaf, P.; Ahrens, L. Pilot-Scale Continuous Foam Fractionation for the Removal of Per- and Polyfluoroalkyl Substances (PFAS) from Landfill Leachate. *ACS ES&T Water* **2022**, *2*, 841−851.

(23) Lyu, X. J.; Liu, Y.; Chen, C.; Sima, M.; Lyu, J. F.; Ma, Z. Y.; Huang, S. Enhanced Use of Foam Fractionation in the Photodegradation of Perfluorooctane Sulfonate (PFOS). *Sep. Purif. Technol.* **2020**, *253*, 117488.

(24) Meng, P.; Deng, S.; Maimaiti, A.; Wang, B.; Huang, J.; Wang, Y.; Cousins, I. T.; Yu, G. Efficient Removal of Perfluorooctane Sulfonate from Aqueous Film-Forming Foam Solution by Aeration-Foam Collection. *Chemosphere* **2018**, *203*, 263−270.

(25) Burns, D. J.; Hinrichsen, H. M.; Stevenson, P.; Murphy, P. J. C. Commercial-scale remediation of per- and polyfluoroalkyl substances from a landfill leachate catchment using Surface-Active Foam Fractionation (SAFF). *Remed. J.* **2022**, *32*, 139−150.

(26) CDM Smith. PFAS Destruction. https://www.cdmsmith.com/en/Client-Solutions/Insights/PFAS-Destruction (accessed Dec 16, 2022).

(27) Martínez-Huitle, C. A.; Rodrigo, M. A.; Sirés, I.; Scialdone, O. Single and Coupled Electrochemical Processes and Reactors for the Abatement of Organic Water Pollutants: A Critical Review. *Chem. Rev.* **2015**, *115*, 13362−13407.

(28) Nzeribe, B. N.; Crimi, M.; Mededovic Thagard, S.; Holsen, T. M. Physico-Chemical Processes for the Treatment of Per- And Polyfluoroalkyl Substances (PFAS): A Review. *Crit. Rev. Environ. Sci. Technol.* **2019**, *49*, 866−915.

(29) Zhuo, Q.; Deng, S.; Yang, B.; Huang, J.; Wang, B.; Zhang, T.; Yu, G. Degradation of Perfluorinated Compounds on a Boron-Doped Diamond Electrode. *Electrochim. Acta* **2012**, *77*, 17−22.

(30) Barisci, S.; Suri, R. Electrooxidation of Short and Long Chain Perfluorocarboxylic Acids Using Boron Doped Diamond Electrodes. *Chemosphere* **2020**, *243*, 125349.

(31) Radjenovic, J.; Duinslaeger, N.; Avval, S. S.; Chaplin, B. P. Facing the Challenge of Poly- and Perfluoroalkyl Substances in Water: Is Electrochemical Oxidation the Answer? *Environ. Sci. Technol.* **2020**, *54*, 14815−14829.

(32) Pierpaoli, M.; Szopińska, M.; Wilk, B. K.; Sobaszek, M.; Łuczkiewicz, A.; Bogdanowicz, R.; Fudala-Książek, S. Electrochemical Oxidation of PFOA and PFOS in Landfill Leachates at Low and Highly Boron-Doped Diamond Electrodes. *J. Hazard. Mater.* **2021**, *403*, 123606.

(33) Schaefer, C. E.; Andaya, C.; Burant, A.; Condee, C. W.; Urtiaga, A.; Strathmann, T. J.; Higgins, C. P. Electrochemical Treatment of Perfluorooctanoic Acid and Perfluorooctane Sulfonate: Insights into

Mechanisms and Application to Groundwater Treatment. *Chem. Eng. J.* **2017**, *317*, 424−432.
(34) Schaefer, C. E.; Choyke, S.; Ferguson, P. L.; Andaya, C.; Burant, A.; Maizel, A.; Strathmann, T. J.; Higgins, C. P. Electrochemical Transformations of Perfluoroalkyl Acid (PFAA) Precursors and PFAAs in Groundwater Impacted with Aqueous Film Forming Foams. *Environ. Sci. Technol.* **2018**, *52*, 10689−10697.
(35) Trautmann, A. M.; Schell, H.; Schmidt, K. R.; Mangold, K. M.; Tiehm, A. Electrochemical Degradation of Perfluoroalkyl and Polyfluoroalkyl Substances (PFASs) in Groundwater. *Water Sci. Technol.* **2015**, *71*, 1569−1575.
(36) Schaefer, C. E.; Andaya, C.; Maizel, A.; Higgins, C. P. Assessing Continued Electrochemical Treatment of Groundwater Impacted by Aqueous Film-Forming Foams. *J. Environ. Eng.* **2019**, *145*, 06019007.
(37) Guan, B.; Zhi, J.; Zhang, X.; Murakami, T.; Fujishima, A. Electrochemical Route for Fluorinated Modification of Boron-Doped Diamond Surface with Perfluorooctanoic Acid. *Electrochem. Commun.* **2007**, *9*, 2817−2821.
(38) Ochiai, T.; Iizuka, Y.; Nakata, K.; Murakami, T.; Tryk, D. A.; Fujishima, A.; Koide, Y.; Morito, Y. Efficient Electrochemical Decomposition of Perfluorocarboxylic Acids by the Use of a Boron-Doped Diamond Electrode. *Diamond Relat. Mater.* **2011**, *20*, 64−67.
(39) Urtiaga, A.; Fernández-González, C.; Gómez-Lavín, S.; Ortiz, I. Kinetics of the Electrochemical Mineralization of Perfluorooctanoic Acid on Ultrananocrystalline Boron Doped Conductive Diamond Electrodes. *Chemosphere* **2015**, *129*, 20−26.
(40) Carter, K. E.; Farrell, J. Oxidative Destruction of Perfluorooctane Sulfonate Using Boron-Doped Diamond Film Electrodes. *Environ. Sci. Technol.* **2008**, *42*, 6111−6115.
(41) Maldonado, V. Y.; Landis, G. M.; Ensch, M.; Becker, M. F.; Witt, S. E.; Rusinek, C. A. A Flow-through Cell for the Electrochemical Oxidation of Perfluoroalkyl Substances in Landfill Leachates. *J. Water Process Eng.* **2021**, *43*, 102210.
(42) Ensch, M.; Rusinek, C. A.; Becker, M. F.; Schuelke, T. A Combined Current Density Technique for the Electrochemical Oxidation of Perfluorooctanoic Acid (PFOA) with Boron-Doped Diamond. *Water Environ. J.* **2021**, *35*, 158−165.
(43) Hamers, T.; Smit, M. G. D.; Murk, A. J.; Koeman, J. H. Biological and Chemical Analysis of the Toxic Potency of Pesticides in Rainwater. *Chemosphere* **2001**, *45*, 609−624.
(44) Hamers, T.; Kortenkamp, A.; Scholze, M.; Molenaar, D.; Cenijn, P. H.; Weiss, J. M. Transthyretin-Binding Activity of Complex Mixtures Representing the Composition of Thyroid-Hormone Disrupting Contaminants in House Dust and Human Serum. *Environ. Health Perspect.* **2020**, *128*, 017015.
(45) Rizzo, L. Bioassays as a Tool for Evaluating Advanced Oxidation Processes in Water and Wastewater Treatment. *Water Res.* **2011**, *45*, 4311−4340.
(46) Wilk, B. K.; Szopińska, M.; Sobaszek, M.; Pierpaoli, M.; Błaszczyk, A.; Luczkiewicz, A.; Fudala-Ksiazek, S. Electrochemical Oxidation of Landfill Leachate Using Boron-Doped Diamond Anodes: Pollution Degradation Rate, Energy Efficiency and Toxicity Assessment. *Environ. Sci. Pollut. Res.* **2022**, *29*, 65625−65641.
(47) Trojanowicz, M.; Bojanowska-Czajka, A.; Bartosiewicz, I.; Kulisa, K. Advanced Oxidation/Reduction Processes Treatment for Aqueous Perfluorooctanoate (PFOA) and Perfluorooctanesulfonate (PFOS) − A Review of Recent Advances. *Chem. Eng. J.* **2018**, *336*, 170−199.
(48) Uwayezu, J. N.; Carabante, I.; Lejon, T.; van Hees, P.; Karlsson, P.; Hollman, P.; Kumpiene, J. Electrochemical Degradation of Per- and Poly-Fluoroalkyl Substances Using Boron-Doped Diamond Electrodes. *J. Environ. Manage.* **2021**, *290*, 112573.
(49) Casas, G.; Martínez-Varela, A.; Roscales, J. L.; Vila-Costa, M.; Dachs, J.; Jiménez, B. Enrichment of Perfluoroalkyl Substances in the Sea-Surface Microlayer and Sea-Spray Aerosols in the Southern Ocean. *Environ. Pollut.* **2020**, *267*, 115512.
(50) Houtz, E. F.; Sedlak, D. L. Oxidative Conversion as a Means of Detecting Precursors to Perfluoroalkyl Acids in Urban Runoff. *Environ. Sci. Technol.* **2012**, *46*, 9342−9349.
(51) Kärrman, A.; Yeung, L. W. Y.; Spaan, K. M.; Lange, F. T.; Nguyen, M. A.; Plassmann, M.; de Wit, C. A.; Scheurer, M.; Awad, R.; Benskin, J. P. Can Determination of Extractable Organofluorine (EOF) Be Standardized? First Interlaboratory Comparisons of EOF and Fluorine Mass Balance in Sludge and Water Matrices. *Environ. Sci.: Processes Impacts* **2021**, *23*, 1458−1465.
(52) Schultes, L.; Vestergren, R.; Volkova, K.; Westberg, E.; Jacobson, T.; Benskin, J. P. Per- and Polyfluoroalkyl Substances and Fluorine Mass Balance in Cosmetic Products from the Swedish Market: Implications for Environmental Emissions and Human Exposure. *Environ. Sci.: Processes Impacts* **2018**, *20*, 1680−1690.
(53) Weiss, J. M.; Andersson, P. L.; Lamoree, M. H.; Leonards, P. E. G.; van Leeuwen, S. P. J.; Hamers, T. Competitive Binding of Poly- and Perfluorinated Compounds to the Thyroid Hormone Transport Protein Transthyretin. *Toxicol. Sci.* **2009**, *109*, 206−216.
(54) Villa, S.; Vighi, M.; Finizio, A. Experimental and Predicted Acute Toxicity of Antibacterial Compounds and Their Mixtures Using the Luminescent Bacterium Vibrio Fischeri. *Chemosphere* **2014**, *108*, 239−244.
(55) Liao, Z.; Farrell, J. Electrochemical Oxidation of Perfluorobutane Sulfonate Using Boron-Doped Diamond Film Electrodes. *J. Appl. Electrochem.* **2009**, *39*, 1993−1999.
(56) Smith, S. J.; Lewis, J.; Wiberg, K.; Wall, E.; Ahrens, L. Foam Fractionation for Removal of Per- and Polyfluoroalkyl Substances: Towards Closing the Mass Balance. *Sci. Total Environ.* **2023**, *871*, 162050.
(57) Nienhauser, A. B.; Ersan, M. S.; Lin, Z.; Perreault, F.; Westerhoff, P.; Garcia-Segura, S. Boron-Doped Diamond Electrodes Degrade Short- and Long-Chain per- and Polyfluorinated Alkyl Substances in Real Industrial Wastewaters. *J. Environ. Chem. Eng.* **2022**, *10*, 107192.
(58) Campos-Pereira, H.; Makselon, J.; Kleja, D. B.; Prater, I.; Kögel-Knabner, I.; Ahrens, L.; Gustafsson, J. P. Binding of Per- and Polyfluoroalkyl Substances (PFASs) by Organic Soil Materials with Different Structural Composition − Charge- and Concentration-Dependent Sorption Behavior. *Chemosphere* **2022**, *297*, 134167.
(59) Ahrens, L.; Harner, T.; Shoeib, M.; Koblizkova, M.; Reiner, E. J. Characterization of Two Passive Air Samplers for Per- and Polyfluoroalkyl Substances. *Environ. Sci. Technol.* **2013**, *47*, 14024−14033.
(60) Shoeib, M.; Harner, T.; Lee, C. L.; Lane, D.; Zhu, J. Sorbent-Impregnated Polyurethane Foam Disk for Passive Air Sampling of Volatile Fluorinated Chemicals. *Anal. Chem.* **2008**, *80*, 675−682.
(61) Winkens, K.; Koponen, J.; Schuster, J.; Shoeib, M.; Vestergren, R.; Berger, U.; Karvonen, A. M.; Pekkanen, J.; Kiviranta, H.; Cousins, I. T. Perfluoroalkyl Acids and Their Precursors in Indoor Air Sampled in Children's Bedrooms. *Environ. Pollut.* **2017**, *222*, 423−432.
(62) Sharma, S.; Shetti, N. P.; Basu, S.; Nadagouda, M. N.; Aminabhavi, T. M. Remediation of Per- and Polyfluoroalkyls (PFAS) via Electrochemical Methods. *Chem. Eng. J.* **2022**, *430*, 132895.

https://doi.org/10.1021/acsestwater.2c00660
ACS EST Water 2023, 3, 1201−1211

Supplementary information to: Electrochemical oxidation for treatment of PFAS in contaminated water and fractionated foam - a pilot scale study

Sanne J. Smith[1], Mélanie Lauria[2], Lutz Ahrens[1], Philip McCleaf[3], Patrik Hollman[4], Sofia Bjälkefur Seroka[3], Timo Hamers[5], Hans Peter H. Arp[6,7], and Karin Wiberg[1]

[1]*Department of Aquatic Sciences and Assessment, Swedish University of Agricultural Sciences (SLU), P.O. Box 7050, SE-750 07, Uppsala, Sweden*
[3]*Uppsala Water and Waste AB, P.O. Box 1444, SE-751 44, Uppsala, Sweden*
[4]*Nova Diamant AB, Tryffelvägen 17, 75646, Uppsala, Sweden*
[2]*Department of Environmental Science, Stockholm University, Svante Arrhenius Väg 8, 10691, Stockholm, Sweden*
[5]*Amsterdam Institute for Life and Environment (A-LIFE), Vrije Universiteit Amsterdam, De Boelelaan 1085, 1081 HV, Amsterdam, the Netherlands*
[6]*Norwegian Geotechnical Institute (NGI), P.O. Box 3930, Ulleval Stadion, NO-080,6 Oslo, Norway*
[7]*Department of Chemistry, Norwegian University of Science and Technology (NTNU), NO-7491, Trondheim, Norway*

1. PH, VOLTAGE AND TEMPERATURE RESULTS

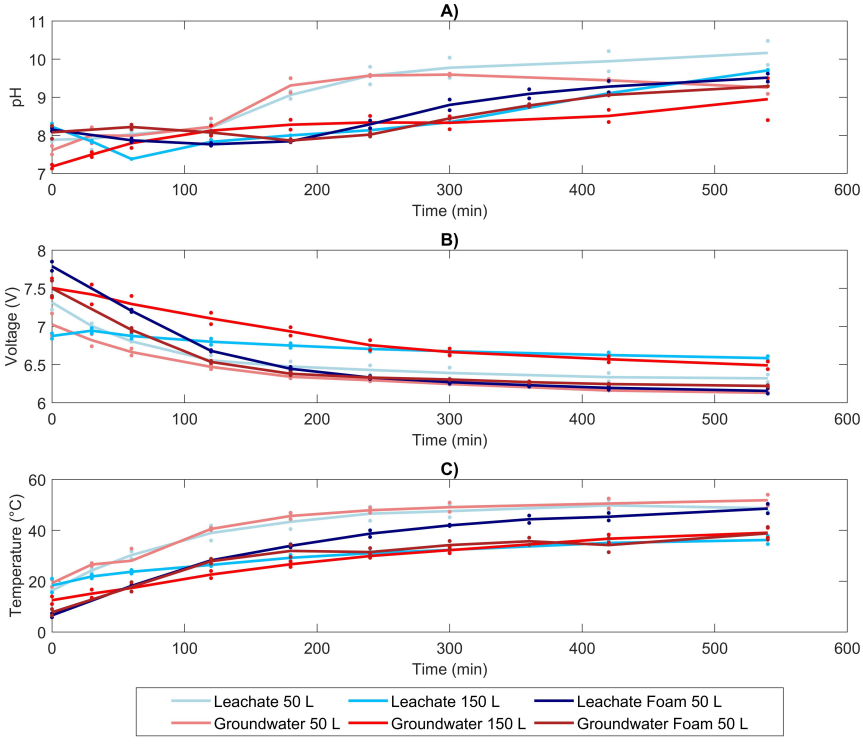

Figure S1. A) pH, B) Voltage (V) and C) Temperature (°C) over time during the electrochemical experiments. The dots represent the individual measurements for each duplicate experiment, whereas the lines connect the means of the two measurements.

2. GENERAL CHEMISTRY RESULTS

Tables S1 and S2 show the mean general chemistry of the water before and after each treatment step. The analysis of the groundwater included a few additional parameters compared to the leachate due to changes in the package offered by the analytical laboratory. Concentrations below the limit of quantification (LOQ) were set to half the LOQ. Effects of the foam fractionation (FF) treatment on the general chemistry were negligible. Conversely, the electrochemical treatment resulted in noticeably decreased dissolved organic carbon (DOC), total organic carbon

(TOC), chemical oxygen demand (COD) and dissolved solids concentrations. In this treatment, organic constituents are mostly degraded by electrochemical oxidation, whereas inorganic salts are removed by precipitation. Conversely, nitrate and to a lesser extent sulfate concentrations increased after electrochemical treatment, due to their formation from the oxidation of ammonium, nitrite and sulfite. Chloride concentrations decreased after electrochemical treatment, which indicates the formation of perchlorate or other high-valent oxidized chlorine species. These byproducts are toxic and would need to be removed in a biological post-treatment step.[1]

Table S1. Mean general chemistry of groundwater before and after each treatment step. Note the reduction of carbonate, calcium, iron, and magnesium concentrations after EO, which indicates the formation of precipitation that could lead to scaling on the electrode.

	Untreated	*FF Effluent*	*EO* 50 *L Effluent*	*EO* 150 *L Effluent*	*Foam*	*EO Foam Effluent*
	$(n = 5)$	$(n = 1)$	$(n = 2)$	$(n = 2)$	$(n = 2)$	$(n = 2)$
Uranium ($\mu g\, L^{-1}$)	35	52	10	22	51	25
Calcium ($mg\, L^{-1}$)	230	230	19	36	200	3.0
Manganese ($\mu g\, L^{-1}$)	1000	1100	400	630	870	340
Sodium ($mg\, L^{-1}$)	680	830	630	640	850	840
Potassium ($mg\, L^{-1}$)	140	180	120	130	190	180
Iron ($mg\, L^{-1}$)	2.1	4.6	1.8	1.4	2.3	2.2
Aluminum ($\mu g\, L^{-1}$)	23	11	35	28	45	42
Copper ($\mu g\, L^{-1}$)	1000	6.0	940	1100	2700	1500
Magnesium ($mg\, L^{-1}$)	75	94	34	63	96	66
DOC ($mg\, L^{-1}$)	34	29	0.25	4.3	52	1.4
TOC ($mg\, L^{-1}$)	35	31	0.25	4.7	81	12
Phosphor ($mg\, L^{-1}$)	0.05	0.09	0.02	0.03	0.07	1.34
Nitrite ($mg\, L^{-1}$)	0.1	0.1	0.6	0.0	0.2	1.3
COD ($mg\, L^{-1}$)	25	15	0.25	0.25	31	0.25
Ammonium ($mg\, L^{-1}$)	4.7	9.7	0.21	0.03	10	0.12
Phosphate ($mg\, L^{-1}$)	0.02	0.02	0.02	0.02	0.02	0.04
Nitrate ($mg\, L^{-1}$)	0.31	0.25	6.3	6.4	0.25	8.2
Fluoride ($mg\, L^{-1}$)	0.62	0.5	0.39	0.39	0.59	0.39
Chloride ($mg\, L^{-1}$)	740	960	0.55	35	920	1.0
Sulfate ($mg\, L^{-1}$)	670	590	690	640	570	580
Turbidity (FNU)	26	72	14	16	33	15
Conductivity ($mS\, m^{-1}$)	450	550	350	350	530	440
pH	7.5	7.8	9.6	9.5	8.1	9.4
Alkalinity ($mg\, HCO_3^-\, L^{-1}$)	980	1300	58	250	1200	450

Table S2. Mean general chemistry of landfill leachate before and after each treatment step. Note the reduction of carbonate, calcium, iron, and magnesium concentrations after EO, which indicates the formation of precipitation that could lead to scaling on the electrode.

	Untreated	*FF Effluent*	*EO* 50 *L Effluent*	*EO* 150 *L Effluent*	*Foam*	*EO Foam Effluent*
	$(n = 5)$	$(n = 1)$	$(n = 2)$	$(n = 2)$	$(n = 2)$	$(n = 2)$
Uranium ($\mu g\, L^{-1}$)	61	50	24	53	44	25
Calcium ($mg\, L^{-1}$)	150	150	4.4	6.3	140	2.4
Manganese ($\mu g\, L^{-1}$)	380	460	200	200	450	240
Sodium ($mg\, L^{-1}$)	640	720	660	630	700	720
Iron ($mg\, L^{-1}$)	2.7	3.7	2.0	1.8	6.8	5.2
Aluminum ($\mu g\, L^{-1}$)	42	18	34	33	79	81
Magnesium ($mg\, L^{-1}$)	61	59	30	47	56	38
DOC ($mg\, L^{-1}$)	43	44	1.8	6.9	45	1.5
TOC ($mg\, L^{-1}$)	44	44	1.5	6.8	47	1.6
Phosphor ($mg\, L^{-1}$)	0.28	0.9	0.08	0.09	0.45	0.34
Nitrite ($mg\, L^{-1}$)	11	1.0	9.1	0.12	1.1	3.7
COD ($mg\, L^{-1}$)	27	25	0.50	0.50	25	0.14
Nitrate ($mg\, L^{-1}$)	41	11	53	92	16	43
Fluoride ($mg\, L^{-1}$)	0.23	0.25	0.36	0.05	0.14	0.14
Chloride ($mg\, L^{-1}$)	900	1000	2.5	44	930	1.0
Sulfate ($mg\, L^{-1}$)	220	130	250	250	120	130
Conductivity ($mS\, m^{-1}$)	470	500	360	360	470	380
pH	7.8	7.6	11	9.6	8.1	9.8
Alkalinity ($mg\, HCO_3^-\, L^{-1}$)	1100	1200	360	400	1200	520

3. AEROSOL ANALYSIS

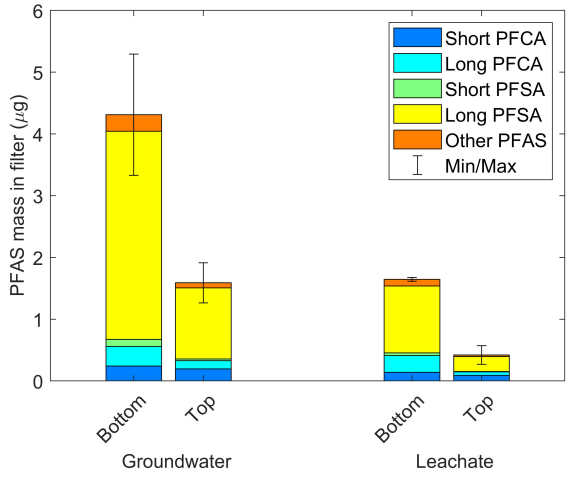

Figure S2. Measured PFAS mass in the aerosol filters placed on top of the inlet cell during the electrochemical treatment of the fractionated foam. Air exiting this tank passed through the bottom filter before passing through the top filter. Error bars represent the minimum and maximum ΣPFAS mass detected over the duplicate runs.

The quartz microfiber filters used for aerosol collection were extracted according to a modified protocol described by Casas *et al.*.[2] Each filter was transferred to a 50 mL polypropylene (PP) tube and 50 µL of an internal standard (IS) mixture containing 50 ng mL^{-1} of each individual compound was added.[3] One blank with a clean filter and one blank without filter were included as well. Then, 15 mL of methanol was added to each tube, after which they were vortexed briefly and sonicated for 20 min. The methanol was decanted into a second PP tube, and the extraction was repeated twice with 5 mL of methanol. The combined methanol fractions were concentrated to 0.5 mL under a gentle stream of N_2 (N-EVAP™112, Organomation Associates Inc., USA) and transferred to 1.5 mL Eppendorf tubes. Each PP tube was rinsed three times with methanol, which was added to the corresponding Eppendorf tube, and the extracts were concentrated to 0.5 mL under N_2 again. Finally, the Eppendorf tubes were centrifuged for 15 min at 4000 rpm (Eppendorf centrifuge 5424R) and 150 µL supernatant was transferred to an analytical PP insert vial for UPLC-MS/MS analysis according to the same protocol as for the water and foam extracts, see section 4 and Smith *et al.*, 2022.[3]

The LOQs for the determination of the aerosol mass per filter are given in Table S3. These LOQs correspond to either the instrument LOQ of 0.1 ng, or the highest mass detected in the extraction blanks. In the data analysis, values below the LOQ were set to 0, since the reported concentrations correspond to minimum concentrations. The field blank contained a ΣPFAS mass of 57 ng, the majority of which was PFOS (45 ng). This high concentration indicates that PFAS had already been emitted to the air during previous runs with the electrochemical system, which contaminated the field blank. However, as illustrated in Figure S2, the PFAS levels in the filters used during electrochemical runs were much higher than in the field blank.

Although the PFAS levels in the bottom filters were clearly higher, PFAS were detected in the top filters at high concentrations as well. Hence, PFAS passed through the bottom filter during the runs. This breakthrough could be due to saturation of the bottom filters. Alternatively, PFAS from the air surrounding the system may have adsorbed to the top filter. Nonetheless, for further calculations, we assumed that the PFAS found in both filters originated from the treatment. Since it is possible that not all PFAS in the exhaust gas was caught in the filters, calculated concentrations represent minimum values.

Faradays law, given in Equation S1, was used for the calculation of the H_2 gas formation rate ($r_{H_2}, L\,s^{-1}$) in the electrochemical system, with F Faradays constant (98465 $C\,mol^{-1}$), I the current (231 A), Z the number of electrons per H_2 molecule formed (2) and V_m the molar volume of an ideal gas (22.4 L). For simplicity, we assumed a cathodic current efficiency towards the reduction of water of 100 % and ignored the formation of gaseous byproducts at the anode. Exhaust gas PFAS concentrations were subsequently calculated as per Equation S2, with M_{tot} the total PFAS mass from both filters and t_{tot} the total treatment time (32400 s). It should be noted that this calculation is an approximation.

$$r_{H_2} = \frac{I}{F \cdot Z} \cdot V_m \tag{S1}$$

$$C_{gas} = \frac{M_{tot}}{t_{tot} \cdot r_{H_2}} \tag{S2}$$

Table S3. LOQ in aerosol filters

Compound	$LOQ\,(ng\,filter^{-1})$
Perfluorobutanoic acid (PFBA)	1.9
Perfluoropentanoic acid (PFPeA)	0.1
Perfluorobutane sulfonate (PFBS)	0.1
Perfluorohexanoic acid (PFHxA)	0.1
4:2 Fluorotelomer sulfonic acid (4:2 FTSA)	0.2
Hexafluoropropylene oxide dimer acid (HFPO-DA)	0.2
Perfluoropentane sulfonate (PFPeS)	0.1
Perfluoroheptanoic acid (PFHpA)	0.1
4,8-dioxa-3H-perfluorononanoic acid (NaDONA)	0.1
Perfluorohexane sulfonate (PFHxS)	0.2
Perfluorooctanoic acid (PFOA)	0.1
6:2 Fluorotelomer sulfonate (6:2 FTSA)	0.5
Perfluoroheptane sulfonate (PFHpS)	0.1
Perfluoroethyl-cyclohexane sulfonate (PFECHS)	0.1
Perfluorononanoic acid (PFNA)	0.1
Perfluorooctane sulfonamide (FOSA)	0.2
Perfluorooctane sulfonate (PFOS)	4.6
Perfluorodecanoic acid (PFDA)	0.2
8:2 Fluorotelomer sulfonate (8:2 FTSA)	0.2
9-chloro-hexadecafluoro-3-oxanonane sulfonate (9Cl-PF3ONS)	0.1
Perfluorononane sulfonate (PFNS)	0.1
Perfluoroundecanoic acid (PFUnDA)	0.5
N-methyl-perfluorooctane sulfonamido acetic acid (MeFOSAA)	0.1
N-ethyl-perfluorooctane sulfonamido acetic acid (EtFOSAA)	0.1
Perfluorodecane sulfonate (PFDS)	0.1
Perfluorododecanoic acid (PFDoDA)	0.3
11-chloro-eicosafluoro-3-oxaundecane-1-sulfonic acid (11Cl-PF3OUdS)	0.1
Perfluorotridecanoic acid (PFTriDA)	0.1
Perfluorotetradecanoic acid (PFTeDA)	1.9

4. ANALYTICAL METHOD

All laboratory glassware used in the extractions was burned at 400 °C overnight and all equipment was rinsed three times with methanol before use. Samples were filtered through glass microfiber filters (47 mm diameter, Whatman™, China), split into two when the analysis was done in duplicate, weighed and spiked with 100 µL of a 50 ng mL^{-1} internal standard mixture in methanol (Wellington Laboratories, MPFAC-24 ES with 13C3-HFPO-DA added individually). The samples were then extracted on Oasis WAX cartridges (6 mL, 150 mg, 30 µm, Waters) as described in Smith *et al.*, 2022[3] and concentrated to 1 mL under nitrogen. Target analysis was done on a SCIEX Triple Quad™ UPLC-MS/MS system (USA) and included 29 target compounds, which are listed in Table S4 together with quality control data. A Phenomenex Kinetix® 1.7 µm C18 precolumn was used to trap PFAS contamination from the mobile phases and LC system prior to extract injection. The organic mobile phase was methanol and the inorganic mobile phase was 10 mM ammonium acetate in Milli-Q water. Extracts were injected on a Phenomenex Gemini® 3 µm C18 HPLC column with a Phenomenex KJ0-4282 analytical guard column, all at 40 °C. MS/MS operation was done in scheduled multiple reaction monitoring (MRM) mode with negative electrospray ionization. Compounds with branched and linear isomers were reported as their summed concentrations. The limit of quantification in the water samples was defined as the lowest concentration with a consistent signal to noise ratio of 10, which was 0.2 ng L^{-1} in the FF samples and 0.4 ng L^{-1} in the EO samples. Of all water samples analyzed for target PFAS in this study (n = 248), the maximum contribution of non-detects to the ΣPFAS concentration was 1.6 %, which was deemed

negligible. Hence, concentrations of PFAS below the LOQ were set to 0. For further details on the analytical method, see Smith *et al.*, 2022.[3]

The mean detected masses of each compound over all analyzed blanks (n = 19) are given in Table S4, with values below the LOQ set to zero. This includes laboratory blanks (n = 6), Milli-Q blanks (n = 11) and TOPA blanks (n = 2). For laboratory blanks, IS was spiked directly on a preconditioned cartridge prior to elution. For Milli-Q blanks, 125 mL Milli-Q water was extracted instead of sample. TOPA blanks were 125 mL Milli-Q water on which a TOP assay was performed. Each extraction batch contained at least one blank. In all cases, detected blank concentrations were negligible compared to sample concentrations. For two samples, outlying PFBA concentrations of > 730 ng L^{-1} were removed from the analysis, i.e. $n = 3$ instead of 4. Mean concentrations of these samples were 220 ng L^{-1} (min – max: 190 – 260 ng L^{-1}) and 200 ng L^{-1} (min – max: 190 – 230 ng L^{-1}) after removal of these outliers.

Table S4 also gives the mean, min and max recovery of native-spiked Milli-Q and matrix samples (n = 6 for both). Spiked amounts ranged from 5 to 25 ng and matrices included groundwater, leachate, groundwater foam, leachate foam and groundwater electrochemical effluent. For recovery determination, matrix samples were filtered, split in three and one of three samples was spiked with the appropriate amount of a 250 ng mL^{-1} native PFAS mixture in methanol. The remaining two samples were analyzed normally, and the recovery was calculated as the weight-normalized difference in concentration between the spiked extract and the mean of the reference extracts. Most outlying recoveries originated from when low amounts of PFAS were spiked to matrices with high natural PFAS contamination. E.g., when 10 ng PFAS was spiked to a natural extract concentration of 100 ng mL^{-1}, a method variability of 10 % could already cause a recovery variation up to 200 %.

Table S4. Analytical method - quality control data

Compound	*Mean blank detection* ($ng\ mL_{Extract}^{-1}$)	*Recovery* (%), *as mean* ($min - max$)
PFBA	0.20	131 (102-293)
PFPeA	0.25	113 (95-170)
PFBS	0.16	110 (68-154)
PFHxA	0.06	130 (91-231)
4:2 FTSA	<LOQ	98 (59-151)
HFPO-DA	0.01	142 (61-342)
PFPeS	<LOQ	108 (57-275)
PFHpA	0.14	111 (79-178)
NaDONA	<LOQ	141 (76-298)
PFHxS	0.02	103 (63-164)
PFOA	0.05	119 (60-262)
6:2 FTSA	0.59	84 (15-136)
PFHpS	0.01	104 (66-126)
PFECHS	<LOQ	109 (60-170)
PFNA	<LOQ	109 (75-154)
FOSA	0.01	101 (68-167)
PFOS	0.53	90 (44-124)
PFDA	<LOQ	109 (60-185)
8:2 FTSA	0.02	105 (66-150)
9Cl-PF3ONS	<LOQ	74 (25-124)
PFNS	<LOQ	107 (72-187)
PFUnDA	0.02	89 (44-173)
Me-FOSAA	<LOQ	103 (72-136)
Et-FOSAA	<LOQ	97 (64-134)
PFDS	<LOQ	83 (60-108)
PFDoDA	<LOQ	101 (70-154)
11Cl-PF3OUdS	<LOQ	69 (35-102)
PFTriDA	<LOQ	127 (89-186)
PFTeDA	0.01	102 (68-138)

5. TOTAL OXIDIZABLE PRECURSOR (TOP) ASSAYS

A. Methods

After filtration as described in section 4, 2 g potassium persulfate ($K_2S_2O_8$, Sigma Aldrich, USA) and 1.9 mL 10 M sodium hydroxide (NaOH, Sigma Aldrich, USA) were added to each 125 mL sample. For the influent samples of the electrochemical runs with fractionated foam, 50 mL collapsed foam sample was used instead and the amounts of chemicals added were reduced accordingly. Samples were left in a water bath at 85 °C for six hours, cooled in an ice bath and adjusted to a pH of 6-8 by gradually adding 30 % hydrogen chloride (HCl, Merck, Germany). Solid phase extraction and UPLC-MS/MS analysis were subsequently done as for the normal target PFAS analysis.

B. Results

Table S5 shows the mean recoveries of individual PFAA and total PFAS after total oxidizable precursor (TOP) assays for all analyzed samples ($n = 32$). Concentrations prior to oxidation below the LOQ were set to the LOQ, and n indicates the number of samples for which the concentrations in both the reference samples and the oxidized samples were above the LOQ. It should be noted that this choice is somewhat arbitrary and results in a recovery of zero when both the reference and the oxidized sample concentrations are below the LOQ. Since the total concentration of all precursors included in the target analysis was negligible (< 5 % of ΣPFAS in all reference and oxidized samples) and

individual precursor concentrations were often below the LOQ, oxidiation efficiencies were difficult to determine.

The samples included influent and effluent from all FF and EO experiments for both groundwater and leachate, including the foam ($n = 2$ for each sample type). There were no differences in TOP assay recovery between the groundwater and leachate samples, so all sample types were grouped together. Overall, a minor decrease in PFAS concentrations after the TOP assay was measured, which indicates that no considerable concentrations of precursors were present in the groundwater or leachate. Probably, this is because all PFAS originate from the landfill, where any precursors were already degraded due to the high biological activity and long storage time before leaching. The observed decreases in concentrations were small and can be explained by analytical uncertainties.

Table S5. Recovery in TOP assay samples and corresponding standard deviation. When the concentrations in the reference sample prior to oxidation were below LOQ, these were set to the LOQ, such that the denominator was non-zero. n indicates the number of samples for which all concentrations (i.e. before and after oxidation) were above the LOQ.

Compound	*Mean recovery* $\pm$ *sd*	*n*
PFBA	0.80 ± 0.19	32
PFPeA	0.99 ± 0.19	32
PFHxA	0.99 ± 0.31	32
PFHpA	0.97 ± 0.31	32
PFOA	0.84 ± 0.15	32
PFNA	0.77 ± 0.34	28
PFDA	3.57 ± 8.20	26
PFUnDA	1.07 ± 1.80	17
PFDoDA	0.01 ± 0.07	1
PFTriDA	0.05 ± 0.21	2
PFTeDA	0.09 ± 0.39	2
PFBS	0.93 ± 0.10	32
PFPeS	0.93 ± 0.10	32
PFHxS	0.88 ± 0.07	32
PFHpS	0.80 ± 0.16	32
PFOS	0.87 ± 0.20	32
PFNS	0.21 ± 0.49	6
PFDS	0.01 ± 0.07	1
4:2 FTSA	0.42 ± 0.59	12
6:2 FTSA	0.55 ± 0.51	19
8:2 FTSA	0.45 ± 0.78	11
HFPO-DA	0.94 ± 2.12	8
NaDONA	0.21 ± 0.53	5
PFECHS	0.79 ± 0.12	32
FOSA	1.31 ± 0.91	29
9Cl-PF3ONS	0.01 ± 0.07	1
11Cl-PF3OUdS	0.01 ± 0.07	1
Me-FOSAA	0.51 ± 0.60	18
Et-FOSAA	0.80 ± 0.46	28
ΣPFAS	0.87 ± 0.10	32

6. EXTRACTABLE ORGANOFLUORINE (EOF)

A. Method

In addition to the influent and effluent water samples, three high volume negative blanks (750 mL MilliQ water), three low volume negative blanks (5 mL MilliQ water), three fluoride blanks (750 mL 0.69 mg L^{-1} F^-) and five positive blanks (three 750 mL MilliQ water spiked with 50 ng and two 750 mL spiked with 150 ng of each of the 29 PFAS included in the target analysis) were included in the extraction and subsequent analysis. The extraction protocol was the same as described above for the target PFAS analysis, but to account for the higher volume, 500 mg WAX cartridges (6 mL, 500 mg, 60 µm, Waters) were used instead of 150 mg and the second elution step was done with 8 mL instead of 4 mL 0.1 % ammonium hydroxide in methanol.

To minimize background contamination, the sample extract carriers (ceramic boats), containing glass wool for better dispersion of the extracts' fluids, were baked at 1100 °C prior to analysis. Each run started and finished with an 8 points calibration curve (100 µL of 0.025 ng F μL^{-1} to 10 ng μL^{-1} of F^- solution, resulting in 2.5 to 1000 ng F^- total combusted) and a mid-level calibration standard was run repeatedly to monitor instrumental drift. The calibration curve showed very good linearity with $R^2 > 0.99$. To evaluate combustion efficiency, a mixture of PFOA and PFOS was combusted at the beginning, middle and end of each run. The PFOA and PFOS mixture average recovery was 92 % (n = 6; min – max: 79 % – 104 %), ensuring a good combustion efficiency of the instrument. Aliquots of 50 µL of extracts were combusted.

Combustion of samples was achieved at 1100 °C in a combustion furnace (HF-210, Mitsubishi) under oxygen (400 mL min^{-1}), argon (200 mL min^{-1}) and argon mixed with water vapour (100 mL min^{-1}) flow for around 5 min. Combustion gases were absorbed in MilliQ water using a gas absorber unit (GA-210, Mitsubishi), 200 µL aliquots of the absorption solution were injected onto the ion chromatograph (Dionex Integrion HPIC, Thermo Fisher Scientific) equipped with an anion exchange column (Dionex IonPac™ AG19-4µm 2x50 mm guard column and Dionex IonPac™ AS19-4µm 2x250 mm analytical column) operated at 35 °C. Chromatographic separation was achieved by running a gradient of aqueous hydroxide mobile phase ramping from 8 mM to 60 mM at a flow rate of 0.25 mL min^{-1} and fluoride was detected by a conductivity detector.

No differences between the low volume and high volume extraction blanks were observed, with an average of 9 ng F combusted, extrapolated to 49 ng L^{-1} in the water. Therefore, the mean EOF concentration in the extraction blanks (n = 6, 3 x 5 mL and 3 x 750 mL) was subtracted from the samples in all cases. The LOQ for EOF analysis was defined as the average concentration plus three times the standard deviation in the method blanks (62.6 ng F L^{-1}) and no samples were found to be below it. The known EOF concentrations based on the measured target PFAS concentrations were calculated as described in Schultes *et al*. (2018).[4]

B. Results and quality control

The mean recovery of positive blanks (50 ng or 150 ng of the 29 PFAS included in the targeted analysis) was 70 % (n=5; min – max: 62 % – 92 %), ensuring satisfactory EOF recovery. Recovery of fluoride in the fluoride blanks was only 0.45 % (n = 3; min – max: 0.18 % – 0.59 %). Nonetheless, since the fluoride concentration in the water samples ranged between <0.1 mg L^{-1} and 0.69 mg L^{-1} (Tables S1 and S2), fluoride may have contributed to the measured EOF concentrations, which were between 0.2 and 14 µg L^{-1}. When assuming the mean fluoride recovery of 0.45 %, the theoretical contribution of fluoride to the measured EOF ranged between 19 % and 1261 % (mean: 192 %). However, no significant correlation between aqueous fluoride concentrations and EOF concentrations were found ($p = 0.23$, fluoride concentrations below LOQ were set to the LOQ). This lack of correlation indicates that the fluoride removal during sample extraction was sufficient, but the exact effect of fluoride on the EOF concentrations remains uncertain.

A quantitative comparison between the measured EOF concentrations and the known EOF from the target PFAS concentrations was difficult to make. In the target PFAS analysis, concentrations were determined based on the peak area ratio with corresponding internal standards (IS). Due to the nature of the method, EOF concentrations were not IS-corrected, which means that target PFAS concentrations were not directly comparable to EOF concentrations. If EOF concentrations were corrected using the mean recovery of the spiked blanks, EOF concentrations were on average 82 % higher (min – max: 11 % – 358 %) than the known EOF concentration from the target PFAS concentrations. If EOF concentrations were not recovery-corrected, the concentrations were on average 27 % higher (min – max: -23 % – 220 %) than expected. Since the combustion efficiency and EOF recovery varied, the real difference is probably somewhere in between these values. Over all samples, a significant correlation between the known EOF from the target PFAS and the measured EOF was found (Pearson's $r = 0.89$, $p \approx 10^{-11}$), indicating that target PFAS concentrations were good indicators of the relative EOF concentrations.

The higher-than-expected EOF concentrations can be explained by the presence of extractable PFAS that were not included in our targeted method, and that do not degrade to target PFAS in the TOP assay. Examples of such are ultrashort-chain,[5] unsaturated[6] or chlorinated PFAS.[7] Fluorinated organic molecules that are not perfluorinated may have contributed to the measured EOF concentrations as well. The contribution of ultrashort-chain PFAS to the EOF content is uncertain. Generally, extra washing steps are included in the extraction procedure for EOF to remove fluoride, with the drawback that ultrashort-chain PFAS are lost as well.[8] Since we used the same extracts for bioassay and EOF analysis, these extra washing steps were omitted (but fluoride recovery was nonetheless only 0.45 %, as outlined above). Hence, more short-chain PFAS may have been recovered in the extracts and contributed to the measured EOF concentrations than is generally the case in EOF analysis. Efforts to identify these unknown fluorinated compounds with non-target methods are currently ongoing.

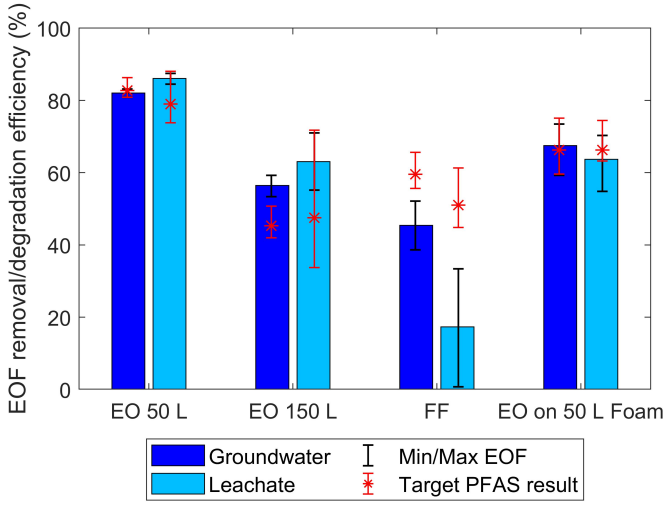

Figure S3. EOF removal (FF) or degradation (EO) efficiency of the different treatments, compared to the result based on total target PFAS concentrations. Black error bars represent the min/max of the EOF results, red error bars the min/max of the target PFAS results, and red asterisks the mean target PFAS result.

The EOF degradation efficiencies in the EO tests with 50 L volume were similar to the degradation of target PFAS, see Figure S3. Conversely, the mean EOF degradation was slightly higher than the target PFAS degradation at 150 L volume. Possibly, this indicates the formation of fluorinated byproducts in the EO at a high specific charge, i.e. at lower treated volumes. Accordingly, the EOF degradation would be higher than the target PFAS degradation at all treatment volumes, due to the presence of more degradable substances such as unsaturated or chlorinated PFAS. However, in the 50 L tests, this higher PFAS degradation is cancelled out by the formation of fluorinated byproducts. This hypothesis is strengthened by the slightly lower toxicity measured in the TTR-binding assay on the effluent of the 150 L EO experiments as compared to the 50 L experiments, see main text Figure 4. However, measurement uncertainties were high and experiments were only done in duplicate, so more research is needed to look further into the formation of fluorinated byproducts.

Conversely, the EOF removal in the foam fractionation was on average 45 % lower than the removal of target PFAS. This indicates the presence of PFAS that are not susceptible to removal by FF, such as ultrashort-chain PFAS or non-amphiphilic compounds.

7. BIOASSAYS

In addition to the influent and effluent water extracts, the high volume negative blanks and the high concentration positive blanks (150 ng of each PFAS included in the target analysis in 750 mL MilliQ water) were included in both bioassays as well.

A. Method - TTR binding assay

Transthyretin-binding experiments were performed in black 96-well polystyrene nonbinding plates (Greiner Bio-One) as described in Hamers *et al.*, 2020.[9] Briefly, a fluorescent conjugate of T_4 and fluorescein 5-isothiocyanate (FITC) was used. This FITC-T_4 conjugate emits increased fluorescence when bound to TTR, so the presence of TTR-binding compounds in an incubated extract will lead to a decreased fluorescence emission compared to a blank incubation. The fluorescence was measured twice for each extract in duplicate sample dilution curves and the data were fit to dose-response curves, to derive the concentration of sample extract (% of well volume) causing 50 % inhibition of TTR-binding by FITC-T_4 (EC_{50}). Using the EC_{50} value of PFOS (289 nM), PFOS-equivalent concentrations in the original water samples were calculated, i.e. a theoretical aqueous concentration of PFOS that in the same dilution as the extract would lead to the EC_{50} determined for the extract.

Duplicate sample dilution curves were prepared at 1, 0.3, 0.1, 0.03, 0.01, 0.003, 0.001 and 0 % of the final total well volume (200 µL). The methanol fraction was kept constant at 1 % of the total well volume for all dilutions. Initial dilutions in 100 µL Tris-HCl buffer at pH 8 were shaken for 5 min at 900 rpm and the background fluorescence was measured in arbitrary fluorescence units (AFU) at λ_{ex} = 490 nm and λ_{em} = 518 nm. Subsequently, 50 µL 110 nM fluorescein 5-isothiocyanate thyroxine (FITC-T_4) in Tris-HCl buffer was added to each well and the fluorescence was measured again after shaking for 5 min. Finally, 50 µL 0.12 µM transthyretin (TTR) in TRIS-HCl buffer was added and the fluorescence was measured in the presence of both FITC-T_4 and TTR. Influent and effluent samples from

each experiment were always incubated on the same 96-well plate.

The fraction of FITC-T_4 bound to TTR (f_{bound}) at each dilution i was calculated according to Equation S3, with F_{TTR} and F_{FT4} the fluorescence after addition of TTR and FITC-T_4, respectively. These data were fit to the inhibition curve given in Equation S4, with x the sample concentration (% of well volume), by minimizing the sum of squared errors between the calculated data $f_{bound,calc}$ and average measured data f_{bound} to find optimized values for the EC_{50} (% of well volume) and hill slope s.

$$f_{bound,i} = \frac{[F_{TTR} - F_{FT4}]_{sample\ i}}{[F_{TTR} - F_{FT4}]_{blank}} \cdot 100\% \tag{S3}$$

$$f_{bound,calc} = \frac{100}{1 + (\frac{x}{EC_{50}})^s} \tag{S4}$$

The measured EC_{50} values (% well volume) were subsequently expressed in PFOS-equivalent concentrations in the original sample as per Equation S5, with $EC_{50,PFOS}$ the average optimized EC_{50} value of PFOS ($2.89 \cdot 10^{-7}$ M). The factor 3750 is the concentration factor from sample to extract (0.75 L to 200 µL). The expected PFOS-equivalent concentration of each sample was calculated as in Equation S6, with C_i and $EC_{50,ref,i}$ the original aqueous concentration (M) and predetermined EC_{50} (M) of compound i, respectively. For compounds without a predetermined EC_{50} value ($n = 10$, with a total contribution to the mean influent $\Sigma PFAS$ concentration of 10 %) the EC_{50} value of PFDS was assumed, which was the highest value of all included compounds (34.8 µM). Because each experiment was carried out in duplicate and each extract was analyzed in duplicate, n = 4 for each data point, but these data points are not independent. Hence, statistical significance was not calculated, because the independent sample size was only 2.

$$C_{PFOS-eqv,\,meas}(M) = \frac{100}{3750} \cdot \frac{EC_{50,PFOS}}{EC_{50,extract}} \tag{S5}$$

$$C_{PFOS-eqv,\,calc}(M) = \sum \frac{C_i \cdot EC_{50,PFOS}}{EC_{50,ref,i}} \tag{S6}$$

B. Method - *A. fischeri* bioluminescence assay

White lumitrac polystyrene 96-well plates (Greiner Bio-One) were washed under hot tap water and rinsed thoroughly with demineralized water. Duplicate dilution curves at 1, 0.33, 0.1, 0.033, 0.01 and 0.033 % of the total well volume (200 µL) were prepared in 100 µL 50 mM KPi buffer with 2 % NaCl. The methanol fraction was kept constant at 1 %. 100 µL *A. fischeri* bacteria suspension in NaCl buffer, prepared according to the instructions from the provider (Modern Water), was automatically injected into each well, and the luminescence was measured after 15 and 30 minutes. These results were similar, so only the results after 30 min exposure are shown. Each plate also contained duplicate dilution curves containing 200, 60, 20, 6, 2, 0.6, 0.2 and 0.06 µM triclosan in 1 % DMSO in NaCl buffer, as well as duplicate DMSO and MeOH blanks. The differences in luminescence between the samples and the blanks were fitted to Equation S4 and expressed in triclosan equivalent concentrations identically as for the TTR-binding tests, using the triclosan EC_{50} measured on the corresponding plate.The antibacterial agent triclosan was used for the expression of the toxicity because an EC_{50} of PFOS individually could not be determined with the *A. fischeri* assay.

C. Quality control - TTR binding assay

All extracts from the untreated groundwater and leachate had a yellow color, leading to a visible coloring of the wells with high extract concentration. The blank fluorescence measurements, i.e. before the addition of FITC-T_4, showed non-zero values in the wells with high sample concentrations. However, there was no significant difference between the increase in fluorescence after FITC-T_4 addition to samples with and without background fluorescence, indicating that the total fluorescence is additive in nature. The mean EC_{50} values of the negative and positive control extracts as well as of pure methanol and a 29 µg L^{-1} ΣPFAS stock solution in methanol were all at least 4 times higher than that of the least active effluent sample when all were expressed in PFOS-eq. Negative controls often yielded linear response curves, which occurred when the highest concentration (% well volume) did not generate a measurable response, in which case EC_{50} values could not be determined. The low response of the positive controls confirmed that PFAS were not the primary cause of the TTR-binding activity of the water samples.

D. Quality control - *A. fischeri* bioluminescence assay

To assess any decrease in luminescence caused by light absorption rather than mortality of the bacteria, the absorption of each extract dilution curve at 490 nm wavelength was measured.[10] *A. fischeri* emit light around this wavelength[11] and from the absorption data, the percentage of light that is transmitted through the well was calculated according to Equation S7. All data are given in Table S6 and the transmission was always higher than 85 %, indicating that toxicity is the dominating cause for decreased light emission. However, the electrochemical influent always had a higher absorption than the effluent, which may have contributed to the difference in toxicity measured between electrochemical influent and effluent samples.

$$\%_{transmitted} = 10^{2 - Abs_{Sample} + Abs_{Blank}} \tag{S7}$$

For the *A. fischeri* bioluminescence assay, measurable activity was also found in the positive and negative control extracts, although both at least two times lower than in any of the sample extracts. The negative and positive controls had mean triclosan equivalent concentrations of 7 and 10 nM respectively, compared to 22 nM in the sample with the next lowest activity (groundwater 150 L EO effluent). The measurable activity in the negative (Milli-Q) control indicates that some of the sample response may have come from the extraction procedure. The similar activities in the negative and positive controls indicate that PFAS are not mainly responsible for the response in the *A. fischeri* bioluminescence assay.

Table S6. Transmission of light at 490 nm (%) through *A. fischeri* bioluminescence sample dilution curves. EO: electrochemical oxidation, FF: foam fractionation, GW: groundwater, Leach: leachate, I: influent, E: effluent

Sample	1 %	0.33 %	0.10 %	0.03 %	0.01 %	0.003 %
EO GW 50L I1	92.9	98.6	100	102	101	102
EO GW 50L I2	92.5	98.1	100	101	101	102
EO GW 50L E1	100	101	101	102	102	102
EO GW 50L E2	99.9	101	101	102	102	102
EO Leach 50L I1	89.8	96.9	99.7	101	102	101
EO Leach 50L I2	87.4	95.9	98.6	101	102	101
EO Leach 50L E1	101	102	102	102	102	101
EO Leach 50L E2	100	100	100	100	100	100
EO GW 150L I1	93.5	98.6	99.4	102	102	102
EO GW 150L I2	94.3	98.6	99.6	102	102	102
EO GW 150L E1	101	102	102	102	102	102
EO GW 150L E2	101	102	102	103	102	103
EO Leach 150L I1	88.4	96.4	99.6	101	101	101
EO Leach 150L I2	88.2	96.5	99.7	101	99.2	101
EO Leach 150L E1	101	103	102	102	102	101
EO Leach 150L E2	102	102	102	102	102	101
FF GW I1	95.0	98.3	100	101	101	101
FF GW I2	95.5	98.5	100	101	101	101
FF GW E1	95.6	98.8	100	101	101	101
FF GW E2	95.5	97.3	99.6	101	101	101
FF Leach I1	89.8	95.4	99.2	100	101	101
FF Leach I2	89.7	96.8	99.0	100	98.4	101
FF Leach E1	90.0	96.7	98.8	101	101	101
FF Leach E2	91.1	97.5	98.8	101	101	101
EO GW Foam I1	96.8	97.7	100	101	101	100
EO GW Foam I2	95.5	98.5	100	100	101	101
EO GW Foam E1	101	101	101	101	101	101
EO GW Foam E2	101	101	101	100	100	101
EO Leach Foam I1	90.8	97.0	99.2	100	100	101
EO Leach Foam I2	91.3	97.4	99.0	100	100	101
EO Leach Foam E1	101	101	101	101	101	101
EO Leach Foam E2	101	101	100	101	101	101
Mean of blanks	99.2	99.6	99.4	99.9	100	99.8
Methanol blanks – not diluted			100	99.4	100	100

8. MODEL EQUATIONS

The coupled numerical model to describe the degradation of PFAS and the formation of degradation products (that are subsequently degraded) is based on the design of the electrochemical cell (Figure S4). The model will be described by first deriving the ordinary differential equations (ODEs) to describe concentration change in the electrochemical cell (section A), discretizing the ODEs (section B), and finally coupling the parent compounds to the transformation compounds (Section C)

A. From mass balance to ODEs

First, the concentration in the inlet tank (C_1) is calculated from a simple mass balance based on inflow and outflow. It is assumed that there is no reactive degradation of PFAS here. The concentration in the inflow into the inlet tank is equal to the concentration in the effluent from the electrochemical cell, which is denoted as C_N. The mass balance over the inlet tank can then be written as follows, with V_1 the volume of the inlet tank (L) and Q the flow rate $(L\,min^{-1})$:

$$V_1 \cdot \frac{dC_1}{dt} = Q \cdot C_N - Q \cdot C_1 \tag{S8}$$

$$\frac{dC_1}{dt} = \frac{Q}{V_1} \cdot C_N - \frac{Q}{V_1} \cdot C_1 \tag{S9}$$

The concentration in the electrochemical cell is a function of both time and place in the reactor, hence the ordinary differential equations are derived from a flux balance. A denotes the cross-sectional area of the reactor and v the velocity of the flow, both are assumed constant in time as well as space. R is the reaction term, which is also a function of time and space. A small segment of the electrochemical cell between z and $z + dz$ is considered:

$$A \cdot dz \cdot \frac{dC(t,z)}{dt} = v_z \cdot A \cdot C_{z,t} - v_{z+dz} \cdot A \cdot C_{z+dz,t} + R \cdot d_z \cdot A \tag{S10}$$

$$\frac{dC(t,z)}{dt} = \frac{v_z \cdot A \cdot C_{z,t} - v_{z+dz} \cdot A \cdot C_{z+dz,t}}{A \cdot dz} + R \tag{S11}$$

Implementing the assumption that v is constant over space as well as time, this can be rewritten as:

$$\frac{dC(t,z)}{dt} = -v \cdot \frac{dC(t,z)}{dz} + R \tag{S12}$$

B. Discretization of ODEs

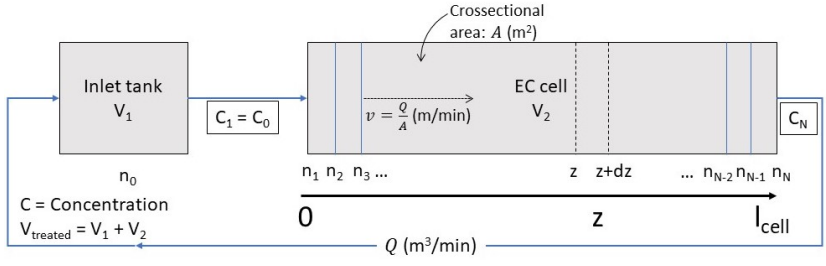

Figure S4. Discretization of the electrochemical reactor

The electrochemical cell is divided into N different nodes over its length, denoted by the subscript n, as illustrated in Figure S4. The concentration in node 1 is assumed equal to the concentration in the inlet tank. The differential equation for the concentration in node 1 is thus equal to Equation S9. The ODE for the concentration in the remaining nodes is:

$$\frac{dC_n}{dt} = \frac{Q}{A_{cell}} \cdot [\frac{dC}{dz}]_n + R_{n-1} \tag{S13}$$

$\frac{dC}{dz}$ for nodes $n = 2 \ldots N$ is calculated using a backward difference as:

$$[\frac{dC}{dz}]_n = \frac{C_n - C_{n-1}}{z_n - z_{n-1}} \tag{S14}$$

and implemented in the equation above.

C. Coupling of ODEs for different compounds

The reaction term R is different for each compound and consists of the sum of formation and degradation reactions. Electrochemical PFAS degradation follows a step-wise pathway, where the chain is shortened by subsequent loss of one CF_2 group.[12] As explained in the main text, perfluorosulfonic acids (PFSA) can degrade to shorter chain PFSA as well as to perfluorocarboxylic acids (PFCA). Conversely, PFCA only degrade to shorter chain PFCA. Finally, formation of both PFCA and PFSA from precursors can occur. Because the TOP assay results did not indicate the presence of any PFAA precursors, PFOS and PFOA precursor concentrations and kinetic constants were set to zero, and no other PFAA precursors were included in the model. For all PFSA, the reaction term then equates to

$$R_i(n) = -k_i \cdot C_i(n-1) + k_{i+1} \cdot C_{i+1}(n-1) \tag{S15}$$

with C_i and k_i the concentration of the PFSA with chain length i and the kinetic constant of the degradation of that same PFSA, respectively. Similarly, C_{i+1} and k_{i+1} are the concentration and kinetic constant for degradation of the PFSA with chain length $i+1$, respectively. For PFCA, additionally, degradation reactions of PFSA with the same chain length are added as formation reactions to this term, each with a corresponding kinetic constant.

As an example, for PFHpA, the total discretized ODE in nodes $n = 2 \dots N$ is then given as:

$$\begin{aligned} \frac{dC_{PFHpA}}{dt}(z,t) = Q/A_{cell} \cdot \frac{C_{PFHpA,n} - C_{PFHpA,n-1}}{z_n - z_{n-1}} \dots \\ - k_{PFHpA} \cdot C_{PFHpA,n-1} + k_{PFOA} \cdot C_{PFOA,n-1} + k_{PFHpS \to PFHpA} \cdot C_{PFHpS,n-1} \end{aligned} \tag{S16}$$

An overview of all kinetic constants included in the model is given in Table S7. As described in the methods section of the main text, the constants were obtained by minimization of the sum of squared errors between the model and experimental results. These kinetic constants are observational and may represent multiple combined reactions, each following a slightly different mechanism but leading to the same degradation products.[12] All reactions given in this table were included in the model, but some of the rate constants were set to zero to exclude certain degradation pathways. Formed perfluoropropanoic acid (PFPrA) concentrations were used for checking of the mole balance, which closed for every simulation. The entire model code is available on request to the corresponding author.

Table S7. Kinetic constants included in the model. The constants calibrated based on the results from the run with 50 L groundwater were used in all model simulations, but separate constants were also calibrated for the experiments with fractionated foam. Certain reaction pathways were excluded by setting the corresponding kinetic constant to 0. It should be noted that these rate constants depend on the current and will be different at current intensities other than the one used in this study (231 A, 25 mA cm^{-2}).

k	*Reaction*	*Value* (min^{-1})	*Value* (min^{-1})	*Value* (min^{-1})
	Calibration using	*GW 50 L*	*Leach Foam*	*GW Foam*
k_1	$Precursors \to PFOA$	0	0	0
k_2	$Precursors \to PFOS$	0	0	0
k_3	$PFOS \to PFHpS$	0	0	0
k_4	$PFHpS \to PFHxS$	0	0	0
k_5	$PFHxS \to PFPeS$	0.0032	0.0009	0.0001
k_6	$PFPeS \to PFBS$	0.0105	0.0019	0.0000
k_7	$PFBS \to PFPrS$	0	0	0
k_8	$PFOS \to PFOA$	0.0092	0.0000	0.0009
k_9	$PFHpS \to PFHpA$	0.0059	0.0000	0.0011
k_{10}	$PFHxS \to PFHxA$	0	0	0
k_{11}	$PFPeS \to PFPeA$	0	0	0
k_{12}	$PFBS \to PFBA$	0.0047	0.0022	0.0009
k_{13}	$PFOA \to PFHpA$	0.0169	0.0105	0.0101
k_{14}	$PFHpA \to PFHxA$	0.0402	0.0276	0.0297
k_{15}	$PFHxA \to PFPeA$	0.0341	0.0350	0.0384
k_{16}	$PFPeA \to PFBA$	0.0560	0.0647	0.0694
k_{17}	$PFBA \to PFPrA$	0.0484	0.0340	0.0481

D. Pseudocode

The ODEs describing the degradation or formation of each compound are combined in the pseudocode shown in Algorithm S1. This set of ODEs is solved in Matlab R2020b using the ode23 solver. Its output is a matrix containing the stacked concentrations of all compounds over time (rows) and axial position (columns). The size of this matrix is $n_{time} \times (n_{compounds} \cdot N)$, with n_{time} the number of time points evaluated, $n_{compounds}$ the number of compounds included in the model and N the length of the position vector. Restructuring this matrix appropriately yields the $n_{compounds} \times n_{time}$ matrix containing the concentrations of all compounds in the inlet tank over time.

Algorithm S1. Model Pseudocode

procedure MYODECOUPLED($Q, V1, Acell, k, z, C$)
  $dCdt(1) = Q/V1 \cdot (C(end) - C(1))$ ▷ set dC/dt in first node (inlet tank)
  for $i \in 1:13$ **do** ▷ Loop over the number of included compounds
    for $n \in 2:N$ **do** ▷ Loop over the length of the z vector
      $dCdz(i,n) = (C(n) - C(n-1))/(z(n) - z(n-1))$
      $dCdt(i,n) = -Q/Acell \cdot dCdz(i,n) + R(i,n)$
      ▷ R defines the reaction term for each compound i at node n
  $Reshape(dCdt)$
  ▷ Save C as column vector that stacks the ODEs for each compound at each node n

9. ELECTROCHEMICAL OXIDATION - ADDITIONAL RESULTS

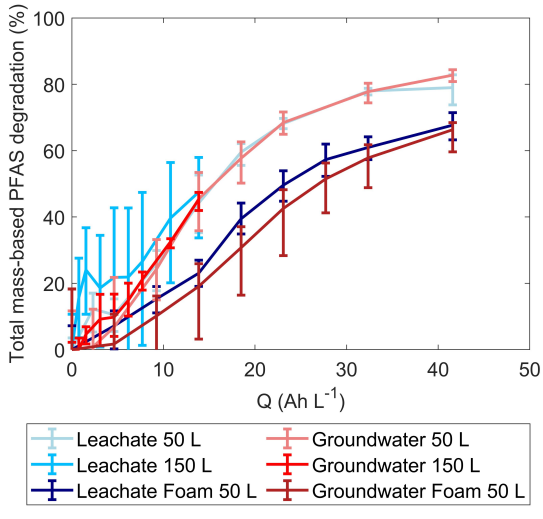

Figure S5. ΣPFAS degradation versus specific charge Q

The specific charge Q (Ah L^{-1}) is defined in equation S17, with V the total treated volume (L), t the treatment time (h) and J the current (A). Q can be used to calculate the energy consumption (W, $kWh\,m^{-3}$) of the electrochemical oxidation, as per equation S18, with U (V) the time-averaged voltage of the cell (see figure S1). This can subsequently be normalized per log removal of PFOS or PFOA using equation S19 (W_n), with C_0 and C_{end} the PFOS/PFOA concentration at the start and end of the EO treatment, respectively. For the log-normalization of the energy demand over the entire treatment train, C_0 was set to the concentration in the influent to the FF process, and C_{end} to the concentration in the effluent from the EO on the fractionated foam. The so obtained value for W_n was then multiplied with 0.1, since only 10 % of the influent water ended up as foam and was thus subjected to EO treatment.

$$Q = \frac{t \cdot J}{V} \tag{S17}$$

$$W = Q \cdot U \tag{S18}$$

$$W_n = \frac{W}{log_{10}(C_0/C_{end})} \tag{S19}$$

Table S8. Mean PFAS concentrations in the groundwater before treatment and after each treatment step. The foam concentrations reported here include the samples taken during the FF experiment (n = 4) as well as the samples from the bulk foam prior to EO (n = 4), whereas degradation efficiencies during EO were calculated based on the concentrations of the bulk foam exclusively.

PFAS	*Untreated*	*FF Effluent*	*EO* 50 *L Effluent*	*EO* 150 *L Effluent*	*Foam*	*EO Foam Effluent*
	$(n = 12)$	$(n = 4)$	$(n = 4)$	$(n = 4)$	$(n = 8)$	$(n = 4)$
PFBA	220	240	30	150	200	300
PFPeA	250	290	14	140	330	200
PFBS	170	190	140	130	310	360
PFHxA	500	470	13	210	1400	190
4:2 FTSA	0.45	<LOQ	<LOQ	0.1	0.092	<LOQ
HFPO-DA	<LOQ	<LOQ	<LOQ	<LOQ	1.9	<LOQ
PFPeS	59	28	59	66	410	580
PFHpA	260	78	11	140	1800	230
NaDONA	<LOQ	<LOQ	<LOQ	<LOQ	<LOQ	<LOQ
PFHxS	350	43	160	280	2700	2600
PFOA	930	88	17	230	8300	500
6:2 FTSA	8.4	<LOQ	2.2	3.4	110	<LOQ
PFHpS	19	1.3	4.6	13	160	140
PFECHS	33	3.8	11	22	370	370
PFNA	12	0.66	<LOQ	2	120	6.4
FOSA	1.5	0.3	0.16	<LOQ	10	0.26
PFOS	220	15	29	100	1800	930
PFDA	1.5	1.7	<LOQ	<LOQ	14	0.22
8:2 FTSA	<LOQ	0.81	<LOQ	<LOQ	1	<LOQ
9Cl-PF3ONS	<LOQ	<LOQ	<LOQ	<LOQ	<LOQ	<LOQ
PFNS	<LOQ	<LOQ	<LOQ	<LOQ	0.22	0.79
PFUnDA	0.23	2.5	<LOQ	0.24	0.073	<LOQ
Me-FOSAA	0.8	<LOQ	<LOQ	<LOQ	5.5	<LOQ
Et-FOSAA	4.9	0.46	0.1	0.7	27	0.86
PFDS	<LOQ	<LOQ	<LOQ	<LOQ	<LOQ	<LOQ
PFDoDA	0.17	1.4	0.15	<LOQ	<LOQ	<LOQ
11Cl-PF3OUdS	<LOQ	<LOQ	<LOQ	<LOQ	<LOQ	<LOQ
PFTriDA	<LOQ	0.4	<LOQ	<LOQ	<LOQ	<LOQ
PFTeDA	0.15	0.13	0.43	<LOQ	<LOQ	<LOQ

Table S9. Mean PFAS concentrations in the leachate before treatment and after each treatment step. The foam concentrations reported here include the samples taken during the FF experiment (n = 4) as well as the samples from the bulk foam prior to EO (n = 4), whereas degradation efficiencies during EO were calculated based on the concentrations of the bulk foam exclusively.

PFAS	*Untreated* ($n = 12$)	*FF Effluent* ($n = 4$)	*EO* 50 *L Effluent* ($n = 4$)	*EO* 150 *L Effluent* ($n = 4$)	*Foam* ($n = 8$)	*EO Foam Effluent* ($n = 4$)
PFBA	200	180	67	130	150	150
PFPeA	230	200	13	110	190	65
PFBS	120	110	95	110	150	140
PFHxA	390	330	26	160	560	59
4:2 FTSA	0.48	0.53	<LOQ	<LOQ	0.92	<LOQ
HFPO-DA	0.88	<LOQ	<LOQ	<LOQ	<LOQ	<LOQ
PFPeS	22	12	24	28	57	77
PFHpA	210	69	20	120	450	80
NaDONA	0.025	<LOQ	<LOQ	<LOQ	0.1	<LOQ
PFHxS	120	17	77	110	200	230
PFOA	570	54	49	260	780	160
6:2 FTSA	15	2.7	2.9	13	29	4
PFHpS	9.6	0.62	3.9	8.6	10	13
PFECHS	32	3.1	17	30	42	48
PFNA	11	1	1.2	4.7	15	4.2
FOSA	2.6	0.38	0.22	<LOQ	3.1	0.42
PFOS	190	11	41	120	160	150
PFDA	4.4	0.56	0.26	1.1	5	0.62
8:2 FTSA	0.28	0.27	<LOQ	0.14	1.1	<LOQ
9Cl-PF3ONS	<LOQ	<LOQ	<LOQ	<LOQ	<LOQ	<LOQ
PFNS	0.034	<LOQ	<LOQ	<LOQ	0.011	<LOQ
PFUnDA	0.45	0.21	0.65	0.29	0.83	0.11
Me-FOSAA	4.1	0.55	<LOQ	0.38	4.8	<LOQ
Et-FOSAA	18	2.3	0.87	2.6	20	0.55
PFDS	<LOQ	<LOQ	<LOQ	<LOQ	<LOQ	<LOQ
PFDoDA	1.3	0.16	1.9	0.2	0.2	<LOQ
11Cl-PF3OUdS	<LOQ	<LOQ	<LOQ	<LOQ	<LOQ	<LOQ
PFTriDA	0.19	0.11	0.68	<LOQ	<LOQ	<LOQ
PFTeDA	0.75	0.11	2.1	0.11	0.079	0.23

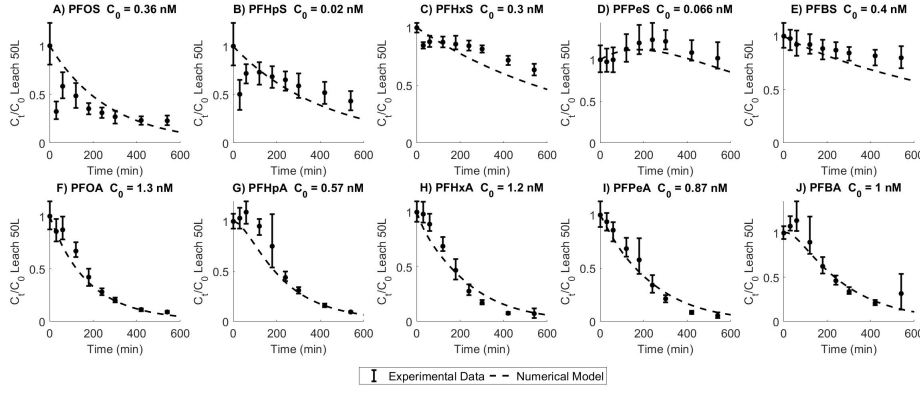

Figure S6. Individual degradation of PFSA and PFCA with chain lengths up to 8 for the EO run with 50 L leachate. Error bars represent min and max values based on the experimental and analytical duplicates (i.e. n = 4), dots represent the means and the dotted line is the model prediction with calibrated kinetic constants, see Table S7.

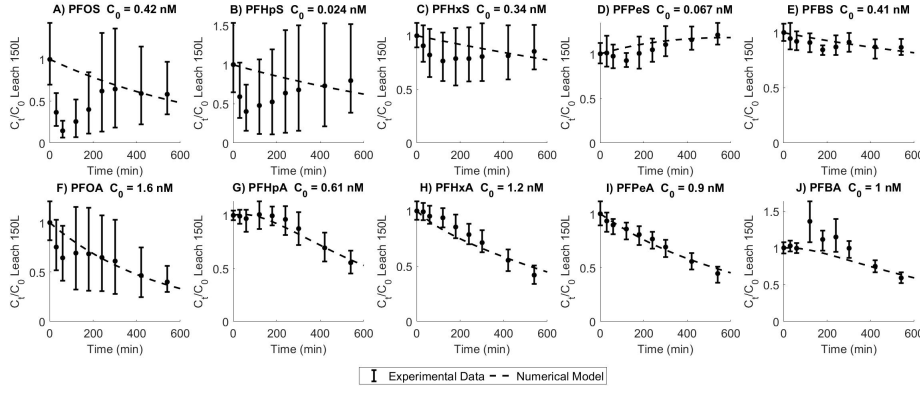

Figure S7. Individual degradation of PFSA and PFCA with chain lengths up to 8 for the EO run with 150 L leachate. Error bars represent min and max values based on the experimental and analytical duplicates (i.e. n = 4), dots represent the means and the dotted line is the model prediction with calibrated kinetic constants, see Table S7.

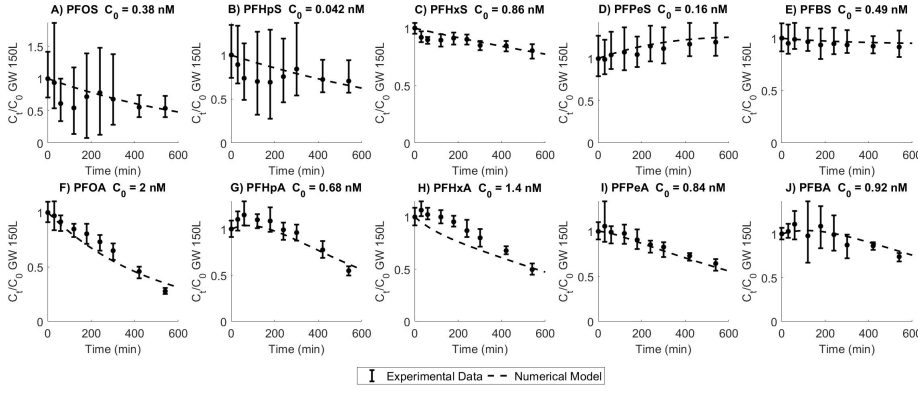

Figure S8. Individual degradation of PFSA and PFCA with chain lengths up to 8 for the EO run with 150 L groundwater. Error bars represent min and max values based on the experimental and analytical duplicates (i.e. n = 4), dots represent the means and the dotted line is the model prediction with calibrated kinetic constants, see Table S7.

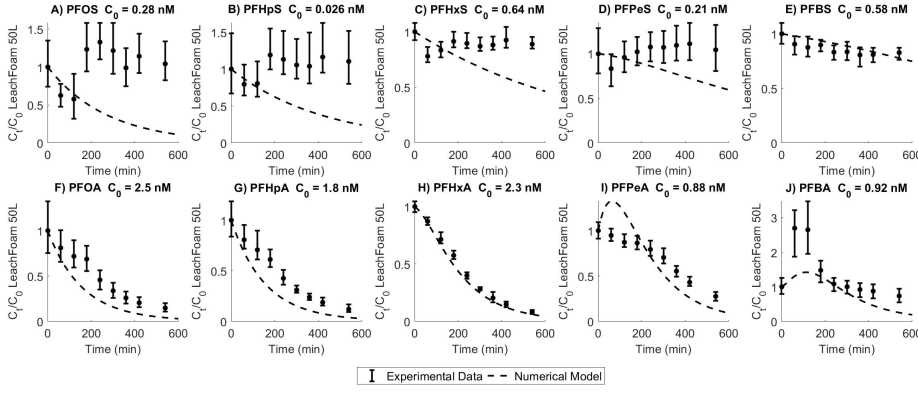

Figure S9. Individual degradation of PFSA and PFCA with chain lengths up to 8 for the EO run with 50 L leachate foam, using the kinetic constants calibrated based on the results from the 50 L GW experiment. Error bars represent min and max values based on the experimental and analytical duplicates (i.e. n = 4), dots represent the means and the dotted line is the model prediction with calibrated kinetic constants, see Table S7.

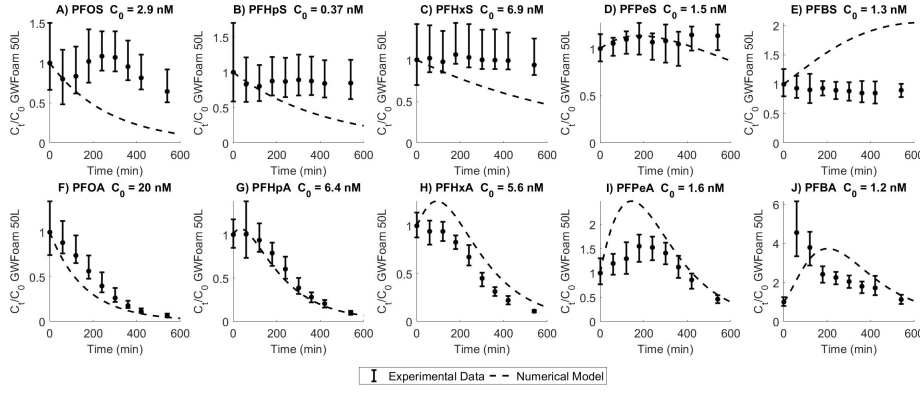

Figure S10. Individual degradation of PFSA and PFCA with chain lengths up to 8 for the EO run with 50 L groundwater foam, using the kinetic constants calibrated based on the results from the 50 L GW experiment. Error bars represent min and max values based on the experimental and analytical duplicates (i.e. n = 4), dots represent the means and the dotted line is the model prediction with calibrated kinetic constants, see Table S7.

Figures S11 and S12 show the model fits when the kinetic constants were calibrated based on the results from each EO experiment with fractionated foam. These kinetic constants are given in the last two columns of Table S7. The degradation rate constants of especially long-chain PFCA and PFSA were much lower than the constants calibrated based on the experiment with 50 L GW. This indicates that the reaction may have been hindered by matrix effects, electrode scaling or a change in pathway. Moreover, the higher initial concentrations may have caused a shift to a reaction-limited degradation, where zero-order kinetics are more appropriate. The concentrations of short-chained PFCA are still not reproduced very accurately, indicating that the degradation pathway may not be included correctly. More fundamental research into the degradation mechanism of PFSA is needed to refine this part of the model.

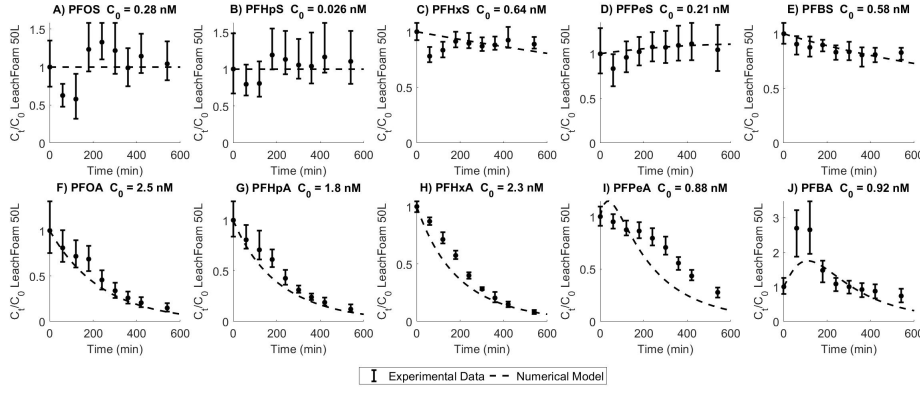

Figure S11. Individual degradation of PFSA and PFCA with chain lengths up to 8 for the EO run with 50 L leachate foam, using the kinetic constants calibrated based on the results from this experiment. Error bars represent min and max values based on the experimental and analytical duplicates (i.e. n = 4), dots represent the means and the dotted line is the model prediction with calibrated kinetic constants, see Table S7.

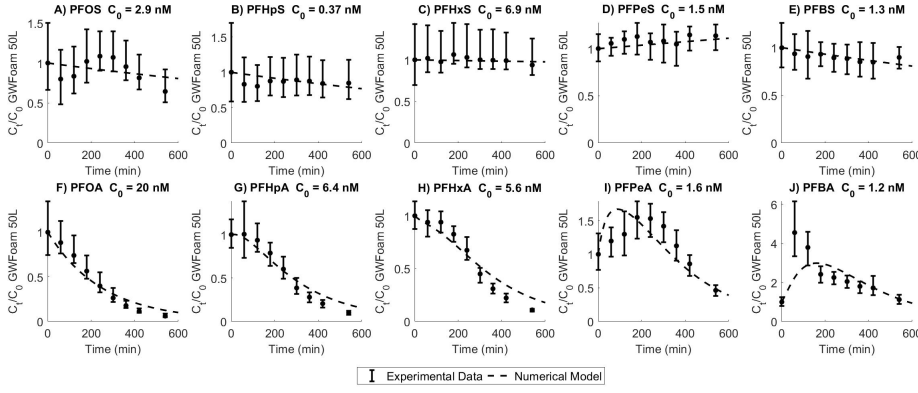

Figure S12. Individual degradation of PFSA and PFCA with chain lengths up to 8 for the EO run with 50 L groundwater foam, using the kinetic constants calibrated based on the results from this experiment. Error bars represent min and max values based on the experimental and analytical duplicates (i.e. n = 4), dots represent the means and the dotted line is the model prediction with calibrated kinetic constants, see Table S7.

REFERENCES

(1) Schaefer, C. E.; Andaya, C.; Burant, A.; Condee, C. W.; Urtiaga, A.; Strathmann, T. J.; Higgins, C. P. Electrochemical treatment of perfluorooctanoic acid and perfluorooctane sulfonate: Insights into mechanisms and application to groundwater treatment. *Chem. Eng. J.* **2017**, *317*, 424–432.

(2) Casas, G.; Martínez-Varela, A.; Roscales, J. L.; Vila-Costa, M.; Dachs, J.; Jiménez, B. Enrichment of perfluoroalkyl substances in the sea-surface microlayer and sea-spray aerosols in the Southern Ocean. *Environ. Pollut.* **2020**, *267*, 115512.

(3) Smith, S. J.; Wiberg, K.; McCleaf, P.; Ahrens, L. Pilot-scale continuous foam fractionation for the removal of per- and polyfluoroalkyl substances (PFAS) from landfill leachate. *ACS EST Water* **2022**, *2*, 841–851.

(4) Schultes, L.; Vestergren, R.; Volkova, K.; Westberg, E.; Jacobson, T.; Benskin, J. P. Per- and polyfluoroalkyl substances and fluorine mass balance in cosmetic products from the Swedish market: Implications for environmental emissions and human exposure. *Environmental Science: Processes and Impacts* **2018**, *20*, 1680–1690.

(5) Ateia, M.; Maroli, A.; Tharayil, N.; Karanfil, T. The overlooked short- and ultrashort-chain poly- and perfluorinated substances: A review. *Chemosphere* **2019**, *220*, 866–882.

(6) McDonough, C. A.; Higgins, C. P.; Choyke, S.; Barton, K. E.; Mass, S.; Starling, A. P.; Adgate, J. L. Unsaturated PFOS and other PFASs in human serum and drinking water from an AFFF-impacted community. *Environmental Science and Technology* **2021**, *55*, 8139–8148.

(7) McCord, J. P.; Strynar, M. J.; Washington, J. W.; Bergman, E. L.; Goodrow, S. M. Emerging chlorinated polyfluorinated polyether compounds impacting the waters of southwestern new jersey identified by use of nontargeted analysis. *Environmental Science and Technology Letters* **2020**, *7*, 903–908.

(8) Kärrman, A.; Yeung, L. W.; Spaan, K. M.; Lange, F. T.; Nguyen, M. A.; Plassmann, M.; De Wit, C. A.; Scheurer, M.; Awad, R.; Benskin, J. P. Can determination of extractable organofluorine (EOF) be standardized? First interlaboratory comparisons of EOF and fluorine mass balance in sludge and water matrices. *Environmental Science: Processes and Impacts* **2021**, *23*, 1458–1465.

(9) Hamers, T.; Kortenkamp, A.; Scholze, M.; Molenaar, D.; Cenijn, P. H.; Weiss, J. M. Transthyretin-binding activity of complex mixtures representing the composition of thyroid-hormone disrupting contaminants in house dust and human serum. *Environ. Health Perspect.* **2020**, *128*, 1–15.

(10) Verweij, W.; Durand, A.; Maas, J.; Van der Grinten, E. *Protocols belonging to the report 'Toxicity measurements in concentrated water samples '*; tech. rep.; 2010.

(11) Daubner, S. C.; Astorga, A. M.; Leisman, G. B.; Baldwin, T. O. Yellow light emission of vibrio fischeri strain Y-1 : purification and characterization of the energy-accepting yellow fluorescent protein. *Proc. Natl. Acad. Sci. U.S.A.* **1987**, *84*, 8912–8916.

(12) Radjenovic, J.; Duinslaeger, N.; Avval, S. S.; Chaplin, B. P. Facing the Challenge of Poly- and Perfluoroalkyl Substances in Water: Is Electrochemical Oxidation the Answer? *Environ. Sci. Technol.* **2020**, *54*, 14815–14829.

IV

ACS ES&T Engineering

pubs.acs.org/estengg

Article

Integrated Treatment of Per- and Polyfluoroalkyl Substances in Existing Wastewater Treatment Plants—Scoping the Potential of Foam Partitioning

Sanne J. Smith,* Chantal Keane, Lutz Ahrens, and Karin Wiberg

Cite This: https://doi.org/10.1021/acsestengg.3c00091

Read Online

ACCESS | Metrics & More | Article Recommendations | Supporting Information

ABSTRACT: Foam fractionation is becoming increasingly popular as a treatment technology for water contaminated with per- and polyfluoroalkyl substances (PFAS). At many existing wastewater treatment facilities, particularly in aerated treatment steps, foam formation is frequently observed. This study aimed to investigate if foam fractionation for the removal of PFAS could be integrated with such existing treatment processes. Influent, effluent, water under the foam, and foam were sampled from ten different wastewater treatment facilities where foam formation was observed. These samples were analyzed for the concentration of 29 PFAS, also after the total oxidizable precursor (TOP) assay. Enrichment factors were defined as the PFAS concentration in the foam divided by the PFAS concentration in the influent. Although foam partitioning did not lead to decreased ∑PFAS concentrations from influent to effluent in any of the plants, certain long-chain PFAS were removed with efficiencies up to 76%. Moreover, ∑PFAS enrichment factors in the foam ranged up to 10^5, and enrichment factors of individual PFAS ranged even up to 10^6. Moving bed biofilm reactors (MBBRs) were more effective at enriching PFAS in the foam than activated sludge processes. Altogether, these high enrichment factors demonstrate that foam partitioning in existing wastewater treatment plants is a promising option for integrated removal. Promoting foam formation and removing foam from the water surface with skimming devices may improve the removal efficiencies further. These findings have important implications for PFAS removal and sampling strategies at wastewater treatment plants.

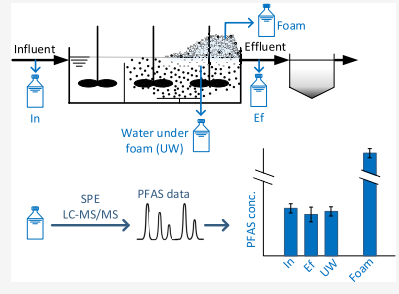

KEYWORDS: *per- and polyfluoroalkyl substances, wastewater treatment, foaming, activated sludge, moving bed biofilm reactors*

INTRODUCTION

Per- and polyfluoroalkyl substances (PFAS) are environmental pollutants mostly known for their high persistency in the environment.[1] The wide group of PFAS is characterized by the presence of at least one perfluorinated methyl or methylene carbon atom in their molecular structure,[2] and can be split into long- and short-chain compounds, depending on how many of such $-CF_2-$ moieties they contain.[3] Typically, perfluorosulfonic acids (PFSA) are considered to be short-chain for a chain length below or equal to five ($C_nF_{2n+1}SO_3H$, $n \leq 5$) and perfluorocarboxylic acids (PFCA) for a chain length below or equal to six ($C_nF_{2n+1}COOH$, $n \leq 6$). Several PFAS have been shown to be bioaccumulative and toxic, although data are scarce for most PFAS.[4,5] PFAS, particularly perfluoroalkyl acids (PFAA), have become ubiquitous in the environment due to their widespread use and high mobility and persistency, with groundwater concentrations ranging from below quantification limits (typically few ng L^{-1}) to mg L^{-1}, depending on the proximity of contamination sources.[6,7] Effluents from wastewater treatment plants treating municipal wastewater, industrial process water, or landfill leachate are considered major discharge routes of PFAS,[8,9] and removing PFAS from these effluents prior to discharge is an important downstream strategy for preventing continued emissions.

PFAS are mostly not removed with conventional primary and secondary treatment steps for wastewater, although some (typically <50%) adsorption to sludge may occur.[10] On the other hand, precursor PFAS may degrade to PFAA in biological processes, leading to higher PFAA concentrations in effluent than in influent.[11] Existing wastewater treatment technologies that are effective for the removal of PFAS from water include nanofiltration,[12] ion exchange,[13] and adsorption to activated carbon,[14] but these technologies are energetically and financially costly, particularly for complex matrices. Extensive pretreatment is often required, and in the case of ion exchange and granular activated carbon, regeneration of

Received: February 28, 2023
Revised: July 18, 2023
Accepted: July 19, 2023

the sorbent is necessary after approximately every 5000−50,000 bed volumes treated, to prevent breakthrough of especially short-chain PFAS.[15,16] In Switzerland, adding treatment with powdered activated carbon to all conventional municipal wastewater treatment plants was estimated to increase the costs of wastewater treatment by approximately 30%.[17,18]

Recently, foam fractionation has been established as a comparatively inexpensive and environmentally friendly treatment technology capable of achieving competitive PFAS removal.[19−23] Foam fractionation exploits the high surface activity that many PFAS share. It works by introducing air bubbles at the bottom of a water column, to which the surface-active PFAS molecules adsorb. If surfactant concentrations in the water are high enough, a PFAS-enriched foam can subsequently be separated from the liquid phase, resulting in a relatively PFAS-free effluent. The sequestered collapsed foamate is only a small fraction (<1 − 10%)[19,24] of the initial volume and can undergo destructive treatment. Foam fractionation removes long-chain PFAS better than short-chain PFAS because long-chain PFAS have higher air−water sorption coefficients and are thus more surface-active.[21] Removal efficiencies for long-chain PFAS typically exceed 95%, whereas, e.g., the short-chain perfluorobutanoic acid (PFBA) is often not removed at all.[24,25]

Many existing wastewater treatment plants use aeration as part of their treatment train. Often, the formation of foam is observed on the water's surface of such treatment processes, which in the case of biological treatment is typically associated with the presence of filamentous microorganisms.[26] The stability of this foam depends on the presence of three components: air bubbles, surfactants, and hydrophobic particles.[27,28] Certain undesirable bacteria strains may exacerbate foam formation by producing biosurfactants and by partitioning into the foam and thereby preventing foam collapse.[27−29] Generally, excessive foam formation is conceived as problematic, since it complicates process control; the foam may overflow onto surrounding areas, and wind-blown foam or aerosols may lead to spreading of contaminants.[26,29] Conversely, the aim of this study was to investigate whether foam formation could instead be exploited for the integrated removal of PFAS within existing treatment processes.

The study included various wastewater treatment technologies: activated sludge, moving bed biofilm reactor (MBBR), electrocoagulation, and ozonation. Activated sludge is a well-known biological treatment technology for the removal of organic matter and can be extended to include nitrification, denitrification, and biological phosphorus removal.[30] MBBR is a type of suspended biofilm reactor, where biofilm grows on plastic carriers that are kept in suspension in the reaction tank. Typically, MBBRs are used for organic matter removal, nitrification, and denitrification. Electrocoagulation is a physicochemical treatment process where metal cations are introduced into the water using sacrificial anodes in an electrochemical cell.[31] These cations form coagulating complexes that destabilize colloidal particles and adsorb contaminants, which are then easily removed from the water by flotation, settling, or filtration. Finally, ozonation is an oxidation process mostly used as a tertiary treatment for the degradation of organic micropollutants such as pharmaceuticals and biocides.[32]

Specific objectives of this study were to (i) measure PFAS concentrations in foam on the surface of wastewater treatment plants; (ii) use these foam concentrations to assess if PFAS enrichment in the foam leads to measurable PFAS removal, and (iii) evaluate if the enrichment of PFAS in the foam is affected by the treatment process, the general chemistry of the influent water, or the presence of oxidizable precursors.

MATERIALS AND METHODS

Site Selection. Ten full-scale wastewater treatment plants from Sweden, The Netherlands, Belgium, Spain, and Australia where foam formation was observed were included in the project. An overview of these plants is given in Table 1. Plants were selected such that a wide variety of water types, treatment processes, geographical locations, and PFAS concentrations were included. The study focused specifically on processes that did not already have PFAS removal or foam formation as part of their design, i.e., no dissolved air flotation or foam fractionation plants were included. "Wastewater treatment" is used as terminology throughout this paper, but treated water types also included landfill leachate, industrial process water, and contaminated stormwater runoff, in addition to municipal wastewater.

Table 1. Overview of Wastewater Treatment Plants, MBBR = Moving Bed Biofilm Reactor

site	treatment process	water type	location	time of sampling (2022)
(A)	MBBR	landfill leachate	Sweden	August
(B)	MBBR	industrial process water	Sweden	August
(C)	MBBR	municipal wastewater	Sweden	December
(D)	activated sludge	landfill leachate	The Netherlands	November
(E)	activated sludge	landfill leachate	The Netherlands	October
(F)	activated sludge	municipal wastewater[a]	Belgium	September
(G)	activated sludge	municipal wastewater	Spain	September
(H)	activated sludge	municipal wastewater[b]	Australia	September
(I)	electrocoagulation	stormwater runoff from landfill[c]	The Netherlands	September
(J)	ozonation	municipal wastewater	Sweden	December

[a]The influent was sampled before sand filtration instead of right before the activated sludge reactor. [b]The influent to this site contained approximately 30% industrial wastewater. [c]Specifically, the stormwater runoff came from the bottom ash storage area on the landfill.

Sample Collection. From each treatment plant, four 250 mL of grab samples from each of the following matrices were collected into clean high-density polyethylene (HDPE) or polypropylene (PP) bottles for PFAS analysis: the influent to the foaming process (i.e., MBBR, activated sludge, electrocoagulation, or ozonation), the effluent from the foaming process, and water from approximately 1 m under the foam. Additionally, samples from the foam were taken for PFAS analysis, which was collapsed to liquid phase prior to transport, and 1 L of influent to the foaming process was sampled for general chemistry analysis. Foam samples were collected into

https://doi.org/10.1021/acsestengg.3c00091
ACS EST Engg. XXXX, XXX, XXX−XXX

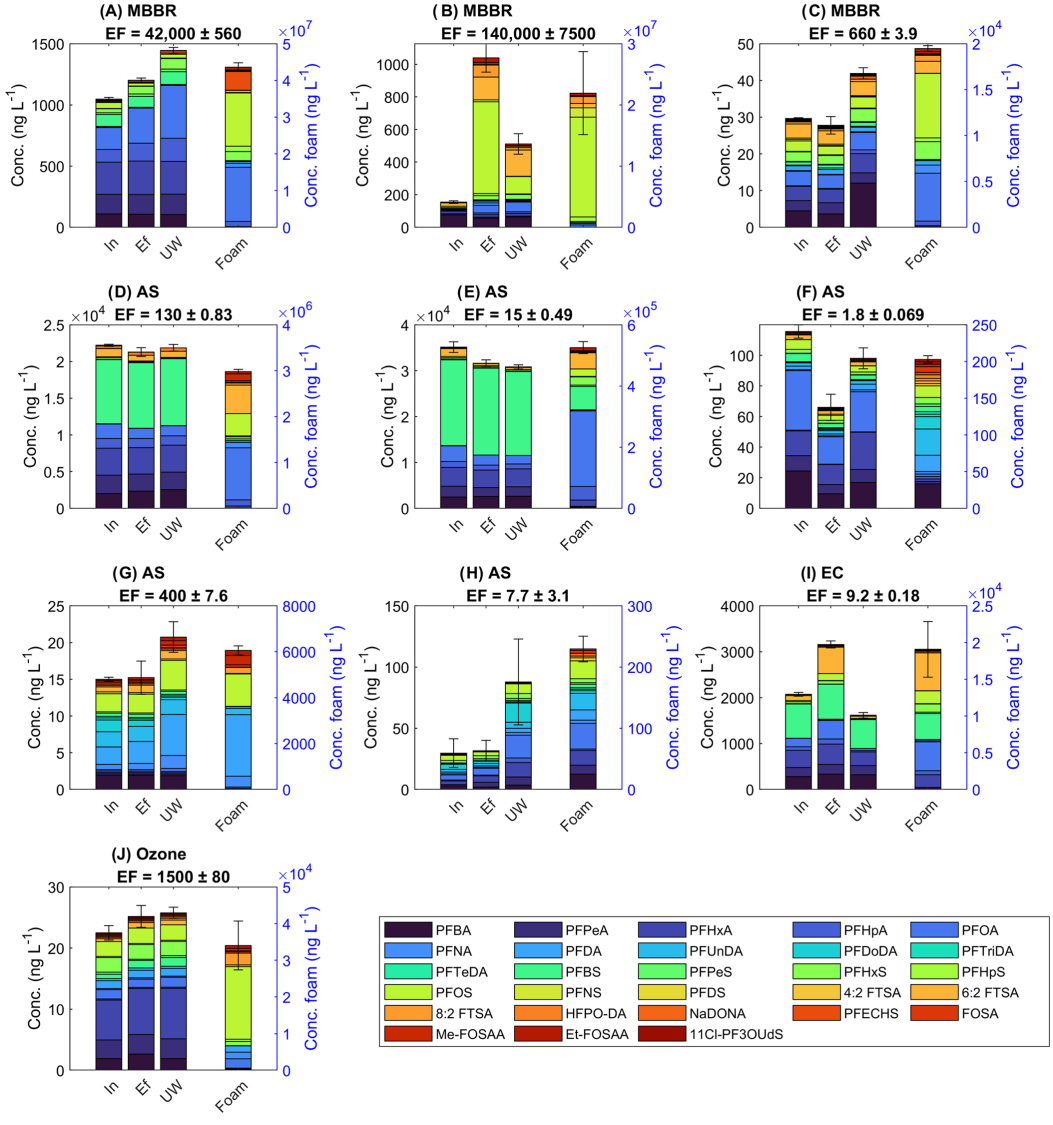

Figure 1. PFAS concentrations (ng L^{-1}) in the influent (In), effluent (Ef), water under the foam (UW), and foamate (Foam) for all treatment plants included in the study (see Table 1, labels of the subplots correspond to the site identifiers). MBBR = moving bed biofilm reactor, AS = activated sludge, EC = electrocoagulation, and Ozone = ozonation. Foamate concentrations are on a different scale, represented by the blue *y*-axis on the right. Titles give the enrichment factor (EF), calculated as per eq 2, with the corresponding standard deviation. Error bars represent the standard deviation (n = 3) over the ∑PFAS concentrations for each sample type. Repeated figures with concentrations below LOQ set to zero or the LOQ, instead of 0.5·LOQ, are given in Figures SI 1 and 2. For the mean concentration data, see Table SI 6.

HDPE or PP containers by scooping up foam from the water surface and were either left to collapse spontaneously or forced to collapse under warm air with a heat gun or by mechanical stirring. The sampled volume of collapsed foam differed per plant, and the volume that was analyzed is given in Table SI 3. The reachability of the foam and the availability of equipment were different for each plant, so the exact equipment used for foam sampling varied between plants as well. Samples from sites (C) to (I) were shipped cooled to the Swedish University of Agricultural Sciences (SLU), Uppsala, Sweden, where they were analyzed in our laboratory. Sites (A) and (B) were located sufficiently close to enable manual transport of the samples. All PFAS samples were stored at ∼4 °C until extraction, which was always done within 2 weeks after arrival

https://doi.org/10.1021/acsestengg.3c00091
ACS EST Engg. XXXX, XXX, XXX−XXX

in the laboratory. General chemistry samples were stored at −20 °C prior to shipment to ALS Scandinavia, Danderyd, Sweden, for analysis of metals, fluoride, chloride, phosphorus, nitrogen, and total organic carbon (TOC) concentrations and conductivity, pH, and turbidity.

Analysis. Three of the water samples for each matrix type (influent, effluent, and water under the foam) were filtered, extracted, and analyzed for the concentrations of 29 PFAS (for full names, see Table SI 1), using a previously established method.[24] In brief, 125 mL samples were sonicated, filtered through glass microfiber filters (Whatman, 0.7 μm pore size, China), and spiked with 5 ng absolute each of 20 internal standards,[24] and solid-phase extraction (SPE) was performed using Oasis WAX cartridges (6 mL, 150 mg, 30 μm, Waters, Ireland). Extracts were analyzed on a SCIEX Triple Quad 3500 ultraperformance liquid chromatography−tandem mass spectrometry (UPLC-MS/MS) system, using scheduled multiple reaction monitoring (sMRM) mode with negative electrospray ionization. An eleven-point calibration curve was used, with concentrations between 0.05 and 900 ng mL^{-1}, see SI Section 1.2. Because of this wide concentration range, seven PFAS were quantified based on quadratic calibration curves instead of linear, see SI Table 2. The quantification was done according to the isotope dilution method and using the IS, as described previously.[24] For compounds with linear as well as branched isomers, only summed concentrations were measured. Median relative standard deviations of the triplicates' ∑PFAS concentrations were 2.6, 7.7, 3.7, and 3.5% for all influent, effluent, water under the foam, and foam samples, respectively.

To minimize matrix effects and stay in the concentration range of the calibration curve, foamate samples were diluted prior to filtration and extraction. Depending on the aqueous PFAS concentrations at the corresponding treatment plant, a foamate volume between 0.25 and 10 mL was diluted with Milli-Q water to a total volume of 50 mL. The exact volume of foamate that was used for each treatment plant is given in Table SI 3. For site (A), a foamate dilution series was analyzed to confirm that the reported concentrations were independent of the volume used. These results are given in Table SI 4, and quality control results of spiked samples are given in Table SI 5. All foamate concentrations are given per unit volume of collapsed foam, i.e., in the liquid phase.

On the fourth sample for each sample type, i.e., influent, effluent, water under the foam, and foamate, a total oxidizable precursor (TOP) assay was performed using a method developed by Houtz and Sedlak.[33] The TOP assay is a tool to quantify concentrations of precursors, which can be transformed to PFAA upon oxidation.[33,34] In brief, 2 g of potassium persulfate ($K_2S_2O_8$, Sigma-Aldrich) and 1.9 mL of 10 M sodium hydroxide (NaOH, Sigma-Aldrich) were added to each 125 mL sample. For the 50 mL diluted foamate samples, 0.8 g of $K_2S_2O_8$ and 0.76 mL of 10 M NaOH were used instead. Samples were placed in a water bath at 80 °C for 6 h, cooled in ice, and gradually adjusted to a pH of 6−8 by adding 30% hydrogen chloride (HCl, Merck, Germany). Filtration, SPE, and UPLC-MS/MS analysis were subsequently done, as described above.

Seven laboratory blanks (cartridges preconditioned, IS-spiked, and eluted without the addition of any sample), five Milli-Q blanks (50 mL of Milli-Q extracted and analyzed as normal samples), and seven TOP blanks (125 mL of Milli-Q on which a TOP assay was performed) were included. Method limits of quantification (LOQs) were calculated based on the detected concentrations in the blanks, see SI Section 1.1, and are given in Table SI 1. For all PFAS, LOQs ranged between 0.4 and 4 ng L^{-1} for the water and between 5 and 2000 ng L^{-1} in the foamate.

Data Handling. All data handling, plotting, and statistical analyses were done in Matlab, version 2020b. PFAS removal efficiencies (RE) were calculated as per eq 1, with C_{In} and C_{Ef} being the mean concentration of the influent and effluent samples, respectively (n = 3 for each). PFAS enrichment factors (EF) were calculated using eq 2, with C_{foam} being the mean concentration foamate samples (n = 3).

$$\mathrm{RE} = \left(1 - \frac{C_{Ef}}{C_{In}}\right) \times 100\% \tag{1}$$

$$\mathrm{EF} = \frac{C_{foam}}{C_{In}} \tag{2}$$

PFAS concentrations and enrichment factors were log-transformed prior to any correlation analyses. When a PFAS was not detected above the LOQ in any of the samples at a site, its concentration was set to zero for all samples from that site. When a PFAS was detected in at least one sample from a site, concentrations below the LOQ were set to half the LOQ unless stated otherwise. To illustrate the range of uncertainty caused by the inclusion of non-detect concentrations, certain figures have been repeated in the SI, with non-detect concentrations set to zero or the LOQ instead (Figures SI 1 and 2 and 4−7). For the correlation analysis on the metal, chloride, and fluoride concentrations, concentrations below the LOQ were set to half the LOQ. Any correlations with mercury were ignored because of the high proportion (50%) of non-detects.

RESULTS AND DISCUSSION

∑PFAS Removal Due to Foam Partitioning. Out of the 29 targeted PFAS, all except 9Cl-PF3ONS were detected in at least one sample. As visualized in Figure 1, the concentrations and compositions of the 28 detected PFAS varied widely between the different treatment plants, but PFAS concentrations were consistently higher in the foamate than in the influent to the treatment process. The only treatment plant with considerable removal of ∑PFAS from influent to effluent was site F, the activated sludge municipal WWTP in Belgium, with a mean ∑PFAS removal of 43%. However, this was coincidentally also the plant with the lowest ∑PFAS enrichment in the foam, and the PFAS removal from influent to the water under the foam was only 15%. Therefore, the PFAS removal here was probably not caused by accumulation of PFAS in the foam but by PFAS adsorption to sludge.

In all other plants, the ∑PFAS concentrations from influent to effluent were either unchanged (<10% difference, sites C, D, E, G, and H) or increased (sites A, B, I, and J). For site J, the 13% higher PFAS concentrations in the effluent may be due to precursor degradation, since increased PFAS concentrations were measured in the influent after the TOP assay (see Figure SI 3), and the ozonation treatment used at this plant may result in precursor degradation.[35] Additionally, for all sites, variability in the treated water may have resulted in higher effluent than influent concentrations, since concentrations were based on grab samples during one occasion rather than time-integrated samples. The effluent water at site B was still

https://doi.org/10.1021/acsestengg.3c00091
ACS EST Engg. XXXX, XXX, XXX−XXX

rather foamy, so it is possible that the effluent samples included some foam, leading to the 570% higher effluent concentrations compared to the influent. This explanation is especially probable considering the extremely high mean ∑PFAS concentrations in the foamate at site B of 22 mg L^{-1}.

Electrocoagulation has been found to remove PFAS on a laboratory scale, which is generally believed to occur because PFAS adsorb to the formed metal flocs.[36,37] It has even been shown that PFAS partitioning into the foam formed during electrocoagulation plays a role in the removal mechanism, particularly when the electrocoagulation process is operated at a high current density.[38] In the current study, no ∑PFAS removal from influent to effluent was found in plant I, a full-scale electrocoagulation reactor with iron electrodes (Figure 1I). PFAS removal by sorption to the iron flocs was not found either, since the effluent concentrations were higher than the influent concentrations.

Overall, while there is clear evidence of PFAS enrichment in the foam, this mechanism did not seem to result in considerable ∑PFAS removal from the influent in any of the investigated treatment plants. A reason for this could be that the foam was not actually removed at any of the plants, but instead left on the water surface to eventually collapse back into the effluent. To test this hypothesis, water under the foam was also sampled at all plants, and >10% ∑PFAS removal from the influent to the water under the foam was found at sites E (12%) and I (22%), as well as the aforementioned site F (15%). While these removal efficiencies are still not very high, they give some indication that removing the foam from the water surface may increase the ∑PFAS removal efficiency, leading to lower concentrations in the water under the foam as well as the effluent.

An additional explanation for the lack of ∑PFAS removal from influent to effluent, despite the high enrichment factors, is the possible discrepancy in retention time between foam and water. All treatment plants included in the study were in continuous operation, but none were regularly skimming foam from the surface. Accordingly, particularly in plants where a high buildup of foam was observed, the high PFAS concentrations in the foam probably reflected the PFAS removal over multiple hydraulic retention times (HRT). Because the foam volumes or flow rates were not measured, it is impossible to quantify the importance of this source of uncertainty. Nonetheless, for plant B, which had the highest enrichment factor, the dosing of anti-foaming agent was stopped less than one HRT before sampling the foam, and foam buildup occurred very quickly. Thus, while long-term accretion of PFAS in the foam layer may have somewhat distorted the measured enrichment factors, it was unlikely to cause the high enrichment measured at all plants.

Long-Chain PFAA Removal Due to Foam Partitioning. When focusing on the total concentration of long-chain PFAA only, instead of on ∑PFAS concentrations, some removal from influent to effluent was measured at sites C (7%), D (37%), E (46%), and H (12%), in addition to the aforementioned site F (46%). Specifically, at site D, mean perfluorooctane sulfonic acid (PFOS) and perfluorooctanoic acid (PFOA) removal efficiencies were 58 and 30%, respectively. At site E, these were 76% and 36%. For these two sites (D and E), similar long-chain PFAA removal efficiencies were obtained from the influent to the water under the foam, indicating that foam partitioning contributes to the removal mechanism. For site I, an even higher mean ∑long-chain PFAA removal from influent to the water under the foam of 74% was measured, with PFOS and PFOA removal at 57 and 76%, respectively. All of these sites treated water with comparatively high PFAS concentrations, which may have contributed to the measurable concentration decrease of long-chain PFAA.

Attributing the decreased effluent concentrations of long-chain PFAA entirely to accumulation in foam is not realistic. Sites D and E were both activated sludge plants, and since long-chain PFAA are known to be susceptible to adsorption to sludge, this is another probable mechanism for the removal of these compounds. However, since sludge concentrations and sludge production rates were not measured in this study, it was impossible to quantify the relative contribution of PFAS adsorption to sludge. The extent of removal with sludge depends on a combination of operational and solution parameters, e.g., solid retention time, pH, and wastewater composition. In the literature, reported PFAS removal due to adsorption to sludge ranges from zero to nearly full removal, although values > 80% were only achieved in processes with extremely high sludge concentrations and retention times.[10] Estimating the contribution of sludge adsorption to the total removal is further complicated by the degradation of precursors. In fact, increased PFAA concentrations in the effluent are more commonly reported than decreased concentrations, and analytical techniques such as the TOP assay have only recently become common.[10,34]

Implementing Foam Stimulation to Increase Removal. While no evidence of ∑PFAS removal due to foam partitioning was found at any of the plants, there were indications that PFAS removal may occur when foam formation would be stimulated rather than prevented. Lower ∑PFAS concentrations were measured in the water under the foam for some plants, long-chain PFAA were occasionally removed to some extent, and the ∑PFAS concentrations in the foamate were up to 10^5 times higher than those in the influent. Particularly, these extremely high enrichment factors from influent to foam indicate promise for using foam formation as an integrated removal mechanism. Although PFAS concentrations in the foamate were very high, the total volume of foam compared to the volume of influent water was probably negligible from a mass balance perspective. The reported concentrations were measured in the collapsed, liquid foamate. Actual foam has a very low density, and the foamate thus constitutes only a very small fraction of the treated influent volume.

Foam control strategies are common at wastewater treatment plants, particularly chemical methods, such as dosing of anti-foaming agents or disinfectants.[26,39] Additionally, design decisions may be made to minimize foam formation, e.g., lowering the sludge retention time in activated sludge, operating at lower aeration rates, or implementing anoxic, anaerobic, or aerobic selector systems.[26] Such selector systems aim to provide unfavorable conditions for the growth of foam-causing filamentous microorganisms.[39] If tanks are mechanically stirred, this may also lead to foam collapse instead of buildup. When foam formation is to be exploited as a PFAS removal technology, foam removal devices that skim foam from the water surface should be installed instead. Designing the treatment process to stimulate foam formation rather than prevent it could possibly enhance the removal efficiency significantly as compared to the values reported here.

An attempt to quantify the increase in foam formation that would be required for the significant removal of long-chain

https://doi.org/10.1021/acsestengg.3c00091
ACS EST Engg. XXXX, XXX, XXX−XXX

PFAA is presented in SI Section 2.4. The derivation of the equation used for this quantification, eq SI 1, relied on several assumptions.[40] Most importantly, adsorption to sludge and reactive transformation of PFAA were ignored, and the foam wetness was assumed to remain constant with increasing foam fraction, i.e., the ratio of foamate flow over influent flow. In other words, the increase in foamate flow was assumed to be entirely due to an increase in foam film surface area available for PFAS sorption, rather than an increase in liquid fraction of the foam. The need for these assumptions inherently compromises the reliability of the analysis, and the results should be seen as rough estimations only, but they indicated that high removal of long-chain PFAA with foam might be possible at certain plants. Specifically, a sevenfold increase in foam fraction could result in a ∑long-chain PFAA removal of ∼80% at sites D and E. Additionally, at site J, a removal of >99% would possibly require a foam fraction of only 3%. More detailed results are given in Figure SI 6.

Enrichment Factors for Individual PFAS. From the literature on foam fractionation, it is known that long-chain PFAS are more susceptible to foam partitioning than short-chain PFAS.[24,25,41] As visualized in Figure 2, the enrichment

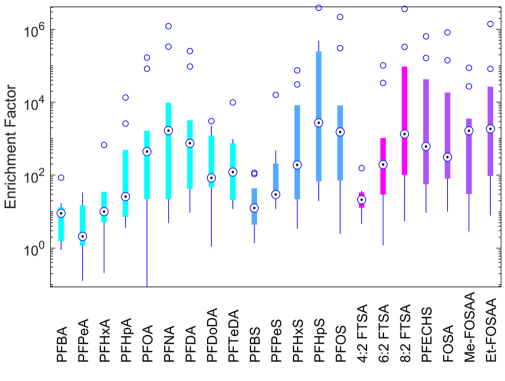

Figure 2. Box plot of enrichment factors across the different sites for individual PFAS. PFCA are colored light blue, PFSA dark blue, FTSA magenta, and the other PFAS purple. Compounds of the same class have an increasing molecular weight from left to right. Only PFAS that were detected at at least eight of the sites were included, i.e., $8 \leq n \leq 10$. The bottom and top of each box represent the 25th to the 75th percentile, respectively. The black dot encircled in blue represents the median, and whiskers go to the most extreme data points, excluding outliers. Outliers (blue circles) are values more than 1.5 interquartile range from the bottom or top of the box. Full names of all PFAS are given in Table SI 1.

factors found across all treatment plants included in this study were indeed generally higher for longer-chained compounds. Nonetheless, the spread in enrichment factor per PFAS was very wide. For example, the enrichment factor of perfluoroheptane sulfonic acid (PFHpS) ranged over six orders of magnitude. The study included a variety of water matrices, treatment processes, and plant designs, and PFAS, dissolved solids, and organic carbon concentrations also varied widely between the ten sites. The density of the foam was not measured but was observed to vary between the plants. Because of all of these changing variables, it is unsurprising that a high variability in the enrichment factors was found.

Effect of Treatment Process and Water Type. Over the ten treatment plants, ∑PFAS concentrations in the influent, effluent, and water under the foam correlated strongly with each other (all $r > 0.97$, all $p < 10^{-5}$). Conversely, foamate ∑PFAS concentrations only correlated significantly with effluent concentrations ($r = 0.63$, $p = 0.049$) but not with ∑PFAS concentrations in the influent or the water under the foam. Enrichment factors correlated significantly with foamate ∑PFAS concentrations ($r = 0.76$, $p = 0.01$) but not with ∑PFAS concentrations in any of the other sample types. Moreover, enrichment factors did not correlate significantly with the fraction of short-chain or long-chain PFAA of the influent ∑PFAS concentrations (all $p > 0.05$). These correlations indicate that the magnitude of PFAS enrichment in foam is relatively independent of the aqueous PFAS concentrations and composition profiles, but instead depends on foam characteristics. The correlations described here were similar for all inclusion methods of non-detect concentrations.

Figure 3a shows the ∑PFAS enrichment factor of all sites grouped by treatment process. MBBRs appear particularly effective at enriching PFAS in foam, with significantly higher enrichment factors than activated sludge processes (1-way ANOVA, $p = 0.04$, followed by Tukey's honestly significant difference procedure). This difference was not significant ($p > 0.05$) when all non-detect concentrations were set to zero (see also Figure SI 6). Possibly, this higher enrichment is because MBBRs do not contain suspended sludge, contrary to activated sludge processes. The presence of suspended sludge may have decreased the PFAS enrichment by adsorbing the PFAS prior to its incorporation in the foam. Similarly, the foam from activated sludge plants generally contained a lot of floating sludge. This floating sludge layer may have prevented the foam from building up, thereby preventing the formation of dry, highly PFAS-enriched foam.

The ozonation plant (J) also had a very high mean enrichment factor of 1500. In a study by Dai et al., higher PFAS removal efficiencies were found with ozonated air fractionation than with conventional foam fractionation.[42] Dai et al. hypothesized that an increased PFAS affinity for a gas bubble surrounded by hydroxyl radicals formed in the ozonation process boosted the accumulation of PFAS in the ozonated foam, due to the affinity of the hydrophilic PFAS head groups to these radicals. Possibly, this effect also played a role in the high enrichment measured in the foam from site J. Additionally, precursor degradation may have increased the foam concentrations even further.[34] The influent, effluent, and water under the foam concentrations all increased after the TOP assay, but the foamate concentration did not (Figure SI 3). Since the foam is formed by being in contact with ozone bubbles, the vast majority of the precursors had probably already degraded in the foam, thereby increasing the measured target PFAS concentrations. In contrast, the influent still contained precursors, which were not measured in the target PFAS analysis. When considering the concentrations after the TOP assay, the enrichment factor was thus only 620 instead of 1500. A similar effect may have played a role at sites C, G, and H, which also had lower enrichment factors after the TOP assay, but here, precursors would have been oxidized by oxygen or biodegradation rather than ozone.

Effect of General Chemistry. There were no clear differences in enrichment factor between the different water types, as illustrated in Figure 3b. Moreover, no significant correlations between the enrichment factor and any of the

https://doi.org/10.1021/acsestengg.3c00091
ACS EST Engg. XXXX, XXX, XXX−XXX

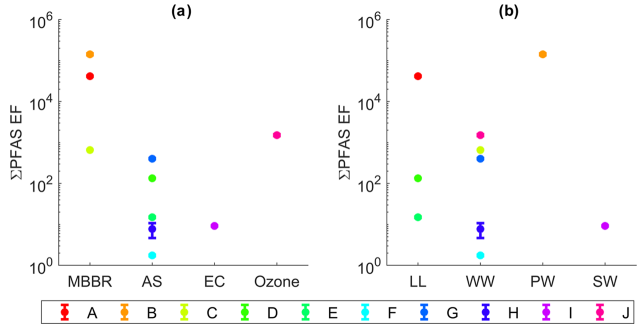

Figure 3. ∑PFAS enrichment factors (EF) grouped by (a) treatment process and (b) water type. MBBR = moving bed biofilm reactor, AS = activated sludge, EC = electrocoagulation, Ozone = ozonation, LL = landfill leachate, WW = wastewater, PW = process water, and SW = stormwater runoff from landfill bottom ash collection site. The letters in the legend correspond to the site identifiers given in Table 1. Error bars represent the standard deviation (sd) within the EF for each plant (n = 3 for foamate as well as influent concentrations) but are difficult to see for all plants except H because the sd was relatively small. Repeated figures with concentrations below the LOQ set to zero or the LOQ, instead of 0.5·LOQ, are given in Figures SI 7 and 8.

tested general chemistry parameters were found (Pearson's r, all $p > 0.05$). Removal efficiencies of ∑PFAS ($r = 0.67$, $p = 0.049$) and ∑long-chain PFAS ($r = 0.77$, $p = 0.02$) only correlated significantly with total phosphorus concentrations but not with any of the other general chemistry parameters. The removal efficiencies from site B were excluded from the correlation analyses with general chemistry, since these were strongly negative (see Figure 1B) and thus not realistic. Altogether, this lack of strong correlations indicates that PFAS enrichment and removal were mostly independent of the measured general chemistry parameters in the influent. This differs from foam fractionation results reported in the literature, where higher concentrations of certain metal ions and higher conductivity were found to correlate with a higher PFAS removal.[21,22] A full overview of the general chemistry results is given in Table SI 7.

Role of Precursors. Precursors degrade to PFCA in the TOP assay,[33] so the fraction of PFCA is expected to increase after the TOP assay. The fraction of PFCA in the total PFAS concentrations was indeed higher after the TOP assay for 90% of the samples (total n = 40). The only samples with a decreased fraction of PFCA were the effluents of site B (−19%), E (−7%), and H (−4%) and the water under the foam of site F (−2%). At site B, PFOS concentrations in the effluent nearly doubled after the TOP assay (see Figures 1 and SI 3), which caused a decreased fraction of PFCA after the TOP assay. Probably, PFOS precursors were present at this site in high concentrations. For the remaining sites, the relative decrease in PFCA concentrations was probably due to measurement uncertainties combined with generally low precursor concentrations in these water types.

As mentioned previously, lower enrichment factors were measured after the TOP assay at sites C, G, H, and J, probably because of precursor degradation in the foam at the treatment site. In contrast, higher enrichment factors were measured after the TOP assay at sites B (22% increase), D (39%), E (44%), F (260%), and I (53%) (see Figures 1 and SI 3). When more precursors are present in the foam than in the influent, precursors are enriched in the foam, and a higher enrichment factor will be measured after the TOP assay. Accordingly, these higher enrichment factors indicate that precursors were enriched in the foam at sites B, D, E, F, and I. Since some well-known precursors are used as surfactants (e.g., perfluoroalkyl phosphonic acids (PFPAs) and polyfluoroalkyl phosphoric acid esters (PAPs)),[3,33] it is unsurprising that oxidizable precursors were susceptible to enrichment in the foam.

■ ENVIRONMENTAL IMPLICATIONS

This study aimed to evaluate the potential of using existing wastewater treatment plants as foam fractionators for the removal of PFAS. The results were twofold. On the one hand, no removal of ∑PFAS was measured at any of the investigated sites that could be attributed to foam partitioning. On the other hand, the high enrichment factors of PFAS in foam show promise for combining conventional wastewater treatment with foam fractionation, and >35% removal of long-chain PFAA was measured at two of the investigated sites. A preliminary mass balance analysis showed that >80% long-chain PFAA removal with foam may be achievable at reasonable (<5%) foam fractions in certain plants. Full-scale attempts to implement foam skimming are required to assess the viability of integrated foam fractionation for PFAS removal and to see if higher removal efficiencies can be achieved.

Despite its exploratory nature, the study showed that MBBRs may be particularly effective for the separation of PFAS in foam, but artificially increasing the foam formation would be necessary to achieve quantifiable PFAS removal. Combining stimulated foam formation with full-scale foam removal in an MBBR would thus be a fruitful area for future work. Additionally, it would be interesting to investigate if this high PFAS enrichment in foam is also found in other compact biofilm-based processes, such as aerobic granular sludge (Nereda)[43] and membrane bioreactors (MBRs).[44,45] Finally, further research should include measurement of foam characteristics to better understand the role these variables play in the enrichment of PFAS. Various methods have been developed to quantifiably evaluate foam on wastewater, such as measuring foam rating, volume, foam power, foam stability, and scum index,[46] and these may generate further insight into what determines the level of PFAS enrichment in foam.

A downside of using existing plants for the removal of PFAS, rather than specifically designed systems, is that the plant

https://doi.org/10.1021/acsestengg.3c00091
ACS EST Engg. XXXX, XXX, XXX−XXX

performance in terms of chemical oxygen demand (COD), nutrient, or micropollutants removal must not be compromised. Each process investigated in this study was designed for a specific treatment objective, and it should be ensured that artificially promoting foam formation for the removal of PFAS does not influence the achievement of that objective. This may limit process options such as modifying the aeration rate or dosing surfactants that are available in traditional foam fractionation for the removal of PFAS.

In addition to the implications related to integrated PFAS removal, the findings presented here also have important implications for sampling strategies. When influent and effluent to a wastewater treatment process are sampled to determine PFAS concentrations, the inclusion or exclusion of foam from the sample may affect the measured concentrations significantly. This is particularly important when grab samples are taken from the water surface, as this increases the likelihood of including foam in the sample, thus overestimating the PFAS concentrations. There is, therefore, a definite need for standardized sampling methods when effluent concentrations are measured for checking the compliance with permitted concentrations.

■ ASSOCIATED CONTENT

Supporting Information

The Supporting Information is available free of charge at https://pubs.acs.org/doi/10.1021/acsestengg.3c00091.

Overview of LOQs; volumes used for the extraction of foamate and quality control results; Figures 1 and 3 repeated with alternative handling of concentrations below the LOQ; mean PFAS concentrations; TOP assay results; approximate quantification of the required foam fraction for increased PFAS removal and general chemistry results (PDF)

■ AUTHOR INFORMATION

Corresponding Author

Sanne J. Smith − *Department of Aquatic Sciences and Assessment, Swedish University of Agricultural Sciences (SLU), SE-750 07 Uppsala, Sweden;* orcid.org/0000-0002-3487-0528; Email: sanne.smith@slu.se

Authors

Chantal Keane − *Queensland Alliance for Environmental Health Sciences, University of Queensland, Woolloongabba, QLD 4102, Australia;* orcid.org/0000-0003-1003-3896

Lutz Ahrens − *Department of Aquatic Sciences and Assessment, Swedish University of Agricultural Sciences (SLU), SE-750 07 Uppsala, Sweden;* orcid.org/0000-0002-5430-6764

Karin Wiberg − *Department of Aquatic Sciences and Assessment, Swedish University of Agricultural Sciences (SLU), SE-750 07 Uppsala, Sweden*

Complete contact information is available at: https://pubs.acs.org/10.1021/acsestengg.3c00091

Author Contributions

CRediT: **Sanne J. Smith** conceptualization, data curation, formal analysis, investigation, visualization, writing-original draft; **Chantal Keane** data curation, methodology, writing-review & editing; **Lutz Ahrens** conceptualization, funding acquisition, writing-review & editing; **Karin Wiberg** conceptualization, supervision, writing-review & editing.

Notes

The authors declare no competing financial interest.

■ ACKNOWLEDGMENTS

This project has received funding from the European Union's Horizon 2020 research and innovation program under the Marie Skłodowska-Curie grant agreement No. 860665 (PERFORCE3). The authors would further like to thank the personnel from all participating wastewater treatment plants for their assistance in the sample collection: Sofia Bjälkefur Seroka (Uppsala Vatten & Avfall AB), Robert Sehlén (Tekniska Verken I Linköping AB), Joakim Thorstensson (Eskilstuna Strängnäs Energi & Miljö), Marthe de Graaff (Evides Industriewater), John Smit (NV Afvalzorg Holding), Lennert Dockx (Aquafin), Robert Bijlsma and Elena Pitarch (Universitat Jaume I), Santiago Querol, Ernesto Santateresa, Nuria Zamorano and Elena Zuriaga (Sociedad de Fomento Agrícola Castellonense), and everyone else who preferred to remain anonymous.

■ REFERENCES

(1) Cousins, I. T.; Dewitt, J. C.; Glüge, J.; Goldenman, G.; Herzke, D.; Lohmann, R.; Ng, C. A.; Scheringer, M.; Wang, Z. The High Persistence of PFAS Is Sufficient for Their Management as a Chemical Class. *Environ. Sci.: Processes Impacts* **2020**, *22*, 2307−2312.

(2) Wang, Z.; Buser, A. M.; Cousins, I. T.; Demattio, S.; Drost, W.; Johansson, O.; Ohno, K.; Patlewicz, G.; Richard, A. M.; Walker, G. W.; White, G. S.; Leinala, E. A New OECD Definition for Per- And Polyfluoroalkyl Substances. *Environ. Sci. Technol.* **2021**, *55*, 15575−15578.

(3) Buck, R. C.; Franklin, J.; Berger, U.; Conder, J. M.; Cousins, I. T.; Voogt, P. De; Jensen, A. A.; Kannan, K.; Mabury, S. A.; van Leeuwen, S. P. J. Perfluoroalkyl and Polyfluoroalkyl Substances in the Environment: Terminology, Classification, and Origins. *Integr. Environ. Assess. Manage.* **2011**, *7*, 513−541.

(4) Wang, Z.; Dewitt, J. C.; Higgins, C. P.; Cousins, I. T. A Never-Ending Story of Per- and Polyfluoroalkyl Substances (PFASs)? *Environ. Sci. Technol.* **2017**, *51*, 2508−2518.

(5) Evich, M. G.; Davis, M. J. B.; McCord, J. P.; Acrey, B.; Awkerman, J. A.; Knappe, D. R. U.; Lindstrom, A. B.; Speth, T. F.; Tebes-Stevens, C.; Strynar, M. J.; Wang, Z.; Weber, E. J.; Henderson, W. M.; Washington, J. W. Per- and Polyfluoroalkyl Substances in the Environment. *Science* **2022**, *375*, No. eabg9065.

(6) Ahrens, L. Polyfluoroalkyl Compounds in the Aquatic Environment: A Review of Their Occurrence and Fate. *J. Environ. Monit.* **2011**, *13*, 20−31.

(7) Johnson, G. R.; Brusseau, M. L.; Carroll, K. C.; Tick, G. R.; Duncan, C. M. Global Distributions, Source-Type Dependencies, and Concentration Ranges of per- and Polyfluoroalkyl Substances in Groundwater. *Sci. Total Environ.* **2022**, *841*, No. 156602.

(8) Clara, M.; Scheffknecht, C.; Scharf, S.; Weiss, S.; Gans, O. Emissions of Perfluorinated Alkylated Substances (PFAS) from Point Sources - Identification of Relevant Branches. *Water Sci. Technol.* **2008**, *58*, 59−66.

(9) Benskin, J. P.; Li, B.; Ikonomou, M. G.; Grace, J. R.; Li, L. Y. Per- and Polyfluoroalkyl Substances in Landfill Leachate: Patterns, Time Trends, and Sources. *Environ. Sci. Technol.* **2012**, *46*, 11532−11540.

(10) Lenka, S. P.; Kah, M.; Padhye, L. P. A Review of the Occurrence, Transformation, and Removal of Poly- and Perfluoroalkyl Substances (PFAS) in Wastewater Treatment Plants. *Water Res.* **2021**, *199*, No. 117187.

(11) Ahrens, L.; Bundschuh, M. Fate and Effects of Poly- and Perfluoroalkyl Substances in the Aquatic Environment: A Review. *Environ. Toxicol. Chem.* **2014**, *33*, 1921−1929.

(12) Franke, V.; McCleaf, P.; Lindegren, K.; Ahrens, L. Efficient Removal of Per- And Polyfluoroalkyl Substances (PFASs) in Drinking Water Treatment: Nanofiltration Combined with Active Carbon or Anion Exchange. *Environ. Sci. Water Res. Technol.* **2019**, *5*, 1836−1843.
(13) Schuricht, F.; Borovinskaya, E. S.; Reschetilowski, W. Removal of Perfluorinated Surfactants from Wastewater by Adsorption and Ion Exchange — Influence of Material Properties, Sorption Mechanism and Modeling. *J. Environ. Sci.* **2017**, *54*, 160−170.
(14) Vu, C. T.; Wu, T. Recent Progress in Adsorptive Removal of Per- and Poly-Fluoroalkyl Substances (PFAS) from Water/Wastewater. *Crit. Rev. Environ. Sci. Technol.* **2020**, 90−129.
(15) McCleaf, P.; Englund, S.; Östlund, A.; Lindegren, K.; Wiberg, K.; Ahrens, L. Removal Efficiency of Multiple Poly- and Perfluoroalkyl Substances (PFASs) in Drinking Water Using Granular Activated Carbon (GAC) and Anion Exchange (AE) Column Tests. *Water Res.* **2017**, *120*, 77−87.
(16) Franke, V.; Ullberg, M.; McCleaf, P.; Wålinder, M.; Köhler, S. J.; Ahrens, L. The Price of Really Clean Water: Combining Nanofiltration with Granular Activated Carbon and Anion Exchange Resins for the Removal of Per- And Polyfluoroalkyl Substances (PFASs) in Drinking Water Production. *ACS ES&T Water* **2021**, *1*, 782−795.
(17) Eggen, R. I. L.; Hollender, J.; Joss, A.; Schärer, M.; Stamm, C. Reducing the Discharge of Micropollutants in the Aquatic Environment: The Benefits of Upgrading Wastewater Treatment Plants. *Environ. Sci. Technol.* **2014**, *48*, 7683−7689.
(18) Margot, J.; Kienle, C.; Magnet, A.; Weil, M.; Rossi, L.; de Alencastro, L. F.; Abegglen, C.; Thonney, D.; Chèvre, N.; Schärer, M.; Barry, D. A. Treatment of Micropollutants in Municipal Wastewater: Ozone or Powdered Activated Carbon? *Sci. Total Environ.* **2013**, *461*−*462*, 480−498.
(19) Meng, P.; Deng, S.; Maimaiti, A.; Wang, B.; Huang, J.; Wang, Y.; Cousins, I. T.; Yu, G. Efficient Removal of Perfluorooctane Sulfonate from Aqueous Film-Forming Foam Solution by Aeration-Foam Collection. *Chemosphere* **2018**, *203*, 263−270.
(20) Burns, D. J.; Stevenson, P.; Murphy, P. J. C. PFAS Removal from Groundwaters Using Surface-Active Foam Fractionation. *Remediation* **2021**, *31*, 19−33.
(21) Buckley, T.; Karanam, K.; Xu, X.; Shukla, P.; Firouzi, M.; Rudolph, V. Effect of Mono- and Di-Valent Cations on PFAS Removal from Water Using Foam Fractionation − A Modelling and Experimental Study. *Sep. Purif. Technol.* **2022**, *286*, No. 120508.
(22) Smith, S. J.; Lewis, J.; Wiberg, K.; Wall, E.; Ahrens, L. Foam Fractionation for Removal of Per- and Polyfluoroalkyl Substances: Towards Closing the Mass Balance. *Sci. Total Environ.* **2023**, *871*, No. 162050.
(23) Buckley, T.; Karanam, K.; Han, H.; Vo, H. N. P.; Shukla, P.; Firouzi, M.; Rudolph, V. Effect of Different Co-Foaming Agents on PFAS Removal from the Environment by Foam Fractionation. *Water Res.* **2023**, *230*, No. 119532.
(24) Smith, S. J.; Wiberg, K.; McCleaf, P.; Ahrens, L. Pilot-Scale Continuous Foam Fractionation for the Removal of Per- and Polyfluoroalkyl Substances (PFAS) from Landfill Leachate. *ACS ES&T Water* **2022**, *2*, 841−851.
(25) McCleaf, P.; Kjellgren, Y.; Ahrens, L. Foam Fractionation Removal of Multiple Per- and Polyfluoroalkyl Substances from Landfill Leachate. *AWWA Water Sci.* **2021**, *3*, No. e1238.
(26) Tipping, B. P. J.; Member, C. Foaming in Activated-Sludge Processes: An Operator's Overview. *Water Environ. J.* **1995**, *9*, 281−289.
(27) Heard, J.; Harvey, E.; Johnson, B. B.; Wells, J. D.; Angove, M. J. The Effect of Filamentous Bacteria on Foam Production and Stability. *Colloids Surf., B* **2008**, *63*, 21−26.
(28) Petrovski, S.; Dyson, Z. A.; Quill, E. S.; McIlroy, S. J.; Tillett, D.; Seviour, R. J. An Examination of the Mechanisms for Stable Foam Formation in Activated Sludge Systems. *Water Res.* **2011**, *45*, 2146−2154.
(29) Stratton, H. M.; Seviour, R. J.; Soddell, J. A.; Blackall, L. L.; Muip, D. The Opportunistic Pathogen Nocardia Farcinica Is a Foam-Producing Bacterium in Activated Sludge Plants. *Lett. Appl. Microbiol.* **1996**, *22*, 342−346.
(30) la Cour Jansen, J.; Arvin, E.; Henze, M.; Harremoës, P. *Wastewater Treatment - Biological and Chemical Processes*, 4th ed.; Kristoffersen, P. B., Ed.; Polyteknisk Forlag, 2019.
(31) Kabdaşlı, I.; Arslan-Alaton, I.; Ölmez-Hancı, T.; Tünay, O. Electrocoagulation Applications for Industrial Wastewaters: A Critical Review. *Environ. Technol. Rev.* **2012**, *1*, 2−45.
(32) Derco, J.; Gotvajn, A. Ž.; Čižmárová, O.; Dudáš, J.; Sumegová, L.; Simovičová, K. Removal of Micropollutants by Ozone-Based Processes. *Processes* **2021**, *9*, No. 1013.
(33) Houtz, E. F.; Sedlak, D. L. Oxidative Conversion as a Means of Detecting Precursors to Perfluoroalkyl Acids in Urban Runoff. *Environ. Sci. Technol.* **2012**, *46*, 9342−9349.
(34) Houtz, E. F.; Sutton, R.; Park, J. S.; Sedlak, M. Poly- and Perfluoroalkyl Substances in Wastewater: Significance of Unknown Precursors, Manufacturing Shifts, and Likely AFFF Impacts. *Water Res.* **2016**, *95*, 142−149.
(35) Kaiser, A. M.; Saracevic, E.; Schaar, H. P.; Weiss, S.; Hornek-Gausterer, R. Ozone as Oxidizing Agent for the Total Oxidizable Precursor (TOP) Assay and as a Preceding Step for Activated Carbon Treatments Concerning per- and Polyfluoroalkyl Substance Removal. *J. Environ. Manage.* **2021**, *300*, No. 113692.
(36) Lin, H.; Wang, Y.; Niu, J.; Yue, Z.; Huang, Q. Efficient Sorption and Removal of Perfluoroalkyl Acids (PFAAs) from Aqueous Solution by Metal Hydroxides Generated in Situ by Electrocoagulation. *Environ. Sci. Technol.* **2015**, *49*, 10562−10569.
(37) Yang, B.; Han, Y.; Yu, G.; Zhuo, Q.; Deng, S.; Wu, J.; Zhang, P. Efficient Removal of Perfluoroalkyl Acids (PFAAs) from Aqueous Solution by Electrocoagulation Using Iron Electrode. *Chem. Eng. J.* **2016**, *303*, 384−390.
(38) Shi, H.; Chiang, S. Y.; Wang, Y.; Wang, Y.; Liang, S.; Zhou, J.; Fontanez, R.; Gao, S.; Huang, Q. An Electrocoagulation and Electrooxidation Treatment Train to Remove and Degrade Per- and Polyfluoroalkyl Substances in Aqueous Solution. *Sci. Total Environ.* **2021**, *788*, No. 147723.
(39) Jolis, D.; Mitch, A. A.; Marneri, M.; Ho, C.-F. Effects of Anaerobic Selector Hydraulic Retention Time on Biological Foam Control and Enhanced Biological Phosphorus Removal in a Pure-Oxygen Activated Sludge System. *Water Environ. Res.* **2007**, *79*, 472−478.
(40) Stevenson, P.; Li, X. *Foam Fractionation - Principles and Process Design*, 1st ed.; Taylor & Francis: Boca Raton, 2014.
(41) Vo, P. H. N.; Buckley, T.; Xu, X.; Nguyen, T. M. H.; Rudolph, V.; Shukla, P. Foam Fractionation of Per- and Polyfluoroalkyl Substances (PFASs) in Landfill Leachate Using Different Cosurfactants. *Chemosphere* **2023**, *310*, No. 136869.
(42) Dai, X.; Xie, Z.; Dorian, B.; Gray, S.; Zhang, J. Comparative Study of PFAS Treatment by UV, UV/Ozone, and Fractionations with Air and Ozonated Air. *Environ. Sci. Water Res. Technol.* **2019**, *5*, 1897−1907.
(43) Pronk, M.; de Kreuk, M. K.; de Bruin, B.; Kamminga, P.; Kleerebezem, R.; van Loosdrecht, M. C. M. Full Scale Performance of the Aerobic Granular Sludge Process for Sewage Treatment. *Water Res.* **2015**, *84*, 207−217.
(44) Al-Asheh, S.; Bagheri, M.; Aidan, A. Membrane Bioreactor for Wastewater Treatment: A Review. *Case Stud. Chem. Environ. Eng.* **2021**, *4*, No. 100109.
(45) Di Bella, G.; Torregrossa, M. Foaming in Membrane Bioreactors: Identification of the Causes. *J. Environ. Manage.* **2013**, *128*, 453−461.
(46) Collivignarelli, M. C.; Baldi, M.; Abbà, A.; Caccamo, F. M.; Miino, M. C.; Rada, E. C.; Torretta, V. Foams in Wastewater Treatment Plants: From Causes to Control Methods. *Appl. Sci.* **2020**, *10*, No. 2716.

https://doi.org/10.1021/acsestengg.3c00091
ACS EST Engg. XXXX, XXX, XXX−XXX

Supplementary information to:
Integrated treatment of per- and polyfluoroalkyl substances in existing water treatment plants – scoping the potential of foam partitioning

Sanne J. Smith[1*], Chantal Keane[2], Lutz Ahrens[1] and Karin Wiberg[1]

[1]Department of Aquatic Sciences and Assessment, Swedish University of Agricultural Sciences (SLU), P.O. Box 7050, SE-750 07, Uppsala, Sweden
[2]University of Queensland, Queensland alliance for Environmental Health Sciences, Woolloongabba, QLD 4102, Australia
E-mail contact: sanne.smith@slu.se

---

1. Supplementary methods

1.1 Limits of quantification

Method limits of quantification (LOQs) for the sample extracts were calculated using Equation SI 1, with $\langle C_{blank} \rangle$ and $sd_{C_{blank}}$ the mean and standard deviation of the extract concentrations in the blanks (*n = 12*), respectively. Outlying blank concentrations (defined as being more than three standard deviations away from the mean) were removed prior to LOQ calculations, and concentrations below the instrument quantification limit (0.05 ng mL^{-1}) were set to 0.05 ng mL^{-1}. For the calculation of the LOQ of TOP assay samples, the concentrations in the TOP blanks (*n* = 7) were used instead. Because the volume of foamate extracted was lower than that of water, LOQs for water samples were lower than those for foam samples. The LOQs as given in Table SI 2 were converted based on the volume of sample extracted to give the LOQ in each sample.

$$LOQ = \langle C_{blank} \rangle + 10 \cdot sd_{C_{blank}}$$

Equation SI 1

Table SI 1: LOQs in sample extracts and extracts of samples after the TOP assay. The LOQs in the samples varied based on the extracted sample volume. An extract LOQ of 0.05 ng mL^{-1} corresponds to a sample LOQ of 0.4 ng L^{-1} for a sample of 125 mL, 5 ng L^{-1} for a sample of 10 mL (the highest foamate volume extracted) and 200 ng L^{-1} for a sample of 0.25 mL (the lowest foamate volume extracted).

Compound	LOQ normal extracts (ng mL^{-1})	LOQ TOP extracts (ng mL^{-1})
Perfluorobutanoic acid (PFBA)	0.50	1.5
Perfluoropentanoic acid (PFPeA)	0.05	0.85
Perfluorobutane sulfonate (PFBS)	0.12	0.06
Perfluorohexanoic acid (PFHxA)	0.05	0.71
4:2 Fluorotelomer sulfonic acid (4:2 FTSA)	0.05	0.05
hexafluoropropylene oxide dimer acid (HFPO-DA)	0.05	0.05
Perfluoropentane sulfonate (PFPeS)	0.05	0.05
Perfluoroheptanoic acid (PFHpA)	0.05	0.05
4,8-dioxa-3H-perfluorononanoic acid (NaDONA)	0.05	0.05
Perfluorohexane sulfonate (PFHxS)	0.13	0.21
Perfluorooctanoic acid (PFOA)	0.05	1.1
6:2 Fluorotelomer sulfonate (6:2 FTSA)	0.05	1.1
Perfluoroheptane sulfonate (PFHpS)	0.05	0.05
Perfluoroethyl-cyclohexane sulfonate (PFECHS)	0.05	0.05
Perfluorononanoic acid (PFNA)	0.05	0.05
Perfluorooctane sulfonamide (FOSA)	0.05	0.05
Perfluorooctane sulfonate (PFOS)	0.24	0.35
Perfluorodecanoic acid (PFDA)	0.34	0.37
8:2 Fluorotelomer sulfonate (8:2 FTSA)	0.05	0.05
9-chloro-hexadecafluoro-3-oxanonane sulfonate (9Cl-PF3ONS)	0.07	0.08
Perfluorononane sulfonate (PFNS)	0.05	0.05
Perfluoroundecanoic acid (PFUnDA)	0.54	0.24
N-methyl-perfluorooctane sulfonamido acetic acid (MeFOSAA)	0.05	0.05
N-ethyl-perfluorooctane sulfonamido acetic acid (EtFOSAA)	0.05	0.05
Perfluorodecane sulfonate (PFDS)	0.05	0.05
Perfluorododecanoic acid (PFDoDA)	0.09	0.11
11-chloro-eicosafluoro-3-oxaundecane-1-sulfonic acid (11Cl-PF3OUdS)	0.05	0.05
Perfluorotridecanoic acid (PFTriDA)	0.05	0.05
Perfluorotetradecanoic acid (PFTeDA)	0.05	0.05

1.2 Calibration curve

The calibration curve concentrations were 0.05, 0.1, 0.5, 1, 5, 10, 50, 100, 250, 500 and 900 ng mL^{-1}. A calibration curve was run before and after all samples from one site. Because the variation in PFAS concentrations between the different samples and the different sites was large, it was necessary to use a calibration curve that included a wide range of concentrations. For some compounds, this curve was not linear over the full concentration range. When necessary, certain points of the calibration curve were excluded or the regression was changed to quadratic, to ensure a good fit of all calibration curve points ($R^2 \geq 0.99$). All compounds with excluded concentration points or a non-linear regression are shown in Table SI 2. Extract concentrations outside of the range of the calibration curve (> 900 ng mL^{-1}) were extrapolated based on the curve's regression equation. This only applied to at most three compounds at four sites, with the concentrations always being acceptably close to the highest included standard concentration.

Table SI 2: Compounds with changed calibration curve regression methods. For compounds not included in this table, all concentration points were included and a linear regression was used. ◊PFBA: the 900 ng mL^{-1} point was included for site D, because PFBA concentrations were >500 ng mL^{-1} in some of the sample extracts of this site. °4:2 FTSA and NaDONA: R^2 was 0.98 for the calibration curve regression of one site (I and A, respectively) for each of these compounds.

Component	Regression	Excluded concentrations (ng mL^{-1})
PFBA◊	Quadratic	900
PFPeA	Quadratic	
4:2 FTSA°	Quadratic	250, 500, 900
HFPO-DA	Quadratic	500, 900
NaDONA°	Linear	250, 500, 900
6:2 FTSA	Linear	900
FOSA	Linear	500, 900
8:2 FTSA	Quadratic	900
9Cl-PF3ONS	Quadratic	500, 900
PFECHS	Quadratic	
Me-FOSAA	Linear	900
PFDoDA	Linear	900
11Cl-PF3OUdS	Linear	250, 500, 900
PFTriDA	Linear	250, 500, 900
PFTeDA	Linear	250, 500, 900

1.3 Foamate extraction

Table SI 3: Volumes of foamate extracted for each site. The foamate was always diluted to 50 mL with Milli-Q water prior to extraction.

Site	Volume of foamate (mL)
A	0.25
B	0.25
C	5.00
D	0.25
E	0.25
F	7.50
G	7.50
H	10.0
I	1.00
J	2.50

Table SI 4: Mean PFAS concentrations (µg L^{-1}) in foamate from site A for different extracted volumes (n = 2 for each volume), always diluted to a total volume of 50 mL. In the calculation of the relative standard deviation (%), samples for which both concentrations were below the LOQ were excluded. When the concentration in one duplicate was above the LOQ, the concentration in the duplicate below the LOQ was set to the LOQ. For some compounds, concentrations could not be determined at high extracted volumes, because matrix interference pushed the compound peak out of the sMRM window. Cells have been left blank when this was the case. Relative errors were always low, except when the concentrations were very close to the quantification limits (e.g. 4:2 FTSA, PFDoDA and PFTeDA) and thus had a high analytical uncertainty.

	Extracted Volume					**Relative standard deviation (%)**
	0.1 mL	0.25 mL	0.5 mL	1 mL	2.5 mL	
Compound	**Concentration (µg L^{-1})**					
PFBA	<5.0	<2.0	<1.0	0.69	0.62	9%
PFPeA	1.5	1.4	1.3	1.5	1.5	5%
PFBS	13	11	11	11	12	7%
PFHxA	180	170	180	190	190	4%
4:2 FTSA	0.61	0.22	0.16	0.12	0.11	83%
HFPO-DA	1.3	1.1	1.1	1.3	1.1	14%
PFPeS	190	260	300	360	400	26%
PFHpA	1300	1300	1400	1200	1200	8%
NaDONA	0.83	0.61	0.60	0.58	0.48	28%
PFHxS	3000	3100	2700	2700	2100	13%
PFOA	16000	14000	12000	9800		20%
6:2 FTSA	550	620	530	510		11%
PFHpS	1400	1500	1500			4%
PFECHS	3500	3500	3400			3%
PFNA	1100	1100	1000	1000		6%
FOSA	200	190	170	170		9%
PFOS	19000	17000	16000			8%
PFDA	480	520	490	470		8%
8:2 FTSA	79	78	63			11%
9Cl-PF3ONS	<0.74	<0.30	<0.15	0.08		N/A
PFNS	69	79				13%
PFUnDA	16	19	13	12		22%
Me-FOSAA	150	150				3%
Et-FOSAA	730	620				11%
PFDS	3.9	3.3	3.3			13%
PFDoDA	7.1	3.9	4.1	2.1		60%
11Cl-PF3OUdS	<0.50	<0.20	<0.10	<0.05	<0.02	N/A
PFTriDA	0.53	0.26	0.35	0.15	0.07	66%
PFTeDA	9.1	0.42	5.4	0.06	0.23	186%

Table SI 5: Recoveries (%, as mean (min – max)) of Milli-Q spiked with 2.5 and 10 ng of each PFAS, and foamate samples spiked with 25 ng of each PFAS. Recoveries well above or below 100 % were often due to high concentrations in the unspiked foamate samples. E.g., when the concentration of an unspiked foamate extract was 250 ng mL^{-1}, a method variability of 10 % may have already caused a recovery of 0 % or 200 %. Recovery of 9Cl-PF3ONS in the foamate samples was consistently low, which indicates that matrix suppression decreased the signal. Since this compound was not detected in any of the samples, it was left out of the data analysis and its low recovery thus did not affect the presented results. The stock solution used to spike the 10 ng Milli-Q samples and the foam samples from Site A was probably contaminated with PFBA, leading to recoveries that were a factor two too high. A different stock solution was used for the remaining samples, in which the recovery of PFBA was always within an acceptable range.

Compound	Spiked Milli-Q (50 mL)		Spiked Foamate (with 25 ng, n = 3 for all)			
	2.5 ng (n = 2)	**10 ng** (n = 3)	**Site A**	**Site C**	**Site D**	**Site J**
PFBA	117 (113 - 122)	209 (202 - 215)	226 (213 - 245)	97 (96 - 98)	126 (124 - 129)	101 (97 - 109)
PFPeA	110 (107 - 112)	142 (138 - 145)	145 (139 - 152)	99 (97 - 101)	118 (116 - 120)	106 (104 - 107)
PFBS	109 (106 - 113)	118 (117 - 119)	126 (122 - 133)	100 (98 - 103)	120 (116 - 124)	112 (108 - 114)
PFHxA	111 (107 - 114)	111 (106 - 119)	149 (137 - 164)	127 (124 - 130)	124 (118 - 128)	125 (122 - 128)
4:2 FTSA	102 (91 - 113)	106 (98 - 115)	116 (108 - 127)	80 (78 - 82)	100 (99 - 101)	88 (81 - 95)
HFPO-DA	102 (98 - 105)	114 (97 - 130)	237 (222 - 255)	189 (176 - 207)	175 (156 - 188)	170 (160 - 183)
PFPeS	94 (91 - 98)	103 (98 - 105)	248 (229 - 275)	88 (84 - 92)	117 (111 - 121)	78 (73 - 81)
PFHpA	100 (94 - 105)	108 (93 - 116)	143 (-3 - 299)	111 (108 - 114)	125 (103 - 146)	136 (130 - 144)
NaDONA	136 (134 - 138)	138 (123 - 152)	146 (141 - 154)	169 (149 - 195)	174 (137 - 195)	210 (195 - 230)
PFHxS	81 (81 - 81)	88 (87 - 89)	130 (-40 - 433)	73 (69 - 77)	92 (87 - 98)	78 (75 - 81)
PFOA	107 (95 - 118)	112 (102 - 124)	658 (19 - 1064)	111 (98 - 121)	217 (152 - 272)	124 (122 - 128)
6:2 FTSA	114 (107 - 121)	116 (110 - 126)	110 (57 - 164)	100 (97 - 103)	184 (174 - 192)	113 (110 - 114)
PFHpS	123 (120 - 125)	130 (124 - 137)	260 (111 - 361)	134 (132 - 136)	132 (127 - 136)	129 (114 - 143)
PFECHS	75 (73 - 77)	100 (93 - 109)	-3222 (-5431 - 943)	130 (127 - 133)	144 (140 - 147)	122 (115 - 130)
PFNA	88 (83 - 93)	112 (105 - 120)	262 (157 - 377)	108 (102 - 111)	123 (120 - 128)	107 (100 - 118)
FOSA	102 (100 - 104)	113 (100 - 128)	124 (96 - 151)	102 (99 - 104)	118 (115 - 121)	100 (94 - 108)
PFOS	74 (74 - 75)	86 (84 - 89)	439 (-1282 - 1572)	68 (41 - 104)	153 (122 - 195)	62 (-32 - 173)
PFDA	73 (72 - 74)	80 (78 - 82)	236 (166 - 300)	103 (96 - 109)	105 (96 - 120)	91 (83 - 106)
8:2 FTSA	113 (111 - 114)	130 (126 - 134)	141 (125 - 152)	77 (74 - 81)	99 (93 - 106)	89 (77 - 105)
9Cl-PF3ONS	91 (87 - 94)	122 (119 - 126)	49 (48 - 52)	29 (28 - 30)	44 (44 - 45)	30 (29 - 32)
PFNS	111 (98 - 124)	127 (125 - 130)	378 (334 - 405)	120 (119 - 120)	151 (145 - 156)	117 (111 - 125)
PFUnDA	51 (49 - 53)	60 (56 - 64)	154 (150 - 162)	107 (102 - 111)	100 (90 - 105)	97 (93 - 105)
Me-FOSAA	111 (110 - 112)	118 (102 - 130)	129 (97 - 150)	104 (99 - 111)	133 (109 - 152)	98 (92 - 109)
Et-FOSAA	102 (100 - 104)	114 (113 - 117)	149 (60 - 282)	91 (89 - 93)	118 (112 - 124)	91 (84 - 101)
PFDS	97 (95 - 99)	109 (105 - 114)	434 (401 - 459)	89 (86 - 92)	151 (147 - 154)	97 (95 - 101)
PFDoDA	110 (104 - 115)	126 (122 - 132)	202 (189 - 214)	134 (131 - 137)	131 (123 - 137)	130 (118 - 146)
11Cl-PF3OUdS	69 (63 - 76)	92 (87 - 95)	285 (274 - 302)	105 (104 - 107)	77 (74 - 79)	73 (66 - 79)
PFTriDA	112 (99 - 124)	145 (141 - 151)	231 (190 - 288)	88 (87 - 89)	131 (114 - 149)	148 (121 - 198)
PFTeDA	91 (82 - 101)	111 (103 - 116)	137 (108 - 175)	91 (85 - 95)	120 (111 - 129)	99 (95 - 101)

2. Supplementary Results

2.1 Figure 1 repeated with alternative handling of concentrations below the LOQ

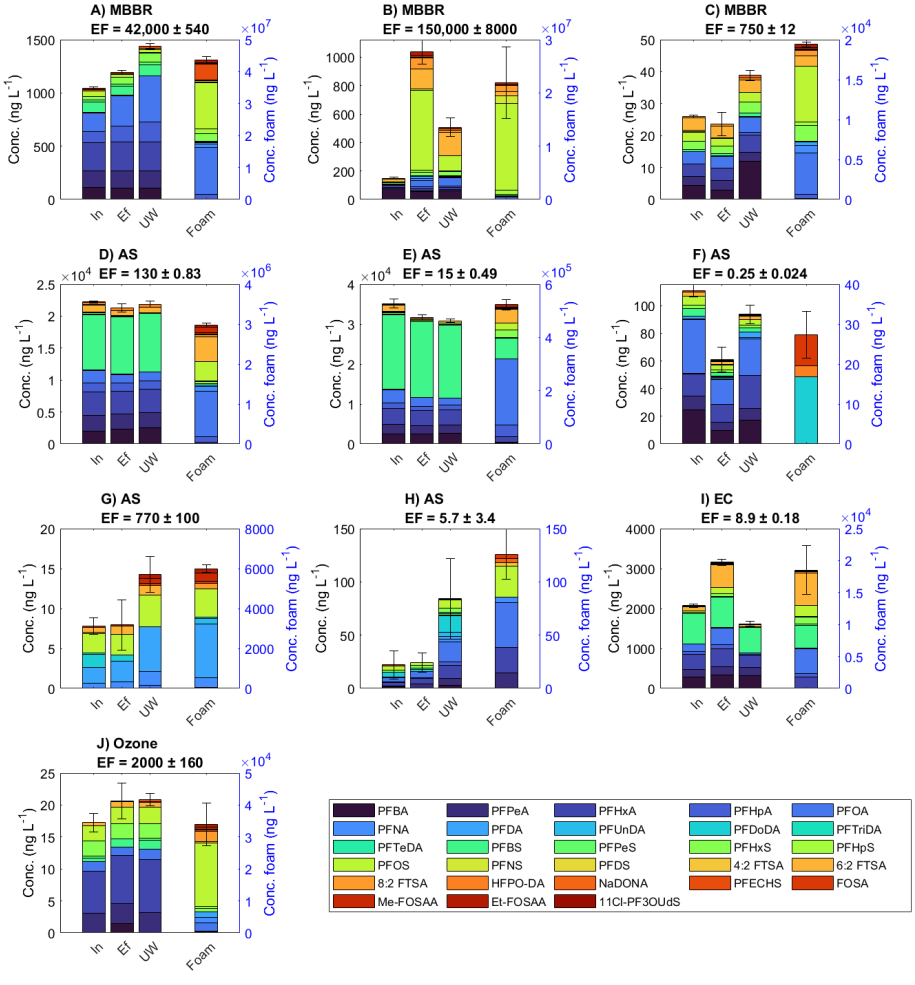

Figure SI 1: PFAS concentrations in the influent (In), effluent (Ef), water under the foam (UW) and foamate (Foam) for all treatment plants included in the study (see main text Table 1, labels of the subplots correspond to the site identifiers), with concentration below the LOQ set to zero. MBBR = moving bed biofilm reactor, AS = activated sludge, EC = electrocoagulation, Ozone = ozonation.

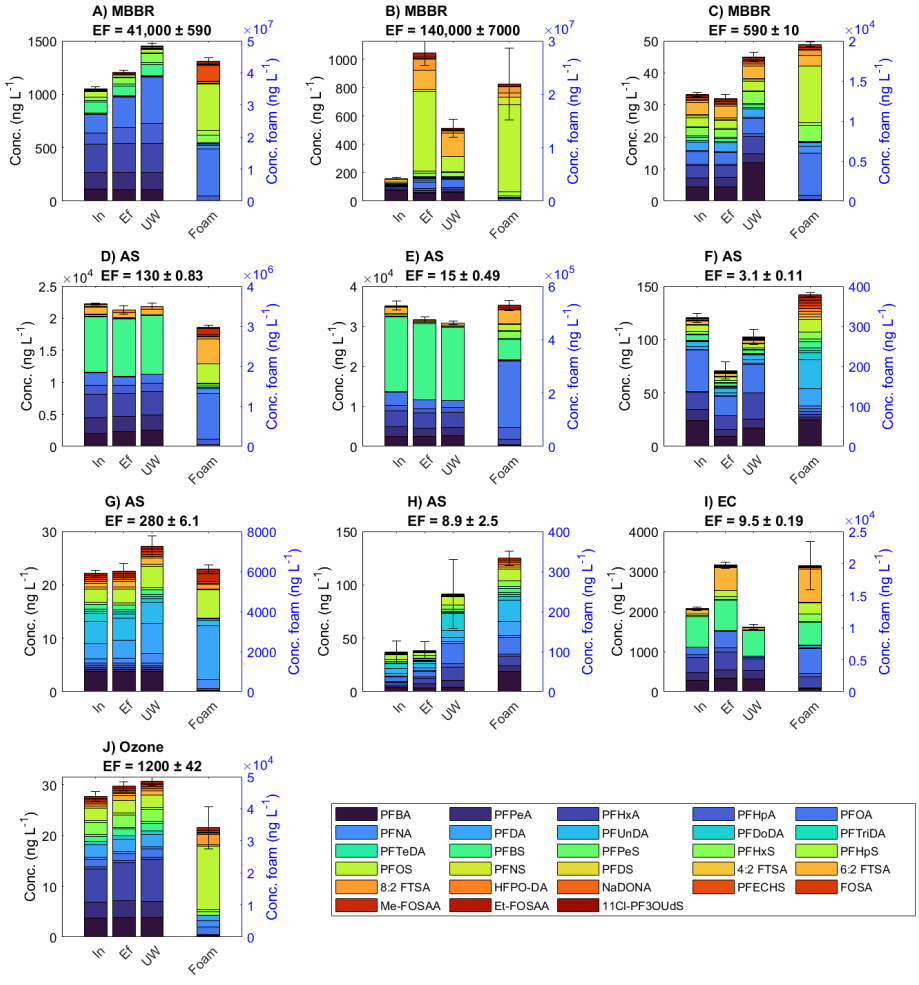

Figure SI 2: PFAS concentrations in the influent (In), effluent (Ef), water under the foam (UW) and foamate (Foam) for all treatment plants included in the study (see main text Table 1, labels of the subplots correspond to the site identifiers), with concentrations below the LOQ set to the LOQ. MBBR = moving bed biofilm reactor, AS = activated sludge, EC = electrocoagulation, Ozone = ozonation.

2.2 Mean PFAS concentrations for each site

Table SI 6: Mean PFAS concentrations (ng L^{-1}) in influent, effluent, water under the foam and foam for each site (A-J) included in the study. W When all triplicates had concentrations below the LOQ, the concentration is reported as < LOQ. When at least one triplicate had a concentration above the LOQ, the other triplicates' concentrations were set to half the LOQ, and the average of the three values was reported.

Conc. (ng L^{-1})	A				B				C			
	In	**Ef**	**UW**	**Foam**	**In**	**Ef**	**UW**	**Foam**	**In**	**Ef**	**UW**	**Foam**
PFBA	110	110	100	<2000	77	56	63	<2000	4.5	3.7	12	<100
PFPeA	160	160	170	380	6.7	6.3	5.5	<200	2.8	3	2.8	<10
PFBS	98	88	100	11000	2.1	2.1	2.5	<440	0.83	0.74	1	<22
PFHxA	260	270	270	180000	15	15	16	<200	3.9	3.7	5.2	130
4:2 FTSA	0.64	<0.40	0.3	<200	<0.40	<0.40	<0.40	<200	0.38	0.38	<0.38	11
HFPO-DA	<0.42	<0.40	<0.42	1500	3	5.2	8.5	<200	<0.40	<0.40	<0.40	<10
PFPeS	14	19	22	220000	2	2.9	3.9	240	<0.39	<0.40	<0.38	92
PFHpA	100	150	190	1400000	6	12	10	<200	<0.39	<0.40	1	500
NaDONA	<0.42	<0.40	<0.42	780	<0.40	<0.40	<0.40	<200	<0.39	<0.40	0.83	12
PFHxS	33	62	85	2500000	5.4	26	29	170000	2.5	2.4	3.5	2000
PFOA	180	290	430	15000000	2.4	46	60	400000	3.9	3.6	4.7	5200
6:2 FTSA	5.4	6.8	9	550000	21	140	160	720000	3.8	3.6	3.8	1300
PFHpS	3	3.2	5.3	1500000	<0.39	13	4.1	750000	<0.39	<0.40	<0.38	400
PFECHS	7.9	12	19	5000000	<0.39	0.62	0.3	32000	<0.39	<0.40	<0.38	120
PFNA	3.2	2.4	3.5	1100000	<0.39	15	3.6	230000	<0.39	<0.40	<0.38	890
FOSA	1.5	0.59	0.88	220000	<0.39	9.7	3.3	160000	<0.39	<0.40	<0.38	21
PFOS	48	24	30	14000000	7.5	560	110	16000000	2.8	2.3	3	7000
PFDA	1.9	<2.70	<2.80	470000	<2.60	10	2.9	120000	<2.60	<2.70	<2.60	480
8:2 FTSA	<0.42	0.37	<0.42	69000	0.31	74	15	1100000	0.56	0.51	0.64	640
9Cl-PF3ONS	<0.59	<0.59	<0.59	<300	<0.59	<0.59	<0.59	<300	<0.59	<0.59	<0.59	<15
PFNS	<0.42	<0.40	<0.42	150000	<0.39	11	2.3	1500000	0.42	<0.40	<0.38	21
PFUnDA	<4.50	<4.30	<4.50	21000	<4.10	<4.10	<4.30	9500	<4.30	<4.30	<4.30	<110
Me-FOSAA	2.5	<0.40	0.32	220000	<0.39	<0.38	<0.40	5200	<0.39	<0.40	<0.38	240
Et-FOSAA	9.4	1.5	1.9	780000	0.27	28	10	380000	<0.39	<0.40	<0.38	360
PFDS	<0.42	<0.40	<0.42	29000	<0.39	<0.38	<0.40	7300	<0.40	<0.40	<0.40	<10
PFDoDA	1.3	<0.73	0.7	3900	<0.70	<0.70	0.58	790	<0.72	<0.72	<0.72	<18
11Cl-PF3OUdS	<0.40	<0.40	<0.40	<200	<0.40	<0.40	<0.40	<200	<0.40	<0.40	<0.40	<10
PFTriDA	<0.42	<0.40	<0.42	230	0.28	0.27	0.47	<200	<0.40	<0.40	<0.40	<10
PFTeDA	<0.42	<0.40	<0.42	200	<0.39	0.53	0.94	1900	<0.39	0.43	0.26	<10

Table SI 6 continued

Conc. (ng L^{-1})	D				E				F			
	In	**Ef**	**UW**	**Foam**	**In**	**Ef**	**UW**	**Foam**	**In**	**Ef**	**UW**	**Foam**
PFBA	2000	2300	2600	3600	2500	2600	2600	3800	24	9.5	17	<67
PFPeA	2500	2300	2400	4100	2400	1900	2100	2800	10	6.2	8.5	<6.7
PFBS	8700	8900	9100	39000	19000	19000	18000	76000	5.4	2.8	3.1	<15
PFHxA	3700	3600	3700	44000	4100	3800	3900	21000	16	13	24	<6.7
4:2 FTSA	12	15	14	<200	22	6.3	5.5	<200	<0.39	0.68	<0.40	<6.7
HFPO-DA	350	430	450	12000	92	85	100	1100	<0.39	0.35	<0.40	5.1
PFPeS	45	47	45	2500	140	120	120	4000	<0.39	<0.38	<0.40	<6.7
PFHpA	1300	1200	1300	130000	1300	1100	1100	45000	0.47	<0.38	<0.40	<6.7
NaDONA	1.7	3	3.7	620	<0.39	1.5	1.5	<200	<0.40	<0.40	<0.40	<6.7
PFHxS	230	110	100	44000	300	290	270	27000	2.4	1.8	1.7	<17
PFOA	2000	1400	1400	1100000	3400	2200	1900	250000	39	18	26	<6.7
6:2 FTSA	1100	780	820	620000	1700	470	430	53000	2.9	2.2	2.5	<6.9
PFHpS	5.3	5.5	4.9	22000	20	13	8.8	2000	<0.40	<0.40	<0.40	<6.7
PFECHS	2.9	3.3	3.3	5900	9.2	7.4	5.4	850	0.36	<0.38	<0.40	<6.7
PFNA	44	21	18	120000	42	16	11	1900	0.69	0.69	1.1	<6.7
FOSA	1.9	1.4	1	34000	5.8	2.4	1.9	1400	0.77	0.53	0.54	7.7
PFOS	89	37	30	490000	300	73	57	24000	6.4	3.3	4	<31
PFDA	11	1.7	<2.50	36000	16	2.3	<2.50	<1300	2.4	<2.50	3.8	<45
8:2 FTSA	18	2.6	3.4	44000	18	<0.37	<0.37	<200	<0.39	0.46	0.29	<6.7
9Cl-PF3ONS	<0.59	<0.59	<0.59	<300	<0.59	<0.59	<0.59	<300	<0.59	<0.59	<0.59	<9.8
PFNS	<0.40	<0.40	<0.40	<200	<0.39	<0.37	<0.37	180	<0.40	<0.40	<0.40	<6.7
PFUnDA	<4.00	<3.90	<4.00	<2100	<4.20	<4.00	<4.00	<2100	<4.10	<4.10	<4.30	<71
Me-FOSAA	72	6.1	4.5	150000	95	2.8	2.6	2900	<0.39	<0.38	<0.40	<6.7
Et-FOSAA	6.2	2.3	2.4	49000	97	9.4	12	10000	0.43	0.35	0.66	<6.7
PFDS	<0.40	<0.40	<0.40	<200	<0.40	<0.40	<0.40	<200	<0.40	<0.40	<0.40	<6.7
PFDoDA	<0.72	<0.72	<0.72	<360	1.2	<0.67	<0.68	<360	<0.70	0.76	<0.72	17
11Cl-PF3OUdS	<0.40	<0.40	<0.40	<200	<0.40	<0.40	<0.40	<200	<0.39	<0.38	0.28	<6.7
PFTriDA	<0.40	<0.40	<0.40	<200	0.27	<0.37	<0.37	<200	<0.39	0.69	<0.40	<6.7
PFTeDA	<0.38	0.39	0.55	<200	0.46	<0.37	<0.37	<200	<0.39	0.58	<0.40	<6.7

Table SI 6 continued

Conc. (ng L^{-1})	G				H				I			
	In	**Ef**	**UW**	**Foam**	**In**	**Ef**	**UW**	**Foam**	**In**	**Ef**	**UW**	**Foam**
PFBA	<3.9	<3.8	<3.8	<67	2.8	<3.7	3.5	<50	280	330	320	<500
PFPeA	<0.39	<0.38	<0.38	<6.7	1.2	4	6.6	14	200	210	200	<50
PFBS	<0.86	<0.85	<0.84	<15	<0.94	1.5	1.2	<11	750	760	630	3500
PFHxA	<0.39	<0.38	<0.38	6.8	3	5.1	12	24	380	440	300	1700
4:2 FTSA	0.26	<0.38	<0.38	5	<0.42	<0.37	0.27	5	0.67	0.75	0.59	<50
HFPO-DA	<0.40	<0.40	<0.40	<6.7	<0.40	<0.40	<0.40	<5.0	23	24	14	160
PFPeS	<0.40	<0.40	<0.40	<6.7	<0.42	<0.37	1.5	<5.0	6.2	5.3	2.8	170
PFHpA	<0.39	<0.38	<0.38	<6.7	0.69	0.75	3.6	<5.0	77	110	30	540
NaDONA	<0.40	<0.40	<0.40	<6.7	<0.42	<0.37	<0.38	4.6	<0.40	<0.40	<0.40	<50
PFHxS	<1.0	<1.0	<1.0	<17	1.9	2.4	4	<13	40	70	11	1100
PFOA	<0.39	<0.38	0.42	60	4.2	5.6	19	42	180	400	43	4000
6:2 FTSA	0.67	1	1.2	20	<0.44	<0.39	0.64	<5.2	110	580	53	5200
PFHpS	<0.39	<0.38	<0.38	6.9	<0.40	<0.40	<0.40	<5.0	2.7	8	0.54	53
PFECHS	<0.39	<0.38	<0.38	12	<0.40	<0.40	<0.40	<5.0	2.3	4.8	0.74	89
PFNA	0.69	0.84	1.7	470	0.92	0.57	2.2	5.4	2.4	13	0.27	51
FOSA	0.27	<0.38	0.37	100	<0.42	<0.37	<0.38	4.7	1.1	5.4	0.61	87
PFOS	2.4	2.6	4	1400	4.3	3	7.9	29	24	150	11	1700
PFDA	2.4	3	5.6	2700	<2.8	<2.5	3.4	<34	3	11	<2.7	<340
8:2 FTSA	<0.39	<0.38	<0.38	260	<0.40	<0.40	<0.40	<5.0	<0.39	5.8	<0.40	<50
9Cl-PF3ONS	<0.59	<0.59	<0.59	<9.8	<0.59	<0.59	<0.59	<7.4	<0.59	<0.59	<0.59	<74
PFNS	<0.40	<0.40	<0.40	<6.7	<0.40	<0.40	<0.40	<5.0	<0.40	<0.40	<0.40	<50
PFUnDA	<4.1	<4.1	<4.0	270	<4.5	<4.0	5	<54	<4.3	<4.3	<4.3	<540
Me-FOSAA	<0.39	<0.38	0.59	410	0.88	<0.37	<0.38	<5.0	1.1	5.3	0.29	40
Et-FOSAA	<0.39	0.27	0.5	220	<0.40	<0.40	<0.40	<5.0	1.3	13	0.81	75
PFDS	<0.40	<0.40	<0.40	<6.7	<0.40	<0.40	<0.40	<5.0	<0.40	<0.40	<0.40	<50
PFDoDA	1.6	0.83	<0.68	73	4.2	1.9	16	<9.1	1.4	1.4	1.2	91
11Cl-PF3OUdS	<0.40	<0.40	<0.40	<6.7	<0.40	<0.40	<0.40	<5.0	<0.40	<0.40	<0.40	<50
PFTriDA	0.29	<0.38	<0.38	<6.7	<0.42	<0.37	0.72	<5.0	<0.40	<0.40	<0.40	<50
PFTeDA	<0.39	<0.38	<0.38	4.7	<0.42	<0.37	0.27	<5.0	<0.40	<0.40	<0.40	<50

Table SI 6 continued

Conc. (ng L^{-1})	J			
	In	**Ef**	**UW**	**Foam**
PFBA	<3.8	2.7	<3.8	160
PFPeA	3.1	3.2	3.2	100
PFBS	0.71	1.3	1.4	31
PFHxA	6.5	7.5	8.3	230
4:2 FTSA	<0.40	<0.40	<0.40	<20
HFPO-DA	<0.40	<0.40	<0.40	<20
PFPeS	0.34	<0.38	0.33	<20
PFHpA	<0.38	<0.38	<0.38	93
NaDONA	<0.40	<0.40	<0.40	<20
PFHxS	2.4	2.4	2.3	1100
PFOA	1.5	1.4	1.6	2500
6:2 FTSA	0.47	0.87	0.78	490
PFHpS	<0.38	<0.38	<0.38	640
PFECHS	<0.38	<0.38	0.32	320
PFNA	<0.38	<0.38	<0.38	1800
FOSA	<0.38	<0.38	<0.38	260
PFOS	2.4	2.5	2.5	20000
PFDA	<2.5	<2.5	<2.6	1700
8:2 FTSA	<0.38	0.26	0.29	3200
9Cl-PF3ONS	<0.59	<0.59	<0.59	<30
PFNS	<0.40	<0.40	<0.40	<20
PFUnDA	<4.3	<4.3	<4.3	<210
Me-FOSAA	<0.38	<0.38	<0.38	670
Et-FOSAA	<0.38	<0.38	<0.38	820
PFDS	<0.40	<0.40	<0.40	<20
PFDoDA	<0.69	<0.69	<0.69	35
11Cl-PF3OUdS	<0.40	<0.40	<0.40	<20
PFTriDA	<0.40	<0.40	<0.40	<20
PFTeDA	<0.40	<0.40	<0.40	<20

2.3 Concentrations after the TOP assay

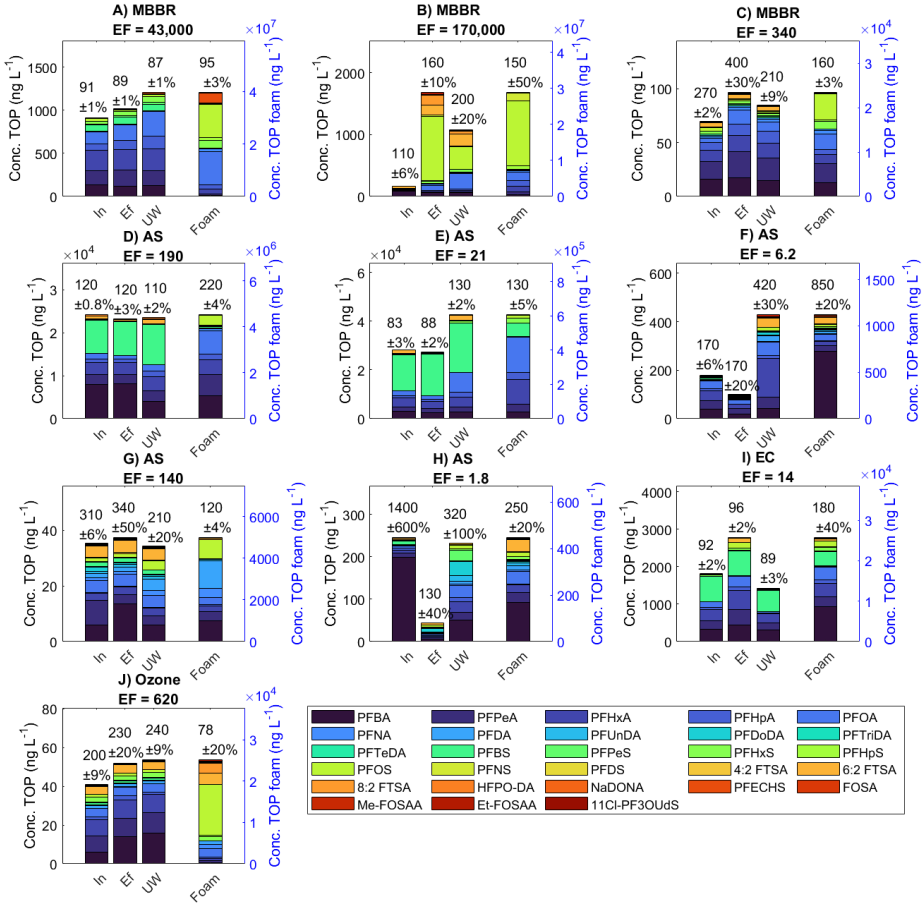

Figure SI 3: PFAS concentrations after the TOP assay in the influent (In), effluent (Ef), water under the foam (UW) and foamate (Foam) for all treatment plants included in the study (see main text Table 1, labels of the subplots correspond to the site identifiers). Concentrations below the LOQ were set to 0.5·LOQ. Foamate concentrations are presented on the y-axis on the right. Titles give the enrichment factors (EF) calculated based on the concentrations after TOP. The text above the bars gives the molar percentage of PFAS compared to the target measurement, i.e. percentages above 100 % indicate an increased ΣPFAS concentration due to precursor degradation. Concentrations below 100 % are probably due to measurement uncertainties. The standard deviations are based only on the variability in target concentrations (n = 3), since TOP assays were done without replicates. MBBR = moving bed biofilm reactor, AS = activated sludge, EC = electrocoagulation, Ozone = ozonation.

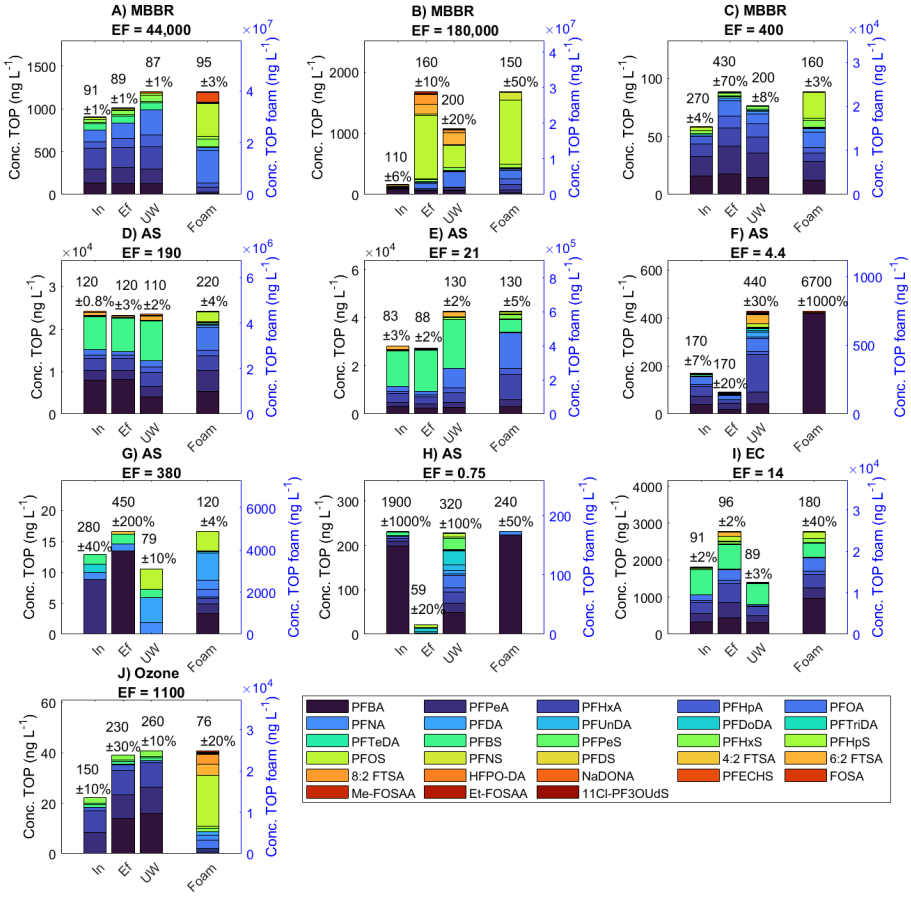

Figure SI 4: PFAS concentrations after the TOP assay in the influent (In), effluent (Ef), water under the foam (UW) and foamate (Foam) for all treatment plants included in the study (see main text Table 1, labels of the subplots correspond to the site identifiers), with concentrations below the LOQ set to zero. MBBR = moving bed biofilm reactor, AS = activated sludge, EC = electrocoagulation, Ozone = ozonation.

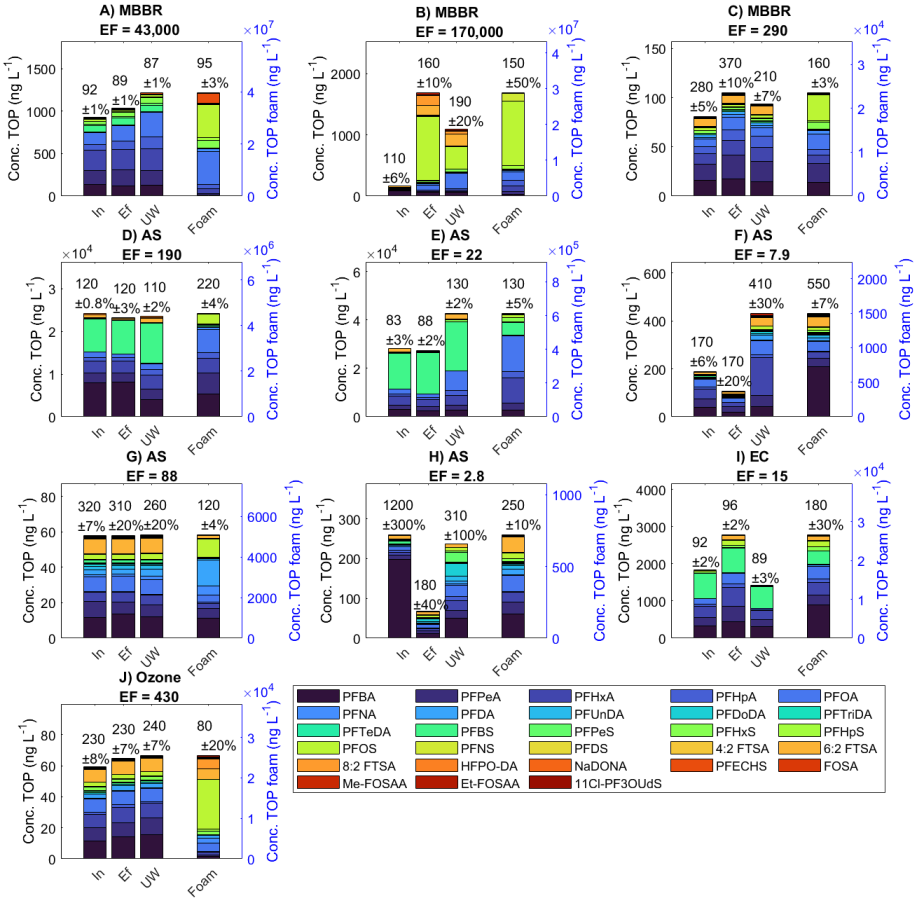

Figure SI 5: PFAS concentrations after the TOP assay in the influent (In), effluent (Ef), water under the foam (UW) and foamate (Foam) for all treatment plants included in the study (see main text Table 1, labels of the subplots correspond to the site identifiers), with concentrations below the LOQ set to the LOQ. MBBR = moving bed biofilm reactor, AS = activated sludge, EC = electrocoagulation, Ozone = ozonation.

2.4 Quantification of required foam fraction for increased long-chain PFAA removal

When ignoring sorption to sludge and reactive transformation of precursors into target PFAS, the mass balance over a foam-forming process can be written as follows, provided that the foam would be removed from the top of the reactor:

$$\frac{dVC_{bulk}}{dt} = \varphi_{In}C_{In} - \varphi_{Ef}C_{Ef} - \varphi_{Foam}C_{Foam}$$

Here, V is the volume of the reactor (m^3), C_{bulk}, C_{In}, C_{Ef} and C_{Foam} the PFAS concentration in the reactor, influent, effluent and foam, respectively (all mol m^{-3}), and φ_{In}, φ_{Ef} and φ_{Foam} the influent, effluent and foam flow rate (all $m^3\ hr^{-1}$), respectively. At steady state and constant reactor volume, this means that:

$$\varphi_{In}C_{In} - \varphi_{Ef}C_{Ef} - \varphi_{Foam}C_{Foam} = 0, \text{ and:}$$

$$\varphi_{In} = \varphi_{Ef} + \varphi_{Foam} \rightarrow \varphi_{Ef} = \varphi_{In} - \varphi_{Foam}$$

Then:

$$\varphi_{In}C_{In} = (\varphi_{In} - \varphi_{Foam})C_{Ef} + \varphi_{Foam}C_{Foam}$$

$$C_{In} = (1 - \frac{\varphi_{Foam}}{\varphi_{In}})C_{Ef} + \frac{\varphi_{Foam}}{\varphi_{In}}C_{Foam}$$

$$C_{In} - C_{Ef} = \frac{\varphi_{Foam}}{\varphi_{In}}(C_{Foam} - C_{Ef})$$

$$\frac{\varphi_{Foam}}{\varphi_{In}} = \frac{C_{In} - C_{Ef}}{C_{Foam} - C_{Ef}}$$

At a removal of RE %:

$$C_{Ef} = \left(1 - \frac{RE}{100}\right) C_{In}$$

Then:

$$\frac{\varphi_{Foam}}{\varphi_{In}} = \frac{C_{In} - \left(1 - \frac{RE}{100}\right) C_{In}}{C_{Foam} - \left(1 - \frac{RE}{100}\right) C_{In}} \quad \text{(Foam Fraction)}$$

The next step is to relate the foam concentration to the effluent concentration. Using the analysis by Stevenson and Li (2017)[1], C_{Foam} can be related to C_{Ef} as below, with Γ the surface excess concentration of PFAS (mol m^{-2}) and r_{32} the Sauter mean bubble radius of the foam (m):

$$C_{Foam} = \quad C_{Ef} + \frac{3\Gamma}{r_{32}}$$

The equilibrium relation between the surface excess and the effluent concentration is given by an adsorption isotherm. For simplicity, a Henry's law isotherm is used, which is relatively realistic at low concentrations, with Henry's constant K_H (m):

$$\Gamma = K_H \cdot C_{Ef}$$

Combining the two equations above and introducing the variable $K = \left(1 + \frac{3K_H}{r_{32}}\right)$:

$$C_{Foam} = \quad C_{Ef} + \frac{3K_H \cdot C_{Ef}}{r_{32}} = \left(1 + \frac{3K_H}{r_{32}}\right) C_{Ef} = K \cdot C_{Ef} = K \cdot \left(1 - \frac{RE}{100}\right) C_{In}$$

Using the above definition of C_{Foam} in the equation for the foam fraction:

$$\frac{\varphi_{Foam}}{\varphi_{In}} = \frac{C_{In} - \left(1 - \frac{RE}{100}\right) C_{In}}{K \cdot \left(1 - \frac{RE}{100}\right) \cdot C_{In} - \left(1 - \frac{RE}{100}\right) C_{In}}$$

$$\frac{\varphi_{Foam}}{\varphi_{In}} = \frac{1 - \left(1 - \frac{RE}{100}\right)}{K \cdot \left(1 - \frac{RE}{100}\right) - \left(1 - \frac{RE}{100}\right)}$$

$$\frac{\varphi_{Foam}}{\varphi_{In}} = \frac{\frac{RE}{100}}{\left(1 - \frac{RE}{100}\right) \cdot (K - 1)} \qquad \text{(Equation S1, Foam Fraction)}$$

There are weaknesses in this analysis that must be pointed out. As aforementioned, the analysis ignores adsorption to sludge and reactive transformation of precursors. Secondly, a Henry adsorption isotherm is only realistic at low concentrations and frequently the more accurate, but more complex, Langmuir isotherm is used. Thirdly, in reality, r_{32} is a variable that will often change when the foam fraction increases. Changing the foam fraction without changing the bubble radius is difficult, since the wetness of the foam is a function of bubble size, so K is only an independent constant if the foam fraction is increased without increasing the foam wetness. Finally, as pointed out in the main text, the foam is not removed from the water surface in any of the plants under investigation in this study, and the retention time of the foam was likely higher than that of the water in most plants.

Despite these limitation, Equation S1 may be used to roughly estimate the required foam fraction that would be necessary to achieve certain levels of long-chain PFAA removal. For this calculation, the removal and enrichment of Σlong-chain PFAA were used, since these compounds are removable with foam fractionation, and using summed concentrations moderates the effects of non-detect concentrations. As visible from Figure SI 6b, at sites D and E, an approximately seven-fold increase in volumetric foam formation may already result in a Σlong-chain PFAA removal of 80 %. Since the calculated foam fractions at these two sites were currently both < 0.5 % (Figure SI 6a), this may be achievable. Furthermore, at site J, a removal of > 99 % would require a foam fraction of only 3 % (Figure SI 6a). However, it should be stressed that these calculations are approximations only and that artificially increasing the foam formation while keeping the bubble size (and thus foam wetness and relative surface area) constant may not be possible.

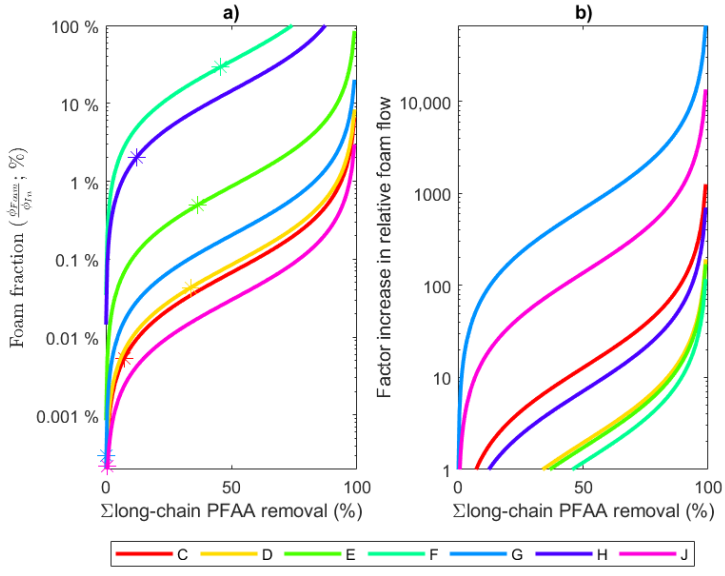

Figure SI 6: Foam fraction (a) and increase in foam fraction (b) required to reach a certain Σlong-chain PFAA removal. Asterisks in a) represent the Σlong-chain PFAA removal and calculated foam fraction as found from the concentrations obtained in this study, i.e. during normal plant operation. Only sites for which the measured Σlong-chain PFAA removal was positive were included, since for the remaining sites the calculated foam fractions would be negative. The letters in the legend correspond to the site identifiers given in main text Table 1. These plots are rough approximations only, since the calculations ignore sorption to sludge and reactive transformation of PFAS and assume the relative surface area of the foam to be constant independent of foam fraction, which is not realistic.

2.4 Figure 3 repeated with alternative handling of concentrations below the LOQ

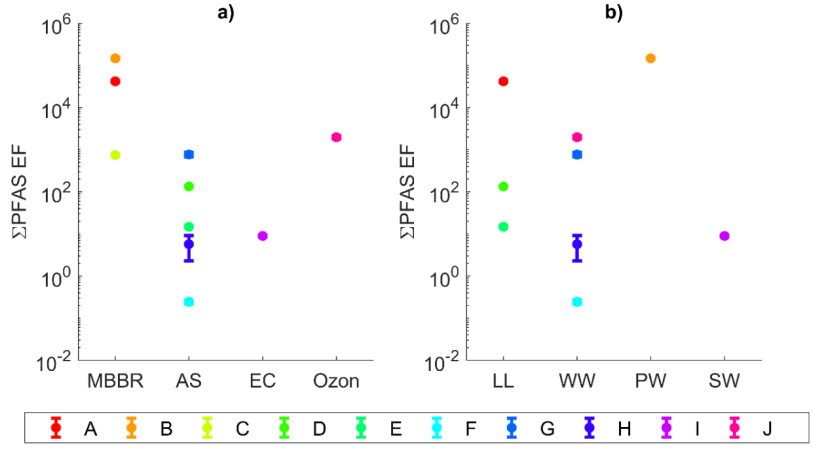

Figure SI 7: ΣPFAS EF grouped by a) treatment process and b) water type, with concentrations below the LOQ set to zero. MBBR = moving bed biofilm reactor, AS = activated sludge, EC = electrocoagulation, Ozon = ozonation, LL = landfill leachate, WW = wastewater, PW = process water, SW = stormwater runoff from landfill bottom ash collection site. Error bars represent the standard deviation (sd) within the EF for each plant (n = 3 for foamate as well as influent concentrations), but are difficult to see for all plants except H, because the sd was relatively small. The letters in the legend correspond to the site identifiers given in main text Table 1.

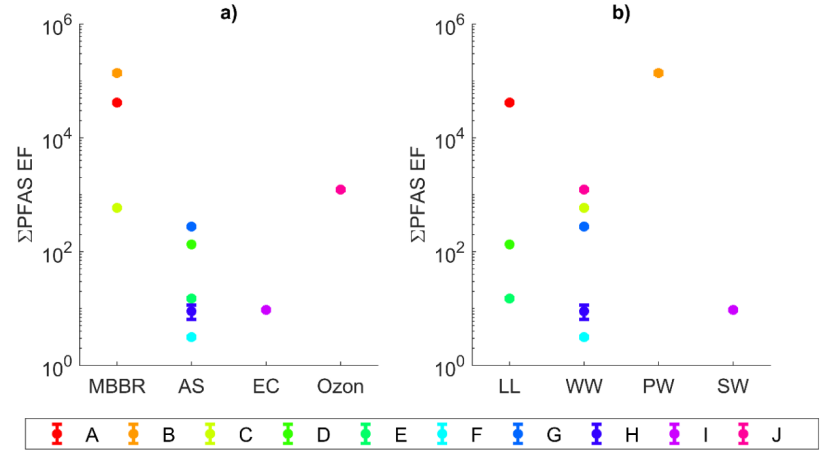

Figure SI 8: ΣPFAS EF grouped by a) treatment process and b) water type, with concentrations below the LOQ set to the LOQ. MBBR = moving bed biofilm reactor, AS = activated sludge, EC = electrocoagulation, Ozon = ozonation, LL = landfill leachate, WW = wastewater, PW = process water, SW = stormwater runoff from landfill bottom ash collection site. Error bars represent the standard deviation (sd) within the EF for each plant (n = 3 for foamate as well as influent concentrations), but are difficult to see for all plants except H, because the sd was relatively small. The letters in the legend correspond to the site identifiers given in main text Table 1.

2.5 General chemistry results

Table SI 7: General chemistry of the influent for all sites.

	A	B	C	D	E	F	G	H	I	J
Aluminum (µg L^{-1})	130	140	1500	67	250	420	310	1300	2000	55
Arsenic (µg L^{-1})	3	<0.5	1	40	110	2.4	5.5	<0.5	5.7	<0.5
Barium (µg L^{-1})	500	3.1	9.0	360	440	31	45	71	100	7.4
Calcium (mg L^{-1})	130	20	44	240	160	76	140	95	190	39
Cadmium (µg L^{-1})	0.15	0.07	<0.05	0.76	1.2	0.14	0.09	0.55	0.98	<0.05
Cobalt (µg L^{-1})	2.3	6.5	0.34	8.9	33	0.64	0.77	0.64	4	1.4
Chromium (µg L^{-1})	1.6	8.4	<0.9	45	350	2.3	3.8	120	7.8	<0.9
Copper (µg L^{-1})	18	43	16	3.3	210	52	17	42	480	5.1
Iron (mg L^{-1})	5.8	29	0.19	0.98	5.6	5.6	2.4	0.85	0.91	0.48
Mercury (µg L^{-1})	<0.02	<0.02	<0.02	<0.02	0.03	0.03	0.02	0.07	0.03	<0.02
Potassium (mg L^{-1})	180	14	21	460	940	25	26	42	450	21
Magnesium (mg L^{-1})	49	2.6	9.0	200	140	9.3	58	3.1	21	6.3
Manganese (µg L^{-1})	380	150	43	1100	760	95	57	35	160	91
Molybdenum (µg L^{-1})	7.4	4.8	2.9	480	27	2.8	1.5	180	140	1.9
Sodium (mg L^{-1})	550	2700	64	1500	6400	110	340	62	1700	74
Nickel (µg L^{-1})	18	21	2.7	140	410	6.3	4.3	3.1	53	2.6
Lead (µg L^{-1})	1.5	2	<0.5	1.1	8.7	11	5.8	41	33	<0.5
Vanadium (µg L^{-1})	1.4	4.4	0.29	39	180	2.1	1.3	3.7	8.5	<0.2
Zinc (µg L^{-1})	25	93	17	42	230	100	80	100	130	20
Chloride (mg L^{-1})	650	1600	100	2300	13000	150	<1.0	67	2700	94
Fluoride (mg L^{-1})	0.24	<0.4	0.44	0.96	4.7	0.27	0.23	1.1	<0.4	0.22
Total phosphorus	0.98	21	1.7	6.7	44	5.1	5.6	7.2	0.21	0.5
Turbidity (FNU)	140	400	14	280	29	100	37	72	270	3.4
Conductivity (mS m^{-1})	360	1100	98	1300	3300	130	300	77	980	72
pH	7.7	8.1	7.7	7.4	7.4	8	7.5	8.5	7.9	7
Total nitrogen (mg L^{-1})	58	85	51	420	1200	55	45	24	18	20
Total organic carbon (TOC, mg L^{-1})	41	1000	30	230	600	120	37	46	85	14

Bibliography

(1) Stevenson, P.; Li, X. *Foam Fractionation - Principles and Process Design*, 1st ed.; Taylor & Francis: Boca Raton, 2014.

Acta Universitatis Agriculturae Sueciae

Doctoral Thesis No. 2023:53

Per- and polyfluoroalkyl substances (PFAS) are anthropogenic persistent chemicals that are notoriously difficult to remove from water. This thesis explored the potential of foam fractionation and electrochemical oxidation as treatment technologies for PFAS-contaminated water. Both technologies could effectively reduce long-chain PFAS concentrations, but short-chain PFAS were more difficult to remove and destroy. Integrating foam fractionation within existing treatment processes could be a promising option for easy PFAS removal, but more research is needed.

Sanne J. Smith received her doctoral education at the Department of Aquatic Sciences and Assessment of the Swedish University of Agricultural Sciences (SLU). She received her master's degree in civil engineering from the Delft University of Technology and bachelor degrees in chemistry and chemical engineering from the University of Groningen.

Acta Universitatis Agriculturae Sueciae presents doctoral theses from the Swedish University of Agricultural Sciences (SLU).

SLU generates knowledge for the sustainable use of biological natural resources. Research, education, extension, as well as environmental monitoring and assessment are used to achieve this goal.

ISSN 1652-6880
ISBN (print version) 978-91-8046-158-0
ISBN (electronic version) 978-91-8046-159-7